DISSERTATION

IDENTIFICATION OF THERAPEUTIC TARGETS IN CANINE BLADDER CANCER: A TRANSLATIONAL MODEL FOR MAPK PATHWAY-TARGETED AND IMMUNE-BASED THERAPIES

Submitted by

Kathryn Elizabeth Cronise

Graduate Degree Program in Cell and Molecular Biology

In partial fulfillment of the requirements

For the Degree of Doctor of Philosophy

Colorado State University

Fort Collins, Colorado

Spring 2021

Doctoral Committee:

Advisor: Dawn Duval
Co-Advisor: Daniel Gustafson

Jennifer DeLuca
Rodney Page
Douglas Thamm

ABSTRACT

IDENTIFICATION OF THERAPEUTIC TARGETS IN CANINE BLADDER CANCER: A TRANSLATIONAL MODEL FOR MAPK PATHWAY-TARGETED AND IMMUNE-BASED THERAPIES

Activating mutations in the proto-oncogene BRAF are drivers of oncogenesis in several human cancers, including melanoma, thyroid and colorectal carcinomas, and hairy-cell leukemia. Small molecule inhibitors targeting oncogenic BRAF demonstrate initial efficacy in approximately 50% of BRAF mutant melanoma patients; however, acquired resistance invariably develops. Other individuals, including the majority of colorectal cancer patients, exhibit intrinsic resistance to BRAF inhibitors. Combined inhibition of BRAF and its downstream target MEK improves the rate and duration of patient response, but resistance remains an issue. Thus, more effective and robust therapies are necessary.

Transitional cell carcinoma (TCC) is the most common bladder cancer in dogs and humans. In this study, we provide a molecular characterization of 11 canine TCC (cTCC) tumors and identified BRAF mutations in 8 out of 11 samples. All BRAF mutations were valine-to-glutamic acid missense substitutions at amino acid residue 596 of canine BRAF (V596E), analogous to the V600E driving variant in human cancer. Additionally, 22 out of 32 formalin-fixed paraffin embedded samples expressed mutant BRAF, indicating an overall prevalence of 70%. Further analysis identified four tumors, three being BRAF mutant, that exhibited increased expression of immune gene markers

and gene signatures associated with complete clinical response to checkpoint inhibition in human bladder cancer. We also found that all TCC tumors overexpress cell cycle, DNA repair, and immune-related genes.

The high prevalence of BRAF mutations in cTCC makes targeting BRAF with small molecule inhibitors an attractive therapeutic option. We explored this possibility *in vitro* and determined that BRAF mutant cTCC cell lines are insensitive to the BRAF inhibitor vemurafenib but are sensitive to the newer, “paradox-breaking” BRAF inhibitor PLX7904. All tested cTCC cell lines were sensitive to the MEK1/2 inhibitors trametinib and selumetinib. A phenomenon observed with single-agent BRAF or MEK inhibition was the reactivation of ERK1/2 within 24 hours post-treatment, suggesting built-in mechanisms of bypassing BRAF and MEK inhibition. We also observed upregulation of genes encoding the ErbB family receptors, EGFR and ERBB2, and the EGFR ligand, EREG, in cTCC cell lines compared to other canine cancer cell lines. Treatment with the pan-ErbB inhibitor sapitinib synergized with BRAF or MEK inhibition in the BRAF mutant Bliley cell line and in the BRAF wild-type Kinsey cell line.

Next, we generated trametinib-resistant clonal derivatives of the BRAF mutant Tyler1 cTCC cell line (Tyler1-TramR). Tyler1-TramR cells exhibited trametinib IC_{50} values over 500 nM and maintained suppression of ERK1/2 phosphorylation for 24 hours following trametinib treatment. This response, combined with the insensitivity of Tyler1-TramR cell lines to the ERK1/2 inhibitor ravoxertinib, suggests that resistance to trametinib is independent of ERK1/2 reactivation. Further analysis of two Tyler1-TramR clones using RNA-Seq identified a loss of epithelial gene markers, while mesenchymal genes and transcription factors controlling the epithelial-to-mesenchymal transition were

upregulated. Analysis of basal cellular metabolism using a Seahorse XF analyzer revealed that one of the Tyler1-TramR clones exhibited altered metabolism compared to the parental Tyler1 characterized by decreased basal and maximal oxygen consumption rates, diminished spare respiratory capacity, and decreased glycolytic reserve. Collectively, these results demonstrate that spontaneous, BRAF mutant cTCC can be utilized as a translational model for investigating novel targeted and immune-based therapies that may improve treatment in both canine and human MAPK-driven cancers.

ACKNOWLEDGEMENTS

None of this could have been possible without the network of support from my advisors, colleagues, family, and friends. First, I thank my advisors, Drs. Dawn Duval and Dan Gustafson, for their consistent support, generous funding, and enthusiasm for scientific discussion and education. I could study all my life and only have but a fraction of the knowledge and expertise that they have. Equally invaluable to my development as a PhD candidate was their imparted freedom to investigate, design, and execute my own ideas and experiments that defend my thesis. I also thank my committee members, Drs. Jake DeLuca, Rod Page, and Doug Thamm for being great resources when I've needed them and for contributing their sound knowledge and guidance.

I offer my many thanks to Drs. Sunetra Das, Dan Regan, and Carol Wilusz for their invaluable mentorship. Sunetra gets an extra shout out for instilling me with confidence when it comes to all things coding. I truly appreciate those who defined my daily life as a graduate student - my colleagues and co-workers within the ACC, including Drs. Joshua Mannheimer, Keagan Collins, Nouf Alyami and Lisa Schlein, Rupa Idate, Barb Rose, Jade Kurihara, Kristen Jackson, Eric Palmer, and Mando Ramirez. You guys made it possible to persevere.

Perhaps the most deserving of acknowledgement is my family. My mother and father, Linda and Paul Cronise, for providing me with everything that I needed to succeed from day 1, and for loving, accepting, and supporting me no matter what. My sister, Kristina Cronise, who, despite being younger than I, has been an amazing role model to me throughout my young and not-so-young adult life. My grandparents, Bill

and Sharon Simms and Paul and Ingrid Cronise, each of whom played an integral part in raising me and had an enormous impact on the person that I am today. And, finally, to my dearest Allister Aradi and Rachel Maison – two of the best things that I've stumbled upon over the last 5.5 years – I could not have done it without you. You two are my Colorado family.

TABLE OF CONTENTS

ABSTRACT ii

ACKNOWLEDGEMENTS v

CHAPTER 1: LITERATURE REVIEW 1
COMPARATIVE ONCOLOGY OF BLADDER CANCER 1
Canine cancer as a model for human cancer 1
Epidemiology of canine and human bladder cancer 4
Clinical and pathological features of canine and human bladder cancer 7
Molecular biology of canine and human bladder cancer 9
Bladder cancer treatment in humans and dogs 15
BRAF SIGNALING IN CANCER 19
Overview of classical MAPK signaling and activation of RAS 19
RAF activation and initiation of a phosphorylation cascade 21
Downstream effects of MAPK signaling 23
BRAF mutations in human cancer 26
Downstream effects of oncogenic BRAF signaling 29
TARGETED THERAPY FOR BRAF-DRIVEN CANCERS 34
Overview of MAPK pathway inhibitors 34
Reactivation of MAPK signaling in BRAF and MEK inhibitor resistance 38
ERK-independent mechanisms of resistance 43
PROJECT RATIONALE 47
REFERENCES 51

CHAPTER 2: A MOLECULAR AND IMMUNE CHARACTERIZATION OF CANINE BLADDER CANCER 81
SUMMARY 81
INTRODUCTION 82
MATERIALS AND METHODS 84
RESULTS 90
DISCUSSION 109
REFERENCES 116

CHAPTER 3: IDENTIFYING THE ERBB/MAPK SIGNALING CASCADE AS A THERAPEUTIC TARGET IN CANINE BLADDER CANCER 123
SUMMARY 123
INTRODUCTION 124
MATERIAL AND METHODS 127
RESULTS 132
DISCUSSION 146
REFERENCES 152

CHAPTER 4: CHARACTERIZING A CANINE MODEL OF ACQUIRED TRAMETINIB RESISTANCE 158

SUMMARY....158
INTRODUCTION....159
MATERIALS AND METHODS....162
RESULTS....168
DISCUSSION....195
REFERENCES....201
CHAPTER 5: CONCLUSIONS AND FUTURE DIRECTIONS....209
CONCLUSIONS....209
FUTURE DIRECTIONS....213
REFERENCES....217

CHAPTER 1

Literature review

COMPARATIVE ONCOLOGY OF BLADDER CANCER

Canine cancer as a model for human cancer

Cancer is the second leading cause of death in the United States, where the lifetime probability of developing an invasive cancer is 40% for men and 39% for women (Siegel et al., 2020). In fact, the American Cancer Society estimated that over 1.8 million new cases will be diagnosed and that over 600,000 people will die from cancer in the U.S. in 2020 (Siegel et al., 2020). Despite these harrowing statistics, cancer survival rates have been on the rise in many countries, including the United States (Allemani et al., 2018). These improvements can be attributed to a decrease in cigarette smoking and improvements in cancer diagnosis and treatment (Siegel et al., 2020).

A major challenge to cancer treatment is the inefficiency of drug development. The road to FDA approval of a novel anticancer drug is a long, arduous, and expensive process (Paul et al., 2010). Ninety-five percent of therapeutic agents entering phase 1 human clinical trials will eventually fail, despite exhibiting effective antitumor activity in the preclinical setting (Day et al., 2015; Paul et al., 2010; Zhang et al., 2020). Murine models have been instrumental in cancer research, where they have been the mainstay for *in vivo* interrogation of mechanisms underlying oncogenesis and preclinical

evaluation of novel therapies (Day et al., 2015; Ireson et al., 2019). However, mouse models are poor predictors of drug efficacy in human patients (Day et al., 2015; Ireson et al., 2019; Johnson et al., 2001; Paul et al., 2010). Specifically, these models fail to recapitulate the complexity of the tumor and its microenvironment, as well as the intricate processes of metastasis and drug resistance (Day et al., 2015; Ireson et al., 2019).

Comparative oncology is the study of spontaneous tumors in companion animals with an emphasis on understanding cancer biology and evaluating novel treatment strategies that could improve cancer treatment in both veterinary and human patients (Khanna et al., 2006; Paoloni and Khanna, 2008). Cancer arises naturally in many species of companion animals, but canine cancers have been the primary focus in the comparative oncology world (LeBlanc and Mazcko, 2020; Paoloni and Khanna, 2008). Roughly 6 million dogs are diagnosed with cancer in the United States each year. In fact, canines have a higher incidence of cancer than humans, with an annual rate of 5,000 new cases per 100,000 individuals versus 500 new cases per 100,000 individuals, respectively (Schiffman and Breen, 2015). Such high incidence makes the dog a particularly appealing model for studies of cancer pathogenesis and the development of anticancer drugs (LeBlanc and Mazcko, 2020).

Research dogs have been extensively used in the preclinical phase of drug development, where they often serve as non-rodent models for assessing the safety of novel compounds. Drug toxicity studies in dogs are more predictive of toxicity in humans than are studies in rodents (Olson et al., 2000). The larger body size of dogs allows for increased sample collection and serial sampling from the same animal, an

advantage that is particularly important when addressing the pharmacokinetics and pharmacodynamics of a novel agent (Paoloni and Khanna, 2008). Additionally, despite man and mouse sharing a more recent common ancestor, dogs and humans exhibit greater genomic sequence similarity with each other than either species shares with the mouse (Kirkness et al., 2003). Genetic diversity is also similar between humans and dogs, whereas laboratory rodents are inbred and, thus, exhibit very little diversity (Lindblad-Toh et al., 2005).

Dogs naturally develop many of the same diseases as humans, including several translationally-relevant cancers (Paoloni and Khanna, 2008; Sargan, 2004). Common canine cancers that also occur in humans include non-Hodgkin lymphoma, melanoma, osteosarcoma, mammary carcinoma, and bladder carcinoma (Dobson et al., 2002; Paoloni and Khanna, 2008). Canine cancers display similar clinical, histological, and biological characteristics to several human cancers (Paoloni and Khanna, 2008). Sarcomas occur much more frequently in dogs than in humans, providing the opportunity for common canine cancers to inform treatment of rare human cancers (Gustafson et al., 2018). For example, dogs develop osteosarcomas at a rate more than ten-times that of humans (Fenger et al., 2014). Several studies of canine osteosarcoma have translated into clinical benefit in human osteosarcoma patients (Chawla et al., 2012; Kurzman et al., 1995; LaRue et al., 1989; MacEwen et al., 1989; Meyers et al., 2005; Paoloni et al., 2010; Withrow and Wilkins, 2010).

Many other factors make the dog a suitable cancer model. In contrast to mouse models of cancer, canine cancers develop spontaneously under the selective pressure of an intact immune system. Similar to human cancers, canine cancers naturally exhibit

tumor heterogeneity, undergo progression and metastasis, and develop drug resistance (Paoloni and Khanna, 2008). Dogs share the same environment as their owners, making them particularly useful for studies of cancer risk factors and prevention. Epidemiological studies of canine cancers indicate shared environmental risk factors for cancer development, including exposure to cigarette smoke (Kelsey et al., 1998). Additionally, sequence analysis of cancer-related genes revealed a greater level of conservation between humans and dogs versus humans and rodents (Paoloni and Khanna, 2008).

Comparative oncology clinical trials serve as intermediates between preclinical murine studies and human clinical trials. Clinical trials in dogs are not constrained by "standard of care" requirements, allowing for assessment of novel treatments in chemotherapy-naïve patients (Paoloni and Khanna, 2007). Canine trials can be completed more expeditiously than human clinical trials. The shorter lifespan of dogs allows for quicker determination of a treatment's impact on time to progression and overall survival (Paoloni and Khanna, 2007). Assessment of novel compounds in tumor-bearing dogs permits determination of an appropriate dosing regimen and schedule, identification of biomarkers, and evaluation of combination therapies (Paoloni and Khanna, 2008). The goals of these studies are to characterize the safety and efficacy of novel compounds while advancing cancer treatment in dogs with the hope of reducing anticancer drug attrition in human clinical trials.

Epidemiology of canine and human bladder cancer

Urinary bladder cancer accounts for 4% of diagnosed human cancers and 2% of diagnosed canine cancers (Fulkerson and Knapp, 2019; Knapp et al., 2014; Siegel et

al., 2020). More than 80,000 people in the United States are expected to be diagnosed with bladder cancer in the year 2020, and nearly 18,000 people are expected to succumb to the disease (Siegel et al., 2020). Based on an estimate of 6 million new canine cancer diagnoses each year in the United States, it is predicted that over 100,000 of these cases will be bladder cancer (Fulkerson and Knapp, 2019; Knapp et al., 2014).

Bladder cancer tends to be a disease of the elderly in both humans and dogs, with median ages of diagnosis of approximately 70 and 11 years, respectively (Knapp et al., 2014; Knowles and Hurst, 2015). Human bladder cancer occurs 3 to 4 times more frequently in males than in females (Knowles and Hurst, 2015; Siegel et al., 2020). In contrast, the incidence of canine bladder cancer is 1.7 to 2 times higher in females than in males (Fulkerson and Knapp, 2019; Knapp et al., 2014). Spayed or neutered dogs are also at increased risk of developing cancer relative to intact dogs, although the reason behind this increased risk is unknown (Bryan et al., 2007; Knapp et al., 2014).

Risk factors common to both humans and canines include genetic predispositions and environmental exposures (Burger et al., 2013; Fulkerson and Knapp, 2019). Tobacco smoking is the greatest environmental risk factor in humans, accounting for half of bladder cancer cases (Burger et al., 2013; Freedman et al., 2011). Differences in smoking habits between men and women are thought to contribute to the increased prevalence of bladder cancer in men (Burger et al., 2013; Freedman et al., 2011). Current smokers are at a higher risk of developing bladder cancer than are former smokers, suggesting that smoking cessation can reduce the risk of developing bladder cancer (Freedman et al., 2011). Interestingly, the hazard ratio for smoking has

increased over the past few decades, potentially due to changes in cigarette formulations (Freedman et al., 2011). Exposure to second hand smoke during childhood and adulthood also increases the risk of developing bladder cancer, particularly for women (Jiang et al., 2007).

Occupational exposure to carcinogens, including aromatic amines, polycyclic aromatic hydrocarbons, and chlorinated hydrocarbons, accounts for up to 20% of bladder cancer cases in humans (Burger et al., 2013). Similarly, environmental exposure to lawn herbicides and topical insecticides is associated with an increased risk of developing TCC in dogs (Glickman et al., 2004; Glickman et al., 1989). Lastly, obesity is a notable bladder cancer risk factor in both humans and dogs (Glickman et al., 1989; Koebnick et al., 2008).

Several inherited genetic factors increase susceptibility to bladder cancer in humans (Burger et al., 2013). For example, polymorphisms in N-acetyltransferase 2 (*NAT2*) and glutathione S-transferase mu 1 (*GSTM1*) are associated with a higher risk of developing bladder cancer (Burger et al., 2013; Garcia-Closas et al., 2005). These enzymes play important roles in the detoxification of carcinogens, including components of tobacco smoke (Hein, 2002; Rebbeck, 1997). *NAT2* and *GSTM1* polymorphisms confer an increased overall risk of bladder cancer and pose an even greater risk to current or former smokers relative to individuals who have never smoked (Garcia-Closas et al., 2005; Rothman et al., 2010). Dogs and other canids are deficient in genes encoding the NAT enzymes (Trepanier et al., 1997). Several genome-wide association studies have identified variants at specific genomic loci that are associated with susceptibility to developing bladder cancer in humans (Rothman et al., 2010).

Many variants occur in regions adjacent to genes with known roles in cancer progression including c-Myc proto-oncogene (*MYC*), tumor protein p63 (*TP63*), telomerase reverse transcriptase (*TERT*), and fibroblast growth factor receptor 3 (*FGFR3*) (Kiemeney et al., 2010; Kiemeney et al., 2008; Rafnar et al., 2009; Rothman et al., 2010).

Scottish terriers demonstrate a strong breed-specific risk of bladder cancer, with roughly a 20-fold increased risk relative to mixed-breed dogs (Knapp et al., 2014). Likewise, breeds such as the Shetland sheepdog, West Highland white terrier, and beagle exhibit a 3- to 6-fold increased risk of developing bladder cancer (Knapp et al., 2014). These breed-specific associations can be used to study potential genetic factors that may contribute to bladder cancer in humans and dogs.

Clinical and pathological features of canine and human bladder cancer

Transitional cell carcinoma (TCC), also known as urothelial carcinoma (UC), is the most common type of bladder cancer in both humans and dogs (Knapp et al., 2014; Knowles and Hurst, 2015). TCCs in humans and dogs are typically broken into two groups: low-grade, papillary tumors and high-grade, non-papillary tumors (Knowles and Hurst, 2015; Meuten and Meuten, 2016). Human TCC tumors in humans are staged according to the classical Tumor-Node-Metastasis (TNM) system (Brierley, 2017; Witjes et al., 2021). The majority (60%) of human TCCs are non-invasive, papillary of low grade (stage Ta) (Knowles and Hurst, 2015). Stage Ta tumors have not yet invaded the basement membrane or muscle tissue of the bladder and are morphologically akin to normal cells (Brierley, 2017; Knowles and Hurst, 2015). Stage T1 tumors, comprising 20% of human TCCs, exhibit invasion of the basement membrane but not muscle tissue

(Brierley, 2017; Knowles and Hurst, 2015). Stage Ta and T1 tumors are referred to as non-muscle-invasive bladder cancers (NMIBCs), which are thought to arise from papillary hyperplasia of the bladder epithelium. NMIBCs bear a five-year survival of 90%, but exhibit a high rate of re-occurrence (~60%) (Knowles and Hurst, 2015).

Roughly 20% of human TCCs are categorized as high-grade, muscle-invasive bladder cancer (MIBC), which are staged T2 and onward, where the tumor has invaded the muscle wall (Brierley, 2017; Knowles and Hurst, 2015). Stages T3 and T4 involve invasion into the perivesical tissue and adjacent organs, respectively (Brierley, 2017). MIBC tumors are thought to arise via flat dysplasia and carcinoma *in situ* (CIS) (Knowles and Hurst, 2015). These tumors are associated with poor five-year survival rates and high rates of metastasis (Knowles and Hurst, 2015).

Canine TCC (cTCC) tumors are staged according to the WHO criteria for canine bladder tumors, which differs from the human criteria. Unlike human TCC, the majority of canine TCCs are muscle-invasive tumors of high-grade (Fulkerson and Knapp, 2019; Knapp et al., 2014). Roughly 75% of cTCC tumors are classified as T2, where the tumor has invaded the bladder wall. The remaining quarter are T3, where the tumor invades the neighboring organs (Knapp et al., 2014). TCC in dogs typically manifests in the trigone of the bladder. These tumors are also involved in the urethra in 55% of cases and the prostate in 30% of male cases (Fulkerson and Knapp, 2019; Meuten and Meuten, 2016). Roughly 15-20% of cTCCs locally metastasize by the time of initial diagnosis and over half of dogs show distant metastases by time of death (Fulkerson and Knapp, 2019; Meuten and Meuten, 2016). This frequency is similar to that of human MIBC, which metastasizes in 50% of cases (Knowles and Hurst, 2015).

The vast majority of humans and dogs with TCC exhibit clinical signs affecting urinary function. Hematuria is the most common symptom, but pollakiruria, cystitis, and dysuria are also common (Fulkerson and Knapp, 2019; Kamat et al., 2016). Diagnosis in humans typically involves a cystoscopy procedure, and a tissue biopsy is collected if TCC is suspected (Witjes et al., 2021). Pathological analysis of the biopsy sample is integral to determining tumor stage and grade. Additional imaging, typically using computed tomography (CT), is performed if metastasis is suspected (Witjes et al., 2021).

In dogs, differential diagnoses that mimic the clinical signs of TCC, like urinary tract infections, are ruled out by routine, non-invasive testing methods (Fulkerson and Knapp, 2019). Negative results prompt the use of cystoscopy-acquired tissue collection. The advanced nature of canine TCCs makes histopathological diagnosis quite simple (Meuten and Meuten, 2016). Histological features that may aid in diagnosis include loss of cell polarity, disorganized cell growth, and cellular atypia. Abnormal nuclear features including clumped chromatin, many mitoses, and prominent nucleoli are also present. Further analysis of uroplakin III expression can be used to confirm bladder as the tissue of origin (Meuten and Meuten, 2016).

Molecular biology of canine and human bladder cancer

MIBC and papillary, low-grade NMIBC tumors are thought to arise via two distinct molecular pathways (Bakkar et al., 2003; Knowles and Hurst, 2015; Spruck et al., 1994; Wu, 2005). Papillary, NMIBC tumors typically harbor activating mutations in oncogenes within the mitogen-activated protein kinase (MAPK) and phosphatidylinositol 3-kinase (PI3K)/protein kinase B (AKT) pathways (Knowles and Hurst, 2015). In contrast, MIBC

is characterized by alterations in regulators of the cell cycle, specifically via inactivation of tumor suppressors including tumor protein p53 (TP53), RB transcriptional corepressor 1 (RB1), and cyclin-dependent kinase inhibitor 2A (CDKN2A) (Atlas, 2014; Knowles and Hurst, 2015; Robertson et al., 2017). While NMIBC tumors are genomically stable and exhibit few chromosomal alterations, MIBC frequently display chromosomal rearrangements and alterations in regulators of DNA damage and repair (Abbosh and Plimack, 2018; Atlas, 2014; Knowles and Hurst, 2015).

TP53 is the most frequently mutated gene in cancer (Kandoth et al., 2013). Mutations in *TP53* are very common in muscle-invasive bladder tumors, where they are associated with higher stage and grade (Fujimoto et al., 1992; Sidransky et al., 1991; Spruck et al., 1994). In contrast, papillary, non-invasive bladder tumors rarely harbor *TP53* mutations (Fujimoto et al., 1992; Spruck et al., 1994). Interestingly, *TP53* variants are frequently observed in CIS and pre-neoplastic dysplasia, suggesting that p53 inactivation is an early event in tumorigenesis of MIBC (Spruck et al., 1994). In 2017, The Cancer Genome Atlas (TCGA) performed a comprehensive molecular analysis of 412 chemotherapy-naïve, high-grade MIBCs, identifying alterations in the p53/cell cycle pathway in 89% of tumors (Robertson et al., 2017). Mutations in *TP53* were identified in 48% of tumors and were mutually exclusive with alterations in MDM2 proto-oncogene (*MDM2*), which encodes an E3-ubiquitin ligase that negatively regulates p53 (Haupt et al., 1997; Momand et al., 1992). Amplification and increased mRNA expression of MDM2 were observed in 6 and 19% of tumors, respectively, suggesting inactivation of p53 function in approximately three-quarters of MIBC (Robertson et al., 2017).

Loss of function of the tumor suppressor RB1 plays a role in MIBC pathogenesis (Knowles and Hurst, 2015). RB1 is a major negative regulator of cell cycle progression (Goodrich et al., 1991; Weinberg, 1995). RB1 binds to and inhibits members of the E2F family transcriptional activators, which regulate expression of genes involved in the G1/S cell cycle transition (Giacinti and Giordano, 2006; Shan et al., 1996). Mutations and focal deletions in *RB1* were identified in 17 and 4% of MBIC tumors, respectively, in the 2017 TCGA genomic analysis (Robertson et al., 2017). Amplification of E2F transcription factor 3 (E2F3) was also observed in 12% of samples (Robertson et al., 2017).

Loss of heterozygosity (LOH) of chromosome 9 is an early step in the pathogenesis of both MIBC and NMIBC that occurs in approximately half of bladder tumors (Cairns et al., 1993; Knowles and Hurst, 2015; Wu, 2005). Several candidate tumor suppressor genes on chromosome 9 are deleted in bladder cancer. Copy number deletion of *CDKN2A* is a particularly common alteration (Knowles and Hurst, 2015; Williamson et al., 1995). *CDKN2A* encodes p16 and $p14^{ARF}$, which play important roles in regulation of the G1/S cell cycle transition and stabilization of p53, respectively (Ruas and Peters, 1998). *CDKN2A* deletions were identified in one-quarter of MIBC patients in the 2017 TCGA study (Robertson et al., 2017). Other deleted genes of interest on chromosome 9 include TSC complex subunit 1 (*TSC1*) (Habuchi et al., 1995; Knowles et al., 2003), patched 1 (*PTCH1*) (Aboulkassim et al., 2003; McGarvey et al., 1998), and BMP/retinoic acid inducible neural specific 1 (*BRINP1*, also known as *DBC1*) (Habuchi et al., 1998).

Alterations in fibroblast growth factor (FGF) signaling are common in human bladder cancer (Knowles and Hurst, 2015). The majority of human NMIBC tumors harbor activating mutations in FGF receptor 3 (*FGFR3*) (Billerey et al., 2001; Burger et al., 2008; Cappellen et al., 1999; Hernandez et al., 2006; van Rhijn et al., 2001). These mutations occur more frequently in tumors of lower pathological stage and grade, and are associated with a better prognosis (Billerey et al., 2001; Burger et al., 2008; Hernandez et al., 2006; van Rhijn et al., 2001; Zieger et al., 2005). Ectopic expression of hotspot *FGFR3* mutations in normal human urothelial cells induces MAPK and phospholipase C gamma (PLCλ**)** activation, oncogenic transformation, and increases proliferation (di Martino et al., 2009). Elevated FGFR3 expression is also observed in NMIBC, albeit, at higher frequencies in FGFR3 mutant tumors of low stage and grade (Tomlinson et al., 2007). Downregulation of microRNAs miR-99a and miR-100 in low-grade NMIBC contributes to elevated FGFR3 expression (Catto et al., 2009). Mutations in *FGFR3* are much less common in MIBC, but increased expression of FGFR3 is observed in 40% of MIBC cases (Tomlinson et al., 2007). Increased expression of FGF receptor 1 (FGFR1) is frequently observed in both NMIBC and MIBC (Tomlinson et al., 2009). Ectopic expression of FGFR1 in immortalized human urothelial cells activates the MAPK pathway and PLCλ in response to FGF2, leading to increased proliferation and survival (Tomlinson et al., 2009). Preferential splicing of FGFR1 transcripts into FGFR1*β* variants is also observed in higher stage and grade TCC, where it promotes increased sensitivity to FGF1 and subsequent MAPK pathway activation (Tomlinson and Knowles, 2010).

Activating alterations in the ErbB family of receptor tyrosine kinases are commonly observed in MIBC and, to a lesser extent, in NMIBC (Knowles and Hurst, 2015). The 2017 TCGA analysis identified mutations in erb-b2 receptor tyrosine kinases 2 and 3 (*ERBB2* and *ERBB3*) in 12% and 10% of MIBC tumors, respectively (Robertson et al., 2017). Amplification and upregulated expression of epidermal growth factor receptor (*EGFR*) and *ERBB2* are also often observed in MIBC (Atlas, 2014; Knowles and Hurst, 2015). Oncogenic mutations in Ras family genes (*HRAS*, *KRAS*, and *NRAS*) occur at similar frequencies in superficial and muscle-invasive TCC (Knowles and Hurst, 2015). Of these genes, *HRAS* is most commonly mutated in bladder cancer, with oncogenic alterations identified in 5 and 12% of MIBC and NMIBC tumors, respectively (Atlas, 2014; Hurst et al., 2017).

A more recent advancement in our understanding of bladder cancer biology was the identification of molecular subtypes that may respond differently to chemotherapeutics. Choi et al. described three molecular subtypes identified in 73 muscle-invasive bladder tumors: basal, luminal, and p53-like (Choi et al., 2014). The basal and luminal subtypes shared biomarkers with the basal and luminal subtypes identified in breast cancer (Choi et al., 2014; Perou et al., 2000). The basal subtype was characterized by high expression of keratins 5,6 and 14, squamous differentiation, and activation of tumor protein p63 (Choi et al., 2014). The luminal subtype was associated with *FGFR3* mutations, increased *FGFR3* expression, and activation of peroxisome proliferator-activated receptor gamma (PPARλ) and estrogen receptor (ER) signaling. Tumors within the p53-like group displayed an active p53 gene expression signature that was not associated with expression of wild-type *TP53*. The basal

subtype was associated with aggressive disease presentation and shorter overall survival, while the p53-like subtype was associated with resistance to cisplatin-based combination chemotherapy (Choi et al., 2014).

In 2017, the TCGA expanded on the previously described molecular subtypes, identifying five different MIBC subtypes: basal/squamous, luminal, luminal-infiltrated, luminal-papillary, and neuronal (Robertson et al., 2017). The neuronal subtype was characterized by high expression of neuronal differentiation and cell cycle genes and was associated with the poorest overall survival out of the five subtypes. The luminal-infiltrated tumors were of low purity and were associated with high expression of epithelial-to-mesenchymal (EMT) markers and wild-type *TP53*; whereas, the luminal-papillary tumors were characterized by papillary histology and high frequencies of alterations in *FGFR3* (Robertson et al., 2017).

Hedegaard et al. identified three molecular classes among NMIBC tumors (Hedegaard et al., 2016). Class I tumors were mainly of papillary histology, lower grade and stage, and were enriched with *FGFR3* mutations. Class I and Class II were described as luminal-like; however, Class II tumors were of higher grade and stage and were associated with *TP53* mutations. Class III was comprised of basal-like tumors, exhibiting expression of basal/stem cell markers similar to basal MIBC, and was enriched in *FGFR3* mutations (Hedegaard et al., 2016).

The molecular landscape of canine bladder cancer is more vaguely defined relative to that of human bladder cancer. One of the most striking features of canine bladder cancer described so far is the disease's high prevalence of BRAF mutations occurring in approximately three-quarters of tumors (Decker et al., 2015; Mochizuki et

al., 2015). Similar to human MIBC, approximately half of cTCC tumors exhibit overexpression of ERBB2, and its expression is associated with higher grade and stage (Jalali Nadoushan et al., 2007; Millanta et al., 2018). In their RNA-Seq analysis of 11 cTCC tumors, Maeda et al. identified the prostaglandin E receptor 2 (PTGER2) and ERBB2 as activated upstream regulators of differentially expressed genes between cTCC and normal bladder (Maeda et al., 2018). Cycooxygenase-2 (COX-2) is an enzyme that catalyzes the synthesis of prostaglandin H_2, a precursor to prostaglandin E_2. Canine TCC primary lesions and metastases exhibit increased expression of COX-2 relative to normal urinary bladder tissue, a feature common to human TCC as well, where it is expressed at high frequencies in CIS and muscle-invasive tumors (Khan et al., 2000; Mohammed et al., 1999; Shirahama, 2000). Recently, Dhawan et al. revealed that canine TCC tumors can be broken into basal and luminal subtypes based on gene expression (Dhawan et al., 2018). Approximately two-thirds of the 29 tumors analyzed were luminal and the remaining one-third were basal. Basal tumors exhibited enrichment of p63 pathway genes, interferon gamma (IFN-λ)-inducible genes, and EMT markers. Luminal tumors had increased expression of PPARG, similar to human luminal MIBC tumors (Choi et al., 2014; Dhawan et al., 2018).

Bladder cancer treatment in humans and dogs

Human non-muscle-invasive TCC tumors are typically removed by transurethral resection (Babjuk et al., 2019). Patients with low-risk tumors typically receive a single local instillation of chemotherapy, such as mitomycin C, following transurethral resection, which can significantly reduce the risk of tumor recurrence (Sylvester et al., 2016). Patients with intermediate- or high-risk tumors usually receive a full course of

Bacillus Calmette-Guerin immunotherapy following tumor resection (Babjuk et al., 2019). Patients are routinely monitored with follow-up cystoscopies and urine analysis (Babjuk et al., 2019). Although treatment of non-invasive TCC yields a 5-year survival rate of 90%, the disease has a high recurrence rate of 50% or greater (Knowles and Hurst, 2015).

For localized MIBC (stage T2-T4a, N0-Nx, M0) the gold standard treatment involves radical cystectomy, where the entire bladder and distal ureters are removed, and pelvic lymph node dissection (Witjes et al., 2021). The procedure also involves removal of the prostate and seminal vesicles or the uterus, urethra, and part of the vagina. Surgical intervention is often non-curative, with roughly 50% of patients experiencing disease relapse (Witjes et al., 2021). Radiation therapy is not recommended in the pre- or post-operative setting for MIBC treatment (Witjes et al., 2021). Neoadjuvant chemotherapy with cisplatin-based combinations aims to decrease the incidence of micrometastases present prior to surgery. Two cisplatin-based combinations are primarily used: methotrexate, vinblastine, doxorubicin, and cisplatin (MVAC) or gemcitabine and cisplatin (GC) (Witjes et al., 2021). A 2016 meta-analysis of outcome data from 15 randomized clinical trials reported significant benefit from neoadjuvant chemotherapy, with an 8% increase in 5-year survival (Yin et al., 2016). Neoadjuvant MVAC was associated with a better overall survival than was GC (Yin et al., 2016). A separate 2016 meta-analysis confirmed increased benefit from neoadjuvant MVAC or GC relative to radical cystectomy alone, using pathological complete response as the primary outcome (Kim et al., 2016). Adequate renal function, is an important pre-requisite for cisplatin-based chemotherapy for MIBC, as cisplatin is

cleared by the kidneys and has possible nephrotoxic effects (Galsky et al., 2011). Other factors that render patients unfit for cisplatin are low performance status, hearing loss, peripheral neuropathy, and heart failure. Unfortunately, since the majority of MBIC patients are of advanced age, approximately half of individuals are considered cisplatin-ineligible (Galsky et al., 2011).

Neoadjuvant immunotherapy with checkpoint inhibitors is currently being investigated for treatment of MIBC, particularly for individuals who are cisplatin-ineligible (Witjes et al., 2021). The phase 2 PURE-01 study evaluating the efficacy of neoadjuvant pembrolizumab, an antibody against programmed cell death protein 1 (PD-1), for treatment of MIBC reported that 42% of patients achieved a complete pathological response (Necchi et al., 2018). High tumor mutational burden and high expression of PD-1 ligand 1 (PD-L1) on tumor and immune cells combined were associated with a better response. Similar results were achieved with the PD-L1 antibody atezolizumab as adjuvant therapy in the phase 2 ABACUS clinical trial, which achieved a pathological complete response rate of 31% (Powles et al., 2019). Neither tumor mutational burden nor PD-L1 expression on tumor cells correlated with outcome in this study; however, the presence of preexisting activated T cells were associated with improved response (Powles et al., 2019).

For MIBC patients with distant metastasis, MVAC or GC is the first-line therapy, followed by immunotherapy with a PD-1 or PD-L1 checkpoint inhibitor, if necessary. Cisplatin-ineligible patients are recommended to receive either a combination of carboplatin and gemcitabine or a checkpoint inhibitor (Witjes et al., 2021).

Unfortunately, for patients with distant metastases, the five-year survival rate is only 5% (Knowles and Hurst, 2015).

Most bladder tumors in dogs are inoperable, as they are frequently located in the trigone of the bladder or the disease is too advanced (Fulkerson and Knapp, 2019). However, surgery may be employed in cases where the tumor is located in the apex of the bladder or for placement of stents to restore urine flow. Treatment with COX inhibitors, chemotherapy, or both is the mainstay therapy (Fulkerson and Knapp, 2019). A study of 94 dogs treated with piroxicam, a nonselective COX-1/-2 inhibitor commonly used for canine TCC disease management, reported a median progression-free interval (PFI) of 120 days and a median survival of 244 days (Knapp et al., 2014). Treatment with combined piroxicam and mitoxantrone yielded a median PFI of 160 days and a median survival of 291 days (Henry et al., 2003). A randomized trial assessing the therapeutic value of combined vinblastine and piroxicam for TCC reported a PFI of 143 days and a median survival of 531 days in the vinblastine arm, and a PFI of 199 days and a median survival of 299 days in the vinblastine/piroxicam arm (Knapp et al., 2016). Treatment of cTCC is typically not curative; however, advances in treatment have improved the quality of life in dogs and have increased the likelihood of disease control (Fulkerson and Knapp, 2019).

BRAF SIGNALING IN CANCER

Overview of classical MAPK signaling and activation of RAS

In the late 1980s, Ray and Sturgill described a soluble, serine/threonine kinase that rapidly phosphorylates microtubule-associated protein 2 (MAP-2) in insulin-treated murine 3T3-L1 adipocytes (Ray and Sturgill, 1987). The activity of this kinase, termed MAP kinase, was dependent upon its own phosphorylation status as a result of insulin treatment (Ray and Sturgill, 1988). When evidence emerged that insulin-stimulated MAP kinase also phosphorylates and activates the ribosomal S6 kinase (S6K-II), it was hypothesized that MAP kinase serves as a major intermediate in a phosphorylation cascade within the insulin signaling pathway (Sturgill et al., 1988). In 1989, Rossomando and colleagues determined that MAP kinase was identical to the previously described pp42, a 42-kD protein that becomes tyrosine-phosphorylated in response to various stimuli including growth factors, viral-transformation, and phorbol ester treatment (Cooper et al., 1982; Cooper and Hunter, 1981; Cooper et al., 1984; Gilmore and Martin, 1983; Martinez et al., 1982; Nakamura et al., 1983; Rossomando et al., 1989). The group suggested the new name “mitogen-activated protein kinase”, to better fit the wide array of mitogens that stimulate its activation (Rossomando et al., 1989).

Over the next decade, an intricate network of kinases would be pieced together into what is now called the mitogen-activated protein kinase (MAPK) signaling pathway, an evolutionarily conserved network responsible for regulating many essential cellular functions including proliferation, differentiation, and apoptosis (Widmann et al., 1999;

Zhang and Liu, 2002). Several different MAPK proteins have been identified, each acting as the downstream kinase in phosphorylation cascades composed of a minimum of three “levels”, whereby a MAP kinase kinase kinase (MAPKKK) activates a MAPK kinase kinase (MAPKK), which then activates the MAPK (Widmann et al., 1999).

The most well described MAPK cascade is the extracellular signal-regulated kinase (ERK) signaling pathway (**Figure 1.1**). Activation of this pathway is typically initiated by binding of a mitogen, such as EGF, to a receptor tyrosine kinase (RTK), which induces ligand binding followed by transautophosphorylation of the RTK intracellular domains (Schlessinger, 2000). This change in RTK conformation and phosphorylation status provides a docking site for the adaptor protein growth factor receptor-bound protein 2 (GRB2), which then recruits the guanine nucleotide exchange factor (GEF) son of sevenless homolog 1 or 2 (SOS1/2, **Figure 1.1**) (Buday and Downward, 1993; Chardin et al., 1993). Recruitment of SOS permits its interaction with the membrane-bound, small GTPase RAS, a major activator of several signaling pathways including MAPK/ERK pathway. The RAS family in mammalians consists of HRAS, KRAS, and NRAS, as well as several RAS-related proteins (Downward, 1990). RAS functions as a molecular switch – inactive when bound to guanosine diphosphate (GDP) and active when bound to guanosine triphosphate (GTP) (Downward, 1990). SOS interaction with RAS promotes exchange of GDP for GTP resulting in RAS activation (**Figure 1.1**) (Buday and Downward, 1993; Chardin et al., 1993).

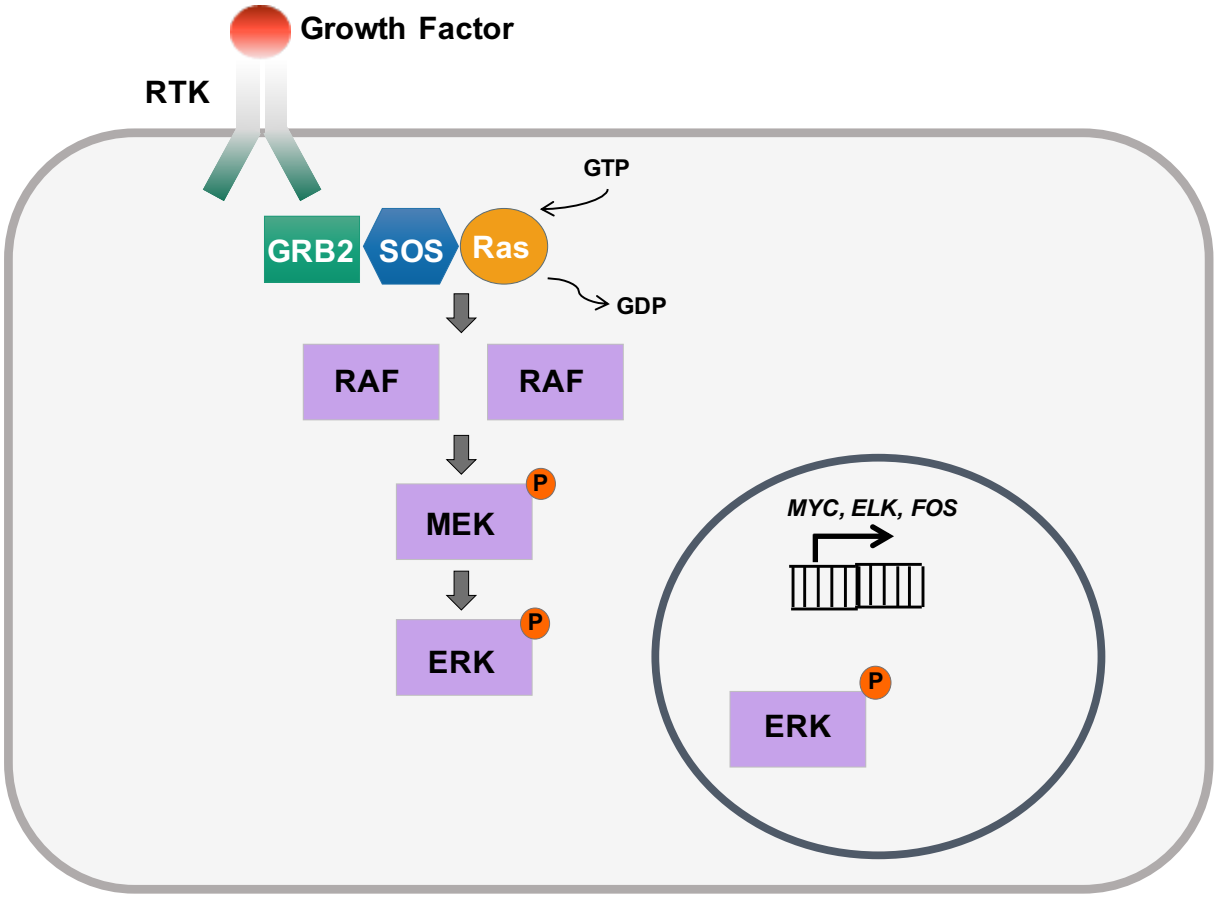

Figure 1.1. **Schematic overview of the MAPK signaling cascade.**

RAF activation and initiation of a phosphorylation cascade

Active RAS recruits its downstream effector RAF, a MAPKKK, to the plasma membrane where it becomes activated (**Figure 1.1**). Mammalian RAF exists in three isoforms: ARAF, BRAF, and CRAF (Bonner et al., 1984; Huebner et al., 1986; Ikawa et al., 1988). These RAF isoforms harbor three distinct evolutionarily conserved domains (CR1, CR2, and CR3). CR1 and CR2 comprise the regulatory elements of RAF, whereas, CR3 is RAF's kinase domain. CR1, which contains the RAS-binding domain (RBD) and a cysteine-rich domain (CRD), is necessary for RAS-stimulated activation of RAF (Lavoie and Therrien, 2015).

In the absence of upstream pathway activation, RAF's RBD and CRD domains associate with its kinase domain, resulting in RAF auto-inhibition (Cutler et al., 1998; Lavoie and Therrien, 2015). This auto-inhibition is further promoted by the binding of 14-3-3 adaptor scaffold proteins to one site within CR2 and another within CR3 (Tzivion et al., 1998). Following conversion of RAS-GDP to RAS-GTP, RAF is recruited to the plasma membrane where it binds to active RAS through its RBD (Moodie et al., 1993; Stokoe et al., 1994; Vojtek et al., 1993; Warne et al., 1993; Zhang et al., 1993). Auto-inhibition is relieved by RAF's binding to RAS as well as by disruption of RAF's interaction with the 14-3-3 protein bound to the CR2 region. The latter occurs via dephosphorylation of 14-3-3's binding site within RAF's CR2 domain by protein phosphatases 1 and 2A (Abraham et al., 2000; Jaumot and Hancock, 2001).

Following relief of auto-inhibition, activation of RAF occurs via homo- and hetero-dimerization and subsequent trans-activation (Farrar et al., 1996; Luo et al., 1996; Rushworth et al., 2006; Weber et al., 2001). Dimerization is promoted by the natural grouping of GTP-bound RAS into nanoclusters within lipid rafts in the plasma membrane and is further stabilized by 14-3-3 protein binding to RAF's CR3 (Plowman et al., 2005; Rushworth et al., 2006; Tian et al., 2007). RAF dimerization results in allosteric activation as a result of stabilizing, conformational changes within RAF's kinase domain. The kinase domain of monomeric wild type RAF is dynamic, shifting between an open and closed conformation (Lavoie et al., 2013). Dimerization stabilizes RAF's kinase domain in the closed conformation, which is made possible in part by movement of its regulatory helix (αC) to an 'in' conformation (Thevakumaran et al., 2015). The αC is typically kept in an 'out' conformation by an inhibitory helix within

RAF's activation segment, activation segment helix 1 (Thevakumaran et al., 2015). Dimerization-induced stabilization of the kinase closed conformation results in parallel alignment of two hydrophobic residues, the regulatory and catalytic spines – a common requirement for kinase catalytic activity (Kornev et al., 2006; Lavoie et al., 2013). In addition to dimerization, activation of all three RAF isoforms requires phosphorylation of two key residues within its activation segment (Baljuls et al., 2008; Chong et al., 2001; Lavoie and Therrien, 2015; Zhang and Guan, 2000). Activation of ARAF and CRAF, but not BRAF, requires additional phosphorylation of serine and tyrosine residues within the N-terminal region (Marais et al., 1997).

Activated RAF then initiates a phosphorylation cascade, whereby it recruits and binds to the MAPKKs MEK1 or MEK2. RAF phosphorylation of MEK at serine residues within MEK's activation segment results in MEK activation (Howe et al., 1992; Kyriakis et al., 1992). MEK1 and MEK2 are dual specificity kinases that, when activated by RAF, can bind to and activate the MAPKs ERK1 and ERK2 by phosphorylating threonine and tyrosine residues within ERK's activation segment (Crews and Erikson, 1992; Rossomando et al., 1992). ERK1/2 has several nuclear and cytoplasmic substrates, which control the essential processes of growth, proliferation, and differentiation (**Figure 1.1**) (Yoon and Seger, 2006; Zhang and Liu, 2002).

Downstream effects of MAPK signaling

The MAPK signaling pathway is a critical regulator of cell proliferation. In 1993, it was discovered that inactivation of ERK1 and ERK2 in Chinese hamster fibroblasts, via either antisense RNA expression or overexpression of a kinase-deficient mutant, results in substantial inhibition of growth factor-induced AP-1 transcriptional activity and cell

growth (Pages et al., 1993). ERK1/2 normally resides in the cytoplasm, but accumulates in the nucleus once activated as a result of extracellular stimulation of upstream receptors (Chen et al., 1992; Lenormand et al., 1993). A major effect of nuclear ERK1/2 signaling is induced expression of immediate early genes, which as the name suggests, are genes that are immediately transcribed following cell exposure to mitogens (Herschman, 1991). Two of these genes encode c-Fos and Jun, which together form the AP-1 transcription factor, a major regulator of genes involved in cell cycle and apoptosis.

c-Fos is transcribed by the ETS transcription factor, ELK1, a well-described ERK1/2 substrate. ELK1 is phosphorylated in its C-terminal region by activated ERK1/2, promoting the formation of a complex between ELK1 and two copies of its cofactor serum response factor (SRF) (Gille et al., 1995). SRF is activated by ribosomal protein S6 kinases (RSKs), which are among the first known cytoplasmic ERK1/2 substrates (Erikson, 1991; Sturgill et al., 1988). Once activated, RSKs translocate into the nucleus to phosphorylate and activate various transcription factors, including SRF. The ELK1/SRF complex binds to the serum response element within the promoter of c-Fos, resulting in its transcription (Gille et al., 1995). c-Fos functions as a molecular sensor for ERK1/2's signal duration (Murphy et al., 2002). Transient MAPK pathway activation results in c-Fos expression; however, upon signal cessation, c-Fos is rapidly degraded. Under sustained MAPK pathway activation, ERK and its downstream target RSK accumulate in the nucleus where they phosphorylate the C-terminal region of c-Fos. These phosphorylation events stabilize c-Fos and prime it for additional phosphorylation by ERK (Murphy et al., 2002).

A cell's decision to divide occurs late in the G1 phase of the cell cycle at the restriction point (Pardee, 1974). Passage through the restriction point is dependent on the phosphorylation state of the tumor suppressor RB1 (Weinberg, 1995). In its unphosphorylated state, RB binds E2F transcription factors, preventing E2F's interaction with the promoters of target genes (Weinberg, 1995). Mitogenic stimulation of the MAPK pathway in G1 results in AP-1 activation and the subsequent transcription of cyclin D1 (Balmanno and Cook, 1999). Cyclin D binds to cyclin dependent kinases 4 and 6 (CDK4/6), increasing their kinase activity, resulting in phosphorylation of RB1 (Ewen et al., 1993; Ezhevsky et al., 1997). Hypophosphorylated RB1 can no longer bind to E2Fs as efficiently, which allows for a sufficient amount of free E2F to activate transcription of genes encoding cyclins E and A. Cyclin E expression results in positive feedback activation of E2F, whereby Cyclin E binds to CDK2, promoting further phosphorylation of RB1 by CDK2 (Hinds et al., 1992). Hyperphosphorylated RB1 can no longer interact with E2F, resulting in further E2F-mediated transcription of genes required for entry into S phase of the cell cycle (Weinberg, 1995).

The MYC proto-oncogene is another immediate early gene transcribed in response the MAPK pathway activation. ERK1/2 also directly phosphorylates MYC on serine 62, enhancing MYC's stability (Sears et al., 2000). MYC associates with MYC associated factor X (MAX) and the MYC-MAX heterodimer binds to E-box sequences within the promoters of target genes (Amati et al., 1993; Blackwood and Eisenman, 1991). MAX can also bind to the transcriptional repressor MAX dimerization protein 1 (MXD, also known as MAD) (Ayer et al., 1993). MXD levels increase during cellular differentiation, resulting in an increase in MXD-bound MAX and repression of MYC

target genes. Under proliferative signaling, MYC-MAX induces expression of cyclin D2 and CDK4, promoting phosphorylation of RB1 (Bouchard et al., 1999; Hermeking et al., 2000). MYC also promotes cell cycle progression by inducing expression of E2F transcription factors (Fernandez et al., 2003).

Activated ERK1/2 induces protein synthesis, in part, due to phosphorylation of cytoplasmic MAPK interacting serine/threonine kinase 1, a kinase that phosphorylates eukaryotic translation initiation factor 4E (eIF4E) (Fukunaga and Hunter, 1997; Waskiewicz et al., 1999). ERK1/2 also regulates protein translation by cooperating with the PI3K/AKT/mTOR pathway. ERK1/2 phosphorylates TSC2, a member of the TSC1/TSC2 complex that negatively regulates mTOR activity (Ma et al., 2005). ERK-activated RSK can also phosphorylate TSC2 (Roux et al., 2004). Phosphorylation of TSC2 disrupts its interaction with TSC1 resulting in increased mTOR signaling, which positively regulates eIF4E and S6 kinase to promote protein translation (Ma and Blenis, 2009).

BRAF mutations in human cancer

A 2018 genomic analysis of 9,125 tumors comprising 33 different cancer types within the TCGA PanCancer Atlas identified RTK/RAS/MAPK as the most frequently altered mitogenic signaling pathway (Sanchez-Vega et al., 2018). Certain tumor types exhibit increased frequencies of MAPK pathway alterations including melanoma (94%), thyroid carcinoma (84%), and pancreatic (78%) and lung adenocarcinomas (74%) (Sanchez-Vega et al., 2018). *KRAS* was the most frequently altered MAPK pathway gene, with alterations particularly common in pancreatic (72%) and lung (33%) adenocarcinomas, as well as in genomically stable colorectal cancer (69%). *BRAF*

was the second most commonly altered MAPK gene, with mutations frequently observed in melanoma (51%), thyroid carcinoma (62%), and microsatellite instable colorectal cancer (56%) (Sanchez-Vega et al., 2018).

RAF's association with cancer actually predates its association with the MAPK signaling pathway. In 1983, *v-raf* was identified as a viral oncogene capable of inducing malignant transformation in NIH 3T3 cells and inducing fibrosarcoma tumorigenesis in mice (Rapp et al., 1983). A key feature of v-raf-transformed NIH 3T3 cells was the constitutive activation of MEK and ERK in the absence of upstream regulation (Kyriakis et al., 1992). Shortly thereafter, *CRAF*, or *RAF1*, was identified as a cellular proto-oncogene in humans, followed by *ARAF* and *BRAF* (Bonner et al., 1984; Bonner et al., 1985; Huebner et al., 1986; Ikawa et al., 1988). The first RAF variants known to cause malignant transformation contained structural alterations at the N-terminal region as a result of truncation or gene fusions (Fukui et al., 1987; Huleihel et al., 1986; Ikawa et al., 1988; Stanton and Cooper, 1987). Future analyses would reveal that the mechanism driving oncogenic activity was loss of the regulatory region containing the RBD (Chuang et al., 1994).

BRAF mutations were first identified in human cancer in 2002, with melanoma exhibiting a particularly high frequency of mutations (Davies et al., 2002). Most of the mutations were T>A transversions resulting in a valine (V) to glutamic acid (E) missense mutation at amino acid residue 600 (described as residue 599 originally) (Davies et al., 2002). Indeed, this variant, termed V600E, represents the vast majority of BRAF mutants identified in human cancer (Lavoie and Therrien, 2015). V600 lies within BRAF's activation segment and mutations at this site result in constitutive BRAF kinase

activity (Wan et al., 2004). Other mutations have been observed at this residue, albeit at much lower frequencies than V600E, including V600K, V600D, and V600R (Lavoie and Therrien, 2015). Missense mutations also occur at other residues within BRAF's activation, as well as within the glycine-rich "P-loop" of the kinase domain (Wan et al., 2004). In addition to missense mutations, certain human cancers, such as pilocytic astrocytoma, exhibit high frequencies of BRAF fusions (Jones et al., 2008; Ross et al., 2016).

Due to its high prevalence in human cancer, the V600E variant of BRAF has been the most widely studied. This variant is located betwixt the two activating phosphorylation sites (T599 and S602) required for activation of wild-type BRAF (Zhang and Guan, 2000). The substitution of glutamic acid at amino acid 600 is thought to mimic these activating phosphorylation events (Lavoie and Therrien, 2015). Additionally, BRAFV600E does not require dimerization for activation (Poulikakos et al., 2011; Roring et al., 2012; Thevakumaran et al., 2015). A key feature in activation of wild-type BRAF is the stabilization of the kinase domain in a closed state as a result of dimerization (Lavoie et al., 2013). BRAFV600E disrupts a key residue within the inhibitory helix AS-H1 that normally functions to keep the kinase domain's regulatory αC helix in an inactive 'out' position. In this manner, the αC helix is maintained in the 'in' position, promoting a stable closed state conformation (Lavoie and Therrien, 2015; Thevakumaran et al., 2015). Additionally, the V600E mutation promotes the formation of a salt bridge (K507-E600) within BRAF's activation segment that provides additional stability to BRAF's active conformation (Thevakumaran et al., 2015).

Downstream effects of oncogenic BRAF signaling

BRAF mutations promote oncogenesis through many mechanisms, which are often context dependent. Similar to the effects of the viral oncogene *v-raf*, transfection of NIH-3T3 cells with BRAFV600E cDNA results in malignant transformation, with approximately 100-fold the transforming capability of wild-type BRAF (Davies et al., 2002). BRAFV600E variants exhibit elevated kinase activity relative to wild-type BRAF,and promote constitutive phosphorylation of endogenous MEK1/2 and ERK1/2 in the absence of activation of RAS (Davies et al., 2002; Wan et al., 2004).

Perhaps the most obvious and well-described consequence of persistent ERK1/2 activation is dysregulation of the cell cycle, resulting in sustained proliferation. Unchecked ERK1/2 signaling results in constitutive expression of key cell cycle genes, such as cyclin D1, and downregulation of the CDK inhibitor $p27^{Kip1}$, which promotes progression from G1 to S phase (Bhatt et al., 2005). Moreover, BRAF knockdown in BRAF mutant melanoma cell lines dramatically reduces DNA synthesis (Karasarides et al., 2004). Knockdown of mutant BRAF specifically in BRAFV600E melanoma cell lines causes growth arrest, apoptosis, and prevents anchorage-independent growth on soft agar (Hingorani et al., 2003; Sumimoto et al., 2004). Inhibition of MEK in BRAF mutant melanoma cell lines produces similar results, suggesting that signaling through the MEK/ERK axis is what potentiates the oncogenic effects of BRAF (Collisson et al., 2003).

In addition to increased proliferation, activated ERK1/2 signaling promotes evasion of cell death pathways. Overexpression of wild-type BRAF in fibroblast cell lines confers protection from cytochrome c-mediated caspase activation (Erhardt et al.,

1999). BRAF knockdown in BRAF mutant melanoma cell lines results in substantial cell death marked by increased activation of caspase 3 and cleavage of PARP (Karasarides et al., 2004). Some of the anti-apoptotic effects of BRAFV600E can be attributed to suppressed expression of the pro-apoptotic proteins BAD and BIM (Boisvert-Adamo and Aplin, 2008; Cartlidge et al., 2008). ERK1/2-mediated phosphorylation of BIM targets it for ubiquitination and proteasomal degradation (Luciano et al., 2003). ERK-mediated activation of RSK promotes increased transcription of the anti-apoptotic proteins BCL2 and MCL1. MCL1 activity is further increased at the protein level, where ERK phosphorylation promotes its stability (Cook et al., 2017).

Increased MAPK signaling as a result of BRAF mutations contributes to cancer invasion and metastasis. The Rho family of GTPases is a subset of the Ras gene family responsible for regulation of cytoskeletal dynamics (Kaibuchi et al., 1999). Alterations in this signaling pathway have been implicated in the migration and invasion of cancer cells (Jaffe and Hall, 2002; Sahai and Marshall, 2002). Stable expression of oncogenic BRAF results in an increase in cell migration and invasion via increased activation of RhoA (Makrodouli et al., 2011). BRAFV600E expression results in ERK-mediated phosphorylation of cortactin, a key component of cancer cell invadopodia, which promotes F-actin nucleation (Lu et al., 2016). ERK1/2 phosphorylation of exocyst component Exo70 also contributes invadopodia formation and secretion of matrix metalloproteinases (MMPs), which are enzymes that play a key role in cancer cell invasion by promoting degradation of the extracellular matrix (ECM) and basement membrane (Lu et al., 2016; Ren and Guo, 2012). Expression of MMP-1, responsible for

degrading collagen types I and III, is increased as a result of oncogenic BRAF signaling (Brinckerhoff et al., 2000; Huntington et al., 2004).

Oncogenic BRAF expression induces a morphology shift in colon adenocarcinoma cells towards a more mesenchymal phenotype (Makrodouli et al., 2011). This shift is characterized by loss of E-cadherin and an increase in expression of N-cadherin and vimentin – a hallmark of the epithelial-to-mesenchymal transition (EMT). The EMT is a natural process that occurs during embryonic development that is exploited by cancer cells as a means of promoting invasion, metastasis, and evasion of apoptosis (Hanahan and Weinberg, 2011). This process is driven by several EMT-inducing transcription factors including SNAIL, TWIST, and ZEB1/2. Expression of oncogenic BRAF in primary melanocytes induces a shift in expression of these transcription factors, whereby expression levels of ZEB1 and TWIST1 increase and expression of ZEB2 and SNAIL2 decrease (Caramel et al., 2013). The change in transcription factor expression is accompanied by an increase in TGF-β target genes and invasion-specific genes (Caramel et al., 2013).

Oncogenic BRAF signaling promotes several metabolic alterations that support tumorigenesis. Cancer cells undergo changes in metabolism in order to meet the energetic requirements necessary for rapid, uncontrolled proliferation (Hanahan and Weinberg, 2011). The “Warburg effect” refers to a feature of this metabolic shift whereby cancer cells prefer to utilize glycolysis to generate ATP in the presence of oxygen, rather than the more efficient mitochondrial oxidative phosphorylation (OxPhos) (Vander Heiden et al., 2009; Warburg, 1956a; Warburg, 1956b).

Oncogenic BRAF promotes glycolytic metabolism via several mechanisms. In melanoma, increased ERK1/2 activation as a result of oncogenic BRAF alters the expression of micropthalmia-associated transcription factor (MITF), a lineage-specific transcription factor controlling melanocyte differentiation as well as cell proliferation, apoptosis, and mitochondrial metabolism (Wellbrock et al., 2008). ERK1/2 phosphorylates MITF, targeting it for proteasomal degradation, resulting in decreased expression of OxPhos genes (Wellbrock et al., 2008) including PPARλ coactivator 1-alpha (PGC-1α), which is a transcriptional coactivator of genes involved in mitochondrial biogenesis (Haq et al., 2013; Lin et al., 2005)

The pro-glycolytic effects of oncogenic BRAF can also be attributed to increased ERK1/2-mediated activation of RSK, whose substrates include 6-phosphofructo-2-kinase/fructose-2,6-bisphosphatase 2 (PFKFB2), which catalyzes the synthesis of fructose-2,6-bisphosphate, resulting in activation of the rate-limiting glycolytic enzyme, 6-phosphofructo-1-kinase (PFK-1). Phosphorylation of PFKFB2 in BRAF mutant melanoma increases PFKFB2's catalytic activity, resulting in increased PFK-1 activity and glycolytic flux (Houles et al., 2018). Selective inhibition of oncogenic BRAF results in downregulation of glucose transporters 1 and 3 (GLUT1/3) and hexokinase 2 (HK2), suggesting a role for oncogenic BRAF signaling in increased expression of key glycolytic components (Parmenter et al., 2014).

Pyruvate dehydrogenase (PDH) acts as a mediator of oncogene-induced senescence in human diploid fibroblasts expressing BRAFV600E (Kaplon et al., 2013). The senescent cells exhibit increased oxidative metabolism relative to cycling cells, which was caused by induction of PDH phosphatase 2 (PDP2) and suppression of PDH

kinase 1 (PDK1), which activate and repress PDH activity, respectively (Kaplon et al., 2013). Interestingly, knockdown of PDP2 or overexpression of PDK1 each permitted cells to bypass oncogene-induced senescence and promote tumorigenesis, suggesting a role for glycolysis in BRAF-mediated oncogenesis (Kaplon et al., 2013).

Melanoma cell lines expressing BRAFV600E mutations exhibit decreased activation of AMP-activated protein kinase (AMPK) (Zheng et al., 2009). AMPK is a critical regulator of cellular energy homeostasis, and its activation by the tumor suppressor serine/threonine kinase 11 (STK11, also known as LKB1) in response to energetic stress results in cell cycle arrest and inhibition of protein synthesis (Zadra et al., 2015). Inhibitory phosphorylation of LKB1 by ERK and p90RSK prevents its activation of AMPK in BRAF mutant melanoma. Thus, oncogenic BRAF is proposed to inhibit the tumor suppressive functions of LKB1-activated AMPK (Zheng et al., 2009).

Tumors typically contain hypoxic regions where the rapid proliferation of cells outgrows the available blood supply. Hypoxia-inducible factor-1 (HIF-1) is the master regulator of cellular adaptation to hypoxia (Wang and Semenza, 1995). In the presence of oxygen, the alpha subunit of HIF-1 (HIF-1α) undergoes proline hydroxylation, facilitating its binding to the E3 ubiquitin ligase von Hippel-Lindau (VHL) that targets HIF-1α for proteasomal degradation (Tanimoto et al., 2000). Conversely, HIF-1α is stabilized under hypoxic conditions, which allows it to interact with HIF-1β and activate transcription of genes involved in metabolism and angiogenesis. Knockdown of oncogenic BRAF decreased the survival of melanoma cells under hypoxic conditions, which was attributed to increased VHL expression and subsequent degradation of HIF-1α (Kumar et al., 2007). This finding suggested that oncogenic BRAF supports

melanoma cell survival under hypoxic conditions by promoting stability of HIF-1α. Overall, BRAF mutations impact a number of cellular attributes identified as “hallmarks of cancer” and, as such, are major drivers of oncogenesis (Hanahan and Weinberg, 2000).

TARGETED THERAPY FOR BRAF-DRIVEN CANCERS

Overview of MAPK pathway inhibitors

Following the identification of BRAF mutations in human cancer, researchers sought to determine whether these alterations confer sensitivity to pharmacological inhibition of the MAPK pathway. In 2006, Solit and colleagues analyzed a panel of melanoma cell lines that were either BRAFV600E mutant, NRASQ61R mutant, or RAS/RAF wild type (Solit et al., 2006). Cell lines were screened against the MEK1/2 inhibitor CI-1040, which reduced phosphorylation of ERK1/2 in all cell lines analyzed independent of mutation status (Sebolt-Leopold et al., 1999; Solit et al., 2006). Interestingly, the growth inhibitory effects of CI-1040 were much more dramatic in BRAFV600E mutant cell lines relative to NRASQ61R or wild type cell lines. Furthermore, the group determined that BRAFV600E mutant cell lines of other lineages were similarly sensitive to the BRAF mutant melanoma cell lines. MEK1/2 inhibition resulted in a decrease in expression of Cyclin D1 and an increase in expression of the tumor suppressor p27, which was followed by a decrease in RB phosphorylation and subsequent arrest in G1 (Solit et al., 2006). This finding indicated that BRAF mutant

cell lines are dependent on the MEK/ERK signaling axis for proliferation and that inhibition of this pathway can be used to selectively target BRAF mutant cancer cells.

Vemurafenib, an ATP-competitive inhibitor of BRAF-V600E, demonstrated strong preclinical antiproliferative effects on the BRAFV600E A375 melanoma cell line and, to a lesser extent, on several BRAF-V600E thyroid carcinoma cell lines (Sala et al., 2008). In A375 cells, vemurafenib induced a dose-dependent decrease in phosphorylation of MEK and a dose-dependent increase in caspase-3 activity and apoptosis. The thyroid carcinoma cell lines analyzed were resistant to vemurafenib-induced cell death (Sala et al., 2008). The antiproliferative effects of vemurafenib were further demonstrated by Yang et al. who analyzed the efficacy of vemurafenib in a panel of 32 cancer cell lines, many of which were BRAF mutant melanoma (Yang et al., 2010). Melanoma cell lines with V600E mutations or other V600 alterations exhibited increased sensitivity relative to wild type cell lines. Vemurafenib treatment decreased ERK1/2 phosphorylation and cyclin D1 expression, and also increased PARP cleavage in support of the anti-proliferative, as well as pro-apoptotic, effects of the drug. Additionally, vemurafenib treatment dramatically inhibited tumor growth and increased mouse survival in BRAF-V600E xenograft models. Furthermore, the plasma concentration of vemurafenib correlated with a decrease in tumor MEK and ERK phosphorylation, suggesting dose-dependent pathway inhibition *in vivo* (Yang et al., 2010).

Vemurafenib treatment in BRAF mutant melanoma cells was shown to activate the intrinsic apoptosis pathway (Beck et al., 2013). A decrease in ERK activation was accompanied by a decrease in the anti-apoptotic proteins BCL2 and MCL1, an increase in the pro-apoptotic BIM, and an increase in caspase cleavage. Vemurafenib also

increased cytosolic concentrations of calcium, triggering endoplasmic reticulum (ER) stress, PRKR-like ER kinase- (PERK)-mediated phosphorylation of eIF2α, and increased expression of activating transcription factor ATF4 (Beck et al., 2013).

A phase 1 clinical trial assessing vemurafenib's safety and efficacy for treatment of BRAF mutant, advanced melanoma showed a remarkable response rate of 81% when patients received a 960 mg oral dose every 12 hours (Flaherty et al., 2010). Analysis of ERK1/2 phosphorylation in pre- and post-treatment tumor biopsies revealed significant MAPK pathway inhibition (Bollag et al., 2010; Flaherty et al., 2010). Interestingly, changes in cytoplasmic, but not nuclear, ERK1/2 phosphorylation correlated with tumor regression (Bollag et al., 2010). Moreover, it was estimated that at least an 80% reduction in cytoplasmic ERK1/2 phosphorylation is necessary to achieve a response (Bollag et al., 2010). In 2011, vemurafenib produced impressive results in a phase 3 clinical trial analyzing its efficacy for treatment of metastatic melanoma, achieving a 48% response rate versus the 5% response rate achieved with the standard of care dacarbazine (Chapman et al., 2011). Unfortunately, despite experiencing an initial response, the majority of vemurafenib-treated patients would eventually experience disease relapse (McArthur et al., 2014). Similar efficacy was seen in clinical trials with another ATP-competitive BRAFV600E inhibitor dabrafenib (Hauschild et al., 2012).

An interesting side effect of BRAFV600E inhibitors is the development of benign skin lesions in sun-exposed areas (Chapman et al., 2011; Flaherty et al., 2010; Hauschild et al., 2012). These lesions are the result of vemurafenib-induced paradoxical MAPK pathway activation in keratinocytes expressing wild-type BRAF

(Bollag et al., 2010). In RAS mutant or BRAF/RAS wild-type cell lines, treatment with a BRAF inhibitor induces BRAF/CRAF and CRAF hetero- and homo-dimerization, respectively (Hatzivassiliou et al., 2010; Poulikakos et al., 2010). While vemurafenib binding inhibits the kinase activity of one RAF promoter, the drug induces dimerization and activation of a second RAF promoter, resulting in increased MAPK signaling and proliferation (Hatzivassiliou et al., 2010; Poulikakos et al., 2010). As a result of this finding, newer BRAF inhibitors that do not cause paradoxical RAF activation in BRAF wild-type cell have been developed (Zhang et al., 2015). The paradox-breaking inhibitors PLX7904 and PLX8394 selectively inhibit cells harboring BRAF mutations, but not cells that are RAS mutant or BRAF/RAS wild-type (Zhang et al., 2015). These drugs not only inhibit BRAF kinase activity, but also prevent BRAF homo-dimerization and hetero-dimerzation with CRAF or ARAF (Yao et al., 2019).

Trametinib is an allosteric, ATP noncompetitive potent inhibitor of MEK1/2 (Gilmartin et al., 2011). The drug binds a region adjacent to MEK's active site and inhibits MEK1/2 kinase activity, preventing MEK-mediated activation of ERK1/2 as well as blocking RAF phosphorylation of MEK1.(Gilmartin et al., 2011). Early preclinical studies with trametinib demonstrated powerful antitumor activity in several BRAF mutant xenograft models (Gilmartin et al., 2011). Trametinib treatment also effectively inhibited growth of KRAS mutant xenograft models, but did not induce tumor regression. Growth of BRAF/KRAS wild-type models was also inhibited by trametinib, albeit to a lesser extant than observed in BRAF or KRAS mutant models (Gilmartin et al., 2011).

In a phase 3 clinical trial, treatment of BRAF mutant melanoma patients with trametinib resulted in an increased response rate and improved progression free and

overall survival relative to treatment with dacarbazine or paclitaxel (Flaherty et al., 2012b). As a monotherapy, trametinib had a 22% response rate, worse than observed with single-agent vemurafenib or dabrafenib (Chapman et al., 2011; Flaherty et al., 2012b; Hauschild et al., 2012). Combining BRAF and MEK inhibitors was found to extend the duration of response in patients with BRAF mutant melanoma relative to BRAF inhibition as a monotherapy (Ascierto et al., 2016; Flaherty et al., 2012a; Long et al., 2014; Robert et al., 2015). BRAF/MEK inhibitor combination therapy also reduces the formation of paradoxical activation-induced benign nevi in melanoma patients (Paraiso et al., 2010). Two FDA-approved combinations are dabrafenib with trametinib and vemurafenib with cobimetinib; however, despite improving the progression-free and overall survival relative to monotherapy, most patients eventually succumb to their disease as a result of acquired resistance (Ascierto et al., 2016; Long et al., 2015; Robert et al., 2015).

Reactivation of MAPK signaling in BRAF and MEK inhibitor resistance

The development of secondary, activating mutations in RAS genes was one of the first described mechanisms of acquired resistance to BRAFV600E inhibitors. NRAS mutations, specifically, were identified in several melanoma cell lines with acquired vemurafenib resistance (**Figure 1.2**). These secondary NRAS mutations provide an alternative means of MAPK pathway activation and promote constitutive ERK1/2 phosphorylation, even in the presence of vemurafenib (Nazarian et al., 2010). Additionally, NRAS mutations were identified in biopsy samples from patients who acquired resistance to vemurafenib (Nazarian et al., 2010). Commonly observed mutations in NRAS associated with BRAF inhibitor resistance occur at amino acid

residue Q61 (Nazarian et al., 2010; Trunzer et al., 2013; Van Allen et al., 2014). This residue is frequently mutated in malignant melanoma and is mutually exclusive with BRAF mutations (Sensi et al., 2006). Activating mutations at this site abolish the intrinsic and GAP-mediated GTPase activity of RAS, resulting in an increase in active, GTP-bound RAS (Simanshu et al., 2017). Loss of negative regulation of RAS can also promote BRAF inhibitor resistance. Neurofibromin 1 (NF1) is a GTPase-activating protein that promotes hydrolysis of RAS-bound GTP, resulting in inactive, GDP-bound RAS (Hattori et al., 1992; Xu et al., 1990). A 2013 RNAi screen aimed at identifying genes whose loss of expression confer resistance to the vemurafenib analog-PLX4720 in the A375 melanoma cell line identified NF1 as the top hit (Whittaker et al., 2013). Loss of NF1 expression or loss-of-function mutations in NF1 resulted in dysregulation of RAS signaling, which permitted increased signaling through CRAF and subsequent reactivation of ERK1/2.

Aberrant splicing of BRAF transcripts is associated with acquired vemurafenib resistance in melanoma patients and cell lines (**Figure 1.2**) (Poulikakos et al., 2011). This alternative splicing yields BRAF isoforms lacking the regulatory RAS-binding domain, promoting enhanced dimerization in the absence of RAS activation (Poulikakos et al., 2011). Two studies reported BRAF splice variants in roughly 30% of melanomas with acquired resistance to vemurafenib or dabrafenib (Poulikakos et al., 2011; Rizos et al., 2014). Increased BRAF signaling via a copy number increase in BRAFV600E or increased CRAF protein expression can also promote acquired resistance to BRAF inhibitors (**Figure 1.2**) (Montagut et al., 2008; Shi et al., 2012).

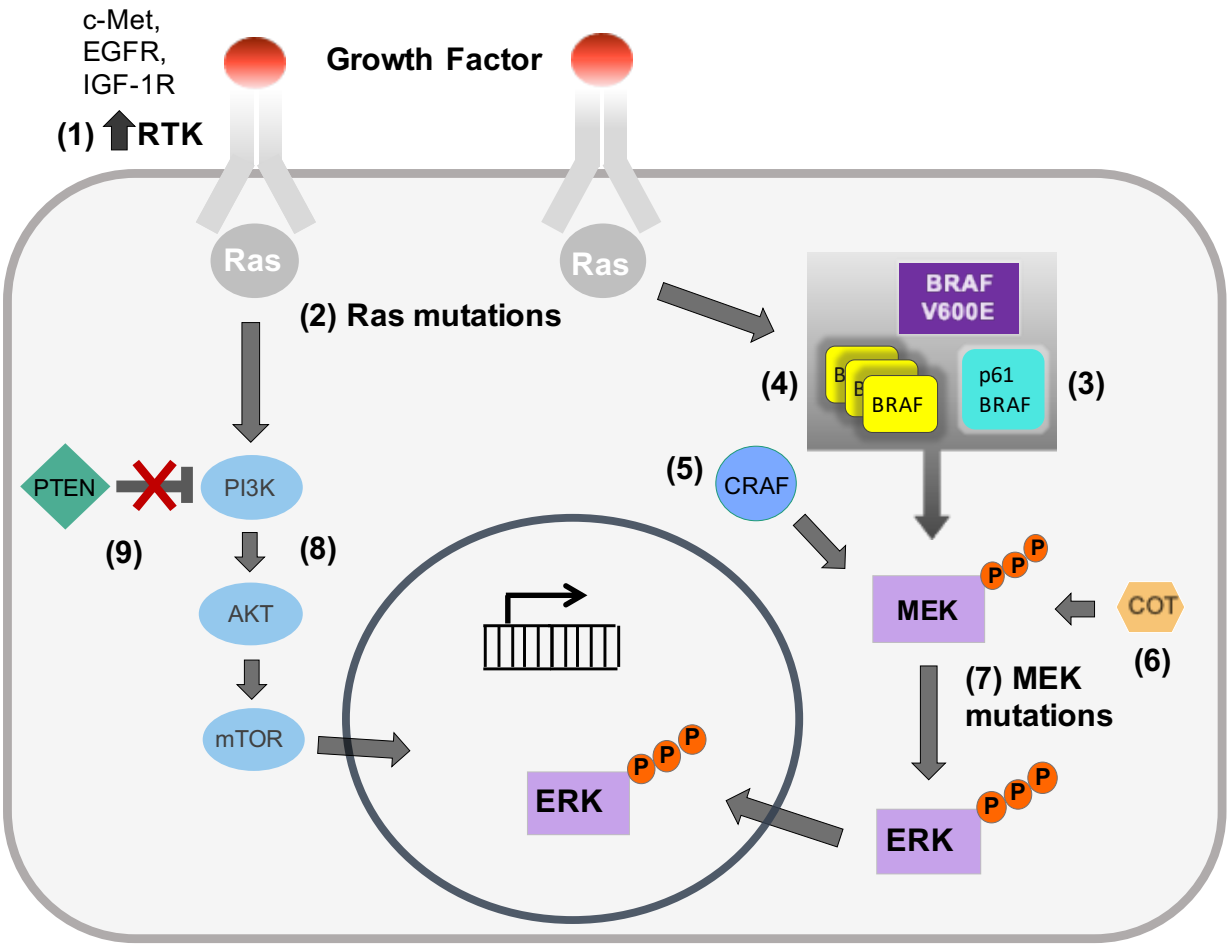

Figure 1.2. Resistance mechanisms to MAPK pathway inhibitors that have been identified in human cancer. 1 – RTK upregulation, 2 – RAS mutation, 3 – BRAF splice isoforms, 4 – BRAF amplification, 5 – Increased signaling through CRAF, 6 – MAPKKK upregulation, 7 – MEK mutations, 8 – Increased signaling through the PI3K/AKT signaling pathway, 9 – loss of PTEN expression or function.

A mutation in *MEK1* was identified in a patient with metastatic melanoma that had a significant clinical response to vemurafenib after 15 weeks on treatment but then rapidly progressed by 23 weeks (**Figure 1.2**) (Wagle et al., 2011). This mutation (C121S) causes an increase in the kinase activity of MEK1, resulting in increased basal activation of the MAPK pathway and rendering melanoma cells resistant to vemurafenib-induced suppression of ERK1/2 phosphorylation (Wagle et al., 2011).

Several other mutations in MEK1 and MEK2 have been identified in patients experiencing acquired resistance to BRAF inhibition (Emery et al., 2009; Rizos et al., 2014; Shi et al., 2014b; Trunzer et al., 2013). Increased expression of other kinases capable of activating MEK provides another means for cancer cells to bypass BRAF inhibition (**Figure 1.2**). COT, encoded by MAP3K8, is a MAPKKK whose overexpression confers resistance to vemurafenib in BRAF mutant melanoma (Johannessen et al., 2010). COT overexpression promotes constitutive phosphorylation of MEK and ERK, even in the presence of vemurafenib.

Increased activation of RTKs has been implicated in resistance to MAPK pathway inhibitors (**Figure 1.2**). Increased expression and activation of PDGFRβ was observed in vemurafenib-resistant melanoma cell lines and later identified in tumors from patients who developed resistance to vemurafenib in early clinical trials (Nazarian et al., 2010). Activation of the ErbB family of receptors is associated with resistance to BRAF inhibition in both melanoma and colorectal cancer. While BRAF-mutant melanomas often show an initial therapeutic response to BRAF inhibition followed by acquired resistance, BRAF-mutant colorectal tumors typically exhibit intrinsic resistance (Kopetz et al., 2015). A common mechanism of resistance in colorectal cancers involves activation of ErbB receptors. BRAF mutant colorectal cancer cell lines exhibit an initial reduction in ERK phosphorylation following treatment with vemurafenib, but fail to maintain this inhibition, showing a rapid rebound in ERK phosphorylation (Corcoran et al., 2012; Prahallad et al., 2012). These cell lines exhibited basal activation of EGFR and ERBB2 that permits increased signaling through RAS and CRAF. Furthermore, an RNAi screen in BRAF mutant colorectal cancer cell lines identified EGFR as a synthetic

lethal target in vemurafenib-treated cells (Prahallad et al., 2012). Increased EGFR expression has also been identified in several BRAF mutant melanoma patients following acquired resistance to BRAF and/or MEK inhibitors (Sun et al., 2014). The SOX10 transcription factor is a negative regulator of TGF-β-induced EGFR expression. Loss of SOX10 expression promotes increased EGFR expression, conferring a selective advantage to BRAF-mutant melanoma cells in the presence of vemurafenib (Sun et al., 2014).

Several mechanisms that promote BRAF inhibitor resistance also promote resistance to MEK inhibition. For instance, amplification of mutant BRAF can promote acquired resistance to the MEK1/2 inhibitor selumetinib in BRAF mutant colorectal cancer cell lines (Corcoran et al., 2010; Little et al., 2011). Similar results were seen in KRAS mutant colorectal cancer cell lines, where amplification of the mutant KRAS allele permitted increased MAPK pathway activation in the presence of selumetinib (Little et al., 2011). In both BRAF and KRAS mutant cases, selumetinib-resistant cell lines exhibited increased basal MEK and ERK activation relative to the parental cell lines and also expressed greater levels of cyclin D1 and AP-1 transcription factors (Little et al., 2011). A later study indicated that the amplification of mutant BRAF, but not mutant KRAS, and subsequent selumetinib resistance in colorectal cancer are reversible upon withdrawal of the inhibitor (Sale et al., 2019). Cells with BRAFV600E amplification were addicted to selumetinib such that inhibitor withdrawal resulted in ERK1/2 hyperactivation and cell cycle arrest or cell death. In contrast, selumetinib withdrawal in cells with KRASG13D amplification induced a ZEB1-dependent EMT (Sale et al., 2019).

Emery et al. performed a MEK1 random mutagenesis screen in BRAFV600E A375 melanoma cells to identify specific variants conferring resistance to the MEK inhibitor selumetinib (Emery et al., 2009). Several variants were identified within the selumetinib binding pocket or the nearby α-helix C, which were predicted to disrupt drug binding. Other variants conferring resistance were clustered at the regulatory N-terminal region of MEK1, disrupting MEK's intrinsic negative regulation (Emery et al., 2009). MEK1 mutations have also been identified in BRAF mutant colorectal cancer models of resistance to the MEK inhibitor RO4927350 (Wang et al., 2011). A variant at residue F129 within the drug binding pocket was found to elicit increased MEK1 intrinsic kinase activity as well as increased binding affinity to CRAF, collectively resulting in greater MEK1 activation (Wang et al., 2011). MEK mutations were also identified as mediators of acquired MEK inhibitor resistance in KRAS-mutant colorectal and breast cancer cell lines; however, these cell lines were sensitive to ERK inhibition, suggesting that they remained dependent on MAPK signaling (Hatzivassiliou et al., 2012).

ERK-independent mechanisms of resistance

Activation of the serine/threonine kinase AKT commonly occurs in cancer resulting in dysregulation of cell growth, survival, and metabolism (Hoxhaj and Manning, 2020). AKT activation occurs following conversion of phosphatidylinositol 4,5-bisphosphate (PIP_2) to phosphatidylinositol (3,4,5)-trisphosphate (PIP_3) by PI3K. Conversely inhibition of AKT signaling occurs via the PTEN tumor suppressor that catalyzes the reverse reaction from PIP_3 to PIP_2 (Hoxhaj and Manning, 2020). BRAF mutant melanoma cell lines that lack PTEN expression were identified as more resistant to apoptosis following treatment with the BRAF inhibitor PLX4720 relative to cell lines

with intact PTEN expression (**Figure 1.2**) (Paraiso et al., 2011). BRAF inhibition resulted in increased AKT phosphorylation in PTEN-negative cell lines, but not PTEN-positive lines, which suppressed expression of the pro-apoptotic BIM (Paraiso et al., 2011). Melanoma cell lines with acquired resistance to BRAF inhibition also exhibited increased phosphorylation and expression of insulin-like growth factor 1 receptor (IGF-1R), which also contributed to increased AKT activation and pro-survival signaling (Paraiso et al., 2011).

A 2014 genomic analysis of melanoma tumors exhibiting acquired resistance to vemurafenib or dabrafenib identified several alterations associated with reactivation of the MAPK pathway or increased signaling through the PI3K/AKT pathway (Shi et al., 2014b). Half of the resistant tumors harbored alterations in only the MAPK pathway, 4% had alterations in just the PI3K/AKT pathway, and 18% harbored alteration in both MAPK and PI3K/AKT. The most common alterations within the MAPK pathway were secondary mutations in NRAS/KRAS, amplification of mutant BRAF, and alternative splicing of BRAF. Alterations in the AKT pathway occurred in genes encoding both positive and negative regulators of the AKT signaling including activating mutations in PIK3CA encoding p110, the catalytic subunit of PI3K, and mutations in AKT1/3. Loss-of-function mutations occurred in genes encoding negative regulators p85β and PHLPP1, which inhibit p110 and AKT, respectively. Deletions and inactivating mutations in PTEN were also identified (Shi et al., 2014b). Activating mutations in AKT1 that increase its association with membrane-bound PIP_3 have also been associated with BRAF inhibitor resistance (Shi et al., 2014a; Shi et al., 2014b).

Expression of Wnt family member 5A (WNT5A) is elevated in melanoma patients and cell lines that are resistant to BRAF inhibition (Anastas et al., 2014). This alteration promotes increased signaling through the Wnt receptor frizzled class receptor 7 (FZD7) and receptor-like tyrosine kinase (RYK), resulting in increased AKT activation and increased tumor growth and resistance to BRAF inhibitors (Anastas et al., 2014). Hepatocyte growth factor (HGF) secretion by cancer-associated stromal cells has been implicated in AKT-mediated resistance to BRAF inhibition in melanoma. In these instances, increased HGF in the tumor microenvironment activates the RTK MET, resulting in increased signaling through both MAPK and PI3K/AKT signaling pathways (Straussman et al., 2012; Wilson et al., 2012). Phosphorylation of BAD occurs as a downstream event of signaling through AKT and, to a lesser extent, ERK, preventing BAD's inhibition of the anti-apoptotic BCL2 and BCL2L1. HGF-mediated resistance to BRAF inhibitors has also been attributed to an increased in BAD phosphorylation, promoting evasion of apoptosis (Perna et al., 2015).

The EMT transcription factor ZEB1 was implicated in resistance, both intrinsic and acquired, to BRAF and MEK inhibitors in BRAF-mutant melanoma (Richard et al., 2016). High basal levels of ZEB1 in melanoma patients correlated with a lack of response to vemurafenib alone or in combination cobimetinib. Additionally, cell lines and patients with acquired resistance to vemurafenib displayed increased ZEB1 expression relative to parental cell lines and pre-treatment biopsies, respectively. Overexpression of ZEB1 in A375 melanoma cells conferred resistance to vemurafenib and cobimetinib, in addition to inducing a "stem-like" phenotype marked by decreased expression of lineage-specific transcription factor MITF (Richard et al., 2016). Indeed,

melanoma patients and cell lines with intrinsic resistance in BRAF and MEK inhibition exhibit decreased expression of MITF and its transcriptional targets relative to sensitive patients and cell lines (Konieczkowski et al., 2014).

Corazao-Rozas et al. demonstrated increased oxygen consumption and reactive oxygen species (ROS) production in vemurafenib-treated BRAF mutant melanoma cells. The group generated vemurafenib-resistant cell lines and observed increased basal and maximal mitochondrial oxygen consumption rates (OCR), as well as greater ROS production, relative to the respective parental cell lines. In this instance, the increased ROS production in resistant cell lines begets a vulnerability to additional oxidative stress (Corazao-Rozas et al., 2013). Treatment of BRAF mutant melanoma with vemurafenib also increases levels of PGC-1α, promoting mitochondrial biogenesis and a shift from aerobic glycoloysis towards OxPhos (Haq et al., 2013).

Gopal et al. observed similar results, identifying increased mitochondrial OxPhos as a mediator of both intrinsic and acquired resistance to selumetinib in BRAF and NRAS mutant melanoma cell lines. Resistant cell lines exhibited increased basal and maximal OCR relative to sensitive lines (Gopal et al., 2014). MEK inhibition increased MITF-induced expression of PGC-1α, resulting in increased OxPhos. Conversely, mTORC1/2 inhibition promoted nuclear exclusion of MITF, resulting in decreased PGC-1α expression and OxPhos. Combined MEK and mTORC1/2 inhibition was synergistic in selumetinib-resistant cell lines with high OxPhos (Gopal et al., 2014). This group later highlighted the therapeutic potential of targeting OxPhos in MAPK inhibitor-resistant, BRAF mutant melanoma models with high basal OxPhos (Vashisht Gopal et al., 2019). The OxPhos inhibitor IACS-010759 (OPi), which inhibits Complex I of the

electron transport chain, significantly inhibited *in vivo* growth of MAPKi-resistant melanomas as a single agent; however, no additional benefit was achieved when combining OPi with either a BRAF or MEK inhibitor (Molina et al., 2018; Vashisht Gopal et al., 2019). Mechanistically, OxPhos inhibition resulted in activation of AMPK, a negative regulator of ERK1/2 and mTORC1, contributing to growth inhibition (Vashisht Gopal et al., 2019).

Melanoma cell lines with decreased basal mitochondrial biogenesis and mass are more intrinsically resistant to BRAF and MEK inhibitors and rely more heavily on OxPhos to meet their energetic needs, rendering them sensitive to disruption of mitochondrial biogenesis with the HSP90 inhibitor gamitrinib (Zhang et al., 2016). Intrinsic resistance to the BRAF inhibitor PLX4720 can be overcome by knockdown of PDH inhibitor PDK1 and subsequent entry into the TCA cycle (Kaplon et al., 2013). Similarly, melanoma cells exhibiting acquired vemurafenib resistance as a result of oncogenic NRAS expression can be re-sensitized to vemurafenib following treatment with the PDK inhibitor dichloroacetate (Parmenter et al., 2014). In conclusion, the means by which cancer cells are able to adapt to MAPK are incredibly diverse, and serve as the motivation for identifying novel combination therapies that may delay or prevent the onset of resistance.

PROJECT RATIONALE

Cancer is the second leading cause of death in the United States. Advancements in cancer diagnostics and treatment, as well as lifestyle changes, have

improved cancer survival rates. A major roadblock to cancer therapy is the inefficiency of anticancer drug development, where 95% of therapeutic agents that enter phase 1 clinical trials fail due to toxicity or a lack of efficacy. While mouse models have been indispensable in the preclinical evaluation of novel cancer therapeutics, they remain poor predictors of drug efficacy or toxicity. Comparative oncology clinical trials aim to partially remedy this issue by serving as an intermediate step between preclinical murine evaluation and human clinical trials. The overarching goal of this dissertation was to investigate the translational potential of canine bladder cancer, or canine transitional cell carcinoma (cTCC), for informing treatment for human cancer using targeted and immune-based therapies.

As highlighted earlier in this chapter, cTCC is highly similar to human muscle-invasive TCC in clinical presentation, risk factors, and histological features. While the molecular biology of human TCC has been extensively characterized, that of cTCC remains poorly defined. We hypothesized that the molecular and immune landscapes of cTCC are similar to that of human muscle-invasive TCC. We tested our hypothesis in Chapter 2 (A Molecular and Immune Characterization of Canine Bladder Cancer), where we performed whole exome sequencing (WES) and RNA sequencing (RNA-Seq) on a panel of 11 cTCC tumors. Four out of 11 tumors harbored V-to-E missense mutations in BRAF, a proto-oncogene within the MAPK signaling pathway, as detected by WES. Sanger sequencing identified BRAF mutations in 8 out of the same 11 cTCC tumors as well as in 22 out of 32 formalin-fixed paraffin-embedded cTCC samples, indicating a prevalence of 70%. Analysis of RNA-Seq gene expression data identified a

subset of four immunologically hot tumors exhibiting high expression of gene signatures associated with complete response to PD-1/PD-L1 blockade.

Based on the findings of Chapter 2, we wanted to further explore BRAF as a possible therapeutic target for cTCC. As described earlier in Chapter 1, BRAF mutations are drivers of oncogenesis in human melanoma as well as in thyroid and colorectal carcinomas. Furthermore, small molecule inhibitors targeting BRAF or its downstream target MEK show initial promise in treating BRAF mutant melanoma; however, approximately half of patients experience disease relapse. BRAF mutant colorectal carcinoma patients are typically intrinsically resistant. Our aim was to determine whether the MAPK pathway is a targetable vulnerability for BRAF mutant cTCC and whether cTCC may serve as a translational model for human MAPK-driven cancers.

To address these possibilities, we performed an *in vitro* characterization of three BRAF mutant and two BRAF wild type cTCC cell lines, as well as four BRAF mutant human cancer cell lines with varying degrees of sensitivity to MAPK pathway-targeted agents. We hypothesized that BRAF mutant cTCC cell lines would exhibit constitutive MAPK pathway activation and would be similar to human BRAF mutant cancer cell lines with regards to sensitivity to BRAF- and MEK-targeted agents. This hypothesis was tested in Chapter 3 (Identifying the ErbB/MAPK Signaling Cascade as a Therapeutic Target in Canine Bladder Cancer). We identified constitutive MAPK signaling in all five cTCC cell lines analyzed, independent of BRAF mutation status. BRAF mutant and wild type cTCC cell lines were highly sensitive to the MEK inhibitor trametinib. Canine and human BRAF mutant cell lines were sensitive to the third-generation BRAF inhibitor

PLX7904. However, most cell lines exhibited MAPK pathway reactivation after 24-hour treatments with BRAF or MEK inhibitors. ErbB receptor (EGFR, ERBB2, and ERBB3) inhibition synergized with BRAF inhibition in a BRAF mutant cTCC cell line and synergized with MEK inhibition in both a BRAF mutant and a BRAF wild type cTCC cell line.

The high degree of cTCC cell line sensitivity to the MEK inhibitor trametinib, combined with the ability of most cTCC lines to bypass MEK inhibition and reactivate downstream ERK, led us to hypothesize that cTCC may be a translational model for interrogating mechanisms of acquired resistance to trametinib. We tested this hypothesis in Chapter 4 (Characterizing a Canine Model of Acquired Trametinib Resistance). Following nine months of exposure to trametinib, six trametinib-resistant (TramR) clones were generated from the BRAF mutant Tyler1 cTCC cell line. TramR clones were insensitive to the ERK inhibitor ravoxertinib and did not reactivate ERK in the presence of trametinib, suggesting an ERK-independent mechanism of resistance. TramR clones exhibited upregulation of EMT gene markers and altered morphology relative to parental Tyler1 cells. Finally, one clone exhibited decreased oxidative metabolism relative to the parental cell line. As highlighted earlier in Chapter 1, EMT and alterations in cellular metabolism have been associated with resistance to MAPK-targeted agents in various models of human BRAF mutant cancer. Overall, the findings of Chapter 4 suggest that long-term exposure to trametinib would likely result in acquired resistance in BRAF mutant cTCC patients and that this model may be used to identify MAPK inhibitor resistance mechanisms and putative combination therapies that may aid in the treatment of canine and human BRAF mutant cancers.

REFERENCES

Abbosh PH and Plimack ER (2018) Molecular and Clinical Insights into the Role and Significance of Mutated DNA Repair Genes in Bladder Cancer. *Bladder Cancer* **4**(1): 9-18.

Aboulkassim TO, LaRue H, Lemieux P, Rousseau F and Fradet Y (2003) Alteration of the PATCHED locus in superficial bladder cancer. *Oncogene* **22**(19): 2967-2971.

Abraham D, Podar K, Pacher M, Kubicek M, Welzel N, Hemmings BA, Dilworth SM, Mischak H, Kolch W and Baccarini M (2000) Raf-1-associated protein phosphatase 2A as a positive regulator of kinase activation. *J Biol Chem* **275**(29): 22300-22304.

Allemani C, Matsuda T, Di Carlo V, Harewood R, Matz M, Niksic M, Bonaventure A, Valkov M, Johnson CJ, Esteve J, Ogunbiyi OJ, Azevedo ESG, Chen WQ, Eser S, Engholm G, Stiller CA, Monnereau A, Woods RR, Visser O, Lim GH, Aitken J, Weir HK, Coleman MP and Group CW (2018) Global surveillance of trends in cancer survival 2000-14 (CONCORD-3): analysis of individual records for 37 513 025 patients diagnosed with one of 18 cancers from 322 population-based registries in 71 countries. *Lancet* **391**(10125): 1023-1075.

Amati B, Brooks MW, Levy N, Littlewood TD, Evan GI and Land H (1993) Oncogenic activity of the c-Myc protein requires dimerization with Max. *Cell* **72**(2): 233-245.

Anastas JN, Kulikauskas RM, Tamir T, Rizos H, Long GV, von Euw EM, Yang PT, Chen HW, Haydu L, Toroni RA, Lucero OM, Chien AJ and Moon RT (2014) WNT5A enhances resistance of melanoma cells to targeted BRAF inhibitors. *J Clin Invest* **124**(7): 2877-2890.

Ascierto PA, McArthur GA, Dreno B, Atkinson V, Liszkay G, Di Giacomo AM, Mandala M, Demidov L, Stroyakovskiy D, Thomas L, de la Cruz-Merino L, Dutriaux C, Garbe C, Yan Y, Wongchenko M, Chang I, Hsu JJ, Koralek DO, Rooney I, Ribas A and Larkin J (2016) Cobimetinib combined with vemurafenib in advanced BRAF(V600)-mutant melanoma (coBRIM): updated efficacy results from a randomised, double-blind, phase 3 trial. *Lancet Oncol* **17**(9): 1248-1260.

Atlas TCG (2014) Comprehensive molecular characterization of urothelial bladder carcinoma. *Nature* **507**(7492): 315-322.

Ayer DE, Kretzner L and Eisenman RN (1993) Mad: a heterodimeric partner for Max that antagonizes Myc transcriptional activity. *Cell* **72**(2): 211-222.

Babjuk M, Burger M, Comperat EM, Gontero P, Mostafid AH, Palou J, van Rhijn BWG, Roupret M, Shariat SF, Sylvester R, Zigeuner R, Capoun O, Cohen D, Escrig JLD, Hernandez V, Peyronnet B, Seisen T and Soukup V (2019) European

Association of Urology Guidelines on Non-muscle-invasive Bladder Cancer (TaT1 and Carcinoma In Situ) - 2019 Update. *Eur Urol* **76**(5): 639-657.

Bakkar AA, Wallerand H, Radvanyi F, Lahaye JB, Pissard S, Lecerf L, Kouyoumdjian JC, Abbou CC, Pairon JC, Jaurand MC, Thiery JP, Chopin DK and de Medina SG (2003) FGFR3 and TP53 gene mutations define two distinct pathways in urothelial cell carcinoma of the bladder. *Cancer Res* **63**(23): 8108-8112.

Baljuls A, Schmitz W, Mueller T, Zahedi RP, Sickmann A, Hekman M and Rapp UR (2008) Positive regulation of A-RAF by phosphorylation of isoform-specific hinge segment and identification of novel phosphorylation sites. *J Biol Chem* **283**(40): 27239-27254.

Balmanno K and Cook SJ (1999) Sustained MAP kinase activation is required for the expression of cyclin D1, p21Cip1 and a subset of AP-1 proteins in CCL39 cells. *Oncogene* **18**(20): 3085-3097.

Beck D, Niessner H, Smalley KS, Flaherty K, Paraiso KH, Busch C, Sinnberg T, Vasseur S, Iovanna JL, Driessen S, Stork B, Wesselborg S, Schaller M, Biedermann T, Bauer J, Lasithiotakis K, Weide B, Eberle J, Schittek B, Schadendorf D, Garbe C, Kulms D and Meier F (2013) Vemurafenib potently induces endoplasmic reticulum stress-mediated apoptosis in BRAFV600E melanoma cells. *Sci Signal* **6**(260): ra7.

Bhatt KV, Spofford LS, Aram G, McMullen M, Pumiglia K and Aplin AE (2005) Adhesion control of cyclin D1 and p27Kip1 levels is deregulated in melanoma cells through BRAF-MEK-ERK signaling. *Oncogene* **24**(21): 3459-3471.

Billerey C, Chopin D, Aubriot-Lorton MH, Ricol D, Gil Diez de Medina S, Van Rhijn B, Bralet MP, Lefrere-Belda MA, Lahaye JB, Abbou CC, Bonaventure J, Zafrani ES, van der Kwast T, Thiery JP and Radvanyi F (2001) Frequent FGFR3 mutations in papillary non-invasive bladder (pTa) tumors. *Am J Pathol* **158**(6): 1955-1959.

Blackwood EM and Eisenman RN (1991) Max: a helix-loop-helix zipper protein that forms a sequence-specific DNA-binding complex with Myc. *Science* **251**(4998): 1211-1217.

Boisvert-Adamo K and Aplin AE (2008) Mutant B-RAF mediates resistance to anoikis via Bad and Bim. *Oncogene* **27**(23): 3301-3312.

Bollag G, Hirth P, Tsai J, Zhang J, Ibrahim PN, Cho H, Spevak W, Zhang C, Zhang Y, Habets G, Burton EA, Wong B, Tsang G, West BL, Powell B, Shellooe R, Marimuthu A, Nguyen H, Zhang KY, Artis DR, Schlessinger J, Su F, Higgins B, Iyer R, D'Andrea K, Koehler A, Stumm M, Lin PS, Lee RJ, Grippo J, Puzanov I, Kim KB, Ribas A, McArthur GA, Sosman JA, Chapman PB, Flaherty KT, Xu X, Nathanson KL and Nolop K (2010) Clinical efficacy of a RAF inhibitor needs broad target blockade in BRAF-mutant melanoma. *Nature* **467**(7315): 596-599.

Bonner T, O'Brien SJ, Nash WG, Rapp UR, Morton CC and Leder P (1984) The human homologs of the raf (mil) oncogene are located on human chromosomes 3 and 4. *Science* **223**(4631): 71-74.

Bonner TI, Kerby SB, Sutrave P, Gunnell MA, Mark G and Rapp UR (1985) Structure and biological activity of human homologs of the raf/mil oncogene. *Mol Cell Biol* **5**(6): 1400-1407.

Bouchard C, Thieke K, Maier A, Saffrich R, Hanley-Hyde J, Ansorge W, Reed S, Sicinski P, Bartek J and Eilers M (1999) Direct induction of cyclin D2 by Myc contributes to cell cycle progression and sequestration of p27. *EMBO J* **18**(19): 5321-5333.

Brierley JD (2017) *TNM Classification of Malignant Tumors*. 8 ed. John Wiley & Sons, Incorperated.

Brinckerhoff CE, Rutter JL and Benbow U (2000) Interstitial collagenases as markers of tumor progression. *Clin Cancer Res* **6**(12): 4823-4830.

Bryan JN, Keeler MR, Henry CJ, Bryan ME, Hahn AW and Caldwell CW (2007) A population study of neutering status as a risk factor for canine prostate cancer. *Prostate* **67**(11): 1174-1181.

Buday L and Downward J (1993) Epidermal growth factor regulates p21ras through the formation of a complex of receptor, Grb2 adapter protein, and Sos nucleotide exchange factor. *Cell* **73**(3): 611-620.

Burger M, Catto JW, Dalbagni G, Grossman HB, Herr H, Karakiewicz P, Kassouf W, Kiemeney LA, La Vecchia C, Shariat S and Lotan Y (2013) Epidemiology and risk factors of urothelial bladder cancer. *Eur Urol* **63**(2): 234-241.

Burger M, van der Aa MN, van Oers JM, Brinkmann A, van der Kwast TH, Steyerberg EC, Stoehr R, Kirkels WJ, Denzinger S, Wild PJ, Wieland WF, Hofstaedter F, Hartmann A and Zwarthoff EC (2008) Prediction of progression of non-muscle-invasive bladder cancer by WHO 1973 and 2004 grading and by FGFR3 mutation status: a prospective study. *Eur Urol* **54**(4): 835-843.

Cairns P, Shaw ME and Knowles MA (1993) Initiation of bladder cancer may involve deletion of a tumour-suppressor gene on chromosome 9. *Oncogene* **8**(4): 1083-1085.

Cappellen D, De Oliveira C, Ricol D, de Medina S, Bourdin J, Sastre-Garau X, Chopin D, Thiery JP and Radvanyi F (1999) Frequent activating mutations of FGFR3 in human bladder and cervix carcinomas. *Nat Genet* **23**(1): 18-20.

Caramel J, Papadogeorgakis E, Hill L, Browne GJ, Richard G, Wierinckx A, Saldanha G, Osborne J, Hutchinson P, Tse G, Lachuer J, Puisieux A, Pringle JH, Ansieau S and Tulchinsky E (2013) A switch in the expression of embryonic EMT-

inducers drives the development of malignant melanoma. *Cancer Cell* **24**(4): 466-480.

Cartlidge RA, Thomas GR, Cagnol S, Jong KA, Molton SA, Finch AJ and McMahon M (2008) Oncogenic BRAF(V600E) inhibits BIM expression to promote melanoma cell survival. *Pigment Cell Melanoma Res* **21**(5): 534-544.

Catto JW, Miah S, Owen HC, Bryant H, Myers K, Dudziec E, Larre S, Milo M, Rehman I, Rosario DJ, Di Martino E, Knowles MA, Meuth M, Harris AL and Hamdy FC (2009) Distinct microRNA alterations characterize high- and low-grade bladder cancer. *Cancer Res* **69**(21): 8472-8481.

Chapman PB, Hauschild A, Robert C, Haanen JB, Ascierto P, Larkin J, Dummer R, Garbe C, Testori A, Maio M, Hogg D, Lorigan P, Lebbe C, Jouary T, Schadendorf D, Ribas A, O'Day SJ, Sosman JA, Kirkwood JM, Eggermont AM, Dreno B, Nolop K, Li J, Nelson B, Hou J, Lee RJ, Flaherty KT, McArthur GA and Group B-S (2011) Improved survival with vemurafenib in melanoma with BRAF V600E mutation. *N Engl J Med* **364**(26): 2507-2516.

Chardin P, Camonis JH, Gale NW, van Aelst L, Schlessinger J, Wigler MH and Bar-Sagi D (1993) Human Sos1: a guanine nucleotide exchange factor for Ras that binds to GRB2. *Science* **260**(5112): 1338-1343.

Chawla SP, Staddon AP, Baker LH, Schuetze SM, Tolcher AW, D'Amato GZ, Blay JY, Mita MM, Sankhala KK, Berk L, Rivera VM, Clackson T, Loewy JW, Haluska FG and Demetri GD (2012) Phase II study of the mammalian target of rapamycin inhibitor ridaforolimus in patients with advanced bone and soft tissue sarcomas. *J Clin Oncol* **30**(1): 78-84.

Chen RH, Sarnecki C and Blenis J (1992) Nuclear localization and regulation of erk- and rsk-encoded protein kinases. *Mol Cell Biol* **12**(3): 915-927.

Choi W, Porten S, Kim S, Willis D, Plimack ER, Hoffman-Censits J, Roth B, Cheng T, Tran M, Lee IL, Melquist J, Bondaruk J, Majewski T, Zhang S, Pretzsch S, Baggerly K, Siefker-Radtke A, Czerniak B, Dinney CP and McConkey DJ (2014) Identification of distinct basal and luminal subtypes of muscle-invasive bladder cancer with different sensitivities to frontline chemotherapy. *Cancer Cell* **25**(2): 152-165.

Chong H, Lee J and Guan KL (2001) Positive and negative regulation of Raf kinase activity and function by phosphorylation. *EMBO J* **20**(14): 3716-3727.

Chuang E, Barnard D, Hettich L, Zhang XF, Avruch J and Marshall MS (1994) Critical binding and regulatory interactions between Ras and Raf occur through a small, stable N-terminal domain of Raf and specific Ras effector residues. *Mol Cell Biol* **14**(8): 5318-5325.

Collisson EA, De A, Suzuki H, Gambhir SS and Kolodney MS (2003) Treatment of metastatic melanoma with an orally available inhibitor of the Ras-Raf-MAPK cascade. *Cancer Res* **63**(18): 5669-5673.

Cook SJ, Stuart K, Gilley R and Sale MJ (2017) Control of cell death and mitochondrial fission by ERK1/2 MAP kinase signalling. *FEBS J* **284**(24): 4177-4195.

Cooper JA, Bowen-Pope DF, Raines E, Ross R and Hunter T (1982) Similar effects of platelet-derived growth factor and epidermal growth factor on the phosphorylation of tyrosine in cellular proteins. *Cell* **31**(1): 263-273.

Cooper JA and Hunter T (1981) Changes in protein phosphorylation in Rous sarcoma virus-transformed chicken embryo cells. *Mol Cell Biol* **1**(2): 165-178.

Cooper JA, Sefton BM and Hunter T (1984) Diverse mitogenic agents induce the phosphorylation of two related 42,000-dalton proteins on tyrosine in quiescent chick cells. *Mol Cell Biol* **4**(1): 30-37.

Corazao-Rozas P, Guerreschi P, Jendoubi M, Andre F, Jonneaux A, Scalbert C, Garcon G, Malet-Martino M, Balayssac S, Rocchi S, Savina A, Formstecher P, Mortier L, Kluza J and Marchetti P (2013) Mitochondrial oxidative stress is the Achille's heel of melanoma cells resistant to Braf-mutant inhibitor. *Oncotarget* **4**(11): 1986-1998.

Corcoran RB, Dias-Santagata D, Bergethon K, Iafrate AJ, Settleman J and Engelman JA (2010) BRAF gene amplification can promote acquired resistance to MEK inhibitors in cancer cells harboring the BRAF V600E mutation. *Sci Signal* **3**(149): ra84.

Corcoran RB, Ebi H, Turke AB, Coffee EM, Nishino M, Cogdill AP, Brown RD, Della Pelle P, Dias-Santagata D, Hung KE, Flaherty KT, Piris A, Wargo JA, Settleman J, Mino-Kenudson M and Engelman JA (2012) EGFR-mediated re-activation of MAPK signaling contributes to insensitivity of BRAF mutant colorectal cancers to RAF inhibition with vemurafenib. *Cancer Discov* **2**(3): 227-235.

Crews CM and Erikson RL (1992) Purification of a murine protein-tyrosine/threonine kinase that phosphorylates and activates the Erk-1 gene product: relationship to the fission yeast byr1 gene product. *Proc Natl Acad Sci U S A* **89**(17): 8205-8209.

Cutler RE, Jr., Stephens RM, Saracino MR and Morrison DK (1998) Autoregulation of the Raf-1 serine/threonine kinase. *Proc Natl Acad Sci U S A* **95**(16): 9214-9219.

Davies H, Bignell GR, Cox C, Stephens P, Edkins S, Clegg S, Teague J, Woffendin H, Garnett MJ, Bottomley W, Davis N, Dicks E, Ewing R, Floyd Y, Gray K, Hall S, Hawes R, Hughes J, Kosmidou V, Menzies A, Mould C, Parker A, Stevens C, Watt S, Hooper S, Wilson R, Jayatilake H, Gusterson BA, Cooper C, Shipley J, Hargrave D, Pritchard-Jones K, Maitland N, Chenevix-Trench G, Riggins GJ,

Bigner DD, Palmieri G, Cossu A, Flanagan A, Nicholson A, Ho JW, Leung SY, Yuen ST, Weber BL, Seigler HF, Darrow TL, Paterson H, Marais R, Marshall CJ, Wooster R, Stratton MR and Futreal PA (2002) Mutations of the BRAF gene in human cancer. *Nature* **417**(6892): 949-954.

Day CP, Merlino G and Van Dyke T (2015) Preclinical mouse cancer models: a maze of opportunities and challenges. *Cell* **163**(1): 39-53.

Decker B, Parker HG, Dhawan D, Kwon EM, Karlins E, Davis BW, Ramos-Vara JA, Bonney PL, McNiel EA, Knapp DW and Ostrander EA (2015) Homologous Mutation to Human BRAF V600E Is Common in Naturally Occurring Canine Bladder Cancer--Evidence for a Relevant Model System and Urine-Based Diagnostic Test. *Mol Cancer Res* **13**(6): 993-1002.

Dhawan D, Hahn NM, Ramos-Vara JA and Knapp DW (2018) Naturally-occurring canine invasive urothelial carcinoma harbors luminal and basal transcriptional subtypes found in human muscle invasive bladder cancer. *PLoS Genet* **14**(8): e1007571.

di Martino E, L'Hote CG, Kennedy W, Tomlinson DC and Knowles MA (2009) Mutant fibroblast growth factor receptor 3 induces intracellular signaling and cellular transformation in a cell type- and mutation-specific manner. *Oncogene* **28**(48): 4306-4316.

Dobson JM, Samuel S, Milstein H, Rogers K and Wood JL (2002) Canine neoplasia in the UK: estimates of incidence rates from a population of insured dogs. *J Small Anim Pract* **43**(6): 240-246.

Downward J (1990) The ras superfamily of small GTP-binding proteins. *Trends Biochem Sci* **15**(12): 469-472.

Emery CM, Vijayendran KG, Zipser MC, Sawyer AM, Niu L, Kim JJ, Hatton C, Chopra R, Oberholzer PA, Karpova MB, MacConaill LE, Zhang J, Gray NS, Sellers WR, Dummer R and Garraway LA (2009) MEK1 mutations confer resistance to MEK and B-RAF inhibition. *Proc Natl Acad Sci U S A* **106**(48): 20411-20416.

Erhardt P, Schremser EJ and Cooper GM (1999) B-Raf inhibits programmed cell death downstream of cytochrome c release from mitochondria by activating the MEK/Erk pathway. *Mol Cell Biol* **19**(8): 5308-5315.

Erikson RL (1991) Structure, expression, and regulation of protein kinases involved in the phosphorylation of ribosomal protein S6. *J Biol Chem* **266**(10): 6007-6010.

Ewen ME, Sluss HK, Sherr CJ, Matsushime H, Kato J and Livingston DM (1993) Functional interactions of the retinoblastoma protein with mammalian D-type cyclins. *Cell* **73**(3): 487-497.

Ezhevsky SA, Nagahara H, Vocero-Akbani AM, Gius DR, Wei MC and Dowdy SF (1997) Hypo-phosphorylation of the retinoblastoma protein (pRb) by cyclin D:Cdk4/6 complexes results in active pRb. *Proc Natl Acad Sci U S A* **94**(20): 10699-10704.

Farrar MA, Alberol-Ila J and Perlmutter RM (1996) Activation of the Raf-1 kinase cascade by coumermycin-induced dimerization. *Nature* **383**(6596): 178-181.

Fenger JM, London CA and Kisseberth WC (2014) Canine osteosarcoma: a naturally occurring disease to inform pediatric oncology. *ILAR J* **55**(1): 69-85.

Fernandez PC, Frank SR, Wang L, Schroeder M, Liu S, Greene J, Cocito A and Amati B (2003) Genomic targets of the human c-Myc protein. *Genes Dev* **17**(9): 1115-1129.

Flaherty KT, Infante JR, Daud A, Gonzalez R, Kefford RF, Sosman J, Hamid O, Schuchter L, Cebon J, Ibrahim N, Kudchadkar R, Burris HA, 3rd, Falchook G, Algazi A, Lewis K, Long GV, Puzanov I, Lebowitz P, Singh A, Little S, Sun P, Allred A, Ouellet D, Kim KB, Patel K and Weber J (2012a) Combined BRAF and MEK inhibition in melanoma with BRAF V600 mutations. *N Engl J Med* **367**(18): 1694-1703.

Flaherty KT, Puzanov I, Kim KB, Ribas A, McArthur GA, Sosman JA, O'Dwyer PJ, Lee RJ, Grippo JF, Nolop K and Chapman PB (2010) Inhibition of mutated, activated BRAF in metastatic melanoma. *N Engl J Med* **363**(9): 809-819.

Flaherty KT, Robert C, Hersey P, Nathan P, Garbe C, Milhem M, Demidov LV, Hassel JC, Rutkowski P, Mohr P, Dummer R, Trefzer U, Larkin JM, Utikal J, Dreno B, Nyakas M, Middleton MR, Becker JC, Casey M, Sherman LJ, Wu FS, Ouellet D, Martin AM, Patel K, Schadendorf D and Group MS (2012b) Improved survival with MEK inhibition in BRAF-mutated melanoma. *N Engl J Med* **367**(2): 107-114.

Freedman ND, Silverman DT, Hollenbeck AR, Schatzkin A and Abnet CC (2011) Association between smoking and risk of bladder cancer among men and women. *JAMA* **306**(7): 737-745.

Fujimoto K, Yamada Y, Okajima E, Kakizoe T, Sasaki H, Sugimura T and Terada M (1992) Frequent association of p53 gene mutation in invasive bladder cancer. *Cancer Res* **52**(6): 1393-1398.

Fukui M, Yamamoto T, Kawai S, Mitsunobu F and Toyoshima K (1987) Molecular cloning and characterization of an activated human c-raf-1 gene. *Mol Cell Biol* **7**(5): 1776-1781.

Fukunaga R and Hunter T (1997) MNK1, a new MAP kinase-activated protein kinase, isolated by a novel expression screening method for identifying protein kinase substrates. *EMBO J* **16**(8): 1921-1933.

Fulkerson CM and Knapp DW (2019) Tumors of the Urinary System, in *Withrow and MacEwen's Small Animal Clinical Oncology (Sxith Edition)* (Vail DM, Thamm DH and Liptak JM eds) pp 645-656, W.B. Saunders, St. Louis (MO).

Galsky MD, Hahn NM, Rosenberg J, Sonpavde G, Hutson T, Oh WK, Dreicer R, Vogelzang N, Sternberg C, Bajorin DF and Bellmunt J (2011) A consensus definition of patients with metastatic urothelial carcinoma who are unfit for cisplatin-based chemotherapy. *Lancet Oncol* **12**(3): 211-214.

Garcia-Closas M, Malats N, Silverman D, Dosemeci M, Kogevinas M, Hein DW, Tardon A, Serra C, Carrato A, Garcia-Closas R, Lloreta J, Castano-Vinyals G, Yeager M, Welch R, Chanock S, Chatterjee N, Wacholder S, Samanic C, Tora M, Fernandez F, Real FX and Rothman N (2005) NAT2 slow acetylation, GSTM1 null genotype, and risk of bladder cancer: results from the Spanish Bladder Cancer Study and meta-analyses. *Lancet* **366**(9486): 649-659.

Giacinti C and Giordano A (2006) RB and cell cycle progression. *Oncogene* **25**(38): 5220-5227.

Gille H, Kortenjann M, Thomae O, Moomaw C, Slaughter C, Cobb MH and Shaw PE (1995) ERK phosphorylation potentiates Elk-1-mediated ternary complex formation and transactivation. *EMBO J* **14**(5): 951-962.

Gilmartin AG, Bleam MR, Groy A, Moss KG, Minthorn EA, Kulkarni SG, Rominger CM, Erskine S, Fisher KE, Yang J, Zappacosta F, Annan R, Sutton D and Laquerre SG (2011) GSK1120212 (JTP-74057) is an inhibitor of MEK activity and activation with favorable pharmacokinetic properties for sustained in vivo pathway inhibition. *Clin Cancer Res* **17**(5): 989-1000.

Gilmore T and Martin GS (1983) Phorbol ester and diacylglycerol induce protein phosphorylation at tyrosine. *Nature* **306**(5942): 487-490.

Glickman LT, Raghavan M, Knapp DW, Bonney PL and Dawson MH (2004) Herbicide exposure and the risk of transitional cell carcinoma of the urinary bladder in Scottish Terriers. *J Am Vet Med Assoc* **224**(8): 1290-1297.

Glickman LT, Schofer FS, McKee LJ, Reif JS and Goldschmidt MH (1989) Epidemiologic study of insecticide exposures, obesity, and risk of bladder cancer in household dogs. *J Toxicol Environ Health* **28**(4): 407-414.

Goodrich DW, Wang NP, Qian YW, Lee EY and Lee WH (1991) The retinoblastoma gene product regulates progression through the G1 phase of the cell cycle. *Cell* **67**(2): 293-302.

Gopal YN, Rizos H, Chen G, Deng W, Frederick DT, Cooper ZA, Scolyer RA, Pupo G, Komurov K, Sehgal V, Zhang J, Patel L, Pereira CG, Broom BM, Mills GB, Ram P, Smith PD, Wargo JA, Long GV and Davies MA (2014) Inhibition of mTORC1/2

overcomes resistance to MAPK pathway inhibitors mediated by PGC1alpha and oxidative phosphorylation in melanoma. *Cancer Res* **74**(23): 7037-7047.

Gustafson DL, Duval DL, Regan DP and Thamm DH (2018) Canine sarcomas as a surrogate for the human disease. *Pharmacol Ther* **188**: 80-96.

Habuchi T, Devlin J, Elder PA and Knowles MA (1995) Detailed deletion mapping of chromosome 9q in bladder cancer: evidence for two tumour suppressor loci. *Oncogene* **11**(8): 1671-1674.

Habuchi T, Luscombe M, Elder PA and Knowles MA (1998) Structure and methylation-based silencing of a gene (DBCCR1) within a candidate bladder cancer tumor suppressor region at 9q32-q33. *Genomics* **48**(3): 277-288.

Hanahan D and Weinberg RA (2000) The hallmarks of cancer. *Cell* **100**(1): 57-70.

Hanahan D and Weinberg RA (2011) Hallmarks of cancer: the next generation. *Cell* **144**(5): 646-674.

Haq R, Shoag J, Andreu-Perez P, Yokoyama S, Edelman H, Rowe GC, Frederick DT, Hurley AD, Nellore A, Kung AL, Wargo JA, Song JS, Fisher DE, Arany Z and Widlund HR (2013) Oncogenic BRAF regulates oxidative metabolism via PGC1alpha and MITF. *Cancer Cell* **23**(3): 302-315.

Hattori S, Maekawa M and Nakamura S (1992) Identification of neurofibromatosis type I gene product as an insoluble GTPase-activating protein toward ras p21. *Oncogene* **7**(3): 481-485.

Hatzivassiliou G, Liu B, O'Brien C, Spoerke JM, Hoeflich KP, Haverty PM, Soriano R, Forrest WF, Heldens S, Chen H, Toy K, Ha C, Zhou W, Song K, Friedman LS, Amler LC, Hampton GM, Moffat J, Belvin M and Lackner MR (2012) ERK inhibition overcomes acquired resistance to MEK inhibitors. *Mol Cancer Ther* **11**(5): 1143-1154.

Hatzivassiliou G, Song K, Yen I, Brandhuber BJ, Anderson DJ, Alvarado R, Ludlam MJ, Stokoe D, Gloor SL, Vigers G, Morales T, Aliagas I, Liu B, Sideris S, Hoeflich KP, Jaiswal BS, Seshagiri S, Koeppen H, Belvin M, Friedman LS and Malek S (2010) RAF inhibitors prime wild-type RAF to activate the MAPK pathway and enhance growth. *Nature* **464**(7287): 431-435.

Haupt Y, Maya R, Kazaz A and Oren M (1997) Mdm2 promotes the rapid degradation of p53. *Nature* **387**(6630): 296-299.

Hauschild A, Grob JJ, Demidov LV, Jouary T, Gutzmer R, Millward M, Rutkowski P, Blank CU, Miller WH, Jr., Kaempgen E, Martin-Algarra S, Karaszewska B, Mauch C, Chiarion-Sileni V, Martin AM, Swann S, Haney P, Mirakhur B, Guckert ME, Goodman V and Chapman PB (2012) Dabrafenib in BRAF-mutated metastatic

melanoma: a multicentre, open-label, phase 3 randomised controlled trial. *Lancet* **380**(9839): 358-365.

Hedegaard J, Lamy P, Nordentoft I, Algaba F, Hoyer S, Ulhoi BP, Vang S, Reinert T, Hermann GG, Mogensen K, Thomsen MBH, Nielsen MM, Marquez M, Segersten U, Aine M, Hoglund M, Birkenkamp-Demtroder K, Fristrup N, Borre M, Hartmann A, Stohr R, Wach S, Keck B, Seitz AK, Nawroth R, Maurer T, Tulic C, Simic T, Junker K, Horstmann M, Harving N, Petersen AC, Calle ML, Steyerberg EW, Beukers W, van Kessel KEM, Jensen JB, Pedersen JS, Malmstrom PU, Malats N, Real FX, Zwarthoff EC, Orntoft TF and Dyrskjot L (2016) Comprehensive Transcriptional Analysis of Early-Stage Urothelial Carcinoma. *Cancer Cell* **30**(1): 27-42.

Hein DW (2002) Molecular genetics and function of NAT1 and NAT2: role in aromatic amine metabolism and carcinogenesis. *Mutat Res* **506-507**: 65-77.

Henry CJ, McCaw DL, Turnquist SE, Tyler JW, Bravo L, Sheafor S, Straw RC, Dernell WS, Madewell BR, Jorgensen L, Scott MA, Higginbotham ML and Chun R (2003) Clinical evaluation of mitoxantrone and piroxicam in a canine model of human invasive urinary bladder carcinoma. *Clin Cancer Res* **9**(2): 906-911.

Hermeking H, Rago C, Schuhmacher M, Li Q, Barrett JF, Obaya AJ, O'Connell BC, Mateyak MK, Tam W, Kohlhuber F, Dang CV, Sedivy JM, Eick D, Vogelstein B and Kinzler KW (2000) Identification of CDK4 as a target of c-MYC. *Proc Natl Acad Sci U S A* **97**(5): 2229-2234.

Hernandez S, Lopez-Knowles E, Lloreta J, Kogevinas M, Amoros A, Tardon A, Carrato A, Serra C, Malats N and Real FX (2006) Prospective study of FGFR3 mutations as a prognostic factor in nonmuscle invasive urothelial bladder carcinomas. *J Clin Oncol* **24**(22): 3664-3671.

Herschman HR (1991) Primary response genes induced by growth factors and tumor promoters. *Annu Rev Biochem* **60**: 281-319.

Hinds PW, Mittnacht S, Dulic V, Arnold A, Reed SI and Weinberg RA (1992) Regulation of retinoblastoma protein functions by ectopic expression of human cyclins. *Cell* **70**(6): 993-1006.

Hingorani SR, Jacobetz MA, Robertson GP, Herlyn M and Tuveson DA (2003) Suppression of BRAF(V599E) in human melanoma abrogates transformation. *Cancer Res* **63**(17): 5198-5202.

Houles T, Gravel SP, Lavoie G, Shin S, Savall M, Meant A, Grondin B, Gaboury L, Yoon SO, St-Pierre J and Roux PP (2018) RSK Regulates PFK-2 Activity to Promote Metabolic Rewiring in Melanoma. *Cancer Res* **78**(9): 2191-2204.

Howe LR, Leevers SJ, Gomez N, Nakielny S, Cohen P and Marshall CJ (1992) Activation of the MAP kinase pathway by the protein kinase raf. *Cell* **71**(2): 335-342.

Hoxhaj G and Manning BD (2020) The PI3K-AKT network at the interface of oncogenic signalling and cancer metabolism. *Nature reviews Cancer* **20**(2): 74-88.

Huebner K, ar-Rushdi A, Griffin CA, Isobe M, Kozak C, Emanuel BS, Nagarajan L, Cleveland JL, Bonner TI, Goldsborough MD and et al. (1986) Actively transcribed genes in the raf oncogene group, located on the X chromosome in mouse and human. *Proc Natl Acad Sci U S A* **83**(11): 3934-3938.

Huleihel M, Goldsborough M, Cleveland J, Gunnell M, Bonner T and Rapp UR (1986) Characterization of murine A-raf, a new oncogene related to the v-raf oncogene. *Mol Cell Biol* **6**(7): 2655-2662.

Huntington JT, Shields JM, Der CJ, Wyatt CA, Benbow U, Slingluff CL, Jr. and Brinckerhoff CE (2004) Overexpression of collagenase 1 (MMP-1) is mediated by the ERK pathway in invasive melanoma cells: role of BRAF mutation and fibroblast growth factor signaling. *J Biol Chem* **279**(32): 33168-33176.

Hurst CD, Alder O, Platt FM, Droop A, Stead LF, Burns JE, Burghel GJ, Jain S, Klimczak LJ, Lindsay H, Roulson JA, Taylor CF, Thygesen H, Cameron AJ, Ridley AJ, Mott HR, Gordenin DA and Knowles MA (2017) Genomic Subtypes of Non-invasive Bladder Cancer with Distinct Metabolic Profile and Female Gender Bias in KDM6A Mutation Frequency. *Cancer Cell* **32**(5): 701-715 e707.

Ikawa S, Fukui M, Ueyama Y, Tamaoki N, Yamamoto T and Toyoshima K (1988) B-raf, a new member of the raf family, is activated by DNA rearrangement. *Mol Cell Biol* **8**(6): 2651-2654.

Ireson CR, Alavijeh MS, Palmer AM, Fowler ER and Jones HJ (2019) The role of mouse tumour models in the discovery and development of anticancer drugs. *Br J Cancer* **121**(2): 101-108.

Jaffe AB and Hall A (2002) Rho GTPases in transformation and metastasis. *Adv Cancer Res* **84**: 57-80.

Jalali Nadoushan MR, Taheri T, Jouian N and Zaeri F (2007) Overexpression of HER-2/neu oncogene and transitional cell carcinoma of bladder. *Urol J* **4**(3): 151-154.

Jaumot M and Hancock JF (2001) Protein phosphatases 1 and 2A promote Raf-1 activation by regulating 14-3-3 interactions. *Oncogene* **20**(30): 3949-3958.

Jiang X, Yuan JM, Skipper PL, Tannenbaum SR and Yu MC (2007) Environmental tobacco smoke and bladder cancer risk in never smokers of Los Angeles County. *Cancer Res* **67**(15): 7540-7545.

Johannessen CM, Boehm JS, Kim SY, Thomas SR, Wardwell L, Johnson LA, Emery CM, Stransky N, Cogdill AP, Barretina J, Caponigro G, Hieronymus H, Murray RR, Salehi-Ashtiani K, Hill DE, Vidal M, Zhao JJ, Yang X, Alkan O, Kim S, Harris JL, Wilson CJ, Myer VE, Finan PM, Root DE, Roberts TM, Golub T, Flaherty KT, Dummer R, Weber BL, Sellers WR, Schlegel R, Wargo JA, Hahn WC and Garraway LA (2010) COT drives resistance to RAF inhibition through MAP kinase pathway reactivation. *Nature* **468**(7326): 968-972.

Johnson JI, Decker S, Zaharevitz D, Rubinstein LV, Venditti JM, Schepartz S, Kalyandrug S, Christian M, Arbuck S, Hollingshead M and Sausville EA (2001) Relationships between drug activity in NCI preclinical in vitro and in vivo models and early clinical trials. *Br J Cancer* **84**(10): 1424-1431.

Jones DT, Kocialkowski S, Liu L, Pearson DM, Backlund LM, Ichimura K and Collins VP (2008) Tandem duplication producing a novel oncogenic BRAF fusion gene defines the majority of pilocytic astrocytomas. *Cancer Res* **68**(21): 8673-8677.

Kaibuchi K, Kuroda S and Amano M (1999) Regulation of the cytoskeleton and cell adhesion by the Rho family GTPases in mammalian cells. *Annu Rev Biochem* **68**: 459-486.

Kamat AM, Hahn NM, Efstathiou JA, Lerner SP, Malmstrom PU, Choi W, Guo CC, Lotan Y and Kassouf W (2016) Bladder cancer. *Lancet* **388**(10061): 2796-2810.

Kandoth C, McLellan MD, Vandin F, Ye K, Niu B, Lu C, Xie M, Zhang Q, McMichael JF, Wyczalkowski MA, Leiserson MDM, Miller CA, Welch JS, Walter MJ, Wendl MC, Ley TJ, Wilson RK, Raphael BJ and Ding L (2013) Mutational landscape and significance across 12 major cancer types. *Nature* **502**(7471): 333-339.

Kaplon J, Zheng L, Meissl K, Chaneton B, Selivanov VA, Mackay G, van der Burg SH, Verdegaal EM, Cascante M, Shlomi T, Gottlieb E and Peeper DS (2013) A key role for mitochondrial gatekeeper pyruvate dehydrogenase in oncogene-induced senescence. *Nature* **498**(7452): 109-112.

Karasarides M, Chiloeches A, Hayward R, Niculescu-Duvaz D, Scanlon I, Friedlos F, Ogilvie L, Hedley D, Martin J, Marshall CJ, Springer CJ and Marais R (2004) B-RAF is a therapeutic target in melanoma. *Oncogene* **23**(37): 6292-6298.

Kelsey JL, Moore AS and Glickman LT (1998) Epidemiologic studies of risk factors for cancer in pet dogs. *Epidemiol Rev* **20**(2): 204-217.

Khan KN, Knapp DW, Denicola DB and Harris RK (2000) Expression of cyclooxygenase-2 in transitional cell carcinoma of the urinary bladder in dogs. *Am J Vet Res* **61**(5): 478-481.

Khanna C, Lindblad-Toh K, Vail D, London C, Bergman P, Barber L, Breen M, Kitchell B, McNeil E, Modiano JF, Niemi S, Comstock KE, Ostrander E, Westmoreland S

and Withrow S (2006) The dog as a cancer model. *Nat Biotechnol* **24**(9): 1065-1066.

Kiemeney LA, Sulem P, Besenbacher S, Vermeulen SH, Sigurdsson A, Thorleifsson G, Gudbjartsson DF, Stacey SN, Gudmundsson J, Zanon C, Kostic J, Masson G, Bjarnason H, Palsson ST, Skarphedinsson OB, Gudjonsson SA, Witjes JA, Grotenhuis AJ, Verhaegh GW, Bishop DT, Sak SC, Choudhury A, Elliott F, Barrett JH, Hurst CD, de Verdier PJ, Ryk C, Rudnai P, Gurzau E, Koppova K, Vineis P, Polidoro S, Guarrera S, Sacerdote C, Campagna M, Placidi D, Arici C, Zeegers MP, Kellen E, Gutierrez BS, Sanz-Velez JI, Sanchez-Zalabardo M, Valdivia G, Garcia-Prats MD, Hengstler JG, Blaszkewicz M, Dietrich H, Ophoff RA, van den Berg LH, Alexiusdottir K, Kristjansson K, Geirsson G, Nikulasson S, Petursdottir V, Kong A, Thorgeirsson T, Mungan NA, Lindblom A, van Es MA, Porru S, Buntinx F, Golka K, Mayordomo JI, Kumar R, Matullo G, Steineck G, Kiltie AE, Aben KK, Jonsson E, Thorsteinsdottir U, Knowles MA, Rafnar T and Stefansson K (2010) A sequence variant at 4p16.3 confers susceptibility to urinary bladder cancer. *Nat Genet* **42**(5): 415-419.

Kiemeney LA, Thorlacius S, Sulem P, Geller F, Aben KK, Stacey SN, Gudmundsson J, Jakobsdottir M, Bergthorsson JT, Sigurdsson A, Blondal T, Witjes JA, Vermeulen SH, Hulsbergen-van de Kaa CA, Swinkels DW, Ploeg M, Cornel EB, Vergunst H, Thorgeirsson TE, Gudbjartsson D, Gudjonsson SA, Thorleifsson G, Kristinsson KT, Mouy M, Snorradottir S, Placidi D, Campagna M, Arici C, Koppova K, Gurzau E, Rudnai P, Kellen E, Polidoro S, Guarrera S, Sacerdote C, Sanchez M, Saez B, Valdivia G, Ryk C, de Verdier P, Lindblom A, Golka K, Bishop DT, Knowles MA, Nikulasson S, Petursdottir V, Jonsson E, Geirsson G, Kristjansson B, Mayordomo JI, Steineck G, Porru S, Buntinx F, Zeegers MP, Fletcher T, Kumar R, Matullo G, Vineis P, Kiltie AE, Gulcher JR, Thorsteinsdottir U, Kong A, Rafnar T and Stefansson K (2008) Sequence variant on 8q24 confers susceptibility to urinary bladder cancer. *Nat Genet* **40**(11): 1307-1312.

Kim HS, Jeong CW, Kwak C, Kim HH and Ku JH (2016) Pathological T0 Following Cisplatin-Based Neoadjuvant Chemotherapy for Muscle-Invasive Bladder Cancer: A Network Meta-analysis. *Clin Cancer Res* **22**(5): 1086-1094.

Kirkness EF, Bafna V, Halpern AL, Levy S, Remington K, Rusch DB, Delcher AL, Pop M, Wang W, Fraser CM and Venter JC (2003) The dog genome: survey sequencing and comparative analysis. *Science* **301**(5641): 1898-1903.

Knapp DW, Ramos-Vara JA, Moore GE, Dhawan D, Bonney PL and Young KE (2014) Urinary bladder cancer in dogs, a naturally occurring model for cancer biology and drug development. *ILAR J* **55**(1): 100-118.

Knapp DW, Ruple-Czerniak A, Ramos-Vara JA, Naughton JF, Fulkerson CM and Honkisz SI (2016) A Nonselective Cyclooxygenase Inhibitor Enhances the Activity of Vinblastine in a Naturally-Occurring Canine Model of Invasive Urothelial Carcinoma. *Bladder Cancer* **2**(2): 241-250.

Knowles MA, Habuchi T, Kennedy W and Cuthbert-Heavens D (2003) Mutation spectrum of the 9q34 tuberous sclerosis gene TSC1 in transitional cell carcinoma of the bladder. *Cancer Res* **63**(22): 7652-7656.

Knowles MA and Hurst CD (2015) Molecular biology of bladder cancer: new insights into pathogenesis and clinical diversity. *Nature reviews Cancer* **15**(1): 25-41.

Koebnick C, Michaud D, Moore SC, Park Y, Hollenbeck A, Ballard-Barbash R, Schatzkin A and Leitzmann MF (2008) Body mass index, physical activity, and bladder cancer in a large prospective study. *Cancer Epidemiol Biomarkers Prev* **17**(5): 1214-1221.

Konieczkowski DJ, Johannessen CM, Abudayyeh O, Kim JW, Cooper ZA, Piris A, Frederick DT, Barzily-Rokni M, Straussman R, Haq R, Fisher DE, Mesirov JP, Hahn WC, Flaherty KT, Wargo JA, Tamayo P and Garraway LA (2014) A melanoma cell state distinction influences sensitivity to MAPK pathway inhibitors. *Cancer Discov* **4**(7): 816-827.

Kopetz S, Desai J, Chan E, Hecht JR, O'Dwyer PJ, Maru D, Morris V, Janku F, Dasari A, Chung W, Issa JP, Gibbs P, James B, Powis G, Nolop KB, Bhattacharya S and Saltz L (2015) Phase II Pilot Study of Vemurafenib in Patients With Metastatic BRAF-Mutated Colorectal Cancer. *J Clin Oncol* **33**(34): 4032-4038.

Kornev AP, Haste NM, Taylor SS and Eyck LF (2006) Surface comparison of active and inactive protein kinases identifies a conserved activation mechanism. *Proc Natl Acad Sci U S A* **103**(47): 17783-17788.

Kumar SM, Yu H, Edwards R, Chen L, Kazianis S, Brafford P, Acs G, Herlyn M and Xu X (2007) Mutant V600E BRAF increases hypoxia inducible factor-1alpha expression in melanoma. *Cancer Res* **67**(7): 3177-3184.

Kurzman ID, MacEwen EG, Rosenthal RC, Fox LE, Keller ET, Helfand SC, Vail DM, Dubielzig RR, Madewell BR, Rodriguez CO, Jr. and et al. (1995) Adjuvant therapy for osteosarcoma in dogs: results of randomized clinical trials using combined liposome-encapsulated muramyl tripeptide and cisplatin. *Clin Cancer Res* **1**(12): 1595-1601.

Kyriakis JM, App H, Zhang XF, Banerjee P, Brautigan DL, Rapp UR and Avruch J (1992) Raf-1 activates MAP kinase-kinase. *Nature* **358**(6385): 417-421.

LaRue SM, Withrow SJ, Powers BE, Wrigley RH, Gillette EL, Schwarz PD, Straw RC and Richter SL (1989) Limb-sparing treatment for osteosarcoma in dogs. *J Am Vet Med Assoc* **195**(12): 1734-1744.

Lavoie H and Therrien M (2015) Regulation of RAF protein kinases in ERK signalling. *Nat Rev Mol Cell Biol* **16**(5): 281-298.

Lavoie H, Thevakumaran N, Gavory G, Li JJ, Padeganeh A, Guiral S, Duchaine J, Mao DY, Bouvier M, Sicheri F and Therrien M (2013) Inhibitors that stabilize a closed RAF kinase domain conformation induce dimerization. *Nat Chem Biol* **9**(7): 428-436.

LeBlanc AK and Mazcko CN (2020) Improving human cancer therapy through the evaluation of pet dogs. *Nature reviews Cancer*.

Lenormand P, Sardet C, Pages G, L'Allemain G, Brunet A and Pouyssegur J (1993) Growth factors induce nuclear translocation of MAP kinases (p42mapk and p44mapk) but not of their activator MAP kinase kinase (p45mapkk) in fibroblasts. *J Cell Biol* **122**(5): 1079-1088.

Lin J, Handschin C and Spiegelman BM (2005) Metabolic control through the PGC-1 family of transcription coactivators. *Cell Metab* **1**(6): 361-370.

Lindblad-Toh K, Wade CM, Mikkelsen TS, Karlsson EK, Jaffe DB, Kamal M, Clamp M, Chang JL, Kulbokas EJ, 3rd, Zody MC, Mauceli E, Xie X, Breen M, Wayne RK, Ostrander EA, Ponting CP, Galibert F, Smith DR, DeJong PJ, Kirkness E, Alvarez P, Biagi T, Brockman W, Butler J, Chin CW, Cook A, Cuff J, Daly MJ, DeCaprio D, Gnerre S, Grabherr M, Kellis M, Kleber M, Bardeleben C, Goodstadt L, Heger A, Hitte C, Kim L, Koepfli KP, Parker HG, Pollinger JP, Searle SM, Sutter NB, Thomas R, Webber C, Baldwin J, Abebe A, Abouelleil A, Aftuck L, Ait-Zahra M, Aldredge T, Allen N, An P, Anderson S, Antoine C, Arachchi H, Aslam A, Ayotte L, Bachantsang P, Barry A, Bayul T, Benamara M, Berlin A, Bessette D, Blitshteyn B, Bloom T, Blye J, Boguslavskiy L, Bonnet C, Boukhgalter B, Brown A, Cahill P, Calixte N, Camarata J, Cheshatsang Y, Chu J, Citroen M, Collymore A, Cooke P, Dawoe T, Daza R, Decktor K, DeGray S, Dhargay N, Dooley K, Dooley K, Dorje P, Dorjee K, Dorris L, Duffey N, Dupes A, Egbiremolen O, Elong R, Falk J, Farina A, Faro S, Ferguson D, Ferreira P, Fisher S, FitzGerald M, Foley K, Foley C, Franke A, Friedrich D, Gage D, Garber M, Gearin G, Giannoukos G, Goode T, Goyette A, Graham J, Grandbois E, Gyaltsen K, Hafez N, Hagopian D, Hagos B, Hall J, Healy C, Hegarty R, Honan T, Horn A, Houde N, Hughes L, Hunnicutt L, Husby M, Jester B, Jones C, Kamat A, Kanga B, Kells C, Khazanovich D, Kieu AC, Kisner P, Kumar M, Lance K, Landers T, Lara M, Lee W, Leger JP, Lennon N, Leuper L, LeVine S, Liu J, Liu X, Lokyitsang Y, Lokyitsang T, Lui A, Macdonald J, Major J, Marabella R, Maru K, Matthews C, McDonough S, Mehta T, Meldrim J, Melnikov A, Meneus L, Mihalev A, Mihova T, Miller K, Mittelman R, Mlenga V, Mulrain L, Munson G, Navidi A, Naylor J, Nguyen T, Nguyen N, Nguyen C, Nguyen T, Nicol R, Norbu N, Norbu C, Novod N, Nyima T, Olandt P, O'Neill B, O'Neill K, Osman S, Oyono L, Patti C, Perrin D, Phunkhang P, Pierre F, Priest M, Rachupka A, Raghuraman S, Rameau R, Ray V, Raymond C, Rege F, Rise C, Rogers J, Rogov P, Sahalie J, Settipalli S, Sharpe T, Shea T, Sheehan M, Sherpa N, Shi J, Shih D, Sloan J, Smith C, Sparrow T, Stalker J, Stange-Thomann N, Stavropoulos S, Stone C, Stone S, Sykes S, Tchuinga P, Tenzing P, Tesfaye S, Thoulutsang D, Thoulutsang Y, Topham K, Topping I, Tsamla T, Vassiliev H, Venkataraman V,

Vo A, Wangchuk T, Wangdi T, Weiand M, Wilkinson J, Wilson A, Yadav S, Yang S, Yang X, Young G, Yu Q, Zainoun J, Zembek L, Zimmer A and Lander ES (2005) Genome sequence, comparative analysis and haplotype structure of the domestic dog. *Nature* **438**(7069): 803-819.

Little AS, Balmanno K, Sale MJ, Newman S, Dry JR, Hampson M, Edwards PA, Smith PD and Cook SJ (2011) Amplification of the driving oncogene, KRAS or BRAF, underpins acquired resistance to MEK1/2 inhibitors in colorectal cancer cells. *Sci Signal* **4**(166): ra17.

Long GV, Stroyakovskiy D, Gogas H, Levchenko E, de Braud F, Larkin J, Garbe C, Jouary T, Hauschild A, Grob JJ, Chiarion Sileni V, Lebbe C, Mandala M, Millward M, Arance A, Bondarenko I, Haanen JB, Hansson J, Utikal J, Ferraresi V, Kovalenko N, Mohr P, Probachai V, Schadendorf D, Nathan P, Robert C, Ribas A, DeMarini DJ, Irani JG, Casey M, Ouellet D, Martin AM, Le N, Patel K and Flaherty K (2014) Combined BRAF and MEK inhibition versus BRAF inhibition alone in melanoma. *N Engl J Med* **371**(20): 1877-1888.

Long GV, Stroyakovskiy D, Gogas H, Levchenko E, de Braud F, Larkin J, Garbe C, Jouary T, Hauschild A, Grob JJ, Chiarion-Sileni V, Lebbe C, Mandala M, Millward M, Arance A, Bondarenko I, Haanen JB, Hansson J, Utikal J, Ferraresi V, Kovalenko N, Mohr P, Probachai V, Schadendorf D, Nathan P, Robert C, Ribas A, DeMarini DJ, Irani JG, Swann S, Legos JJ, Jin F, Mookerjee B and Flaherty K (2015) Dabrafenib and trametinib versus dabrafenib and placebo for Val600 BRAF-mutant melanoma: a multicentre, double-blind, phase 3 randomised controlled trial. *Lancet* **386**(9992): 444-451.

Lu H, Liu S, Zhang G, Kwong LN, Zhu Y, Miller JP, Hu Y, Zhong W, Zeng J, Wu L, Krepler C, Sproesser K, Xiao M, Xu W, Karakousis GC, Schuchter LM, Field J, Zhang PJ, Herlyn M, Xu X and Guo W (2016) Oncogenic BRAF-Mediated Melanoma Cell Invasion. *Cell Rep* **15**(9): 2012-2024.

Luciano F, Jacquel A, Colosetti P, Herrant M, Cagnol S, Pages G and Auberger P (2003) Phosphorylation of Bim-EL by Erk1/2 on serine 69 promotes its degradation via the proteasome pathway and regulates its proapoptotic function. *Oncogene* **22**(43): 6785-6793.

Luo Z, Tzivion G, Belshaw PJ, Vavvas D, Marshall M and Avruch J (1996) Oligomerization activates c-Raf-1 through a Ras-dependent mechanism. *Nature* **383**(6596): 181-185.

Ma L, Chen Z, Erdjument-Bromage H, Tempst P and Pandolfi PP (2005) Phosphorylation and functional inactivation of TSC2 by Erk implications for tuberous sclerosis and cancer pathogenesis. *Cell* **121**(2): 179-193.

Ma XM and Blenis J (2009) Molecular mechanisms of mTOR-mediated translational control. *Nat Rev Mol Cell Biol* **10**(5): 307-318.

MacEwen EG, Kurzman ID, Rosenthal RC, Smith BW, Manley PA, Roush JK and Howard PE (1989) Therapy for osteosarcoma in dogs with intravenous injection of liposome-encapsulated muramyl tripeptide. *J Natl Cancer Inst* **81**(12): 935-938.

Maeda S, Tomiyasu H, Tsuboi M, Inoue A, Ishihara G, Uchikai T, Chambers JK, Uchida K, Yonezawa T and Matsuki N (2018) Comprehensive gene expression analysis of canine invasive urothelial bladder carcinoma by RNA-Seq. *BMC Cancer* **18**(1): 472.

Makrodouli E, Oikonomou E, Koc M, Andera L, Sasazuki T, Shirasawa S and Pintzas A (2011) BRAF and RAS oncogenes regulate Rho GTPase pathways to mediate migration and invasion properties in human colon cancer cells: a comparative study. *Mol Cancer* **10**: 118.

Marais R, Light Y, Paterson HF, Mason CS and Marshall CJ (1997) Differential regulation of Raf-1, A-Raf, and B-Raf by oncogenic ras and tyrosine kinases. *J Biol Chem* **272**(7): 4378-4383.

Martinez R, Nakamura KD and Weber MJ (1982) Identification of phosphotyrosine-containing proteins in untransformed and Rous sarcoma virus-transformed chicken embryo fibroblasts. *Mol Cell Biol* **2**(6): 653-665.

McArthur GA, Chapman PB, Robert C, Larkin J, Haanen JB, Dummer R, Ribas A, Hogg D, Hamid O, Ascierto PA, Garbe C, Testori A, Maio M, Lorigan P, Lebbe C, Jouary T, Schadendorf D, O'Day SJ, Kirkwood JM, Eggermont AM, Dreno B, Sosman JA, Flaherty KT, Yin M, Caro I, Cheng S, Trunzer K and Hauschild A (2014) Safety and efficacy of vemurafenib in BRAF(V600E) and BRAF(V600K) mutation-positive melanoma (BRIM-3): extended follow-up of a phase 3, randomised, open-label study. *Lancet Oncol* **15**(3): 323-332.

McGarvey TW, Maruta Y, Tomaszewski JE, Linnenbach AJ and Malkowicz SB (1998) PTCH gene mutations in invasive transitional cell carcinoma of the bladder. *Oncogene* **17**(9): 1167-1172.

Meuten DJ and Meuten TLK (2016) Tumors of the Urinary System, in *Tumors in Domestic Animals* (Meuten DJ ed) pp 632-688.

Meyers PA, Schwartz CL, Krailo M, Kleinerman ES, Betcher D, Bernstein ML, Conrad E, Ferguson W, Gebhardt M, Goorin AM, Harris MB, Healey J, Huvos A, Link M, Montebello J, Nadel H, Nieder M, Sato J, Siegal G, Weiner M, Wells R, Wold L, Womer R and Grier H (2005) Osteosarcoma: a randomized, prospective trial of the addition of ifosfamide and/or muramyl tripeptide to cisplatin, doxorubicin, and high-dose methotrexate. *J Clin Oncol* **23**(9): 2004-2011.

Millanta F, Impellizeri J, McSherry L, Rocchigiani G, Aurisicchio L and Lubas G (2018) Overexpression of HER-2 via immunohistochemistry in canine urinary bladder

transitional cell carcinoma - A marker of malignancy and possible therapeutic target. *Vet Comp Oncol* **16**(2): 297-300.

Mochizuki H, Kennedy K, Shapiro SG and Breen M (2015) BRAF Mutations in Canine Cancers. *PLoS One* **10**(6): e0129534.

Mohammed SI, Knapp DW, Bostwick DG, Foster RS, Khan KN, Masferrer JL, Woerner BM, Snyder PW and Koki AT (1999) Expression of cyclooxygenase-2 (COX-2) in human invasive transitional cell carcinoma (TCC) of the urinary bladder. *Cancer Res* **59**(22): 5647-5650.

Molina JR, Sun Y, Protopopova M, Gera S, Bandi M, Bristow C, McAfoos T, Morlacchi P, Ackroyd J, Agip AA, Al-Atrash G, Asara J, Bardenhagen J, Carrillo CC, Carroll C, Chang E, Ciurea S, Cross JB, Czako B, Deem A, Daver N, de Groot JF, Dong JW, Feng N, Gao G, Gay J, Do MG, Greer J, Giuliani V, Han J, Han L, Henry VK, Hirst J, Huang S, Jiang Y, Kang Z, Khor T, Konoplev S, Lin YH, Liu G, Lodi A, Lofton T, Ma H, Mahendra M, Matre P, Mullinax R, Peoples M, Petrocchi A, Rodriguez-Canale J, Serreli R, Shi T, Smith M, Tabe Y, Theroff J, Tiziani S, Xu Q, Zhang Q, Muller F, DePinho RA, Toniatti C, Draetta GF, Heffernan TP, Konopleva M, Jones P, Di Francesco ME and Marszalek JR (2018) An inhibitor of oxidative phosphorylation exploits cancer vulnerability. *Nat Med* **24**(7): 1036-1046.

Momand J, Zambetti GP, Olson DC, George D and Levine AJ (1992) The mdm-2 oncogene product forms a complex with the p53 protein and inhibits p53-mediated transactivation. *Cell* **69**(7): 1237-1245.

Montagut C, Sharma SV, Shioda T, McDermott U, Ulman M, Ulkus LE, Dias-Santagata D, Stubbs H, Lee DY, Singh A, Drew L, Haber DA and Settleman J (2008) Elevated CRAF as a potential mechanism of acquired resistance to BRAF inhibition in melanoma. *Cancer Res* **68**(12): 4853-4861.

Moodie SA, Willumsen BM, Weber MJ and Wolfman A (1993) Complexes of Ras.GTP with Raf-1 and mitogen-activated protein kinase kinase. *Science* **260**(5114): 1658-1661.

Murphy LO, Smith S, Chen RH, Fingar DC and Blenis J (2002) Molecular interpretation of ERK signal duration by immediate early gene products. *Nat Cell Biol* **4**(8): 556-564.

Nakamura KD, Martinez R and Weber MJ (1983) Tyrosine phosphorylation of specific proteins after mitogen stimulation of chicken embryo fibroblasts. *Mol Cell Biol* **3**(3): 380-390.

Nazarian R, Shi H, Wang Q, Kong X, Koya RC, Lee H, Chen Z, Lee MK, Attar N, Sazegar H, Chodon T, Nelson SF, McArthur G, Sosman JA, Ribas A and Lo RS (2010) Melanomas acquire resistance to B-RAF(V600E) inhibition by RTK or N-RAS upregulation. *Nature* **468**(7326): 973-977.

Necchi A, Anichini A, Raggi D, Briganti A, Massa S, Luciano R, Colecchia M, Giannatempo P, Mortarini R, Bianchi M, Fare E, Monopoli F, Colombo R, Gallina A, Salonia A, Messina A, Ali SM, Madison R, Ross JS, Chung JH, Salvioni R, Mariani L and Montorsi F (2018) Pembrolizumab as Neoadjuvant Therapy Before Radical Cystectomy in Patients With Muscle-Invasive Urothelial Bladder Carcinoma (PURE-01): An Open-Label, Single-Arm, Phase II Study. *J Clin Oncol* **36**(34): 3353-3360.

Olson H, Betton G, Robinson D, Thomas K, Monro A, Kolaja G, Lilly P, Sanders J, Sipes G, Bracken W, Dorato M, Van Deun K, Smith P, Berger B and Heller A (2000) Concordance of the toxicity of pharmaceuticals in humans and in animals. *Regul Toxicol Pharmacol* **32**(1): 56-67.

Pages G, Lenormand P, L'Allemain G, Chambard JC, Meloche S and Pouyssegur J (1993) Mitogen-activated protein kinases p42mapk and p44mapk are required for fibroblast proliferation. *Proc Natl Acad Sci U S A* **90**(18): 8319-8323.

Paoloni M and Khanna C (2008) Translation of new cancer treatments from pet dogs to humans. *Nature reviews Cancer* **8**(2): 147-156.

Paoloni MC and Khanna C (2007) Comparative oncology today. *Vet Clin North Am Small Anim Pract* **37**(6): 1023-1032; v.

Paoloni MC, Mazcko C, Fox E, Fan T, Lana S, Kisseberth W, Vail DM, Nuckolls K, Osborne T, Yalkowsy S, Gustafson D, Yu Y, Cao L and Khanna C (2010) Rapamycin pharmacokinetic and pharmacodynamic relationships in osteosarcoma: a comparative oncology study in dogs. *PLoS One* **5**(6): e11013.

Paraiso KH, Fedorenko IV, Cantini LP, Munko AC, Hall M, Sondak VK, Messina JL, Flaherty KT and Smalley KS (2010) Recovery of phospho-ERK activity allows melanoma cells to escape from BRAF inhibitor therapy. *Br J Cancer* **102**(12): 1724-1730.

Paraiso KH, Xiang Y, Rebecca VW, Abel EV, Chen YA, Munko AC, Wood E, Fedorenko IV, Sondak VK, Anderson AR, Ribas A, Palma MD, Nathanson KL, Koomen JM, Messina JL and Smalley KS (2011) PTEN loss confers BRAF inhibitor resistance to melanoma cells through the suppression of BIM expression. *Cancer Res* **71**(7): 2750-2760.

Pardee AB (1974) A restriction point for control of normal animal cell proliferation. *Proc Natl Acad Sci U S A* **71**(4): 1286-1290.

Parmenter TJ, Kleinschmidt M, Kinross KM, Bond ST, Li J, Kaadige MR, Rao A, Sheppard KE, Hugo W, Pupo GM, Pearson RB, McGee SL, Long GV, Scolyer RA, Rizos H, Lo RS, Cullinane C, Ayer DE, Ribas A, Johnstone RW, Hicks RJ and McArthur GA (2014) Response of BRAF-mutant melanoma to BRAF inhibition is mediated by a network of transcriptional regulators of glycolysis. *Cancer Discov* **4**(4): 423-433.

Paul SM, Mytelka DS, Dunwiddie CT, Persinger CC, Munos BH, Lindborg SR and Schacht AL (2010) How to improve R&D productivity: the pharmaceutical industry's grand challenge. *Nat Rev Drug Discov* **9**(3): 203-214.

Perna D, Karreth FA, Rust AG, Perez-Mancera PA, Rashid M, Iorio F, Alifrangis C, Arends MJ, Bosenberg MW, Bollag G, Tuveson DA and Adams DJ (2015) BRAF inhibitor resistance mediated by the AKT pathway in an oncogenic BRAF mouse melanoma model. *Proc Natl Acad Sci U S A* **112**(6): E536-545.

Perou CM, Sorlie T, Eisen MB, van de Rijn M, Jeffrey SS, Rees CA, Pollack JR, Ross DT, Johnsen H, Akslen LA, Fluge O, Pergamenschikov A, Williams C, Zhu SX, Lonning PE, Borresen-Dale AL, Brown PO and Botstein D (2000) Molecular portraits of human breast tumours. *Nature* **406**(6797): 747-752.

Plowman SJ, Muncke C, Parton RG and Hancock JF (2005) H-ras, K-ras, and inner plasma membrane raft proteins operate in nanoclusters with differential dependence on the actin cytoskeleton. *Proc Natl Acad Sci U S A* **102**(43): 15500-15505.

Poulikakos PI, Persaud Y, Janakiraman M, Kong X, Ng C, Moriceau G, Shi H, Atefi M, Titz B, Gabay MT, Salton M, Dahlman KB, Tadi M, Wargo JA, Flaherty KT, Kelley MC, Misteli T, Chapman PB, Sosman JA, Graeber TG, Ribas A, Lo RS, Rosen N and Solit DB (2011) RAF inhibitor resistance is mediated by dimerization of aberrantly spliced BRAF(V600E). *Nature* **480**(7377): 387-390.

Poulikakos PI, Zhang C, Bollag G, Shokat KM and Rosen N (2010) RAF inhibitors transactivate RAF dimers and ERK signalling in cells with wild-type BRAF. *Nature* **464**(7287): 427-430.

Powles T, Kockx M, Rodriguez-Vida A, Duran I, Crabb SJ, Van Der Heijden MS, Szabados B, Pous AF, Gravis G, Herranz UA, Protheroe A, Ravaud A, Maillet D, Mendez MJ, Suarez C, Linch M, Prendergast A, van Dam PJ, Stanoeva D, Daelemans S, Mariathasan S, Tea JS, Mousa K, Banchereau R and Castellano D (2019) Clinical efficacy and biomarker analysis of neoadjuvant atezolizumab in operable urothelial carcinoma in the ABACUS trial. *Nat Med* **25**(11): 1706-1714.

Prahallad A, Sun C, Huang S, Di Nicolantonio F, Salazar R, Zecchin D, Beijersbergen RL, Bardelli A and Bernards R (2012) Unresponsiveness of colon cancer to BRAF(V600E) inhibition through feedback activation of EGFR. *Nature* **483**(7387): 100-103.

Rafnar T, Sulem P, Stacey SN, Geller F, Gudmundsson J, Sigurdsson A, Jakobsdottir M, Helgadottir H, Thorlacius S, Aben KK, Blondal T, Thorgeirsson TE, Thorleifsson G, Kristjansson K, Thorisdottir K, Ragnarsson R, Sigurgeirsson B, Skuladottir H, Gudbjartsson T, Isaksson HJ, Einarsson GV, Benediktsdottir KR, Agnarsson BA, Olafsson K, Salvarsdottir A, Bjarnason H, Asgeirsdottir M, Kristinsson KT, Matthiasdottir S, Sveinsdottir SG, Polidoro S, Hoiom V, Botella-Estrada R, Hemminki K, Rudnai P, Bishop DT, Campagna M, Kellen E, Zeegers

MP, de Verdier P, Ferrer A, Isla D, Vidal MJ, Andres R, Saez B, Juberias P, Banzo J, Navarrete S, Tres A, Kan D, Lindblom A, Gurzau E, Koppova K, de Vegt F, Schalken JA, van der Heijden HF, Smit HJ, Termeer RA, Oosterwijk E, van Hooij O, Nagore E, Porru S, Steineck G, Hansson J, Buntinx F, Catalona WJ, Matullo G, Vineis P, Kiltie AE, Mayordomo JI, Kumar R, Kiemeney LA, Frigge ML, Jonsson T, Saemundsson H, Barkardottir RB, Jonsson E, Jonsson S, Olafsson JH, Gulcher JR, Masson G, Gudbjartsson DF, Kong A, Thorsteinsdottir U and Stefansson K (2009) Sequence variants at the TERT-CLPTM1L locus associate with many cancer types. *Nat Genet* **41**(2): 221-227.

Rapp UR, Goldsborough MD, Mark GE, Bonner TI, Groffen J, Reynolds FH, Jr. and Stephenson JR (1983) Structure and biological activity of v-raf, a unique oncogene transduced by a retrovirus. *Proc Natl Acad Sci U S A* **80**(14): 4218-4222.

Ray LB and Sturgill TW (1987) Rapid stimulation by insulin of a serine/threonine kinase in 3T3-L1 adipocytes that phosphorylates microtubule-associated protein 2 in vitro. *Proc Natl Acad Sci U S A* **84**(6): 1502-1506.

Ray LB and Sturgill TW (1988) Insulin-stimulated microtubule-associated protein kinase is phosphorylated on tyrosine and threonine in vivo. *Proc Natl Acad Sci U S A* **85**(11): 3753-3757.

Rebbeck TR (1997) Molecular epidemiology of the human glutathione S-transferase genotypes GSTM1 and GSTT1 in cancer susceptibility. *Cancer Epidemiol Biomarkers Prev* **6**(9): 733-743.

Ren J and Guo W (2012) ERK1/2 regulate exocytosis through direct phosphorylation of the exocyst component Exo70. *Dev Cell* **22**(5): 967-978.

Richard G, Dalle S, Monet MA, Ligier M, Boespflug A, Pommier RM, de la Fouchardiere A, Perier-Muzet M, Depaepe L, Barnault R, Tondeur G, Ansieau S, Thomas E, Bertolotto C, Ballotti R, Mourah S, Battistella M, Lebbe C, Thomas L, Puisieux A and Caramel J (2016) ZEB1-mediated melanoma cell plasticity enhances resistance to MAPK inhibitors. *EMBO Mol Med* **8**(10): 1143-1161.

Rizos H, Menzies AM, Pupo GM, Carlino MS, Fung C, Hyman J, Haydu LE, Mijatov B, Becker TM, Boyd SC, Howle J, Saw R, Thompson JF, Kefford RF, Scolyer RA and Long GV (2014) BRAF inhibitor resistance mechanisms in metastatic melanoma: spectrum and clinical impact. *Clin Cancer Res* **20**(7): 1965-1977.

Robert C, Karaszewska B, Schachter J, Rutkowski P, Mackiewicz A, Stroiakovski D, Lichinitser M, Dummer R, Grange F, Mortier L, Chiarion-Sileni V, Drucis K, Krajsova I, Hauschild A, Lorigan P, Wolter P, Long GV, Flaherty K, Nathan P, Ribas A, Martin AM, Sun P, Crist W, Legos J, Rubin SD, Little SM and Schadendorf D (2015) Improved overall survival in melanoma with combined dabrafenib and trametinib. *N Engl J Med* **372**(1): 30-39.

Robertson AG, Kim J, Al-Ahmadie H, Bellmunt J, Guo G, Cherniack AD, Hinoue T, Laird PW, Hoadley KA, Akbani R, Castro MAA, Gibb EA, Kanchi RS, Gordenin DA, Shukla SA, Sanchez-Vega F, Hansel DE, Czerniak BA, Reuter VE, Su X, de Sa Carvalho B, Chagas VS, Mungall KL, Sadeghi S, Pedamallu CS, Lu Y, Klimczak LJ, Zhang J, Choo C, Ojesina AI, Bullman S, Leraas KM, Lichtenberg TM, Wu CJ, Schultz N, Getz G, Meyerson M, Mills GB, McConkey DJ, Network TR, Weinstein JN, Kwiatkowski DJ and Lerner SP (2017) Comprehensive Molecular Characterization of Muscle-Invasive Bladder Cancer. *Cell* **171**(3): 540-556 e525.

Roring M, Herr R, Fiala GJ, Heilmann K, Braun S, Eisenhardt AE, Halbach S, Capper D, von Deimling A, Schamel WW, Saunders DN and Brummer T (2012) Distinct requirement for an intact dimer interface in wild-type, V600E and kinase-dead B-Raf signalling. *EMBO J* **31**(11): 2629-2647.

Ross JS, Wang K, Chmielecki J, Gay L, Johnson A, Chudnovsky J, Yelensky R, Lipson D, Ali SM, Elvin JA, Vergilio JA, Roels S, Miller VA, Nakamura BN, Gray A, Wong MK and Stephens PJ (2016) The distribution of BRAF gene fusions in solid tumors and response to targeted therapy. *Int J Cancer* **138**(4): 881-890.

Rossomando A, Wu J, Weber MJ and Sturgill TW (1992) The phorbol ester-dependent activator of the mitogen-activated protein kinase p42mapk is a kinase with specificity for the threonine and tyrosine regulatory sites. *Proc Natl Acad Sci U S A* **89**(12): 5221-5225.

Rossomando AJ, Payne DM, Weber MJ and Sturgill TW (1989) Evidence that pp42, a major tyrosine kinase target protein, is a mitogen-activated serine/threonine protein kinase. *Proc Natl Acad Sci U S A* **86**(18): 6940-6943.

Rothman N, Garcia-Closas M, Chatterjee N, Malats N, Wu X, Figueroa JD, Real FX, Van Den Berg D, Matullo G, Baris D, Thun M, Kiemeney LA, Vineis P, De Vivo I, Albanes D, Purdue MP, Rafnar T, Hildebrandt MA, Kiltie AE, Cussenot O, Golka K, Kumar R, Taylor JA, Mayordomo JI, Jacobs KB, Kogevinas M, Hutchinson A, Wang Z, Fu YP, Prokunina-Olsson L, Burdett L, Yeager M, Wheeler W, Tardon A, Serra C, Carrato A, Garcia-Closas R, Lloreta J, Johnson A, Schwenn M, Karagas MR, Schned A, Andriole G, Jr., Grubb R, 3rd, Black A, Jacobs EJ, Diver WR, Gapstur SM, Weinstein SJ, Virtamo J, Cortessis VK, Gago-Dominguez M, Pike MC, Stern MC, Yuan JM, Hunter DJ, McGrath M, Dinney CP, Czerniak B, Chen M, Yang H, Vermeulen SH, Aben KK, Witjes JA, Makkinje RR, Sulem P, Besenbacher S, Stefansson K, Riboli E, Brennan P, Panico S, Navarro C, Allen NE, Bueno-de-Mesquita HB, Trichopoulos D, Caporaso N, Landi MT, Canzian F, Ljungberg B, Tjonneland A, Clavel-Chapelon F, Bishop DT, Teo MT, Knowles MA, Guarrera S, Polidoro S, Ricceri F, Sacerdote C, Allione A, Cancel-Tassin G, Selinski S, Hengstler JG, Dietrich H, Fletcher T, Rudnai P, Gurzau E, Koppova K, Bolick SC, Godfrey A, Xu Z, Sanz-Velez JI, M DG-P, Sanchez M, Valdivia G, Porru S, Benhamou S, Hoover RN, Fraumeni JF, Jr., Silverman DT and Chanock SJ (2010) A multi-stage genome-wide association study of bladder cancer identifies multiple susceptibility loci. *Nat Genet* **42**(11): 978-984.

Roux PP, Ballif BA, Anjum R, Gygi SP and Blenis J (2004) Tumor-promoting phorbol esters and activated Ras inactivate the tuberous sclerosis tumor suppressor complex via p90 ribosomal S6 kinase. *Proc Natl Acad Sci U S A* **101**(37): 13489-13494.

Ruas M and Peters G (1998) The p16INK4a/CDKN2A tumor suppressor and its relatives. *Biochim Biophys Acta* **1378**(2): F115-177.

Rushworth LK, Hindley AD, O'Neill E and Kolch W (2006) Regulation and role of Raf-1/B-Raf heterodimerization. *Mol Cell Biol* **26**(6): 2262-2272.

Sahai E and Marshall CJ (2002) RHO-GTPases and cancer. *Nature reviews Cancer* **2**(2): 133-142.

Sala E, Mologni L, Truffa S, Gaetano C, Bollag GE and Gambacorti-Passerini C (2008) BRAF silencing by short hairpin RNA or chemical blockade by PLX4032 leads to different responses in melanoma and thyroid carcinoma cells. *Mol Cancer Res* **6**(5): 751-759.

Sale MJ, Balmanno K, Saxena J, Ozono E, Wojdyla K, McIntyre RE, Gilley R, Woroniuk A, Howarth KD, Hughes G, Dry JR, Arends MJ, Caro P, Oxley D, Ashton S, Adams DJ, Saez-Rodriguez J, Smith PD and Cook SJ (2019) MEK1/2 inhibitor withdrawal reverses acquired resistance driven by BRAF(V600E) amplification whereas KRAS(G13D) amplification promotes EMT-chemoresistance. *Nat Commun* **10**(1): 2030.

Sanchez-Vega F, Mina M, Armenia J, Chatila WK, Luna A, La KC, Dimitriadoy S, Liu DL, Kantheti HS, Saghafinia S, Chakravarty D, Daian F, Gao Q, Bailey MH, Liang WW, Foltz SM, Shmulevich I, Ding L, Heins Z, Ochoa A, Gross B, Gao J, Zhang H, Kundra R, Kandoth C, Bahceci I, Dervishi L, Dogrusoz U, Zhou W, Shen H, Laird PW, Way GP, Greene CS, Liang H, Xiao Y, Wang C, Iavarone A, Berger AH, Bivona TG, Lazar AJ, Hammer GD, Giordano T, Kwong LN, McArthur G, Huang C, Tward AD, Frederick MJ, McCormick F, Meyerson M, Cancer Genome Atlas Research N, Van Allen EM, Cherniack AD, Ciriello G, Sander C and Schultz N (2018) Oncogenic Signaling Pathways in The Cancer Genome Atlas. *Cell* **173**(2): 321-337 e310.

Sargan DR (2004) IDID: inherited diseases in dogs: web-based information for canine inherited disease genetics. *Mamm Genome* **15**(6): 503-506.

Schiffman JD and Breen M (2015) Comparative oncology: what dogs and other species can teach us about humans with cancer. *Philos Trans R Soc Lond B Biol Sci* **370**(1673).

Schlessinger J (2000) Cell signaling by receptor tyrosine kinases. *Cell* **103**(2): 211-225.

Sears R, Nuckolls F, Haura E, Taya Y, Tamai K and Nevins JR (2000) Multiple Ras-dependent phosphorylation pathways regulate Myc protein stability. *Genes Dev* **14**(19): 2501-2514.

Sebolt-Leopold JS, Dudley DT, Herrera R, Van Becelaere K, Wiland A, Gowan RC, Tecle H, Barrett SD, Bridges A, Przybranowski S, Leopold WR and Saltiel AR (1999) Blockade of the MAP kinase pathway suppresses growth of colon tumors in vivo. *Nat Med* **5**(7): 810-816.

Sensi M, Nicolini G, Petti C, Bersani I, Lozupone F, Molla A, Vegetti C, Nonaka D, Mortarini R, Parmiani G, Fais S and Anichini A (2006) Mutually exclusive NRASQ61R and BRAFV600E mutations at the single-cell level in the same human melanoma. *Oncogene* **25**(24): 3357-3364.

Shan B, Durfee T and Lee WH (1996) Disruption of RB/E2F-1 interaction by single point mutations in E2F-1 enhances S-phase entry and apoptosis. *Proc Natl Acad Sci U S A* **93**(2): 679-684.

Shi H, Hong A, Kong X, Koya RC, Song C, Moriceau G, Hugo W, Yu CC, Ng C, Chodon T, Scolyer RA, Kefford RF, Ribas A, Long GV and Lo RS (2014a) A novel AKT1 mutant amplifies an adaptive melanoma response to BRAF inhibition. *Cancer Discov* **4**(1): 69-79.

Shi H, Hugo W, Kong X, Hong A, Koya RC, Moriceau G, Chodon T, Guo R, Johnson DB, Dahlman KB, Kelley MC, Kefford RF, Chmielowski B, Glaspy JA, Sosman JA, van Baren N, Long GV, Ribas A and Lo RS (2014b) Acquired resistance and clonal evolution in melanoma during BRAF inhibitor therapy. *Cancer Discov* **4**(1): 80-93.

Shi H, Moriceau G, Kong X, Lee MK, Lee H, Koya RC, Ng C, Chodon T, Scolyer RA, Dahlman KB, Sosman JA, Kefford RF, Long GV, Nelson SF, Ribas A and Lo RS (2012) Melanoma whole-exome sequencing identifies (V600E)B-RAF amplification-mediated acquired B-RAF inhibitor resistance. *Nat Commun* **3**: 724.

Shirahama T (2000) Cyclooxygenase-2 expression is up-regulated in transitional cell carcinoma and its preneoplastic lesions in the human urinary bladder. *Clin Cancer Res* **6**(6): 2424-2430.

Sidransky D, Von Eschenbach A, Tsai YC, Jones P, Summerhayes I, Marshall F, Paul M, Green P, Hamilton SR, Frost P and et al. (1991) Identification of p53 gene mutations in bladder cancers and urine samples. *Science* **252**(5006): 706-709.

Siegel RL, Miller KD and Jemal A (2020) Cancer statistics, 2020. *CA Cancer J Clin* **70**(1): 7-30.

Simanshu DK, Nissley DV and McCormick F (2017) RAS Proteins and Their Regulators in Human Disease. *Cell* **170**(1): 17-33.

Solit DB, Garraway LA, Pratilas CA, Sawai A, Getz G, Basso A, Ye Q, Lobo JM, She Y, Osman I, Golub TR, Sebolt-Leopold J, Sellers WR and Rosen N (2006) BRAF mutation predicts sensitivity to MEK inhibition. *Nature* **439**(7074): 358-362.

Spruck CH, 3rd, Ohneseit PF, Gonzalez-Zulueta M, Esrig D, Miyao N, Tsai YC, Lerner SP, Schmutte C, Yang AS, Cote R and et al. (1994) Two molecular pathways to transitional cell carcinoma of the bladder. *Cancer Res* **54**(3): 784-788.

Stanton VP, Jr. and Cooper GM (1987) Activation of human raf transforming genes by deletion of normal amino-terminal coding sequences. *Mol Cell Biol* **7**(3): 1171-1179.

Stokoe D, Macdonald SG, Cadwallader K, Symons M and Hancock JF (1994) Activation of Raf as a result of recruitment to the plasma membrane. *Science* **264**(5164): 1463-1467.

Straussman R, Morikawa T, Shee K, Barzily-Rokni M, Qian ZR, Du J, Davis A, Mongare MM, Gould J, Frederick DT, Cooper ZA, Chapman PB, Solit DB, Ribas A, Lo RS, Flaherty KT, Ogino S, Wargo JA and Golub TR (2012) Tumour micro-environment elicits innate resistance to RAF inhibitors through HGF secretion. *Nature* **487**(7408): 500-504.

Sturgill TW, Ray LB, Erikson E and Maller JL (1988) Insulin-stimulated MAP-2 kinase phosphorylates and activates ribosomal protein S6 kinase II. *Nature* **334**(6184): 715-718.

Sumimoto H, Miyagishi M, Miyoshi H, Yamagata S, Shimizu A, Taira K and Kawakami Y (2004) Inhibition of growth and invasive ability of melanoma by inactivation of mutated BRAF with lentivirus-mediated RNA interference. *Oncogene* **23**(36): 6031-6039.

Sun C, Wang L, Huang S, Heynen GJ, Prahallad A, Robert C, Haanen J, Blank C, Wesseling J, Willems SM, Zecchin D, Hobor S, Bajpe PK, Lieftink C, Mateus C, Vagner S, Grernrum W, Hofland I, Schlicker A, Wessels LF, Beijersbergen RL, Bardelli A, Di Nicolantonio F, Eggermont AM and Bernards R (2014) Reversible and adaptive resistance to BRAF(V600E) inhibition in melanoma. *Nature* **508**(7494): 118-122.

Sylvester RJ, Oosterlinck W, Holmang S, Sydes MR, Birtle A, Gudjonsson S, De Nunzio C, Okamura K, Kaasinen E, Solsona E, Ali-El-Dein B, Tatar CA, Inman BA, N'Dow J, Oddens JR and Babjuk M (2016) Systematic Review and Individual Patient Data Meta-analysis of Randomized Trials Comparing a Single Immediate Instillation of Chemotherapy After Transurethral Resection with Transurethral Resection Alone in Patients with Stage pTa-pT1 Urothelial Carcinoma of the Bladder: Which Patients Benefit from the Instillation? *Eur Urol* **69**(2): 231-244.

Tanimoto K, Makino Y, Pereira T and Poellinger L (2000) Mechanism of regulation of the hypoxia-inducible factor-1 alpha by the von Hippel-Lindau tumor suppressor protein. *EMBO J* **19**(16): 4298-4309.

Thevakumaran N, Lavoie H, Critton DA, Tebben A, Marinier A, Sicheri F and Therrien M (2015) Crystal structure of a BRAF kinase domain monomer explains basis for allosteric regulation. *Nat Struct Mol Biol* **22**(1): 37-43.

Tian T, Harding A, Inder K, Plowman S, Parton RG and Hancock JF (2007) Plasma membrane nanoswitches generate high-fidelity Ras signal transduction. *Nat Cell Biol* **9**(8): 905-914.

Tomlinson DC, Baldo O, Harnden P and Knowles MA (2007) FGFR3 protein expression and its relationship to mutation status and prognostic variables in bladder cancer. *J Pathol* **213**(1): 91-98.

Tomlinson DC and Knowles MA (2010) Altered splicing of FGFR1 is associated with high tumor grade and stage and leads to increased sensitivity to FGF1 in bladder cancer. *Am J Pathol* **177**(5): 2379-2386.

Tomlinson DC, Lamont FR, Shnyder SD and Knowles MA (2009) Fibroblast growth factor receptor 1 promotes proliferation and survival via activation of the mitogen-activated protein kinase pathway in bladder cancer. *Cancer Res* **69**(11): 4613-4620.

Trepanier LA, Ray K, Winand NJ, Spielberg SP and Cribb AE (1997) Cytosolic arylamine N-acetyltransferase (NAT) deficiency in the dog and other canids due to an absence of NAT genes. *Biochem Pharmacol* **54**(1): 73-80.

Trunzer K, Pavlick AC, Schuchter L, Gonzalez R, McArthur GA, Hutson TE, Moschos SJ, Flaherty KT, Kim KB, Weber JS, Hersey P, Long GV, Lawrence D, Ott PA, Amaravadi RK, Lewis KD, Puzanov I, Lo RS, Koehler A, Kockx M, Spleiss O, Schell-Steven A, Gilbert HN, Cockey L, Bollag G, Lee RJ, Joe AK, Sosman JA and Ribas A (2013) Pharmacodynamic effects and mechanisms of resistance to vemurafenib in patients with metastatic melanoma. *J Clin Oncol* **31**(14): 1767-1774.

Tzivion G, Luo Z and Avruch J (1998) A dimeric 14-3-3 protein is an essential cofactor for Raf kinase activity. *Nature* **394**(6688): 88-92.

Van Allen EM, Wagle N, Sucker A, Treacy DJ, Johannessen CM, Goetz EM, Place CS, Taylor-Weiner A, Whittaker S, Kryukov GV, Hodis E, Rosenberg M, McKenna A, Cibulskis K, Farlow D, Zimmer L, Hillen U, Gutzmer R, Goldinger SM, Ugurel S, Gogas HJ, Egberts F, Berking C, Trefzer U, Loquai C, Weide B, Hassel JC, Gabriel SB, Carter SL, Getz G, Garraway LA, Schadendorf D and Dermatologic Cooperative Oncology Group of G (2014) The genetic landscape of clinical resistance to RAF inhibition in metastatic melanoma. *Cancer Discov* **4**(1): 94-109.

van Rhijn BW, Lurkin I, Radvanyi F, Kirkels WJ, van der Kwast TH and Zwarthoff EC (2001) The fibroblast growth factor receptor 3 (FGFR3) mutation is a strong indicator of superficial bladder cancer with low recurrence rate. *Cancer Res* **61**(4): 1265-1268.

Vander Heiden MG, Cantley LC and Thompson CB (2009) Understanding the Warburg effect: the metabolic requirements of cell proliferation. *Science* **324**(5930): 1029-1033.

Vashisht Gopal YN, Gammon S, Prasad R, Knighton B, Pisaneschi F, Roszik J, Feng N, Johnson S, Pramanik S, Sudderth J, Sui D, Hudgens C, Fischer GM, Deng W, Reuben A, Peng W, Wang J, McQuade JL, Tetzlaff MT, Di Francesco ME, Marszalek J, Piwnica-Worms D, DeBerardinis RJ and Davies MA (2019) A Novel Mitochondrial Inhibitor Blocks MAPK Pathway and Overcomes MAPK Inhibitor Resistance in Melanoma. *Clin Cancer Res* **25**(21): 6429-6442.

Vojtek AB, Hollenberg SM and Cooper JA (1993) Mammalian Ras interacts directly with the serine/threonine kinase Raf. *Cell* **74**(1): 205-214.

Wagle N, Emery C, Berger MF, Davis MJ, Sawyer A, Pochanard P, Kehoe SM, Johannessen CM, Macconaill LE, Hahn WC, Meyerson M and Garraway LA (2011) Dissecting therapeutic resistance to RAF inhibition in melanoma by tumor genomic profiling. *J Clin Oncol* **29**(22): 3085-3096.

Wan PT, Garnett MJ, Roe SM, Lee S, Niculescu-Duvaz D, Good VM, Jones CM, Marshall CJ, Springer CJ, Barford D, Marais R and Cancer Genome P (2004) Mechanism of activation of the RAF-ERK signaling pathway by oncogenic mutations of B-RAF. *Cell* **116**(6): 855-867.

Wang GL and Semenza GL (1995) Purification and characterization of hypoxia-inducible factor 1. *J Biol Chem* **270**(3): 1230-1237.

Wang H, Daouti S, Li WH, Wen Y, Rizzo C, Higgins B, Packman K, Rosen N, Boylan JF, Heimbrook D and Niu H (2011) Identification of the MEK1(F129L) activating mutation as a potential mechanism of acquired resistance to MEK inhibition in human cancers carrying the B-RafV600E mutation. *Cancer Res* **71**(16): 5535-5545.

Warburg O (1956a) On respiratory impairment in cancer cells. *Science* **124**(3215): 269-270.

Warburg O (1956b) On the origin of cancer cells. *Science* **123**(3191): 309-314.

Warne PH, Viciana PR and Downward J (1993) Direct interaction of Ras and the amino-terminal region of Raf-1 in vitro. *Nature* **364**(6435): 352-355.

Waskiewicz AJ, Johnson JC, Penn B, Mahalingam M, Kimball SR and Cooper JA (1999) Phosphorylation of the cap-binding protein eukaryotic translation initiation factor 4E by protein kinase Mnk1 in vivo. *Mol Cell Biol* **19**(3): 1871-1880.

Weber CK, Slupsky JR, Kalmes HA and Rapp UR (2001) Active Ras induces heterodimerization of cRaf and BRaf. *Cancer Res* **61**(9): 3595-3598.

Weinberg RA (1995) The retinoblastoma protein and cell cycle control. *Cell* **81**(3): 323-330.

Wellbrock C, Rana S, Paterson H, Pickersgill H, Brummelkamp T and Marais R (2008) Oncogenic BRAF regulates melanoma proliferation through the lineage specific factor MITF. *PLoS One* **3**(7): e2734.

Whittaker SR, Theurillat JP, Van Allen E, Wagle N, Hsiao J, Cowley GS, Schadendorf D, Root DE and Garraway LA (2013) A genome-scale RNA interference screen implicates NF1 loss in resistance to RAF inhibition. *Cancer Discov* **3**(3): 350-362.

Widmann C, Gibson S, Jarpe MB and Johnson GL (1999) Mitogen-activated protein kinase: conservation of a three-kinase module from yeast to human. *Physiol Rev* **79**(1): 143-180.

Williamson MP, Elder PA, Shaw ME, Devlin J and Knowles MA (1995) p16 (CDKN2) is a major deletion target at 9p21 in bladder cancer. *Hum Mol Genet* **4**(9): 1569-1577.

Wilson TR, Fridlyand J, Yan Y, Penuel E, Burton L, Chan E, Peng J, Lin E, Wang Y, Sosman J, Ribas A, Li J, Moffat J, Sutherlin DP, Koeppen H, Merchant M, Neve R and Settleman J (2012) Widespread potential for growth-factor-driven resistance to anticancer kinase inhibitors. *Nature* **487**(7408): 505-509.

Withrow SJ and Wilkins RM (2010) Cross talk from pets to people: translational osteosarcoma treatments. *ILAR J* **51**(3): 208-213.

Witjes JA, Bruins HM, Cathomas R, Comperat EM, Cowan NC, Gakis G, Hernandez V, Linares Espinos E, Lorch A, Neuzillet Y, Rouanne M, Thalmann GN, Veskimae E, Ribal MJ and van der Heijden AG (2021) European Association of Urology Guidelines on Muscle-invasive and Metastatic Bladder Cancer: Summary of the 2020 Guidelines. *Eur Urol* **79**(1): 82-104.

Wu XR (2005) Urothelial tumorigenesis: a tale of divergent pathways. *Nature reviews Cancer* **5**(9): 713-725.

Xu GF, Lin B, Tanaka K, Dunn D, Wood D, Gesteland R, White R, Weiss R and Tamanoi F (1990) The catalytic domain of the neurofibromatosis type 1 gene product stimulates ras GTPase and complements ira mutants of S. cerevisiae. *Cell* **63**(4): 835-841.

Yang H, Higgins B, Kolinsky K, Packman K, Go Z, Iyer R, Kolis S, Zhao S, Lee R, Grippo JF, Schostack K, Simcox ME, Heimbrook D, Bollag G and Su F (2010) RG7204 (PLX4032), a selective BRAFV600E inhibitor, displays potent antitumor activity in preclinical melanoma models. *Cancer Res* **70**(13): 5518-5527.

Yao Z, Gao Y, Su W, Yaeger R, Tao J, Na N, Zhang Y, Zhang C, Rymar A, Tao A, Timaul NM, McGriskin R, Outmezguine NA, Zhao H, Chang Q, Qeriqi B, Barbacid M, de Stanchina E, Hyman DM, Bollag G and Rosen N (2019) RAF inhibitor PLX8394 selectively disrupts BRAF dimers and RAS-independent BRAF-mutant-driven signaling. *Nat Med* **25**(2): 284-291.

Yin M, Joshi M, Meijer RP, Glantz M, Holder S, Harvey HA, Kaag M, Fransen van de Putte EE, Horenblas S and Drabick JJ (2016) Neoadjuvant Chemotherapy for Muscle-Invasive Bladder Cancer: A Systematic Review and Two-Step Meta-Analysis. *Oncologist* **21**(6): 708-715.

Yoon S and Seger R (2006) The extracellular signal-regulated kinase: multiple substrates regulate diverse cellular functions. *Growth Factors* **24**(1): 21-44.

Zadra G, Batista JL and Loda M (2015) Dissecting the Dual Role of AMPK in Cancer: From Experimental to Human Studies. *Mol Cancer Res* **13**(7): 1059-1072.

Zhang BH and Guan KL (2000) Activation of B-Raf kinase requires phosphorylation of the conserved residues Thr598 and Ser601. *EMBO J* **19**(20): 5429-5439.

Zhang C, Spevak W, Zhang Y, Burton EA, Ma Y, Habets G, Zhang J, Lin J, Ewing T, Matusow B, Tsang G, Marimuthu A, Cho H, Wu G, Wang W, Fong D, Nguyen H, Shi S, Womack P, Nespi M, Shellooe R, Carias H, Powell B, Light E, Sanftner L, Walters J, Tsai J, West BL, Visor G, Rezaei H, Lin PS, Nolop K, Ibrahim PN, Hirth P and Bollag G (2015) RAF inhibitors that evade paradoxical MAPK pathway activation. *Nature* **526**(7574): 583-586.

Zhang G, Frederick DT, Wu L, Wei Z, Krepler C, Srinivasan S, Chae YC, Xu X, Choi H, Dimwamwa E, Ope O, Shannan B, Basu D, Zhang D, Guha M, Xiao M, Randell S, Sproesser K, Xu W, Liu J, Karakousis GC, Schuchter LM, Gangadhar TC, Amaravadi RK, Gu M, Xu C, Ghosh A, Xu W, Tian T, Zhang J, Zha S, Liu Q, Brafford P, Weeraratna A, Davies MA, Wargo JA, Avadhani NG, Lu Y, Mills GB, Altieri DC, Flaherty KT and Herlyn M (2016) Targeting mitochondrial biogenesis to overcome drug resistance to MAPK inhibitors. *J Clin Invest* **126**(5): 1834-1856.

Zhang W and Liu HT (2002) MAPK signal pathways in the regulation of cell proliferation in mammalian cells. *Cell Res* **12**(1): 9-18.

Zhang XF, Settleman J, Kyriakis JM, Takeuchi-Suzuki E, Elledge SJ, Marshall MS, Bruder JT, Rapp UR and Avruch J (1993) Normal and oncogenic p21ras proteins bind to the amino-terminal regulatory domain of c-Raf-1. *Nature* **364**(6435): 308-313.

Zhang Z, Zhou L, Xie N, Nice EC, Zhang T, Cui Y and Huang C (2020) Overcoming cancer therapeutic bottleneck by drug repurposing. *Signal Transduct Target Ther* **5**(1): 113.

Zheng B, Jeong JH, Asara JM, Yuan YY, Granter SR, Chin L and Cantley LC (2009) Oncogenic B-RAF negatively regulates the tumor suppressor LKB1 to promote melanoma cell proliferation. *Mol Cell* **33**(2): 237-247.

Zieger K, Dyrskjot L, Wiuf C, Jensen JL, Andersen CL, Jensen KM and Orntoft TF (2005) Role of activating fibroblast growth factor receptor 3 mutations in the development of bladder tumors. *Clin Cancer Res* **11**(21): 7709-7719.

CHAPTER 2

A molecular and immune characterization of canine bladder cancer[1]

SUMMARY

Transitional cell carcinoma (TCC) is the most common bladder cancer in humans and dogs. Approximately one-quarter of human TCCs are muscle-invasive and associated with a high risk of death from metastasis. Canine TCC (cTCC) tumors are typically high-grade and invasive at diagnosis. Canine and human TCCs share similarities in risk factors, histopathology, and clinical presentation, suggesting cTCC may serve as a model for the assessment of novel therapeutics that may inform therapies for human muscle-invasive TCC. The goal of this study was to characterize cTCC at the molecular level to identify drivers of oncogenesis and druggable targets. We performed whole exome sequencing (WES) of 11 cTCC tumors and 3 matched normal samples, identifying 583 variants in known protein-coding genes. The most common variant was a V-to-E missense variant in the proto-oncogene *BRAF*, identified in 4 out of 11 samples via WES and confirmed using Sanger sequencing in 70% of samples. Variants in the cancer-related genes *LRP1B*, *CUL3*, *MSH2*, and *RNF213* were also detected in at least two samples. RNA-Seq was performed to compare the gene expression profiles of cTCC tumors to normal bladder tissue. cTCC tumors exhibited up-regulation of genes involved in the cell cycle, DNA repair, and antiviral

[1] Thank you to the many people who contributed to this chapter: Dawn Duval, Dan Gustafson, Sunetra Das, Dan Regan, Belen Hernandez, Susan Lana, Deanna Dailey, Rodney Page, and Robert McGeacham

immunity. We also analyzed the immune landscape of cTCC using immune gene signatures and immunohistochemical (IHC) analysis. A subset of tumors had characteristics of a hot tumor microenvironment (TME) and was associated with genomic indicators of response to PD-1/PD-L1 blockade in human muscle-invasive bladder cancer.

INTRODUCTION

Bladder cancer comprises over 4% of diagnosed human malignancies in the United States, with an estimated 80,000 new cases diagnosed in 2019 (Siegel et al., 2019). TCC, the most common bladder cancer in humans, is broken into superficial, non-muscle-invasive TCC (~70%) and muscle-invasive TCC (~30%) (Knowles and Hurst, 2015). Non-muscle-invasive bladder cancer has a five-year survival rate of 90%; however, the disease has a high rate of recurrence (Knowles and Hurst, 2015). Muscle-invasive TCC has a poorer prognosis, with a five-year survival rate of 50% for all patients and only 5% for those with distant metastasis (Knowles and Hurst, 2015). Increased focus on cancer as a molecular disease has emphasized the relevance of comparative oncology, providing a translational opportunity to identify mechanisms underlying cancer progression and to evaluate novel therapeutics in spontaneous tumors in companion animals that may inform studies in human cancer patients (Gordon et al., 2009; LeBlanc and Mazcko, 2020).

Similar to humans, most bladder tumors in dogs are TCCs, accounting for 2% of diagnosed canine cancers (Knapp and McMillan, 2013). The majority of cTCCs are

muscle-invasive tumors of intermediate- to high-grade at diagnosis (Knapp et al., 2014). Treatment of cTCC typically consists of cyclooxygenase inhibitors and/or chemotherapeutic agents; however, cTCC has a poor prognosis with a median survival time of less than a year for most treatments (Fulkerson and Knapp, 2015; Knapp and McMillan, 2013). Risk factors common to humans and dogs include living in urban areas, environmental exposure to benzene and polycyclic aromatic hydrocarbons, and prior treatment with cyclophosphamide (Mutsaers et al., 2003). Both species also have race- or breed-associated subpopulations that exhibit increased risk (Knapp et al., 2014; Mutsaers et al., 2003). Additionally, human and canine muscle-invasive TCCs share similarities in histopathology, clinical presentation, and sites of metastasis (Knapp et al., 2014).

The Cancer Genome Atlas performed a comprehensive genomic analysis of 412 chemotherapy-naïve, muscle-invasive human bladder tumors, identifying molecular alterations that may aid in future diagnosis and treatment of the disease (Robertson et al., 2017). Inactivation of the p53/cell cycle pathway occurred in ~90% of tumors, mainly via mutations in *TP53* and *RB1*, copy number loss of *CDKN2A*, and amplification/overexpression of *MDM2* (Robertson et al., 2017). Activating alterations in the RTK/Ras/PI(3)K pathway were common, including mutations in *FGFR3*, *PIK3CA*, and the RAS gene family (Robertson et al., 2017). Human muscle-invasive TCCs also frequently harbor mutations in chromatin modifiers such as histone demethylases and methyltransferases (Gui et al., 2011; Robertson et al., 2017).

In this study, we characterize the molecular features of 11 cTCC tumors by integrating whole exome sequencing and RNA-Seq to identify alterations contributing to pathogenesis as well as putative druggable targets. A major advantage of comparative

oncology is the ability to evaluate novel immunotherapies in naturally occurring tumors under normal immunosurveillance. Thus, we examined the immune landscape of cTCC using both gene expression and immunohistochemistry. Herein, we identify an immunologically hot subset of cTCC tumors exhibiting high expression of gene signatures associated with complete response to PD-1/PD-L1 blockade in human bladder cancer.

MATERIALS AND METHODS

Patients and samples

TCC tumor and matched normal tissue samples were collected through our institution's tumor biorepository program with IACUC approval and informed owner consent. Pathological review identified 11 TCC samples containing >70% tumor by mass. Nine out of 11 patients were male and the average age of diagnosis was 10.9 years (**Table 2.1**). Normal bladder samples were obtained from healthy research hounds.

Table 2.1. Patient and sample characteristics.

Sample Name	Breed	Sex	Age at diagnosis (years)	Matched Normal?	Estimated DFI (days)
Tumor					
T-1025	Airedale Terrier	MC	8.5	N	300
T-113	Mix	MC	13.7	N	102
T-22	Dachshund - Long Haired Standard	MI	11.1	N	480
T-353	Mix	MC	11.8	Y	240
T-36	Mix	MC	7.3	N	95
T-400	Mix	MC	10.4	Y	120
T-500	Shetland sheepdog	FS	8	Y	90
T-522	Dalmatian	FS	13.2	N	690

T-730	Mix	MC	14.7	N	35
T-735	Mix	MC	12.3	N	65
T-868	Mix	MC	9.3	N	150
Normal					
N-6970	Research hound	FI			
N-6994	Research hound	FI			
N-6998	Research hound	FI			

Genomic DNA and RNA Isolation

Tumor and normal tissues were freeze-fractured and homogenized in TRIzol Reagent (Thermo Fisher Scientific, Waltham, MA). RNA and DNA were isolated according to the manufacturer's recommendations. RNA was purified using the RNeasy Cleanup Kit (Qiagen, Hilden, Germany). Genomic DNA was purified using either DNeasy Blood and Tissue or QIAamp DNA Micro Kits (Qiagen).

Whole exome sequencing and analysis pipeline

Three µg of genomic DNA from 11 cTCC tumors and three matched normal samples was fragmented by sonication for a mean fragment size of 300 bp. Fragments were prepared for sequencing and captured using the Canine SureSelect V1 capture kit (53.59 Mb, part number 5190-5452, Agilent, Santa Clara, CA) based on the CanFam2.0 genome assembly. Sequencing was performed on an Illumina HiSeq 2500 (Illumina, San Diego, CA) generating 100 bp, paired-end reads.

FASTQ files were trimmed using Trimmomatic (v0.36) (Bolger et al., 2014). Reads were mapped to CanFam3.1 using BWA-MEM (v0.7.15) (Li and Durbin, 2009). Duplicate reads were identified using the Picard (v1.119) tool MarkDuplicates. Base Quality Score Recalibration was performed on alignment files using the GATK (v4) tools BaseRecalibrator and ApplyBQSR in accordance with GATK best practices (Van der

Auwera et al., 2013). Tumor and matched normal variants were called using Freebayes, with a min-alternate-count of 2 and a min-alternate-fraction of 0.05. Raw variants for tumor and matched normal samples were filtered for a minimum depth (DP) of 10. Raw tumor variants were further filtered for a minimum quality (QUAL) of 1 using SnpEff (v4.3t) (Cingolani et al., 2012).

Tumor variants were then screened against variants from an in-house panel of normals created from 43 canine normal samples, including the 3 matched normals in this study, and previously identified canine germline variants (Bai et al., 2015; Elvers et al., 2015; Plassais et al., 2019) to obtain a list of 3,340 somatic variants after removing variants with genotype 0/0. Annotation of somatic variants was performed using the Ensembl Variant Effect Predictor (v99) (McLaren et al., 2016). Mutational burden was determined by dividing the number of somatic variants in a sample by captured megabases (53.59 Mb).

Sanger sequencing of variants

Sanger sequencing was performed to confirm variants in *BRAF*, *MSH2*, *ARID1A*, *PTPRB,* and *BRCA2* that were identified with WES. An additional 32 formalin-fixed paraffin-embedded (FFPE) TCC samples were also screened for BRAF variants. Diagnosis of FFPE samples was confirmed and DNA was isolated as previously described (Dailey et al., 2015). Polymerase chain reaction was conducted using GoTaq Flexi reagents (Promega, Madison, WI) with the primers listed in **Table 2**. Polymerase chain reaction products were gel isolated (QIAquick Gel Extraction Kit, Qiagen) and sequenced at CSU.

Table 2.2 List of primers used in Sanger sequencing.		
Gene	**5' Primer**	**3' Primer**
BRAF	GCTTGCTTTGCTAGGAAAATG	GTAGCACCTCAGGGTCCAAA
MSH2	AAGTTAATTTATTCCCATAATGGCTTA	CCCAAAGAAAGCCCATAATT
PTPRB	AGAAAGGGCTAGAGGGAAGA	CGTTATGTATCTCAGGGACTGTG
JAK1	CGACAGAAGGTCCCAGATGT	TTCTGGTTCCTGGTGGAGAC
BRCA2	TGACCTTGAGAATATCAATGAGGA	GCTTTCATAACTTCCAAACAGG
ARID1A	GCCATCTCCTCGTCATTTTC	GGCAGGATGGACACACTTCT

RNA-Seq Analysis

RNA sequencing was performed on 11 cTCC tumor samples as well as three normal bladder samples obtained from healthy dogs. A poly(A) selected library was prepared using a Universal mRNA-Seq Library Preparation Kit (NuGEN Technologies, Inc., San Carlos, CA) and sequenced on an Illumina NovaSEQ 6000 generating 150 bp, pair-end reads.

Raw FASTQ reads were trimmed using Trimmomatic (v0.36) (Bolger et al., 2014) and mapped against the CanFam3.1 genome with Tophat (v2.1.0) (Trapnell et al., 2013). Count data was determined using HTseq-Count (v0.11.4) and relative FPKM expression values were extracted using Cufflinks (v2.2.1) (Anders et al., 2015; Trapnell et al., 2010). Genes that are unexpressed or expressed at very low levels were removed by filtering for a minimum count of 10 in at least 3 samples, resulting in 17,225 expressed genes with Ensembl identifiers. Differentially expressed genes (DEGs) were identified using the 'DESeq2' R package (Love et al., 2014), requiring a Benjamini and Hochberg adjusted p-value cutoff of 0.05 and a minimum $\log_2$ fold change of 2 (when comparing tumors to normal bladder samples) or 1 (when comparing between tumors).

Heat maps were generated in R using the 'ComplexHeatmap' package (Gu et al., 2016).

Functional analysis using DAVID

Functional annotation of mutated and/or differentially expressed genes was performed using DAVID functional annotation tool (Huang da et al., 2009a; Huang da et al., 2009b). Genes were screened for enrichment of KEGG pathways as well as Biological Process and Molecular Function Gene Ontology (GO) terms using a p-value cutoff of 0.05 and a minimum gene count of 3.

Gene set enrichment analysis (GSEA)

GSEA software (v4) was used to compare gene expression profiles between sample groups (Mootha et al., 2003; Subramanian et al., 2005). Normalized gene counts were used as input. All runs were performed using the "gene_set" permutation type with default parameters. Samples were screened for enrichment of "Hallmarks" gene sets present in the Molecular Signatures Database (v7.0). Gene sets with FDR q-val < 0.05 were considered to be significantly enriched.

Gene set variation analysis (GSVA)

GSVA was implemented to analyze enrichment of specific gene sets in an unsupervised manner (Hanzelmann et al., 2013). GSVA enrichment scores were estimated using the R package 'GSVA' with $\log_2$-CPM expression values as input. Tumors were analyzed for relative enrichment of previously described immune gene signatures. GSVA enrichment scores were compared between phenotypes using the 'limma' R package as previously described (Hanzelmann et al., 2013; Ritchie et al., 2015).

Immunohistochemical analysis

Archived FFPE tissue samples were obtained from our institution's Diagnostic Laboratory. Available paraffin blocks were routinely processed for hematoxylin and eosin (H&E) staining, as well as IHC. IHC was performed via routine, automated methods on the Leica Bond Max autostainer (Leica Biosystems, Wetzlar, Germany), with the following panel of previously published canine cross-reactive antibodies: rabbit polyclonal anti-human CD3 (pan T lymphocyte marker; Dako, #A0452), monoclonal mouse anti-human Myeloid/Histiocyte antigen (MAC387; Dako, clone MAC387), and mouse anti-human FOXP3 (regulatory T cells; ThermoFisher, clone eBio7979). Antigen retrieval was performed using Leica Epitope Retrieval 2 (Tris-EDTA buffer, pH 9) for 20 min. Detection was performed with PowerVision IHC detection systems (Leica Biosystems), using either a polymeric horseradish peroxidase anti-mouse IgG and DAB chromogen (FOXP3) or polymeric alkaline phosphatase anti-mouse IgG (MAC387) or anti-rabbit IgG (CD3) and Fast Red chromogen. All H&E slides were reviewed by a single pathologist to confirm the diagnosis.

Whole slide brightfield images of IHC stained slides were digitally captured using an Olympus IX83 microscope at 10x magnification. Quantitative image analysis was performed using open source ImageJ software. Tumor tissue regions-of-interest (ROIs) were segmented from adjacent normal tissue by manual outlining in ImageJ in blinded fashion by Dr. Daniel Regan. Following determination of the ROI, positively labeled infiltrating immune cells were counted using the color deconvolution algorithm. Briefly, a positive pixel threshold for all immune cell markers was determined visually by a veterinary pathologist using appropriate isotype-stained control slides. Images were

subjected to color deconvolution, followed by global, automated application of this intensity threshold to all images. Following automated image analysis, positive pixel masks of each image were blindly evaluated by a pathologist to ensure thresholding accuracy. Data was analyzed and expressed as the number of infiltrating immune cells/mm^2 of the ROI of the tumor tissue.

Data Availability

Raw FASTQ sequences from the WES and RNA-Seq analysis were submitted to NCBI's SRA database (Sayers et al., 2019). Sequence data for tumor and normal samples can be found under BioProject PRJNA616374 and PRJNA503860, respectively.

RESULTS

Mutation profile of cTCC

WES analysis identified 3,340 total somatic variants among 11 cTCC tumors. Mutational burden was less than 10 mutations per captured Mb for all samples, ranging from 1.9 to 7.9 mutations/Mb, with a mean of 5.7 mutations/Mb (**Figure 2.1**). C>T transitions were the most prevalent base alteration, comprising 45% of single base substitutions, followed by T>C transitions (18%) and C>A transversions (15%) (**Figure 2.1**). 80% of somatic variants were single nucleotide polymorphisms, while insertions and deletions made up 6 and 7 % of somatic variants, respectively.

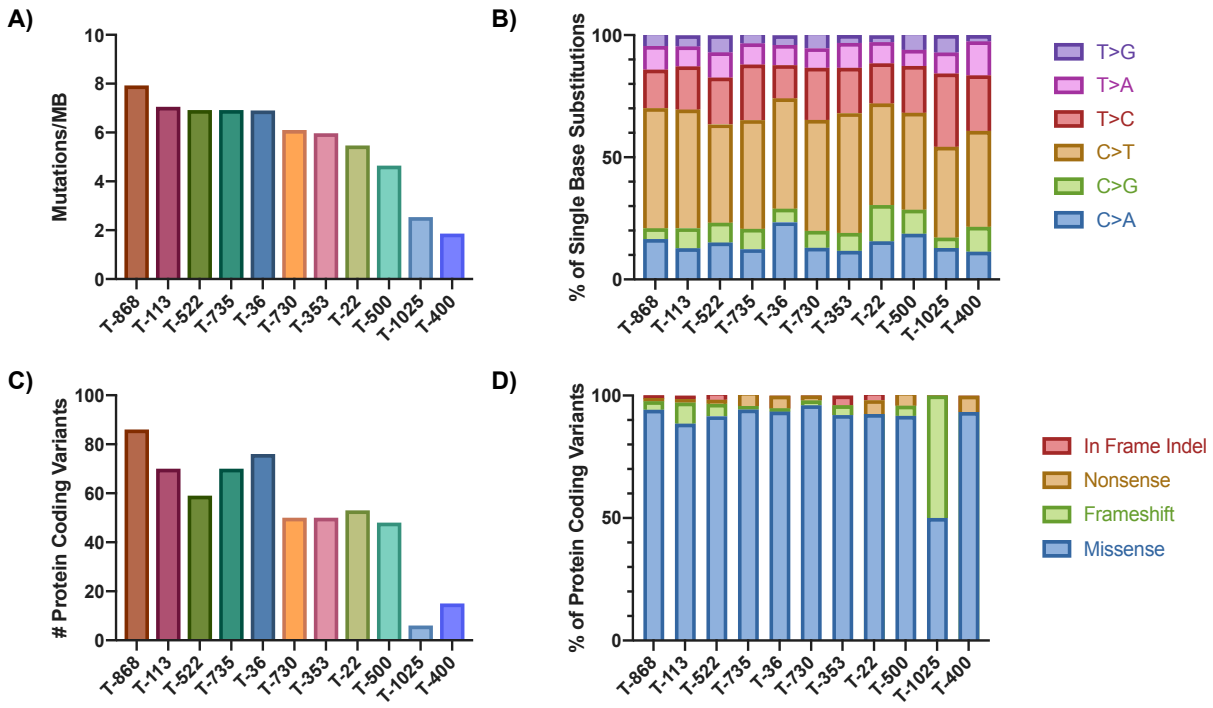

Figure 2.1 Mutation profile of cTCC.
(A) Mutational burden shown as somatic mutations per captured megabase. (B) Relative abundance of single base substitutions for somatic variants. (C) Number of protein-coding variants per sample. (D) Relative abundance of protein coding variants.

Somatic variants were filtered for protein-coding variants, including in-frame indels and missense, frameshift, and nonsense variants. A total of 583 protein-altering variants were identified, ranging from 6 (T-1025) to 86 (T-868) per sample (**Figure 2.1**, **Figure 2.2**). Missense mutations comprised 92% of protein-coding variants (**Figure 2.1**). DAVID functional annotation tool was used to identify enriched pathways and GO terms among the list of protein-coding variants. The top enriched pathways include Axon guidance, Focal adhesion, and MAPK signaling. The top enriched GO Molecular Function and Biological Process terms were “ATP binding” and “negative regulation of neuron apoptosis”, respectively (**Table 2.3**).

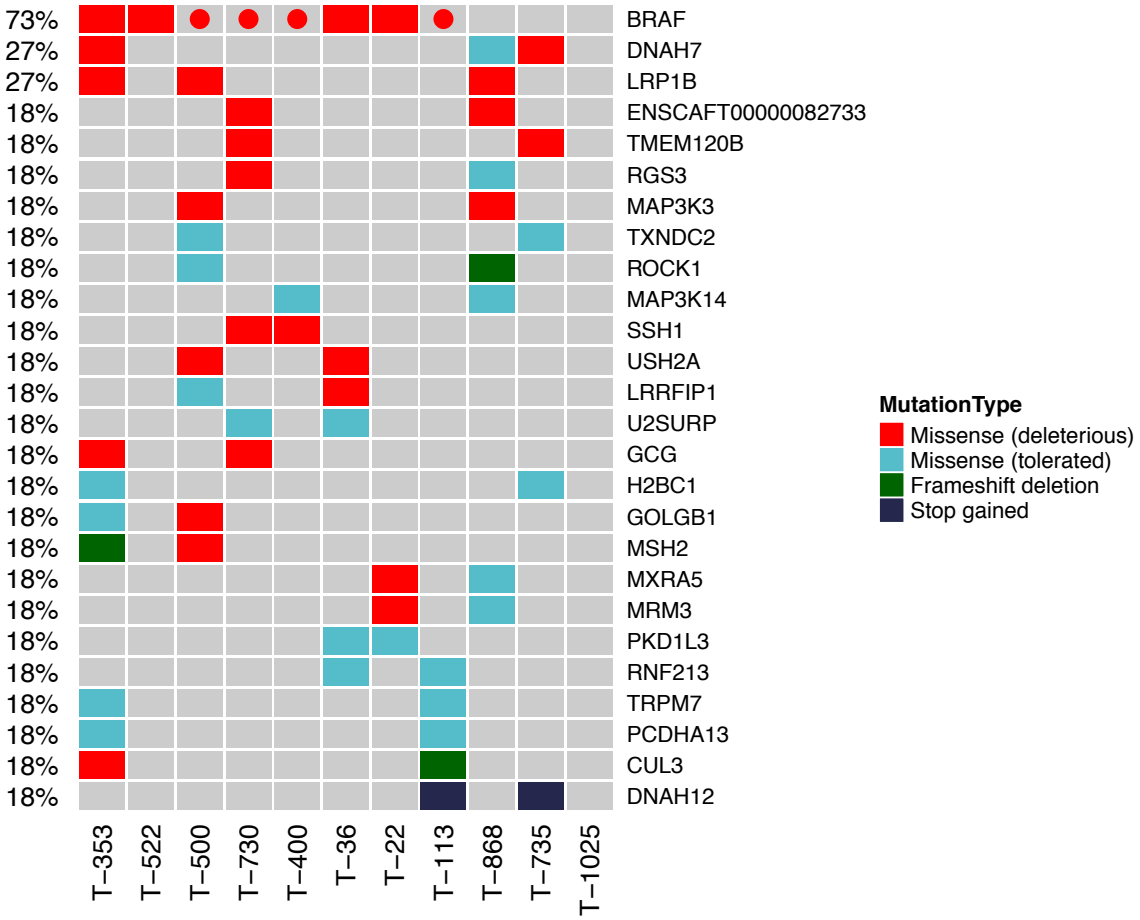

Figure 2.2 Oncoplot of protein-coding variants present in two or more samples. Missense variants with SIFT < 0.05 are considered deleterious. BRAF variants that were detected via Sanger sequencing only are shown as circles.

Table 2.3 Functional annotation of protein-coding variants using DAVID.

Term	Genes	n	p-val
GO:0005524 ATP binding	KIFC2, CLPB, MLH3, TLR9, ACSS1, DDX17, DDX18, DDX60, TOP2B, BRAF, ROCK1, TRPM7, MYH3, RBKS, CFTR, LIG4, NAV3, GMPS, NME7, PRKD1, MAP4K3, HIPK2, PDGFRB, KIF19, YARS2, MAP3K14, SMARCA2, DNAH12, ERBB4, MYO9B, SPO11, DNAH6, EPHB6, MAP3K3, DGKG, CHD1, ABCA13, ABCA12, CSNK1A1, GUCY2F,	61	<0.001

	MYO1A, SMCHD1, FLT1, KIF3A, MSH2, SMG1, AK5, ACACB, DGKI, ATR, WRN, EPHA3, RPS6KA5, EPHA5, ABCC9, UBA1, CCT8, ARAF, JAK1, GRK3, KATNAL2		
GO:0043524 negative regulation of neuron apoptotic process	NRP1, GABRB3, ROCK1, BRAF, MSH2, GRIK2, NR4A2, MECP2, STXBP1, LIG4, HIPK2, SYNGAP1, CHL1	13	<0.001
GO:0016887 ATPase activity	KIFC2, KIF3A, DNAH12, MSH2, MYO9B, KIF19, MLH3, DNAH7, SMARCA2, RNF213, DNAH6	11	<0.001
cfa04360 Axon guidance	EPHA5, EPHB6, NRP1, ROCK1, SEMA6D, RGS3, ROBO2, LRRC4C, ARHGEF12, NFATC3, SLIT2, EPHA3	12	<0.001
GO:0005509 calcium ion binding	SYT7, EDEM2, MMP3, DNAH7, EDEM1, PKD1L3, CIB4, CAPS2, CDH9, DNER, DGKG, FAT1, PLCB1, THBS3, CDH23, ADGRE1, NIN, BRAF, CAPN8, LRP1B, PCDH10, PCDHB1, SLIT2, EPS15, NOTCH3, WDR49, CDH19, NOTCH4	28	0.003
GO:0051276 chromosome organization	RLF, SMCHD1, BRCA2, LIG4	4	0.004
GO:0007156 homophilic cell adhesion via plasma membrane adhesion molecules	CDH9, FAT1, CDH19, PCDH10, PCDHB1, ROBO2, IGSF9B, CDH23	8	0.008
GO:0035556 intracellular signal transduction	PLCZ1, GUCY2F, BRAF, MYO9B, DEPDC1, DGKI, ARHGEF12, PRKD1, RPS6KA5, RGS11, GMIP, MAP3K3, DGKG, ARAF, JAK1, PLCB1	16	0.009
cfa05206 MicroRNAs in cancer	NOTCH3, RPS6KA5, DNMT3A, ROCK1, SERPINB5, TNR, NOTCH4, PDGFRB, STMN1, CDC25B	10	0.012
GO:0051480 regulation of cytosolic calcium ion concentration	HCRTR2, TRPC1, TRPC7, CDH23	4	0.013

BRAF V596E variant identified in 70% of tumors

To identify potential drivers of oncogenesis, protein-coding variants were screened against the COSMIC Cancer Gene Census, identifying 42 variants in 32 cancer-related genes (**Figure 2.3**). BRAF, a kinase that plays a regulatory role in the MAPK signaling pathway, was mutated in 4 out of 11 samples (T-353, T-36, T-522, and T-22). BRAF variants were T>A substitutions resulting in V-to-E missense mutations at amino acid 588 (ENSCAFT00000006305). This variant is homologous to the BRAFV600E oncogenic mutation identified in human melanoma, thyroid, and colorectal cancers (Dankner et al., 2018; Turski et al., 2016). Rapid amplification of cDNA ends was previously used to determine the entire sequence of canine BRAF, identifying the V-to-E mutation in cTCC cell lines at amino acid 596 (GenBank: MN581672) (Cronise et al., 2019). The BRAF variant was detected in 4 additional tumor samples using Sanger sequencing (T-500, T-113, T-400, and T-730). Further examination of WES results confirmed the presence of BRAF variants in these samples below filtering levels. Additionally, BRAF V-to-E mutations were detected in 22 out of 32 FFPE cTCC tumor samples, indicating an overall prevalence of approximately 70%.

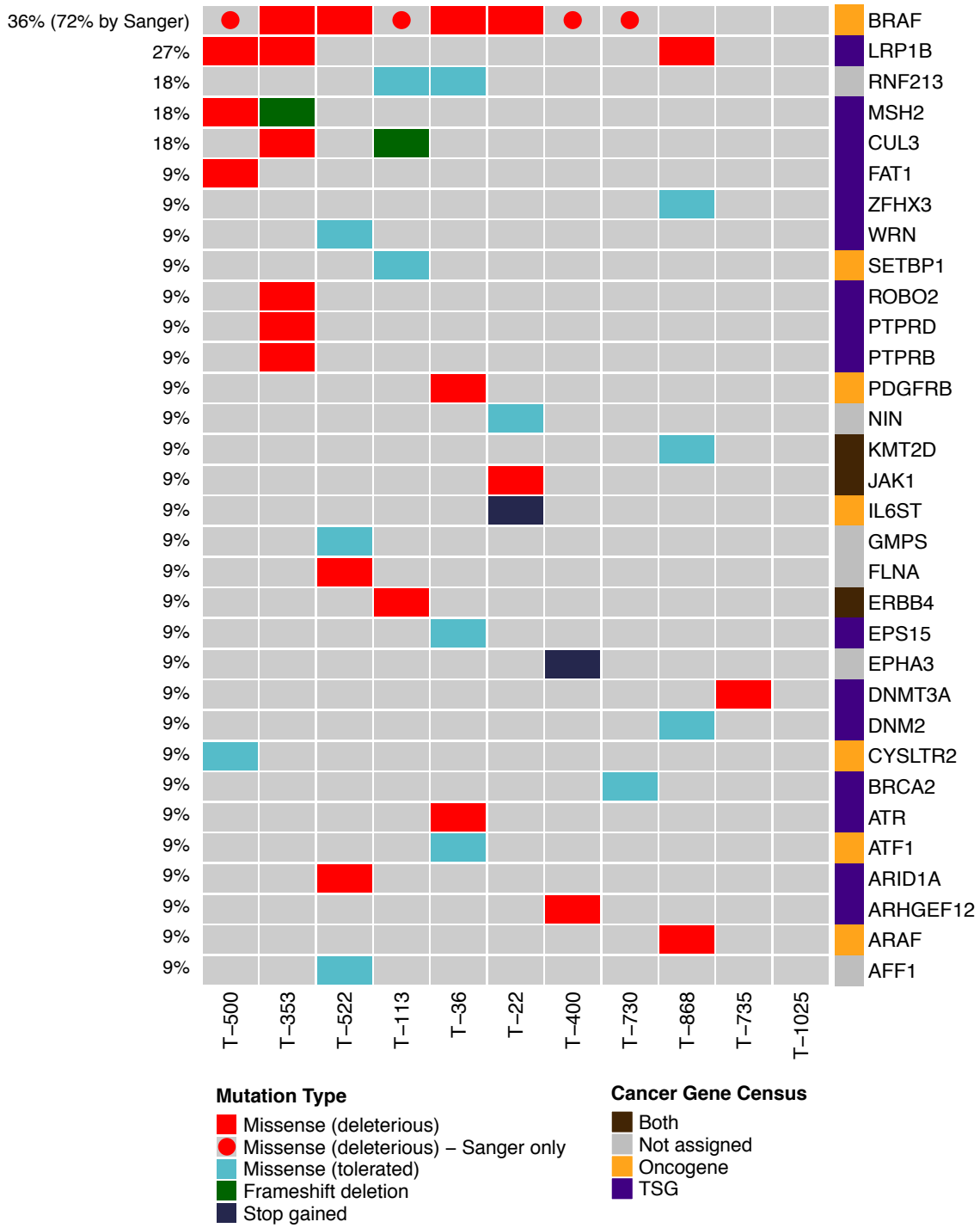

Figure 2.3 Oncoplot of cancer variants.
Oncoplot depicting protein-coding variants in genes present in COSMIC's Cancer Gene Census (v90). Colors on the oncoplot represent the type of variant. Missense variants with SIFT < 0.05 are considered deleterious. BRAF variants that were detected via Sanger sequencing only are shown as circles. Colors next to gene names represent a gene's designation in the Cancer Gene Census.

Deleterious variants in the low-density lipoprotein receptor LRP1B were detected in three samples (T-353, T-500, T-868). Other cancer-related genes that were mutated in more than one sample encode the E3 ubiquitin ligases CUL3 (deleterious missense and frameshift) and RNF213 (tolerated missense) as well as the mismatch repair protein MSH2 (deleterious missense and frameshift). Mutations occurred more frequently in tumor suppressor genes than oncogenes. No cancer gene variants were detected in T-1025.

Transcriptomic alterations in cTCC relative to normal bladder

RNA-Seq analysis was performed to assess the transcriptome of these 11 bladder tumors and three normal bladder samples. Principal component analysis resulted in a clear separation between tumors and normal bladder samples (**Figure 2.4**). BRAF mutant tumors clustered separately from BRAF wild type tumors. Differential gene expression analysis identified 1,219 and 1,347 genes up- and down-regulated in tumor relative to normal tissue, respectively (**Figure 2.4**). Functional analysis of up-regulated DEGs revealed enrichment of cell cycle-related processes as well as DNA repair and immune system processes (**Table 2.4**). Many of the immune terms were related to antiviral immunity. Genes down-regulated in tumors relative to normal bladder samples were associated with extracellular matrix organization, cell adhesion molecules, muscle-related terms, and second messenger signaling (**Table 2.4**).

Gene expression data was also analyzed using GSEA to identify enrichment of MSigDB hallmark gene sets in cTCC tumors relative to normal bladder samples. GSEA identified significant enrichment of gene sets related to cell growth and proliferation in

cTCC tumors: E2F Targets, G2M Checkpoint, Mitotic Spindle, and MTORC1 Signaling (**Figure 2.4**). Additionally, tumor samples exhibited enrichment of Interferon Alpha (IFN-α) Response, Oxidative Phosphorylation, and DNA Repair gene sets. Twelve hallmark gene sets were enriched in normal samples, including Epithelial Mesenchymal Transition (EMT), TNF-α Signaling via NFKB, Myogenesis, and Angiogenesis (**Figure 2.4**).

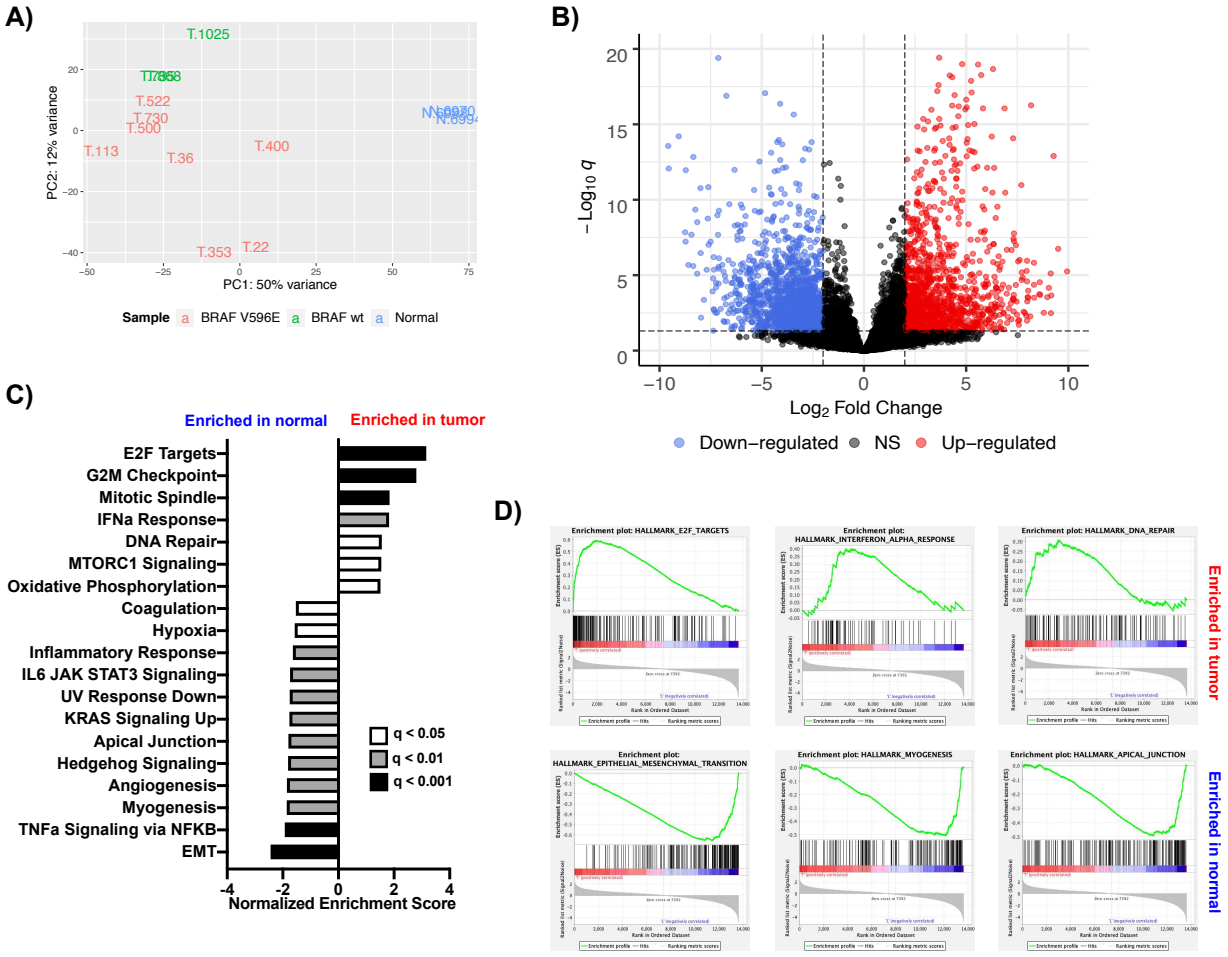

Figure 2.4 RNA-Seq analysis of cTCC tumors and normal bladder.
(A) Principal component analysis of normalized gene counts. (B) 1,219 and 1,347 genes up- (red) and down-regulated (blue) in TCC tumor relative to normal bladder (logFC > 2 and adj. $p < 0.05$). (C) Gene sets significantly enriched in tumor and normal (FDR q-val < 0.05). (D) GSEA enrichment plots for significantly enriched gene sets.

Table 2.4 Functional annotation of DEGs between cTCC tumors and normal bladder tissue.

Process	Terms/Pathways	Genes
Upregulated in tumor		
Immune	T cell receptor signaling pathway	CSF2, LAT, IL5, CD3G, MAPK12, CD3D, CD3E, CD40LG, PAK5, CTLA4, PDCD1
	Immune response	CSF2, IL5, VPREB3, ENPP3, OAS3, CTLA4, OAS1, OAS2, CX3CL1, TNFRSF4, CCL28, LAT, CCL13, OASL, TNFSF11, RELT, AIRE, DLA-DMA, IL12B, BLNK
	2'-5'-oligoadenylate synthetase activity	OAS3, OAS1, OAS2
	Negative regulation of viral genome replication	RNASEL, OASL, ISG15, OAS3, RSAD2, SLPI, OAS1, CCL5, ISG20
	Response to virus	LCN2, GATA3, CDK6, STMN1, MST1R, CCL5, DHX58
	Defense response to virus	IFIT2, RNASEL, OASL, UNC13D, ISG15, DDX60, F2RL1, OAS3, RSAD2, OAS1, OAS2, IL12B, ISG20
Cell Cycle	Cell cycle	CDK1, CDC6, E2F2, PKMYT1, TTK, CHEK1, ESPL1, CDC20, CDK6, MCM2, CDC25C, MCM5, CCNE2, CDC45, CCNB3, CCNB2, PLK1, BUB1, BUB1B, ORC6, ORC1, CCNA2
	DNA replication initiation	CCNE2, CDC6, CDC45, GINS4, ORC6, POLA2, MCM2, MCM10, MCM5
	Mitotic sister chromatid segregation	CDCA8, PLK1, DSN1, CENPA, NEK2, ZWINT, KIF18A, KIF18B, ESPL1, KNSTRN
	Mitotic cytokinesis	KIF23, PLK1, NUSAP1, ANLN, MITD1, STMN1, RACGAP1, KIF20A
DNA Damage	Fanconi anemia pathway	FANCM, RAD51C, FANCI, FANCD2, BRIP1, RMI2, BRCA1, UBE2T, RAD51

	Regulation of double-strand break repair via homologous recombination	TEX15, RAD51AP1, CHEK1, RAD51
	Base-excision repair	RECQL4, DNA2, NEIL3, NEIL1, FEN1
	G2 DNA damage checkpoint	CLSPN, PLK1, DTL, CHEK1, BRCA1
Down-regulated in tumor		
Cell Adhesion	ECM-receptor interaction	TNC, COL3A1, ITGA11, COL2A1, VTN, CHAD, COL6A6, TNR, COL6A3, COL6A1, SV2A, THBS1, COL11A1, THBS3, COL4A4, COL4A3, TNXB, HSPG2, COL4A6, COL4A5, LAMA2, ITGA9, LAMA4, CD36, LAMC3, ITGA5, ITGA8, RELN
	Positive regulation of cell-substrate adhesion	EGFL6, SPOCK2, NPNT, DMP1, CCDC80, VTN, NID1, ECM2, VIT, ABI3BP, EMILIN1, SMOC2, ALOX15, FBLN2
	Heterophilic cell-cell adhesion via plasma membrane cell adhesion molecules	VCAM1, TENM4, SELP, CADM3, TENM1, FAT4, ITGA5, TENM2, NLGN1, CDH2, SELE, DCHS1, SCARF2
Myogenesis	Vascular smooth muscle contraction	KCNMA1, ADCY3, ADCY2, ACTA2, ADCY5, PPP1R12B, CALD1, MRVI1, NPR2, PRKG1, KCNMB1, MYL9, KCNMB2, AGTR1, PTGIR, CACNA1C, MYLK, PPP1R14A
	Dilated cardiomyopathy	ADCY3, CACNA2D1, ADCY2, ADCY5, CACNG7, ITGA11, CACNB2, IGF1, CACNA2D3, TPM2, CACNA2D2, TPM1, TNNT2, ITGA9, DES, ITGA5, DMD, ITGA8, SGCD, CACNA1C, SGCA
	Smooth muscle contraction	PDE4D, BDKRB2, HTR2B, MYLK, HTR2A
Second Messenger Signaling	cGMP-PKG signaling pathway	ADCY3, SLC8A3, ADCY2, GNAI1, ATP1B2, ADCY5, MRVI1, BDKRB2, PRKG1, ADORA1, KCNMB1, KCNMB2, MYL9, ATP2B2, AGTR1,

		ADRA2A, NOS3, AKT3, KCNMA1, SLC8A1, ATP1A3, CREB5, NPR2, PDE2A, KCNJ8, PDE5A, CACNA1C, MYLK
	cAMP signaling pathway	ADCY3, FXYD1, ADCY2, DRD2, ATP1B2, GNAI1, ADCY5, FFAR2, ADORA1, VIPR2, MYL9, ATP2B2, GRIN2D, PDE4B, CAMK2A, AKT3, PTGER2, ATP1A3, GRIA3, PDE4D, CREB5, GRIA4, GRIA1, CACNA1C, TSHR
	Calcium signaling pathway	SLC8A3, ADCY3, SLC8A1, ADCY2, PHKG1, BDKRB2, AGTR1, ATP2B2, P2RX1, HRH2, P2RX3, GRIN2D, PDE1A, CACNA1G, CACNA1H, PLCD4, NOS3, HTR2B, CACNA1C, CAMK2A, MYLK, HTR2A

GSEA was also used to compare the gene expression profiles of BRAF mutant and wild type tumors. BRAF mutant tumors showed significant enrichment of the hallmark gene sets E2F Targets and Myogenesis; whereas, wild type tumors showed significant enrichment of IFN-α and -γ Response gene sets as well as Hedgehog Signaling (**Figure 2.5**). We also analyzed MAPK pathway activity among the tumors since 8 out of 11 harbor BRAF mutations. The MAPK Pathway Activation Score (MPAS) is a gene signature quantifying relative MAPK activity based on expression levels of 10 downstream targets of the MAPK pathway and correlates with sensitivity to MAPK inhibitors in both cell lines and patients (Wagle et al., 2018). The MPAS has previously been applied to a panel of canine cancer cell lines and TCC cell lines exhibited the highest MPAS values relative to other cancer types (Cronise et al., 2019). In this study, all three normal samples and the three BRAF wild type samples had negative MPAS values (**Figure 2.6**). Only three of the BRAF mutant tumors had

positive MPAS values, possibly indicating sensitivity to MAPK pathway inhibitors. T-353, a BRAF mutant tumor, exhibited extremely high MAPK pathway activation relative to the other tumor samples.

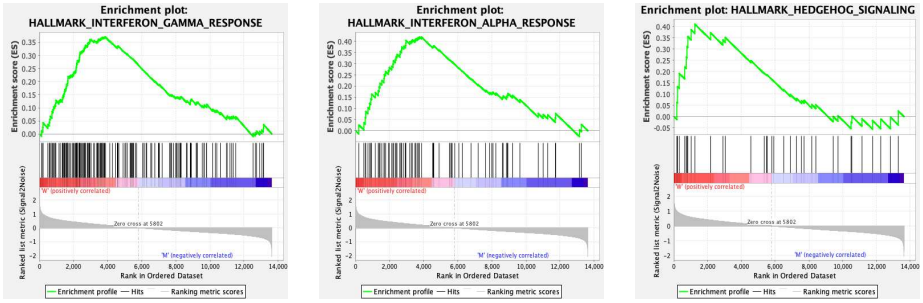

BRAF wild type

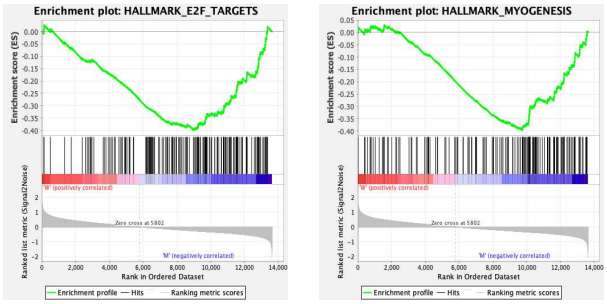

BRAF mutant

Figure 2.5 GSEA of BRAF wild type versus BRAFV596E cTCC tumors.
Enrichment plots of gene sets significantly enriched in BRAF wild type (top) and BRAF mutant (bottom) cTCC tumors (FDR q-val < 0.05)

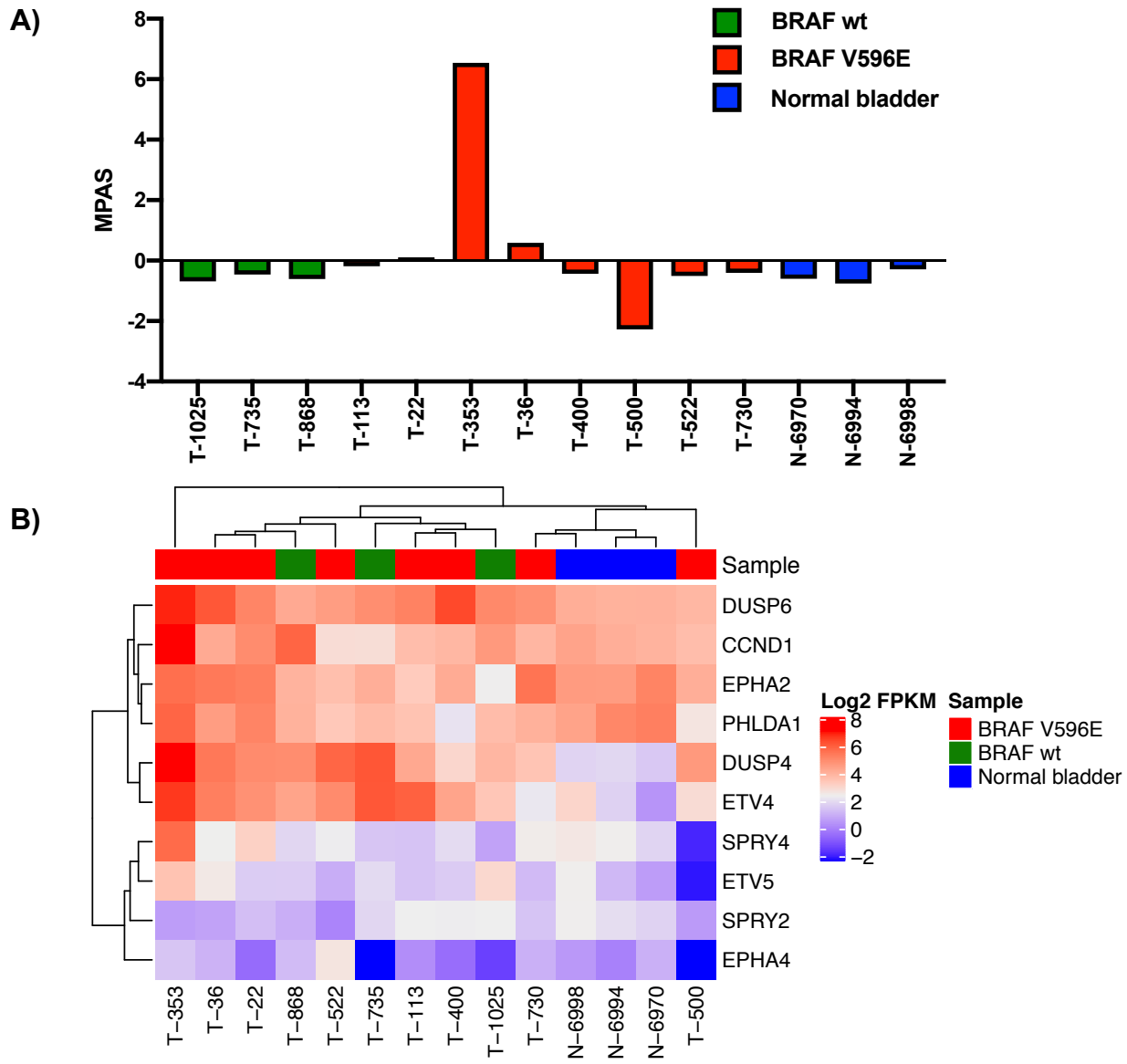

Figure 2.6. MAPK Pathway Activity Scores (MPAS) for cTCC tumors.
(A) Relative MPAS values for cTCC tumors and normal bladder. (B) Heatmap of log_2-transformed MPAS gene expression levels.

Identification of an immunologically hot subset of cTCC

Several immune-related, antiviral genes were upregulated in cTCC tumors relative to normal bladder samples. Additionally, the IFN-α Response gene set was significantly enriched in cTCC tumors relative to normal bladder. We performed

hierarchical clustering of tumor and normal samples based on expression of genes within this gene set and a subset of five tumors with high expression of IFN-α response genes clustered separately from the other tumors and normal bladder samples (**Figure 2.7**).

To determine whether this subset of tumors exhibits an immunologically hot tumor microenvironment, we used GSVA to analyze the relative enrichment of gene sets representing specific immune cell types and processes described by Rooney et al (Rooney et al., 2015). We chose to employ GSVA since this method determines relative enrichment scores for each sample in an unsupervised manner. Clustering of tumors based on their GSVA scores resulted in two distinct clusters representing immunologically hot (T-1025, T-36, T-500, T-730) and cold tumors, termed "TME-Hot" and "TME-Cold", respectively (**Figure 2.7**). T-868, which has high expression of IFN-α response genes, clustered with the TME-Cold tumors. TME-Hot tumors exhibited significant enrichment of gene sets representing cytolytic activity, $CD8^+$ T cells, plasmacytoid dendritic cells (pDCs), co-stimulatory and co-inhibitory receptor expression by antigen presenting cells (APCs) and T cells, major histocompatibility complex (MHC) class I expression, $CD4^+$ regulatory T cells (Tregs), and type I IFN response (**Figure 2.7**).

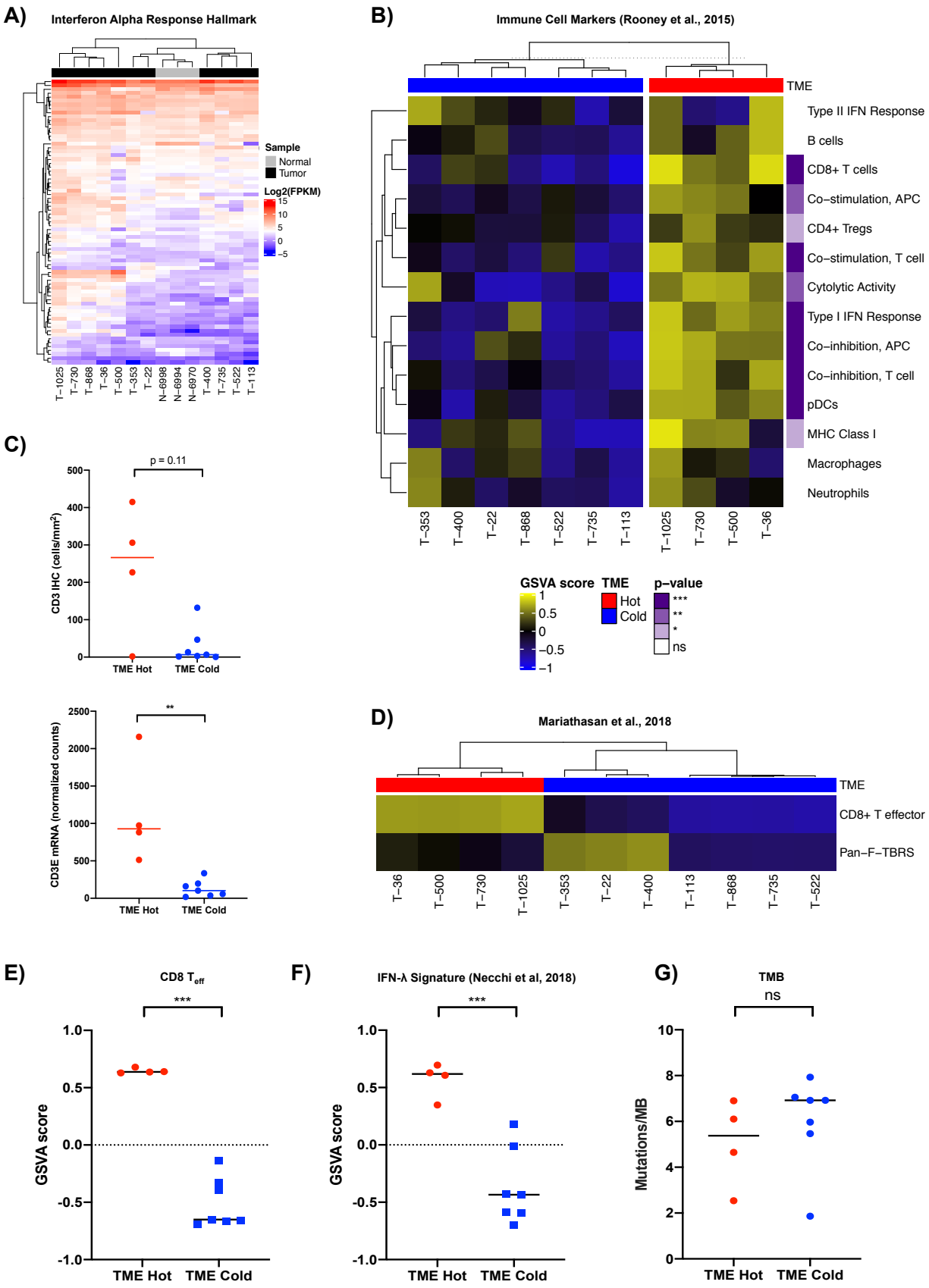
A)
Interferon Alpha Response Hallmark
Sample
Normal
Tumor
Log2(FPKM)
15
10
5
0
−5
T−1025
T−730
T−868
T−36
T−500
T−353
T−22
N−6998
N−6994
N−6970
T−400
T−735
T−522
T−113
B)
Immune Cell Markers (Rooney et al., 2015)
TME
Type II IFN Response
B cells
CD8+ T cells
Co−stimulation, APC
CD4+ Tregs
Co−stimulation, T cell
Cytolytic Activity
Type I IFN Response
Co−inhibition, APC
Co−inhibition, T cell
pDCs
MHC Class I
Macrophages
Neutrophils
T−353
T−400
T−22
T−868
T−522
T−735
T−113
T−1025
T−730
T−500
T−36
GSVA score
1
0.5
0
−0.5
−1
TME
Hot
Cold
p−value
***
**
*
ns
C)
p = 0.11
CD3 IHC (cells/mm²)
500
400
300
200
100
0
TME Hot
TME Cold
**
CD3E mRNA (normalized counts)
2500
2000
1500
1000
500
0
TME Hot
TME Cold
D)
Mariathasan et al., 2018
TME
CD8+ T effector
Pan−F−TBRS
T−36
T−500
T−730
T−1025
T−353
T−22
T−400
T−113
T−868
T−735
T−522
E)
CD8 T$_{eff}$
***
GSVA score
1.0
0.5
0.0
-0.5
-1.0
TME Hot
TME Cold
F)
IFN-λ Signature (Necchi et al, 2018)
***
GSVA score
1.0
0.5
0.0
-0.5
-1.0
TME Hot
TME Cold
G)
TMB
ns
Mutations/MB
10
8
6
4
2
0
TME Hot
TME Cold

Figure 2.7. Identification of an immunologically hot subset of cTCC tumors associated with genomic indicators of response to PD-1/PD-L1 blockade in human bladder cancer.
A) Hierarchical clustering of cTCC tumors and normal bladder based on expression of genes present in the IFN-α Response Hallmark gene set. Colors on the heat map represent log^2-FPKM expression values. (B) Heatmap of GSVA scores for gene sets representing immune cell types and processes described by Rooney et al. Significantly enriched gene sets were determined using linear models and moderated t tests implemented in the 'limma' R package. P-values are represented in purple on the right. (C) CD3 IHC (top) and CD3E mRNA expression (bottom) in TME-Hot versus TME-Cold tumors compared using the Mann Whitney test. (D) Heatmap representing cTCC GSVA scores for CD8 T_{eff} and F-TBRS gene signatures associated with good and bad responses to PD-L1 blockade in human bladder cancer, respectively. (E) CD8 T_{eff} (left) and F) IFN-λ (right) GSVA scores in HME-Hot vs. TME-Cold tumors. Statistical significance was determined same as in panel B. (G) Tumor mutation burden in TME-Hot versus TME-Cold tumors compared using the Mann Whitney test.

IHC analysis was performed to quantify T cell abundance in cTCC tumors. $CD3^+$ T cell counts were variable, ranging from 1 to 415 cells/mm^2 (**Figure 2.8**). Though not statistically different, several TME-Hot tumors had higher T cell infiltration than any of the TME-Low tumors (**Figure 2.7**). Despite exhibiting an immunologically hot gene expression signature, T-730 had very little T cell infiltration. TME-Hot tumors did, however, exhibit significantly higher CD3E mRNA expression (**Figure 2.7**), which was highly correlated with CD3 IHC staining ($p < 0.001$, $R^2 = 0.86$). Tumors with high CD3 staining showed enrichment of the immune-related hallmarks gene sets IFN-α Response, IFN-γ Response, and Allograft Rejection, as well as cell cycle-related gene sets E2F Targets and G2M Checkpoint (**Figure 2.9**). Tumors with low $CD3^+$ staining exhibited enrichment of hallmark gene sets for TNF-α Signaling via NFKB, TGF-β Signaling, and Hypoxia.

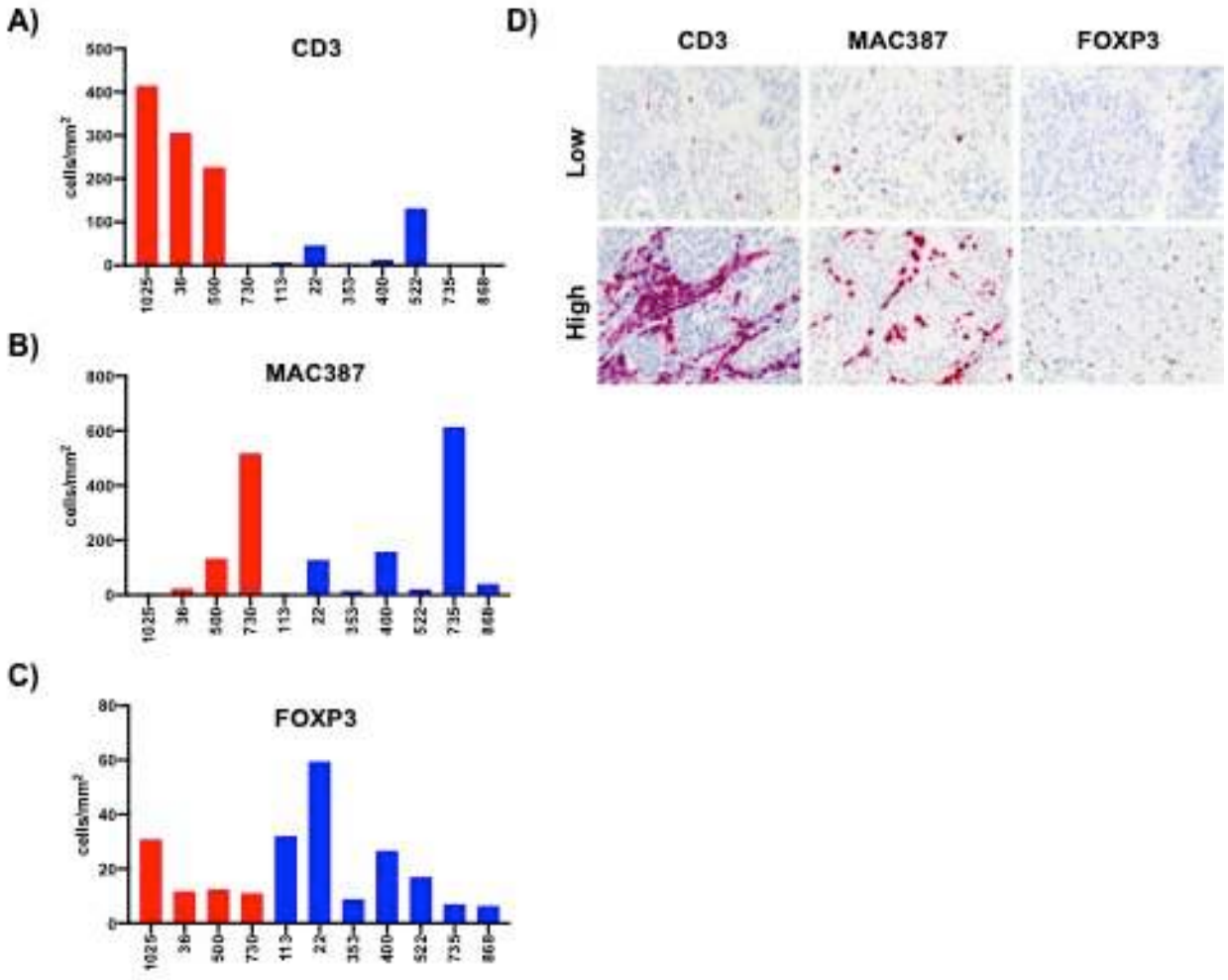

Figure 2.8 IHC analysis of CD3, MAC387, and FOXP3 expression in cTCC tumors. A) Quantification of CD3, (B) MAC387, and (C) FOXP3 expression shown as cells per mm^2. TME-Hot tumors are shown in red and TME-Cold tumors are shown in blue. (D) Representative images of tumors with high and low expression of CD3, MAC387, and FOXP3.

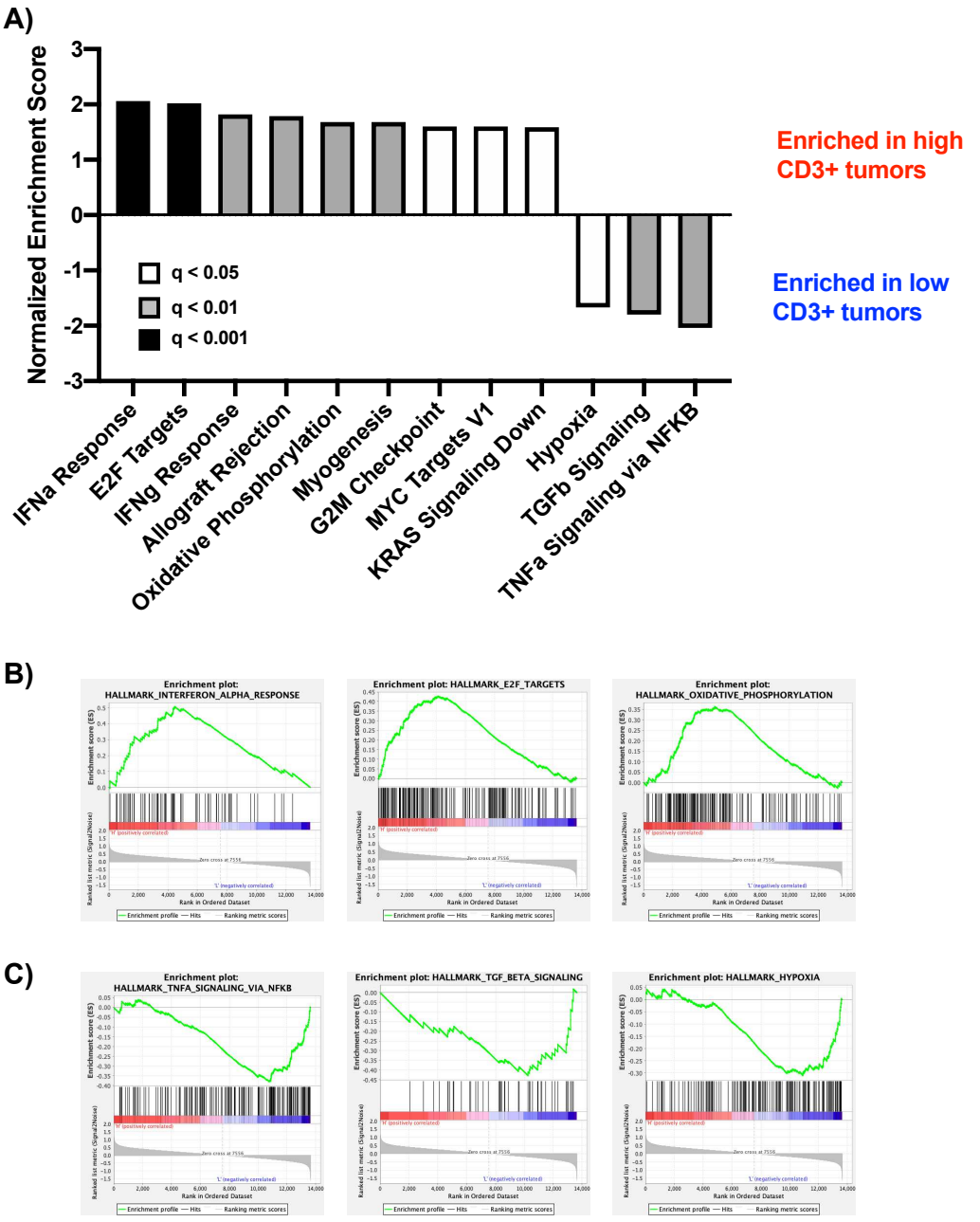

Figure 2.9. GSEA comparing cTCC tumors with high versus low CD3$^+$ T cell infiltration.

(A) Bar plot of normalized enrichment scores for significantly enriched gene sets in high versus low CD3-infiltrated cTCC tumors. (B) Enrichment plots of gene sets enriched in tumors with high and (C) low CD3$^+$ T cell infiltration.

We also stained for MAC387 and FOXP3 expression as a means of quantifying myeloid and Treg cells, respectively (**Figure 2.8**). MAC387$^+$ cell counts ranged from 3 to 614 cell/mm^2 and did not correlate with CD3$^+$ T cell counts ($p=0.24$, $R^2=0.15$). FOXP3$^+$ cell counts ranging from 6 to 60 cells/mm^2 did not correlate with CD3 ($p=0.86$, $R^2=0.004$) or MAC387 staining ($p=0.44$, $R^2=0.07$). However, neither MAC387 nor FOXP3 IHC staining correlated with S100A9 ($p=0.44$, $R^2=0.07$) or FOXP3 ($p=0.70$, $R^2=0.02$) mRNA expression, respectively. These discrepancies between the IHC and gene expression data could be explained by tumor heterogeneity, lack of specificity of the antigen as a cell marker, or subsequent regulatory processes.

TME-Hot cTCCs exhibit high expression of genomic biomarkers of response to PD-1/PD-L1 inhibition in human bladder cancer

Immune checkpoint inhibitors targeting PD-1 and PD-L1 have shown efficacy in a subset of human bladder cancer patients (Balar et al., 2017; Bellmunt et al., 2017). A CD8$^+$ T-effector gene signature (CD8 T_{eff}) has been identified as a genomic indicator of response to the PD-L1 inhibitor atezolizumab in bladder cancer patients enrolled in the phase 2 IMvigor210 clinical trial (Mariathasan et al., 2018; Rosenberg et al., 2016). Additionally, Mariathasan et al. generated a pan-fibroblast TGF-β response signature (F-TBRS) that was associated with lack of response (Mariathasan et al., 2018). We applied these human-derived gene signatures to the canine TCC dataset in this study, generating relative CD8 T_{eff} and F-TBRS scores for each sample using GSVA. Clustering of tumors based on their CD8+ T_{eff} and F-TBRS scores resulted in a clear separation between TME-Hot and TME-Cold tumors (**Figure 2.7**). TME-Hot tumors exhibited significantly higher CD8+ T_{eff} scores relative to TME-Cold tumors (**Figure 2.7**).

Three tumors, all TME-Cold, exhibited high F-TBRS scores (T-353, T-22, T-400), suggestive of TGF-β signaling by cancer-associated fibroblasts (Mariathasan et al., 2018).

We next evaluated an IFN-γ-related gene signature associated with complete response to the PD-1 inhibitor pembrolizumab in the neoadjuvant setting (Ayers et al., 2017; Necchi et al., 2018). Indeed, TME-Hot tumors exhibited significantly higher IFN-γ scores relative to TME-Cold tumors (**Figure 2.7**). High tumor mutation burden (TMB) has also been identified as a correlate of response to PD-1/PD-L1 blockade in several human cancers, including bladder (Rosenberg et al., 2016). Notably, we did not detect a difference in TMB between TME-Hot and TME-Cold tumors (**Figure 2.7**). Overall, these results suggest that the TME-Hot cTCC tumors identified in this study represent a subset of canine bladder cancer patients that may achieve clinical benefit from checkpoint inhibitors targeting the PD-1/PD-L1 axis.

DISCUSSION

Canine cancers have become increasingly established as valuable models for human cancer. Oncology clinical trials in dogs serve to evaluate novel anticancer strategies with the goal of advancing treatment for both canines and humans (Gordon et al., 2009; LeBlanc and Mazcko, 2020). Our genomic characterization of cTCC contributes to the growing body of evidence supporting the comparative relevancy of the disease. We identify novel and previously described drivers of oncogenesis as well as putative therapeutic targets. Additionally, a subset of cTCC tumors in this study

exhibited an inflamed tumor microenvironment with high expression of genomic biomarkers of response to checkpoint inhibition in human bladder cancer.

The mutation profile of the cTCC tumors analyzed in this study was similar to that of human muscle-invasive bladder cancer. cTCC tumors exhibited a mean somatic mutation rate of 5.7 mutations/Mb, similar to 7.7 mutations/Mb reported in human bladder cancer (The Cancer Genome Atlas Research, 2014). Additionally, C>T transitions were the most common single base substitution, consistent with frequencies observed in human cancers, including TCC (Bailey et al., 2018; Robertson et al., 2017). The most common protein-coding variant identified in this study was a BRAF V-to-E missense mutation homologous to the V600E driving variant frequently observed in human cancer (Dankner et al., 2018; Turski et al., 2016). BRAF variants were detected in this study at an overall prevalence of 70%, consistent with other studies of canine bladder cancer (Decker et al., 2015; Mochizuki et al., 2015). Several small molecule inhibitors targeting mutant BRAF, as well as BRAF's downstream target MEK1/2, have been approved for BRAF mutant human cancers; however, intrinsic and acquired drug resistance pose major roadblocks to treatment (Yaeger and Corcoran, 2019). In Chapter 3, we find that BRAF mutant cTCC cell lines are sensitive to the "paradox-breaking" BRAF inhibitor PLX7904 and the MEK inhibitor trametinib (Cronise et al., 2019). However, MAPK pathway reactivation was observed is most cell lines by 24 hours post-treatment, suggesting cTCC may serve as a model for interrogating combination therapies that circumvent resistance to MAPK pathway inhibition (Cronise et al., 2019). Parker et al. recently determined genes and pathways differentially enriched in BRAF mutant versus BRAF wild type cTCC, identifying enrichment of cell

cycle/cell death pathways in BRAF mutant cTCC and enrichment of immune-related gene sets in BRAF wild type cTCC (Parker et al., 2020). Similarly, we observed enrichment of E2F target genes in BRAF mutant tumors and enrichment of IFN-α and IFN-γ response gene sets in BRAF wild type tumors.

In total, 36 mutated genes identified in this study were previously identified in other genomic analyses of cTCC. Nine of these genes are present in the COSMIC Cancer Gene Census (*BRAF, LRP1B, BRCA2, FAT1, PDGFRB, KMT2D, FLNA, ARHGEF12,* and *AFF1*), potentially validating the importance of these alterations in cTCC pathogenesis (Decker et al., 2015; Ramsey et al., 2017). Deleterious missense mutations in *LRP1B* were detected in three tumors analyzed in this study as well as one tumor analyzed by Ramsey et al (Ramsey et al., 2017). LRP1B is a member of the LDL receptor family, and its inactivation has been observed in a number of human cancers, including bladder, where it is predicted to act as a tumor suppressor (Langbein et al., 2002; Tate et al., 2019). Shapiro et al. identified deletions in a region on chromosome 19 containing *LRP1B* (corresponding to chromosome 13 in humans) as a common copy number aberration in canine bladder cancer that is conserved in human bladder cancer (Shapiro et al., 2015). Together, these results suggest that inactivation of LRP1B may be an important feature of cTCC oncogenesis.

Our transcriptomic analysis identified 2,566 differentially expressed genes between cTCC and normal bladder tissue, of which 1,561 (61%) were identified in at least one prior RNA-Seq analysis of canine bladder cancer (Maeda et al., 2018; Parker et al., 2020; Ramsey et al., 2017). Functional analysis of up-regulated DEGs identified in this study revealed enrichment of cell cycle, DNA repair, and immune-related genes

in cTCC tumors. Whereas, genes down-regulated in cTCC were related to focal adhesion, myogenesis, and second messenger signaling. Ramsey et al. performed a comparative analysis of the transcriptomes of canine and human bladder cancer, finding a high level of similarity between the two; whereby, both species exhibit up-regulation of cell cycle and DNA repair machinery and down-regulation of cytoskeletal, cell adhesion, and muscle-related genes (Ramsey et al., 2017).

Activation of ErbB signaling has been previously reported in cTCC (Maeda et al., 2018; Millanta et al., 2018; Parker et al., 2020). Here, we identified up-regulation of *ERBB2* and *ERBB3* by 6- and 7-fold, respectively, in cTCC tumors relative to normal bladder (Supporting Table S5). Up-regulation of these genes was also observed in the transcriptomic analyses by Parker et al. and Ramsey et al. *ERBB2*'s gene product, HER2, is overexpressed in more than half of cTCC tumors (Millanta et al., 2018). Additionally, EGFR and ERBB2 are predicted upstream regulators of overexpressed genes in canine bladder cancer (Maeda et al., 2018). Cronise et al. identified up-regulation of *EGFR* and *ERBB2* expression in cTCC cell lines relative to other canine cancer cell lines and demonstrated synergism between combined ErbB receptor inhibition and BRAF or MEK inhibition (Cronise et al., 2019). Activation of the ErbB family of receptors is also common in human muscle-invasive bladder cancer, specifically via mutations in *ERBB2/ERBB3* and amplification of *EGFR/ERBB2* (The Cancer Genome Atlas Research, 2014).

Immune checkpoint inhibitors targeting PD-1 and PD-L1 have been effective in approximately one-quarter of human bladder cancer patients (Balar et al., 2017; Bellmunt et al., 2017). One of the major challenges to cancer immunotherapy has been

the lack of pre-clinical models that adequately recapitulate the natural process of immunoediting that occurs during tumor development. Canine clinical trials provide the opportunity to evaluate novel immunotherapies in spontaneous tumors in the presence of an intact immune system. Four out of 11 cTCC tumors analyzed in this study exhibited characteristics of a hot tumor microenvironment (TME-Hot) with high expression of gene markers for $CD8^+$ T cells, pDCs, co-inhibitory/co-stimulatory receptor expression by T cells and APCs, cytolytic activity, MHC class I expression, and type I IFN response.

Mariathasan et al. analyzed pre-treatment tumor samples from human metastatic bladder cancer patients treated with the PD-L1 inhibitor atezolizumab, identifying PD-L1 expression on immune cells, TMB, and a CD8 T_{eff} signature as biomarkers of complete response (Mariathasan et al., 2018). This group also derived a signature representing TGF-β signaling by fibroblasts (F-TBRS), which was associated with lack of response. Powles et al. evaluated similar biomarkers of response to atezolizumab as a neoadjuvant therapy for human bladder cancer, identifying CD8 T_{eff} and F-TBRS signatures as indicators of response and resistance, respectively (Powles et al., 2019). Neither PD-L1 expression nor TMB correlated with response in the neoadjuvent setting. The TME-Hot cTCC tumors in this study exhibited strong expression of the CD8 T_{eff} gene signature, as well as a similar IFN-γ gene signature associated with complete response to the PD-1 inhibitor pembrolizumab (Ayers et al., 2017; Necchi et al., 2018). These results suggest that TME-Hot tumors exhibit pre-existing CD8+ T cell immunity and may represent a subset of cTCC that would be responsive to checkpoint inhibitor

therapy. Three TME-Cold tumors exhibited high expression of the F-TBRS signature, consistent with immunosuppressive TGF-β signaling (Mariathasan et al., 2018).

Additionally, three out of four TME-Hot tumors harbor BRAF mutations. BRAF inhibition in human melanoma increases antigen expression, promotes $CD8^+$ lymphocyte infiltration and function, and decreases expression of immunosuppressive cytokines (Frederick et al., 2013; Hugo et al., 2015; Wilmott et al., 2012). Acquired resistance to BRAF inhibition is often accompanied by loss of antigen expression and $CD8^+$ T cell infiltration, but can be partially reversed with the addition of a MEK inhibitor (Frederick et al., 2013; Hugo et al., 2015). Combining BRAF and/or MEK inhibitors with checkpoint inhibitors has been explored in BRAF mutant melanoma; however, toxicity remains a challenge. A triple combination of BRAF, MEK, and PD-1 inhibition causes increased toxicity relative to either BRAF/MEK combined inhibition or PD-1 blockade alone (Ascierto et al., 2019; Ribas et al., 2019). However, this triple combination resulted in increased progression free survival and duration of response relative to combined BRAF/MEK inhibition in a phase II study (Ascierto et al., 2019). Genomic analysis of pre- and post-treatment biopsies of patients receiving the triple combination revealed increased expression of CD8 and MHC Class I and II molecules following treatment, as well as increased expression of the same IFN-γ gene signature used in this study, suggesting an enhanced antitumor immune response (Ayers et al., 2017; Ribas et al., 2019). The prevalence of BRAF mutations in cTCC provides the unique opportunity to evaluate novel strategies combining checkpoint inhibition with BRAF and/or MEK inhibition. Overall, this study emphasizes the importance of conducting

clinical trials for dogs with TCC, where the evaluation of immunotherapies alone and in combination with MAPK-targeted therapies may benefit canines as well as humans.

REFERENCES

Anders S, Pyl PT and Huber W (2015) HTSeq--a Python framework to work with high-throughput sequencing data. *Bioinformatics* **31**(2): 166-169.

Ascierto PA, Ferrucci PF, Fisher R, Del Vecchio M, Atkinson V, Schmidt H, Schachter J, Queirolo P, Long GV, Di Giacomo AM, Svane IM, Lotem M, Bar-Sela G, Couture F, Mookerjee B, Ghori R, Ibrahim N, Moreno BH and Ribas A (2019) Dabrafenib, trametinib and pembrolizumab or placebo in BRAF-mutant melanoma. *Nat Med* **25**(6): 941-946.

Ayers M, Lunceford J, Nebozhyn M, Murphy E, Loboda A, Kaufman DR, Albright A, Cheng JD, Kang SP, Shankaran V, Piha-Paul SA, Yearley J, Seiwert TY, Ribas A and McClanahan TK (2017) IFN-gamma-related mRNA profile predicts clinical response to PD-1 blockade. *J Clin Invest* **127**(8): 2930-2940.

Bai B, Zhao WM, Tang BX, Wang YQ, Wang L, Zhang Z, Yang HC, Liu YH, Zhu JW, Irwin DM, Wang GD and Zhang YP (2015) DoGSD: the dog and wolf genome SNP database. *Nucleic Acids Res* **43**(Database issue): D777-783.

Bailey MH, Tokheim C, Porta-Pardo E, Sengupta S, Bertrand D, Weerasinghe A, Colaprico A, Wendl MC, Kim J, Reardon B, Kwok-Shing Ng P, Jeong KJ, Cao S, Wang Z, Gao J, Gao Q, Wang F, Liu EM, Mularoni L, Rubio-Perez C, Nagarajan N, Cortes-Ciriano I, Zhou DC, Liang WW, Hess JM, Yellapantula VD, Tamborero D, Gonzalez-Perez A, Suphavilai C, Ko JY, Khurana E, Park PJ, Van Allen EM, Liang H, Group MCW, Cancer Genome Atlas Research N, Lawrence MS, Godzik A, Lopez-Bigas N, Stuart J, Wheeler D, Getz G, Chen K, Lazar AJ, Mills GB, Karchin R and Ding L (2018) Comprehensive Characterization of Cancer Driver Genes and Mutations. *Cell* **174**(4): 1034-1035.

Balar AV, Galsky MD, Rosenberg JE, Powles T, Petrylak DP, Bellmunt J, Loriot Y, Necchi A, Hoffman-Censits J, Perez-Gracia JL, Dawson NA, van der Heijden MS, Dreicer R, Srinivas S, Retz MM, Joseph RW, Drakaki A, Vaishampayan UN, Sridhar SS, Quinn DI, Duran I, Shaffer DR, Eigl BJ, Grivas PD, Yu EY, Li S, Kadel EE, 3rd, Boyd Z, Bourgon R, Hegde PS, Mariathasan S, Thastrom A, Abidoye OO, Fine GD, Bajorin DF and Group IMS (2017) Atezolizumab as first-line treatment in cisplatin-ineligible patients with locally advanced and metastatic urothelial carcinoma: a single-arm, multicentre, phase 2 trial. *Lancet* **389**(10064): 67-76.

Bellmunt J, de Wit R, Vaughn DJ, Fradet Y, Lee JL, Fong L, Vogelzang NJ, Climent MA, Petrylak DP, Choueiri TK, Necchi A, Gerritsen W, Gurney H, Quinn DI, Culine S, Sternberg CN, Mai Y, Poehlein CH, Perini RF, Bajorin DF and Investigators K- (2017) Pembrolizumab as Second-Line Therapy for Advanced Urothelial Carcinoma. *N Engl J Med* **376**(11): 1015-1026.

Bolger AM, Lohse M and Usadel B (2014) Trimmomatic: a flexible trimmer for Illumina sequence data. *Bioinformatics* **30**(15): 2114-2120.

Cingolani P, Platts A, Wang le L, Coon M, Nguyen T, Wang L, Land SJ, Lu X and Ruden DM (2012) A program for annotating and predicting the effects of single nucleotide polymorphisms, SnpEff: SNPs in the genome of Drosophila melanogaster strain w1118; iso-2; iso-3. *Fly (Austin)* **6**(2): 80-92.

Cronise KE, Hernandez BG, Gustafson DL and Duval DL (2019) Identifying the ErbB/MAPK Signaling Cascade as a Therapeutic Target in Canine Bladder Cancer. *Molecular pharmacology* **96**(1): 36-46.

Dailey DD, Ehrhart EJ, Duval DL, Bass T and Powers BE (2015) DOG1 is a sensitive and specific immunohistochemical marker for diagnosis of canine gastrointestinal stromal tumors. *J Vet Diagn Invest* **27**(3): 268-277.

Dankner M, Rose AAN, Rajkumar S, Siegel PM and Watson IR (2018) Classifying BRAF alterations in cancer: new rational therapeutic strategies for actionable mutations. *Oncogene* **37**(24): 3183-3199.

Decker B, Parker HG, Dhawan D, Kwon EM, Karlins E, Davis BW, Ramos-Vara JA, Bonney PL, McNiel EA, Knapp DW and Ostrander EA (2015) Homologous Mutation to Human BRAF V600E Is Common in Naturally Occurring Canine Bladder Cancer--Evidence for a Relevant Model System and Urine-Based Diagnostic Test. *Mol Cancer Res* **13**(6): 993-1002.

Elvers I, Turner-Maier J, Swofford R, Koltookian M, Johnson J, Stewart C, Zhang CZ, Schumacher SE, Beroukhim R, Rosenberg M, Thomas R, Mauceli E, Getz G, Palma FD, Modiano JF, Breen M, Lindblad-Toh K and Alfoldi J (2015) Exome sequencing of lymphomas from three dog breeds reveals somatic mutation patterns reflecting genetic background. *Genome Res* **25**(11): 1634-1645.

Frederick DT, Piris A, Cogdill AP, Cooper ZA, Lezcano C, Ferrone CR, Mitra D, Boni A, Newton LP, Liu C, Peng W, Sullivan RJ, Lawrence DP, Hodi FS, Overwijk WW, Lizee G, Murphy GF, Hwu P, Flaherty KT, Fisher DE and Wargo JA (2013) BRAF inhibition is associated with enhanced melanoma antigen expression and a more favorable tumor microenvironment in patients with metastatic melanoma. *Clin Cancer Res* **19**(5): 1225-1231.

Fulkerson CM and Knapp DW (2015) Management of transitional cell carcinoma of the urinary bladder in dogs: a review. *Veterinary journal (London, England : 1997)* **205**(2): 217-225.

Gordon I, Paoloni M, Mazcko C and Khanna C (2009) The Comparative Oncology Trials Consortium: using spontaneously occurring cancers in dogs to inform the cancer drug development pathway. *PLoS Med* **6**(10): e1000161.

Gu Z, Eils R and Schlesner M (2016) Complex heatmaps reveal patterns and correlations in multidimensional genomic data. *Bioinformatics* **32**(18): 2847-2849.

Gui Y, Guo G, Huang Y, Hu X, Tang A, Gao S, Wu R, Chen C, Li X, Zhou L, He M, Li Z, Sun X, Jia W, Chen J, Yang S, Zhou F, Zhao X, Wan S, Ye R, Liang C, Liu Z, Huang P, Liu C, Jiang H, Wang Y, Zheng H, Sun L, Liu X, Jiang Z, Feng D, Chen J, Wu S, Zou J, Zhang Z, Yang R, Zhao J, Xu C, Yin W, Guan Z, Ye J, Zhang H, Li J, Kristiansen K, Nickerson ML, Theodorescu D, Li Y, Zhang X, Li S, Wang J, Yang H, Wang J and Cai Z (2011) Frequent mutations of chromatin remodeling genes in transitional cell carcinoma of the bladder. *Nat Genet* **43**(9): 875-878.

Hanzelmann S, Castelo R and Guinney J (2013) GSVA: gene set variation analysis for microarray and RNA-seq data. *BMC Bioinformatics* **14**: 7.

Huang da W, Sherman BT and Lempicki RA (2009a) Bioinformatics enrichment tools: paths toward the comprehensive functional analysis of large gene lists. *Nucleic Acids Res* **37**(1): 1-13.

Huang da W, Sherman BT and Lempicki RA (2009b) Systematic and integrative analysis of large gene lists using DAVID bioinformatics resources. *Nat Protoc* **4**(1): 44-57.

Hugo W, Shi H, Sun L, Piva M, Song C, Kong X, Moriceau G, Hong A, Dahlman KB, Johnson DB, Sosman JA, Ribas A and Lo RS (2015) Non-genomic and Immune Evolution of Melanoma Acquiring MAPKi Resistance. *Cell* **162**(6): 1271-1285.

Knapp DW and McMillan SK (2013) Tumors of the Urinary System, in *Withrow and MacEwen's Small Animal Clinical Oncology* (Withrow SJ, Page RL and Vail DM eds) pp 572-582, Elsevier Saunders, St. Louis, MO.

Knapp DW, Ramos-Vara JA, Moore GE, Dhawan D, Bonney PL and Young KE (2014) Urinary Bladder Cancer in Dogs, a Naturally Occurring Model for Cancer Biology and Drug Development. *ILAR journal* **55**(1): 100-118.

Knowles MA and Hurst CD (2015) Molecular biology of bladder cancer: new insights into pathogenesis and clinical diversity. *Nature reviews Cancer* **15**(1): 25-41.

Langbein S, Szakacs O, Wilhelm M, Sukosd F, Weber S, Jauch A, Lopez Beltran A, Alken P, Kalble T and Kovacs G (2002) Alteration of the LRP1B gene region is associated with high grade of urothelial cancer. *Laboratory investigation; a journal of technical methods and pathology* **82**(5): 639-643.

LeBlanc AK and Mazcko CN (2020) Improving human cancer therapy through the evaluation of pet dogs. *Nature reviews Cancer*.

Li H and Durbin R (2009) Fast and accurate short read alignment with Burrows-Wheeler transform. *Bioinformatics* **25**(14): 1754-1760.

Love MI, Huber W and Anders S (2014) Moderated estimation of fold change and dispersion for RNA-seq data with DESeq2. *Genome Biol* **15**(12): 550.

Maeda S, Tomiyasu H, Tsuboi M, Inoue A, Ishihara G, Uchikai T, Chambers JK, Uchida K, Yonezawa T and Matsuki N (2018) Comprehensive gene expression analysis of canine invasive urothelial bladder carcinoma by RNA-Seq. *BMC Cancer* **18**(1): 472.

Mariathasan S, Turley SJ, Nickles D, Castiglioni A, Yuen K, Wang Y, Kadel EE, III, Koeppen H, Astarita JL, Cubas R, Jhunjhunwala S, Banchereau R, Yang Y, Guan Y, Chalouni C, Ziai J, Senbabaoglu Y, Santoro S, Sheinson D, Hung J, Giltnane JM, Pierce AA, Mesh K, Lianoglou S, Riegler J, Carano RAD, Eriksson P, Hoglund M, Somarriba L, Halligan DL, van der Heijden MS, Loriot Y, Rosenberg JE, Fong L, Mellman I, Chen DS, Green M, Derleth C, Fine GD, Hegde PS, Bourgon R and Powles T (2018) TGFbeta attenuates tumour response to PD-L1 blockade by contributing to exclusion of T cells. *Nature* **554**(7693): 544-548.

McLaren W, Gil L, Hunt SE, Riat HS, Ritchie GR, Thormann A, Flicek P and Cunningham F (2016) The Ensembl Variant Effect Predictor. *Genome Biol* **17**(1): 122.

Millanta F, Impellizeri J, McSherry L, Rocchigiani G, Aurisicchio L and Lubas G (2018) Overexpression of HER-2 via immunohistochemistry in canine urinary bladder transitional cell carcinoma - A marker of malignancy and possible therapeutic target. *Vet Comp Oncol* **16**(2): 297-300.

Mochizuki H, Kennedy K, Shapiro SG and Breen M (2015) BRAF Mutations in Canine Cancers. *PLoS One* **10**(6): e0129534.

Mootha VK, Lindgren CM, Eriksson KF, Subramanian A, Sihag S, Lehar J, Puigserver P, Carlsson E, Ridderstrale M, Laurila E, Houstis N, Daly MJ, Patterson N, Mesirov JP, Golub TR, Tamayo P, Spiegelman B, Lander ES, Hirschhorn JN, Altshuler D and Groop LC (2003) PGC-1alpha-responsive genes involved in oxidative phosphorylation are coordinately downregulated in human diabetes. *Nat Genet* **34**(3): 267-273.

Mutsaers AJ, Widmer WR and Knapp DW (2003) Canine transitional cell carcinoma. *J Vet Intern Med* **17**(2): 136-144.

Necchi A, Anichini A, Raggi D, Briganti A, Massa S, Luciano R, Colecchia M, Giannatempo P, Mortarini R, Bianchi M, Fare E, Monopoli F, Colombo R, Gallina A, Salonia A, Messina A, Ali SM, Madison R, Ross JS, Chung JH, Salvioni R, Mariani L and Montorsi F (2018) Pembrolizumab as Neoadjuvant Therapy Before Radical Cystectomy in Patients With Muscle-Invasive Urothelial Bladder Carcinoma (PURE-01): An Open-Label, Single-Arm, Phase II Study. *J Clin Oncol* **36**(34): 3353-3360.

Parker HG, Dhawan D, Harris AC, Ramos-Vara JA, Davis BW, Knapp DW and Ostrander EA (2020) RNAseq expression patterns of canine invasive urothelial carcinoma reveal two distinct tumor clusters and shared regions of dysregulation with human bladder tumors. *BMC Cancer* **20**(1): 251.

Plassais J, Kim J, Davis BW, Karyadi DM, Hogan AN, Harris AC, Decker B, Parker HG and Ostrander EA (2019) Whole genome sequencing of canids reveals genomic regions under selection and variants influencing morphology. *Nat Commun* **10**(1): 1489.

Powles T, Kockx M, Rodriguez-Vida A, Duran I, Crabb SJ, Van Der Heijden MS, Szabados B, Pous AF, Gravis G, Herranz UA, Protheroe A, Ravaud A, Maillet D, Mendez MJ, Suarez C, Linch M, Prendergast A, van Dam PJ, Stanoeva D, Daelemans S, Mariathasan S, Tea JS, Mousa K, Banchereau R and Castellano D (2019) Clinical efficacy and biomarker analysis of neoadjuvant atezolizumab in operable urothelial carcinoma in the ABACUS trial. *Nat Med* **25**(11): 1706-1714.

Ramsey SA, Xu T, Goodall C, Rhodes AC, Kashyap A, He J and Bracha S (2017) Cross-species analysis of the canine and human bladder cancer transcriptome and exome. *Genes Chromosomes Cancer* **56**(4): 328-343.

Ribas A, Lawrence D, Atkinson V, Agarwal S, Miller WH, Jr., Carlino MS, Fisher R, Long GV, Hodi FS, Tsoi J, Grasso CS, Mookerjee B, Zhao Q, Ghori R, Moreno BH, Ibrahim N and Hamid O (2019) Combined BRAF and MEK inhibition with PD-1 blockade immunotherapy in BRAF-mutant melanoma. *Nat Med* **25**(6): 936-940.

Ritchie ME, Phipson B, Wu D, Hu Y, Law CW, Shi W and Smyth GK (2015) limma powers differential expression analyses for RNA-sequencing and microarray studies. *Nucleic Acids Res* **43**(7): e47.

Robertson AG, Kim J, Al-Ahmadie H, Bellmunt J, Guo G, Cherniack AD, Hinoue T, Laird PW, Hoadley KA, Akbani R, Castro MAA, Gibb EA, Kanchi RS, Gordenin DA, Shukla SA, Sanchez-Vega F, Hansel DE, Czerniak BA, Reuter VE, Su X, de Sa Carvalho B, Chagas VS, Mungall KL, Sadeghi S, Pedamallu CS, Lu Y, Klimczak LJ, Zhang J, Choo C, Ojesina AI, Bullman S, Leraas KM, Lichtenberg TM, Wu CJ, Schultz N, Getz G, Meyerson M, Mills GB, McConkey DJ, Network TR, Weinstein JN, Kwiatkowski DJ and Lerner SP (2017) Comprehensive Molecular Characterization of Muscle-Invasive Bladder Cancer. *Cell* **171**(3): 540-556 e525.

Rooney MS, Shukla SA, Wu CJ, Getz G and Hacohen N (2015) Molecular and genetic properties of tumors associated with local immune cytolytic activity. *Cell* **160**(1-2): 48-61.

Rosenberg JE, Hoffman-Censits J, Powles T, van der Heijden MS, Balar AV, Necchi A, Dawson N, O'Donnell PH, Balmanoukian A, Loriot Y, Srinivas S, Retz MM, Grivas P, Joseph RW, Galsky MD, Fleming MT, Petrylak DP, Perez-Gracia JL, Burris HA, Castellano D, Canil C, Bellmunt J, Bajorin D, Nickles D, Bourgon R,

Frampton GM, Cui N, Mariathasan S, Abidoye O, Fine GD and Dreicer R (2016) Atezolizumab in patients with locally advanced and metastatic urothelial carcinoma who have progressed following treatment with platinum-based chemotherapy: a single-arm, multicentre, phase 2 trial. *Lancet* **387**(10031): 1909-1920.

Sayers EW, Agarwala R, Bolton EE, Brister JR, Canese K, Clark K, Connor R, Fiorini N, Funk K, Hefferon T, Holmes JB, Kim S, Kimchi A, Kitts PA, Lathrop S, Lu Z, Madden TL, Marchler-Bauer A, Phan L, Schneider VA, Schoch CL, Pruitt KD and Ostell J (2019) Database resources of the National Center for Biotechnology Information. *Nucleic Acids Res* **47**(D1): D23-D28.

Shapiro SG, Raghunath S, Williams C, Motsinger-Reif AA, Cullen JM, Liu T, Albertson D, Ruvolo M, Bergstrom Lucas A, Jin J, Knapp DW, Schiffman JD and Breen M (2015) Canine urothelial carcinoma: genomically aberrant and comparatively relevant. *Chromosome research : an international journal on the molecular, supramolecular and evolutionary aspects of chromosome biology* **23**(2): 311-331.

Siegel RL, Miller KD and Jemal A (2019) Cancer statistics, 2019. *CA Cancer J Clin* **69**(1): 7-34.

Subramanian A, Tamayo P, Mootha VK, Mukherjee S, Ebert BL, Gillette MA, Paulovich A, Pomeroy SL, Golub TR, Lander ES and Mesirov JP (2005) Gene set enrichment analysis: a knowledge-based approach for interpreting genome-wide expression profiles. *Proc Natl Acad Sci U S A* **102**(43): 15545-15550.

Tate JG, Bamford S, Jubb HC, Sondka Z, Beare DM, Bindal N, Boutselakis H, Cole CG, Creatore C, Dawson E, Fish P, Harsha B, Hathaway C, Jupe SC, Kok CY, Noble K, Ponting L, Ramshaw CC, Rye CE, Speedy HE, Stefancsik R, Thompson SL, Wang S, Ward S, Campbell PJ and Forbes SA (2019) COSMIC: the Catalogue Of Somatic Mutations In Cancer. *Nucleic Acids Res* **47**(D1): D941-D947.

The Cancer Genome Atlas Research N (2014) Comprehensive molecular characterization of urothelial bladder carcinoma. *Nature* **507**(7492): 315-322.

Trapnell C, Hendrickson DG, Sauvageau M, Goff L, Rinn JL and Pachter L (2013) Differential analysis of gene regulation at transcript resolution with RNA-seq. *Nat Biotechnol* **31**(1): 46-53.

Trapnell C, Williams BA, Pertea G, Mortazavi A, Kwan G, van Baren MJ, Salzberg SL, Wold BJ and Pachter L (2010) Transcript assembly and quantification by RNA-Seq reveals unannotated transcripts and isoform switching during cell differentiation. *Nat Biotechnol* **28**(5): 511-515.

Turski ML, Vidwans SJ, Janku F, Garrido-Laguna I, Munoz J, Schwab R, Subbiah V, Rodon J and Kurzrock R (2016) Genomically Driven Tumors and Actionability across Histologies: BRAF-Mutant Cancers as a Paradigm. *Mol Cancer Ther* **15**(4): 533-547.

Van der Auwera GA, Carneiro MO, Hartl C, Poplin R, Del Angel G, Levy-Moonshine A, Jordan T, Shakir K, Roazen D, Thibault J, Banks E, Garimella KV, Altshuler D, Gabriel S and DePristo MA (2013) From FastQ data to high confidence variant calls: the Genome Analysis Toolkit best practices pipeline. *Curr Protoc Bioinformatics* **43**: 11 10 11-11 10 33.

Wagle MC, Kirouac D, Klijn C, Liu B, Mahajan S, Junttila M, Moffat J, Merchant M, Huw L, Wongchenko M, Okrah K, Srinivasan S, Mounir Z, Sumiyoshi T, Haverty PM, Yauch RL, Yan Y, Kabbarah O, Hampton G, Amler L, Ramanujan S, Lackner MR and Huang SA (2018) A transcriptional MAPK Pathway Activity Score (MPAS) is a clinically relevant biomarker in multiple cancer types. *NPJ Precis Oncol* **2**(1): 7.

Wilmott JS, Long GV, Howle JR, Haydu LE, Sharma RN, Thompson JF, Kefford RF, Hersey P and Scolyer RA (2012) Selective BRAF inhibitors induce marked T-cell infiltration into human metastatic melanoma. *Clin Cancer Res* **18**(5): 1386-1394.

Yaeger R and Corcoran RB (2019) Targeting Alterations in the RAF-MEK Pathway. *Cancer Discov* **9**(3): 329-341.

CHAPTER 3

Identifying the ErbB/MAPK signaling cascade as a therapeutic target in canine bladder cancer[2]

SUMMARY

Transitional cell carcinoma (TCC) of the bladder comprises 2% of diagnosed canine cancers. TCC tumors are generally inoperable and unresponsive to traditional chemotherapy, indicating a need for more effective therapies. BRAF, a kinase in the mitogen-activated protein kinase (MAPK) pathway, is mutated in 70% of canine TCCs. In this study, we use BRAF mutant and wild-type TCC cell lines to characterize the role of BRAF mutations in TCC pathogenesis and assess the efficacy of inhibition of the MAPK pathway alone and in combination with other gene targets as a treatment for canine TCC. Analysis of MAPK target gene expression and assessment of ERK1/2 phosphorylation following serum starvation indicated constitutive MAPK activity in all TCC cell lines. BRAF mutant TCC cell lines were insensitive to the BRAF inhibitor vemurafenib, with IC_{50} values greater than 5 μM, but exhibited greater sensitivity to a "paradox-breaking" BRAF inhibitor (IC_{50}: 0.2-1 μM). All TCC cell lines had IC_{50} values less than 7 nM to the MEK1/2 inhibitor trametinib independent of their BRAF mutation status. ERK1/2 phosphorylation decreased after 6-hour treatments with MAPK

[2] This chapter was published on May 2, 2019 in Molecular Pharmacology.
Cronise KE, Hernandez BG, Gustafson DL and Duval DL (2019) Identifying the ErbB/MAPK Signaling Cascade as a Therapeutic Target in Canine Bladder Cancer. *Mol Pharmacol* 96(1): 36-46.

inhibitors, but rebounded by 24 hours, suggesting the presence of resistance mechanisms. Microarray analysis identified elevated expression of the ErbB family of receptors and ligands in TCC cell lines. The pan-ErbB inhibitor sapitinib synergized with BRAF inhibition in BRAF mutant Bliley TCC cells and synergized with MEK1/2 inhibition in Bliley and BRAF wild-type Kinsey cells. These findings suggest the potential for combined MAPK and ErbB receptor inhibition as a therapy for canine TCC.

INTRODUCTION

TCC is the most common bladder cancer in humans and dogs, comprising approximately 4 and 2% of diagnosed malignancies in each species, respectively (Knapp and McMillan, 2013; Siegel et al., 2018). Most canine TCCs are muscle-invasive tumors of intermediate- to high-grade, with metastases present in 15% of patients at diagnosis and 50% at death. Canine TCC tumors are typically located in the trigone of the bladder, preventing complete surgical resection in most cases (Knapp and McMillan, 2013). These tumors are treated with cyclooxygenase inhibitors alone or in combination with cytotoxic chemotherapeutics; however, median survival time is typically less than a year for all treatment options, indicating a need for more effective therapies (Fulkerson and Knapp, 2015; Knapp and McMillan, 2013). Canine and human TCCs share similarities in their molecular markers, sites of metastasis, and response to chemotherapeutic agents (Fulkerson et al., 2017). Muscle-invasive bladder cancer is less common in humans than dogs but has a similar poor prognosis (Knowles and Hurst, 2015).

A major distinction between canine and human TCC is the occurrence of activating BRAF mutations in 70% of canine tumors (Decker et al., 2015; Duval et al., 2014; Mochizuki et al., 2015). BRAF is a serine/threonine protein kinase in the MAPK signaling pathway that regulates cell growth, proliferation, differentiation, and apoptosis (Dhillon et al., 2007). Mutations resulting in dysregulation of the MAPK pathway occur in one-third of human cancers, with activating BRAF mutations identified in 50% of malignant melanomas and at lower frequencies in colorectal and thyroid carcinomas (Dankner et al., 2018; Dhillon et al., 2007). Ninety percent of activating BRAF mutations in human cancers are valine-to-glutamic acid missense mutations at amino acid 600 (V600E) in the protein's activation loop (Dhillon et al., 2007). This alteration allows BRAF to signal as a monomer independent of upstream RAS activation, resulting in increased MAPK pathway activity (Dankner et al., 2018).

Several small-molecule inhibitors have been developed to target the MAPK signaling cascade. Vemurafenib, an ATP-competitive inhibitor of BRAFV600E, showed promising antitumor activity in humans with late-stage melanoma, with a 48% response rate compared to 5% with standard-of-care dacarbazine (Chapman et al., 2011). Despite vemurafenib's initial success, the majority of these tumors eventually acquired resistance (Sosman et al., 2012). Combination therapies that include both BRAF inhibitors and inhibitors of MEK1/2, BRAF's downstream target, have shown greater success in melanoma than single-agent treatment, leading to FDA-approval of these combinations for the treatment of metastatic melanoma (Ascierto et al., 2016; Long et al., 2017). Unlike melanoma, colorectal tumors are innately resistant to BRAF inhibition (Kopetz et al., 2015). Various resistance mechanisms to BRAF inhibition have been

identified in human melanoma and colorectal cancer including up-regulation of receptor tyrosine kinases (RTKs), secondary mutations in RAS, and increased signaling through the PI3K/AKT pathway (Mao et al., 2013; Nazarian et al., 2010).

The discovery of a homologous BRAF-activating mutation in canine TCC identifies a compelling new potential drug target for canine TCC treatment; however, additional *in vitro* evaluation of canine BRAF's function and sensitivity to targeted agents is required. The utility of canine cancers as a model for human cancers has become increasingly widespread. Mouse models are poor predictors of anticancer drug efficacy in human patients. Spontaneous tumors in dogs develop under normal immunosurveillance, share molecular and histological features with human cancers, and undergo the processes of metastasis and drug resistance. Additionally, clinical trials in dogs provide the opportunity to evaluate the efficacy of novel treatments in chemotherapy-naïve patients in a shorter amount of time compared to clinical trials in human patients (Gordon et al., 2009).

In this study, we further characterize BRAF mutations in canine TCC cell lines. We assess the ability of BRAF and MEK1/2 targeted agents to inhibit TCC cell growth and block ERK1/2 phosphorylation as a measure of MAPK pathway activation. We use differential gene expression analysis to determine other potential gene targets for TCC treatment, identifying combined inhibition of the MAPK pathway and the ErbB family of receptors as a therapy with synergistic activity in both BRAF mutant and wild-type TCC cell lines. The results of this study not only identify a novel therapy for canine TCC, but also establish canine TCC's value as a model for human MAPK-driven cancers, where

clinical trials in dogs with naturally occurring bladder tumors can inform therapies for human patients.

MATERIAL AND METHODS

Cell lines

Human cell lines were provided by Dr. John Tentler, University of Colorado Anschutz Medical Campus (RKO, HT29, Colo205) or purchased from ATCC (A375) (Manassas, VA). Canine TCC cell lines were provided by Dr. Steve Dow at Colorado State University (Bliley) or Dr. Elizabeth McNiel at Tufts University (Angus1, Kinsey, Tyler1, Tyler2). All cell lines were maintained in Dulbecco's modified Eagle's media supplemented with 10% fetal bovine serum (FBS), 100 units/mL penicillin, 100 µg/ml streptomycin, and 1mM sodium pyruvate (Thermo Fisher Scientific, Waltham, MA). Cells were incubated at 37°C in 5% CO_2 and 100% humidity. Canine cell lines were validated using short tandem repeat analysis with the Canine Stockmarks Genotyping Kit (Thermo Fisher Scientific, Waltham, MA) as previously described (O'Donoghue et al., 2011).

Sequencing of canine BRAF

Total RNA was extracted from the Bliley TCC cell line using the RNeasy Mini Kit (Qiagen, Germantown, MD) and reverse transcribed to cDNA with the ImProm-II Reverse Transcription System (Promega, Madison, WI). Polymerase chain reaction (PCR) amplification of BRAF was performed using the following primers: forward, 5'-CACCATGGAAGCCCTATTGGACAAGTTTGGT-3'; reverse, 5'-

CTTGAAGGCTGCAAATTCTCCGTA-3'. The resulting amplicon was gel extracted with the QIAquick Gel Extraction Kit (Qiagen, Germantown, MD) and cloned into an expression vector using the pcDNA/3.2/GW/D-TOPO Expression Kit (Thermo Fisher Scientific, Waltham, MA). Following transformation into One Shot TOP10 Chemically Competent *E. coli* (Thermo Fisher Scientific, Waltham, MA), individual clones were isolated and sequenced at the Proteomics and Metabolics Facility at Colorado State University.

5' rapid amplification of cDNA ends (5' RACE) with the SMARTer RACE 5'/3' Kit (Takara Bio, Japan) was performed according to the manufacturer's protocol. First-strand cDNA was synthesized from total RNA isolated from the Bliley TCC cell line. 5' RACE PCR using the reverse primer 5'-GATTACGCCAAGCTTTGGCGTGTAAGTAATCCATGCCCTGTGC-3' and SeqAmp DNA Polymerase (Takara Bio, Japan) was performed to obtain a product containing the 5' sequence of BRAF. The 5' RACE PCR product was gel extracted using NucleoSpin Gel and PCR Clean-Up Kit (Takara Bio, Japan) and cloned into the 5' RACE vector with the In-Fusion HD Cloning Kit (Takara Bio, Japan). The resulting construct was transformed into Stellar Competent Cells (Takara Bio, Japan) according to the manufacturer's protocol and individual clones were isolated for sequencing by GENEWIZ (South Plainfield, NJ).

Cell viability assays

Vemurafenib and 5-(2-cyclopropylpyrimidin-5-yl)-3-[3-[[ethyl(methyl)sulfamoyl]amino]-2,6-difluoro-benzoyl]-1*H*-pyrrolo[2,3-*b*]pyridine (PLX7904) are inhibitors of BRAFV600E. Selumetinib and trametinib are inhibitors of

MEK1/2. Sapitinib is an inhibitor of ErbB receptors EGFR, ERBB2 and ERBB3. All inhibitors were purchased from Selleck Chemicals (Houston, TX) and stock solutions were prepared in dimethyl sulfoxide (DMSO) and stored according to the manufacturer's protocol.

Cell lines were plated in 96-well plates at 1,000-5,000 cells/well in 100 μl of complete media and incubated for 24 hours at 37°C. Serial dilutions of inhibitor or DMSO control were prepared in complete media at a 2X concentration and 100 μl was added to each well. Plates were incubated at 37°C for 72 hours and cell proliferation was monitored using the IncuCyte ZOOM Live-Cell Analysis System (Essen BioScience Inc., Ann Arbor, MI). Percent confluence at 72 hours was normalized by dividing by confluence at 0 hours, and relative cell number was determined as a fraction of DMSO control. Dose-response curves were fitted in GraphPad Prism (v7) using a non-linear regression of the logarithm of inhibitor concentration versus fraction of control. Half maximal inhibitory concentration (IC_{50}) values were determined as the concentration of inhibitor corresponding to half the fraction of control on the dose-response curves.

For combination treatments, relative cell number was determined similar to single-agent therapies, and fraction affected was determined as a fraction of DMSO control. Combination indices were calculated for each combination using CalcuSyn (v2.11) software. Representative images of combination treatments were obtained using red-labeled cells (NucLight Rapid Red Reagent, Essen BioScience Inc., Ann Arbor, MI). For both single-agent and combination drug sensitivity assays, three to five independent experiments were conducted for each cell line. Each independent

experiment included three technical replicates for each drug concentration and DMSO control.

Western blotting and antibodies

Cells were lysed by sonication in RIPA buffer (20 mM Tris-HCl, 150 mM NaCl, 1 mM Na_2EDTA, 1 mM EGTA, 1% NP-40, 1% sodium deoxycholate, and 50 mM NaF) supplemented with protease and phosphatase inhibitors (2.5 mM sodium pyrophosphate, 1 mM beta-glycerophosphate, 1mM Na_3VO_4, and 1 ug/ml leupeptin). Lysates were centrifuged at 14,000 rpm to isolate protein fractions and total protein was quantified using the Pierce BCA Protein Assay Kit (Thermo Fisher Scientific, Waltham, MA). Equal amounts of total protein were resolved on 4-20% Criterion TGX Protein Gels (Bio-Rad Laboratories, Hercules, CA) and transferred to PVDF membranes with the TransBlot Turbo Transfer System (Bio-Rad Laboratories, Hercules, CA). Membranes were blocked in Tris-buffered saline with 0.1% Tween-20 (TBST) with 5% bovine serum albumin for one hour at room temperature. Blots were incubated overnight at 4°C with primary antibodies diluted in blocking buffer (phospho-p44/42 MAPK (Thr202/Tyr204) Rabbit mAb #4370 (1:1,000), p44/42 MAPK Rabbit mAb #4695 1:1,000, B-Raf Rabbit mAb #14815 (1:1,000), Cell Signaling Technology, Danvers, MA; α-tubulin #T5168 (1:5,000), Sigma-Aldrich, St. Louis, MO). Membranes were washed three times with TBST, incubated with secondary antibody (goat anti-rabbit IgG HRP-conjugated (1:10,000) or goat anti-mouse IgG HRP-conjugated (1:10,000), Bio-Rad Laboratories, Hercules, CA) at room temperature for an hour, followed by three TBST washes. Blots were developed using Clarity Western ECL Blotting Substrate (Bio-Rad

Laboratories, Hercules, CA) and imaged with a Chemi Doc XES+ System (Bio-Rad Laboratories, Hercules, CA).

Microarray analysis

Total RNA was isolated from cell lines with the RNeasy Mini Kit (Qiagen, Germantown, MD) and microarray analysis was performed at the Functional Genomics Facility at University of Colorado Denver Anschutz Medical Campus using GeneChip Canine Gene 1.0 ST Arrays (Affymetrix, Santa Clara, CA) (Fowles et al., 2017). Gene expression values were determined following robust multi-array average normalization in R (v3.3) using the 'oligo' package (Halper-Stromberg et al., 2011). Differentially expressed genes were determined using a Benjamani & Hochberg false discovery rate cutoff of 0.05 and a fold change of at least 1.5. If multiple probe sets for a single gene were present, the probe set with the highest variance across samples was used.

MPAS score

MAPK Pathway Activity Scores (MPAS) were calculated as previously described based on expression levels of ten MAPK target genes: *CCND1, DUSP4, DUSP6, EPHA2, EPHA4, ETV4, ETV5, PHLDA1, SPRY2, SPRY4* (Wagle et al., 2018). Briefly, z-scores for MPAS genes were determined across all samples using $\log_2$-transformed expression values. MPAS scores for each sample were calculated as MPAS = (sum of z-scores for MPAS genes) / ($\sqrt{10}$).

RESULTS

Canine BRAF is homologous to human BRAF

Reverse transcription PCR was utilized to amplify BRAF's coding sequence from the Bliley TCC cell line. The resulting amplicon, corresponding to predicted canine BRAF AA10-772 (ENSCAFP00000005841), exhibited 99% homology to human BRAF AA62-767 (ENSP00000419060). Since the predicted canine protein was truncated at the amino-terminus compared to human BRAF, 5' RACE was used to determine the N-terminal sequence of canine BRAF, revealing an additional 48 amino acids not present in the predicted canine BRAF sequence (ENSCAFP00000005841). The resulting full length predicted BRAF protein is 763 amino acids and exhibits 98% homology to human BRAF (ENSP00000419060). Our analysis also identified a heterozygous V to E missense mutation at amino acid 596 consistent with previously identified BRAF mutations in TCC tumors (Decker et al., 2015; Duval et al., 2014; Mochizuki et al., 2015). Western blot analysis of BRAF in canine TCC cell lines and the human BRAF V600E A375 melanoma cell line suggests that BRAF is expressed at a similar size and abundance in both humans and dogs (**Figure 3.1**).

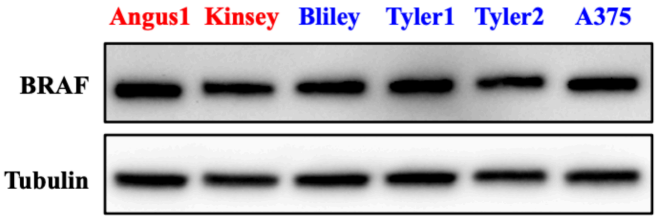

Figure 3.1 Western blot of BRAF protein abundance in canine TCC cell lines and the A375 melanoma cell line.
BRAF wild type cell lines are in red and BRAF mutant cell lines are in blue.

Canine TCC cell lines exhibit constitutive MAPK activity

BRAFV600E mutations result in constitutive MAPK activity in human cancers (Dhillon et al., 2007). A gene expression signature quantifying relative MAPK activity in a variety of human cancers was recently described (Wagle et al., 2018). A MAPK Pathway Activation Score (MPAS) was calculated based on expression levels of 10 gene targets of the MAPK pathway obtained using Canine 1.0ST arrays. MPAS scores were calculated for five TCC cell lines as well as 30 other canine cancer cell lines in the Flint Animal Cancer Center (FACC) cell line panel (Fowles et al., 2017). TCC cell lines exhibited high MPAS values relative to other canine cancer cell lines, suggesting high MAPK pathway activity in TCC cell lines (**Figure 3.2**). To validate these findings, MPAS scores were also calculated using gene expression levels from Canine 2.0 arrays (Fowles et al., 2017). MPAS scores correlated between Canine 1.0ST and Canine 2.0 arrays ($R=0.9263$, $p<0.0001$, **Figure 3.2**).

To determine whether canine TCC cell lines with BRAF mutations exhibit constitutive MAPK pathway activity, cells were cultured for 24 hours in the absence of FBS followed by assessment of ERK1/2 phosphorylation by western blot. Five TCC cell lines were analyzed: three with heterozygous BRAF V596E mutations (Bliley, Tyler1, and Tyler2), one with a heterozygous KRAS G12D mutation (Angus1), and one wild-type for BRAF and KRAS (Kinsey) (Das et al., 2019). ERK1/2 phosphorylation was sustained under serum-starved conditions in BRAF and KRAS mutant cell lines (**Figure 3.2**). Interestingly, the Kinsey cell line, which does not harbor any known activating cancer gene mutations in the MAPK pathway, also showed constitutive ERK1/2 phosphorylation.

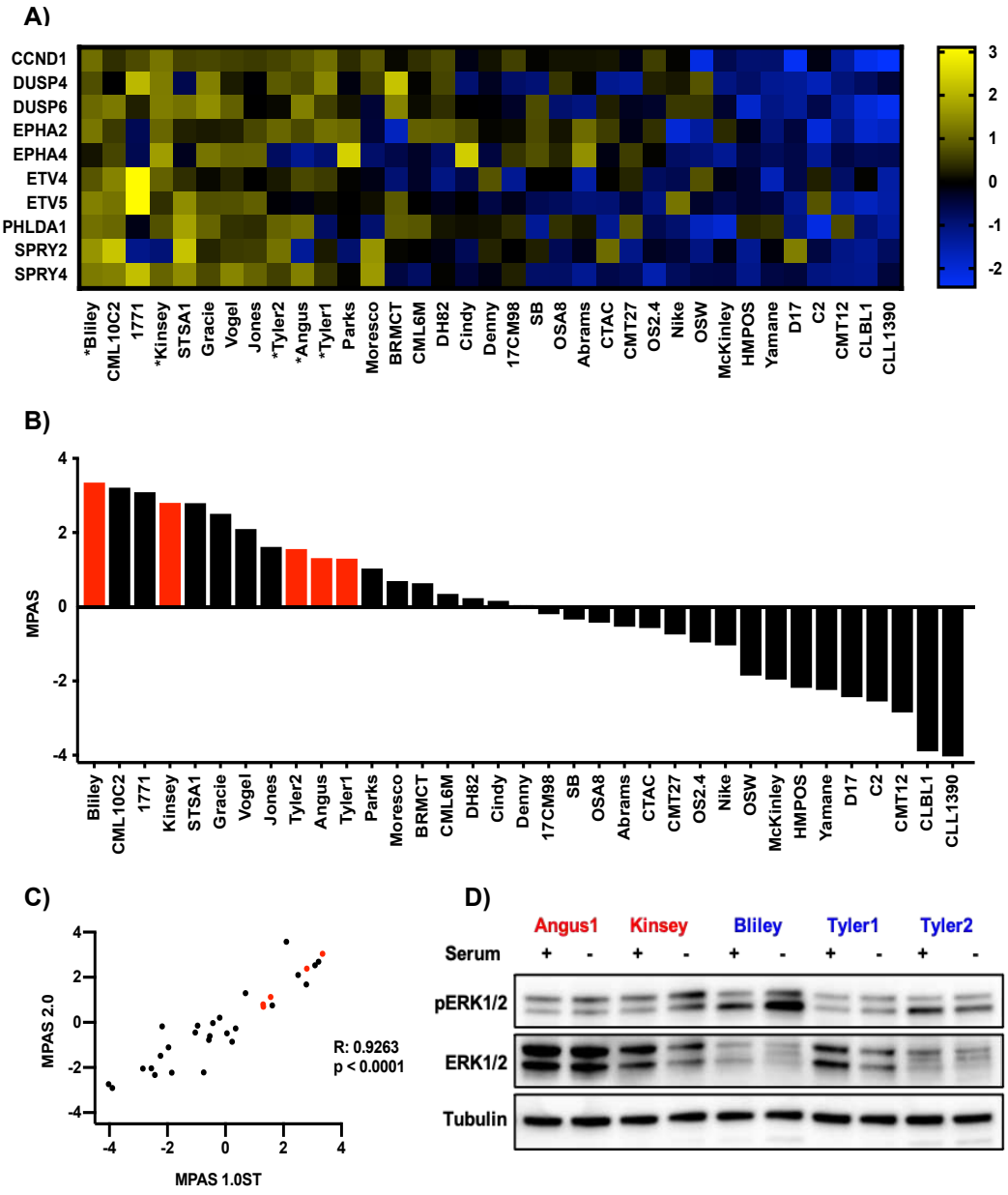

Figure 3.2. Canine TCC cell lines exhibit constitutive MAPK pathway activity. (A) Heat map of z-transformed expression values for MPAS genes in the FACC cell line panel. Asterisks (*) indicate TCC cell lines. (B) MPAS values for FACC cell lines. TCC cell lines are shown in red. (C) MPAS values determined using Canine 1.0ST arrays versus those determined using Canine 2.0 arrays (Pearson r = 0.9263, p < 0.0001). (D) Serum starvation of canine TCC cell lines followed by western blot analysis of ERK1/2 phosphorylation. BRAF mutant cell lines are shown in blue and wild-type are shown in red.

BRAF mutant canine TCC cell lines are insensitive to vemurafenib, but sensitive to a "paradox-breaking" BRAF inhibitor

The effect of BRAF inhibition on TCC cell proliferation was determined using vemurafenib, an ATP-competitive inhibitor of mutant BRAF. Drug sensitivity assays were also conducted in human BRAF mutant melanoma (A375) and colorectal cancer cell lines (RKO, HT29, Colo205) with varying degrees of sensitivity to vemurafenib (Yang et al., 2012). All TCC cell lines had IC_{50} values greater than 5 μM (**Figure 3.3**; **Table 3.1**). Canine TCC cell lines were roughly 10- to 100-fold less sensitive than human BRAF mutant A375, Colo-205 and HT29 cancer cell lines and exhibited levels of sensitivity similar to the RKO colorectal cancer cell line (**Table 3.1**).

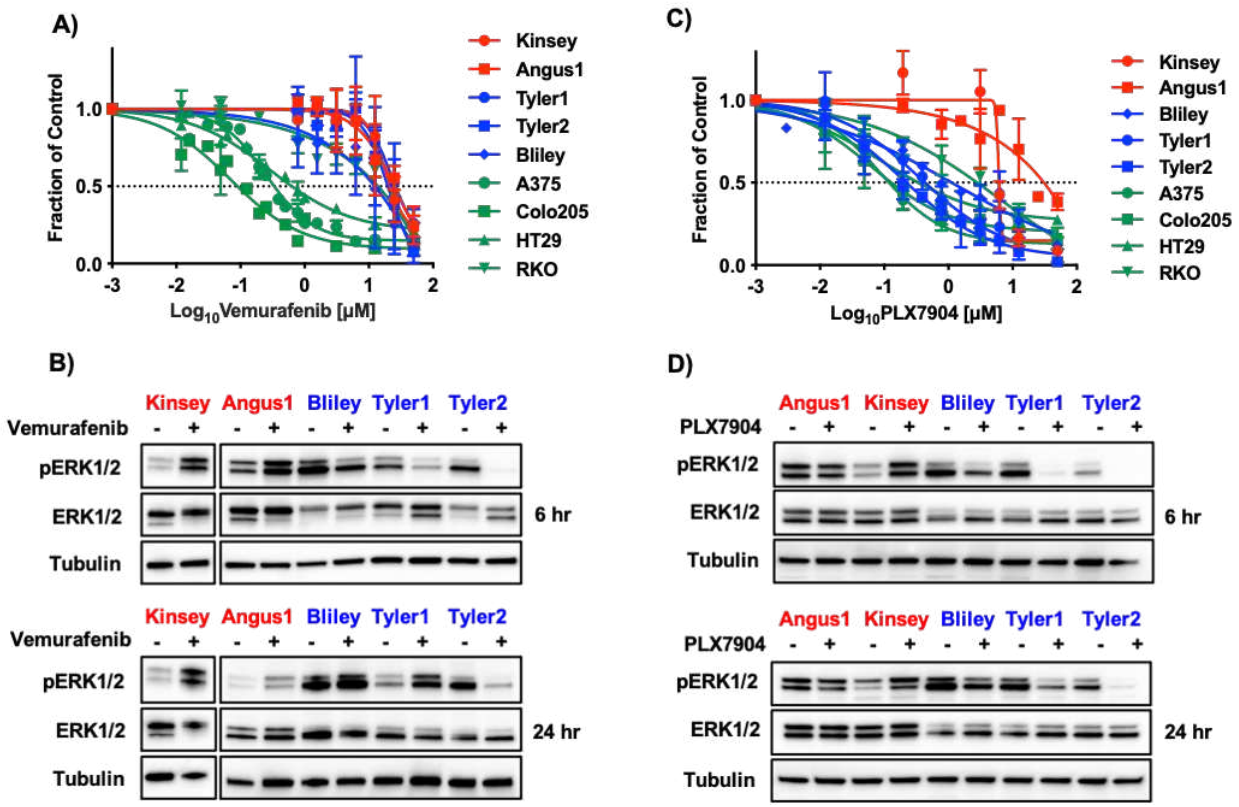

Figure 3.3 BRAF mutant TCC cell lines are sensitive to "paradox-breaking" PLX7904, but insensitive to vemurafenib.
Cell lines were treated with serial dilutions of (A) vemurafenib or (C) PLX7904 for 72 hours. Relative viability at each dose was determined as a fraction of vehicle control. Three to five independent experiments with three technical replicates were conducted for each cell line. Error bars represent the standard deviation of the fraction of control from combined experiments (n=3-5). TCC cell lines were treated with (B) 15 μM vemurafenib or (D) 2 μM PLX7904 for 6 (top) and 24 (bottom) hours and assessed for ERK1/2 phosphorylation via western blot analysis. Western blot analysis of Kinsey cell lysate in (B) was performed on a separate blot. BRAF mutant and wild type canine cell lines are shown in blue and red, respectively. BRAF mutant human cell lines are shown in green.

Table 3.1 IC_{50} values to BRAF and MEK inhibitors in canine and human cancer cell lines. Values shown are the mean and 95% confidence interval of IC_{50} values determined from three to five independent experiments. Each experiment included three technical replicates for each drug concentration. IC_{50} values were rounded to two significant figures.

	Vemurafenib [μM]	PLX7904 [μM]	Selumetinib [nM]	Trametinib [nM]
Canine				
Angus1	19 (7.6 – 48)	21 (6.6 – 69)	150 (41 – 530)	6.2 (1.9 – 20)
Kinsey	20 (9.3 – 45)	6.1 (5.8 – 6.3)	18 (13 – 23)	0.10 (0.019 – 0.56)
Bliley	9.0 (2.8 – 29)	0.96 (0.43 – 2.1)	240 (140 – 410)	1.4 (0.39 – 5.6)
Tyler1	26 (14 – 49)	0.52 (0.18 – 1.5)	140 (47 – 390)	2.2 (0.55 – 9.0)
Tyler2	19 (8.4 – 42)	0.20 (0.072 – 0.58)	390 (100 – 1,500)	3.1 (0.94 – 10)
Human				
A375	0.35 (0.23 – 0.54)	0.11 (0.058 – 0.23)	81 (55 – 120)	1.2 (0.72 – 2.0)
Colo205	0.077 (0.020 – 0.30)	0.10 (0.020 – 0.54)	100 (29 – 360)	0.26 (0.076 – 0.87)
HT29	0.60 (0.25 – 1.4)	0.32 (0.075 – 1.3)	130 (62 – 270)	0.70 (0.17 – 2.9)
RKO	14 (9.5 – 21)	2.8 (1.1 – 7.1)	1,700 (660 – 4,600)	8.6 (0.96 – 78)

To determine whether vemurafenib inhibits MAPK pathway activity in TCC cell lines, ERK1/2 phosphorylation was assessed following 6- and 24-hour treatments with vemurafenib. ERK1/2 phosphorylation was suppressed at 6 hours in BRAF mutant cell lines, but rebounded by 24 hours (**Figure 3.3**). Similarly, colorectal cancer cell lines achieve MAPK pathway reactivation by 24 hours post-treatment, whereas melanoma cell lines maintain pathway suppression (Corcoran et al., 2012). Conversely, vemurafenib treatment increased ERK1/2 phosphorylation in KRAS mutant Angus1 and BRAF/KRAS wild-type Kinsey cells. This response is consistent with paradoxical

activation of the MAPK pathway following BRAF inhibition in KRAS mutant and BRAF/KRAS wild-type human cancer cell lines. Mutant BRAF signals as a monomer, but wild-type BRAF requires dimerization with other RAF isoforms. Binding of BRAF inhibitors to wild-type BRAF stabilizes the formation of dimers resulting in increased MAPK signaling (Hatzivassiliou et al., 2010; Heidorn et al., 2010; Poulikakos et al., 2010).

Since BRAF mutations in canine TCC cell lines are heterozygous, we wanted to investigate whether TCC insensitivity to vemurafenib could be due to paradoxical MAPK pathway activation as a result of the wild-type copy of BRAF. Thus, sensitivity to the "paradox-breaking" BRAF inhibitor PLX7904 was determined in canine and human cells lines. BRAF mutant canine cell lines had IC_{50} values ranging from 0.2 to 1 μM, similar to BRAF mutant human cell lines, whereas wild-type cell lines exhibited IC_{50} values greater than 5 μM (**Figure 3.3**, **Table 3.1**). ERK1/2 phosphorylation decreased in BRAF mutant cell lines following a 6-hour incubation with PLX7904, but rebounded by 24 hours, although the extent of rebound was less than that with vemurafenib (**Figure 3.3**). ERK1/2 phosphorylation remained unchanged in KRAS mutant Angus1 and increased in BRAF/KRAS wild-type Kinsey cells.

Canine TCC cell lines are sensitive to MEK inhibition

To determine whether MAPK inhibition downstream of BRAF is an effective therapeutic option, we targeted MEK in canine and human cell lines with the selective, allosteric MEK1/2 inhibitors selumetinib and trametinib. Canine TCC cell lines exhibited similar degrees of sensitivity to MEK inhibition as human BRAF mutant cell lines. Canine TCC IC_{50} values ranged from 18 to 390 nM and 0.1 to 6.2 nM for selumetinib

and trametinib, respectively. Human cell lines exhibited IC_{50} values of 81 to 1,700 nM and 0.3 to 8.6 nM for selumetinib and trametinib, respectively (**Figure 3.4**, **Table 3.1**). BRAF mutant cell lines in the Genomics of Drug Sensitivity in Cancer database have median IC_{50} values of 640 and 19 nM to selumetinib and trametinib, respectively (Yang et al., 2013). Thus, canine TCC cell lines exhibited sensitivities to MEK inhibition similar to human BRAF mutant cell lines. Interestingly, BRAF/KRAS wild-type Kinsey cells were the most sensitive to MEK inhibition of all tested cell lines. This response is supported by Kinsey's MPAS value, which is the fourth highest in the FACC cell line panel. ERK1/2 phosphorylation was blocked in all cell lines after 6 hours of MEK inhibition but, as with BRAF inhibition, showed a degree of rebound by 24 hours indicating reactivation of the MAPK pathway despite MAPK inhibition (**Figure 3.4**). Combined BRAF and MEK inhibition synergized in BRAF mutant Bliley cells, but not wild-type Kinsey cells (median combination index (CI) of 0.5 versus 1.1, respectively; **Figure 3.5**).

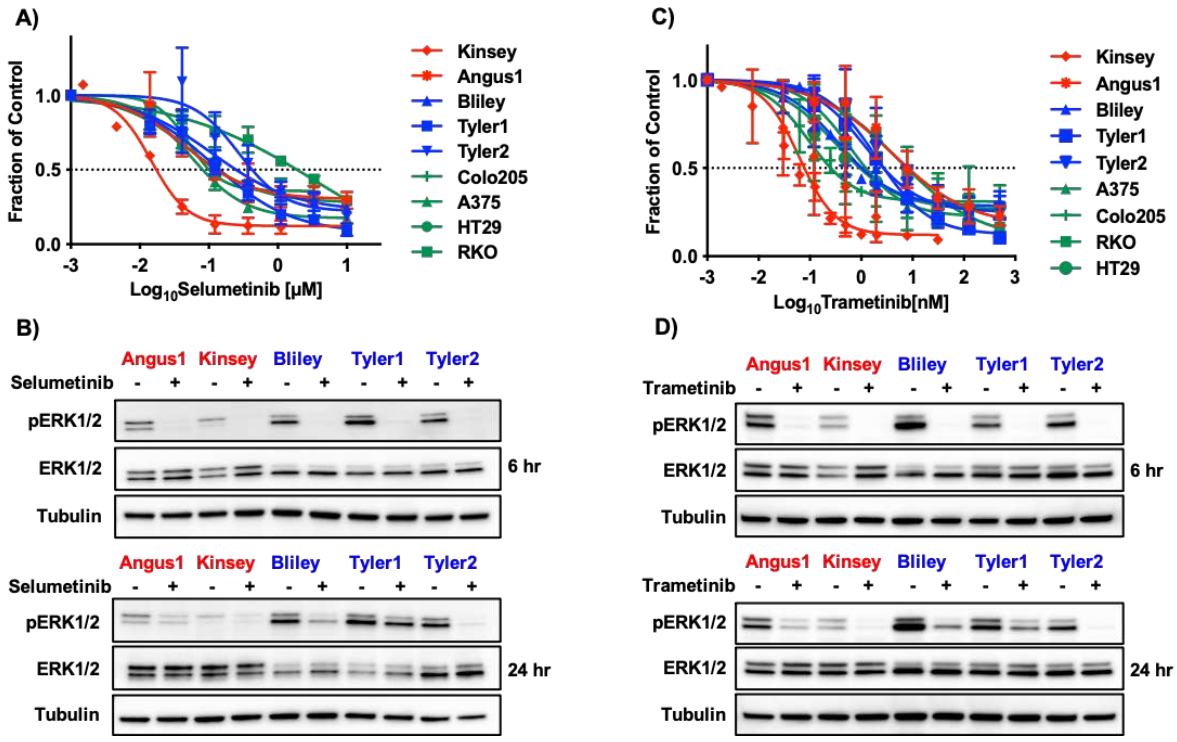

Figure 3.4 Canine TCC cell lines are sensitive to MEK1/2 inhibition.
Cell lines were treated with serial dilutions of (A) selumetinib or (C) trametinib for 72 hours. Relative viability at each dose was determined as a fraction of vehicle control. Three to five independent experiments with three technical replicates were conducted for each cell line. Error bars represent the standard deviation of the fraction of control from combined experiments (n=3-5).. TCC cell lines were treated with (B) 500 nM selumetinib or (D) 25 nM trametinib for 6 (top) and 24 (bottom) hours and assessed for ERK1/2 phosphorylation via western blot analysis. BRAF mutant and wild-type canine cell lines are shown in blue and red, respectively. BRAF mutant human cell lines are shown in green.

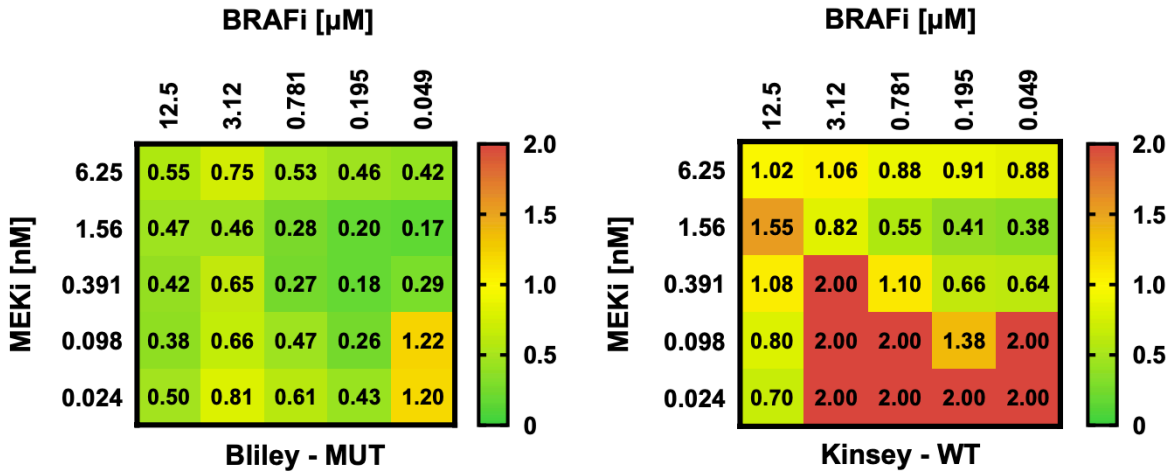

Figure 3.5 Combined BRAF and MEK1/2 inhibition in canine TCC cell lines. Cells were treated with serial dilutions of the "paradox-breaking" BRAF inhibitor PLX7904 (BRAFi) and MEK1/2 inhibitor trametinib (MEKi). Cell proliferation was monitored for 72 hours. Drug synergy was determined using CalcuSyn software. Colors on heat maps represent combination index (CI) values, where CI < 1 is synergistic (green), CI = 1 is additive, and CI > 1 is antagonistic (red)

ErbB signaling is up-regulated in TCC cell lines relative to other canine cancer cell lines

Synthetic lethality has been widely explored as an antitumor strategy. Cancer cells often harbor specific oncogenic alterations that may not be targeted effectively alone but, when targeted in combination with a second gene, elicit a lethal response (O'Neil et al., 2017) . Single-agent treatment of canine TCC cell lines with BRAF or MEK inhibitors yielded an initial attenuation of MAPK pathway activity followed by a rebound in pathway activity by 24 hours of treatment. This short-lived response suggests that MAPK inhibition may not be effective as a monotherapy for TCC treatment. Thus, we sought to identify a second gene target that, when inhibited in combination with BRAF, exhibits a synergistic response. To identify potential candidate targets, we determined

genes differentially expressed in TCC cell lines relative to other canine cancer cell lines. To avoid histotype-specific genes, we limited our analysis to 719 cancer-related genes present in the COSMIC database (v83) (Forbes et al., 2017).

Twenty-nine and nine cancer genes were up- and down-regulated in TCC cell lines relative to other cancer cell lines, respectively (**Figure 3.6**). This analysis revealed up-regulation of genes encoding epidermal growth factor (EGFR) and receptor tyrosine-protein kinase erbB-2 (ErbB2) receptors in TCC cell lines. We then expanded our analysis to all ErbB ligands and receptors present in the KEGG pathway database (hsa04012) (**Figure 3.6**). In addition to up-regulation of genes encoding EGFR and ErbB2 receptors, the ligand epiregulin (EREG) was also up-regulated in TCC cell lines. Additional cancer genes up-regulated in TCC cell lines include *CDH1*, *PPARG*, *NOTCH1*, and *MYC*. Down-regulated genes include *IDH2*, *SMO*, and *ALDH2*.

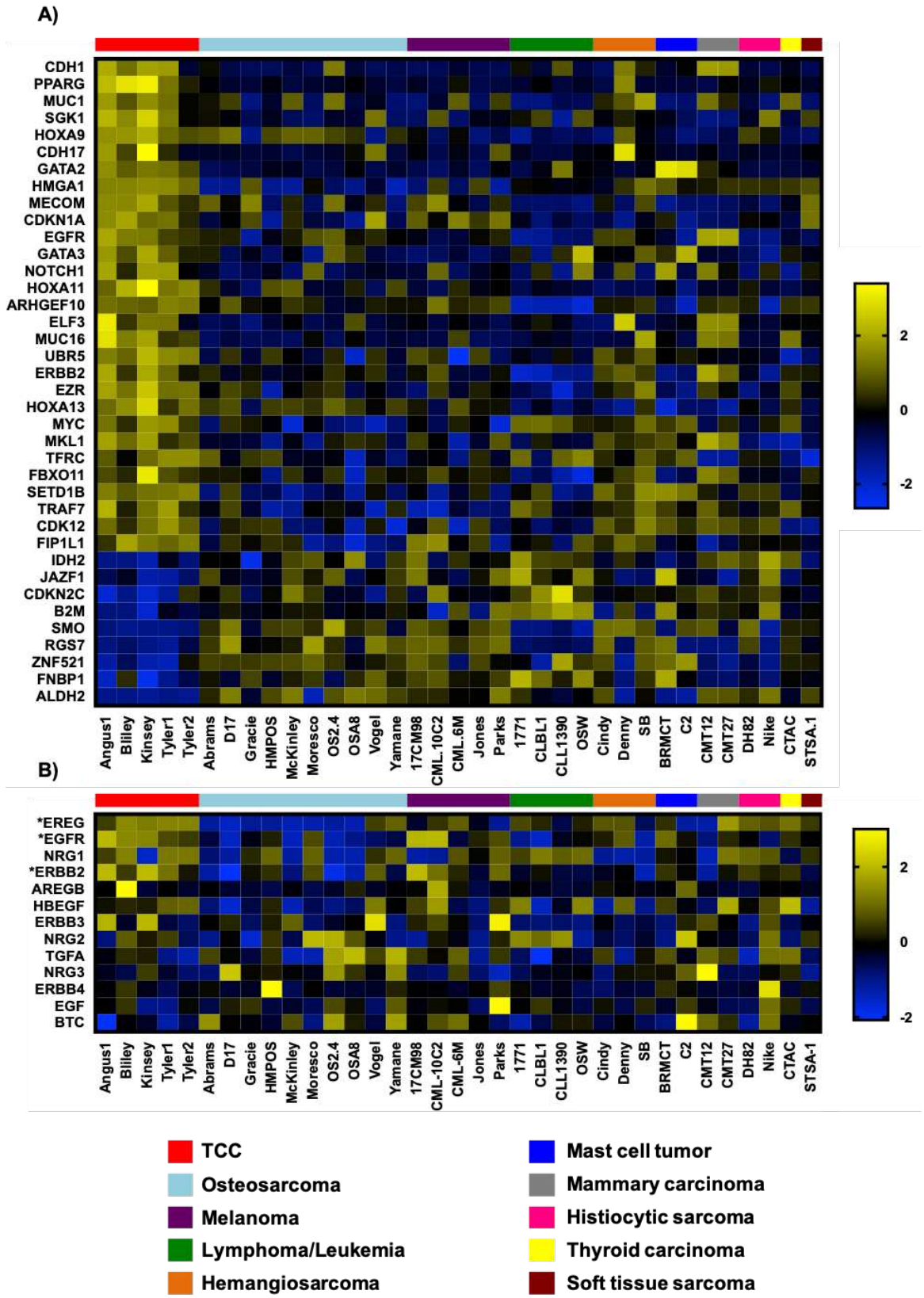
A)
CDH1
PPARG
MUC1
SGK1
HOXA9
CDH17
GATA2
HMGA1
MECOM
CDKN1A
EGFR
GATA3
NOTCH1
HOXA11
ARHGEF10
ELF3
MUC16
UBR5
ERBB2
EZR
HOXA13
MYC
MKL1
TFRC
FBXO11
SETD1B
TRAF7
CDK12
FIP1L1
IDH2
JAZF1
CDKN2C
B2M
SMO
RGS7
ZNF521
FNBP1
ALDH2
Angus1
Bliley
Kinsey
Tyler1
Tyler2
Abrams
D17
Gracie
HMPOS
McKinley
Moresco
OS2.4
OSA8
Vogel
Yamane
17CM98
CML.10C2
CML.6M
Jones
Parks
1771
CLBL1
CLL1390
OSW
Cindy
Denny
SB
BRMCT
C2
CMT12
CMT27
DH82
Nike
CTAC
STSA.1
2
0
-2
B)
*EREG
*EGFR
NRG1
*ERBB2
AREGB
HBEGF
ERBB3
NRG2
TGFA
NRG3
ERBB4
EGF
BTC
Angus1
Bliley
Kinsey
Tyler1
Tyler2
Abrams
D17
Gracie
HMPOS
McKinley
Moresco
OS2.4
OSA8
Vogel
Yamane
17CM98
CML-10C2
CML-6M
Jones
Parks
1771
CLBL1
CLL1390
OSW
Cindy
Denny
SB
BRMCT
C2
CMT12
CMT27
DH82
Nike
CTAC
STSA-1
2
0
-2
TCC
Osteosarcoma
Melanoma
Lymphoma/Leukemia
Hemangiosarcoma
Mast cell tumor
Mammary carcinoma
Histiocytic sarcoma
Thyroid carcinoma
Soft tissue sarcoma

Figure 3.6. Up-regulation of the ErbB signaling cascade in canine TCC cell lines. Microarray analysis was used to analyze gene expression in the FACC panel of canine cancer cell lines. (A) Cancer genes up- or down-regulated in TCC relative to other canine cancer cell lines using a fold change cutoff of 1.5 and $q < 0.05$. (B) Expression of ErbB ligands and receptors (KEGG pathway hsa04012) in FACC cell lines. Asterisks (*) indicate ErbB genes significantly up-regulated in TCC cell lines. Colors on heat maps represent z-transformed expression values. Color bars above heat maps indicate cell line histotype.

Pan-ErbB inhibition synergizes with MAPK inhibition in canine TCC

To determine whether ErbB inhibition alone or in combination with MAPK inhibition may be an effective treatment for canine TCC treatment, TCC cell lines were treated with a pan-ErbB inhibitor sapitinib that targets EGFR, ErbB2, and ErbB3 receptors. All TCC cell lines had IC_{50} values greater than 1 µM. Combination treatments were performed to assess the efficacy of pan-ErbB inhibition with MAPK inhibition. Sapitinib treatment synergized with the "paradox-breaking" BRAFV600E inhibitor PLX7904 in BRAF mutant Bliley cells but not in wild-type Kinsey cells (median CI 0.4 versus 1.4, respectively; **Figure 3.7**). Conversely, pan-ErbB inhibition synergized with MEK inhibition in both Bliley and Kinsey cells (median CI 0.7 and 0.5, respectively; **Figure 3.7**).

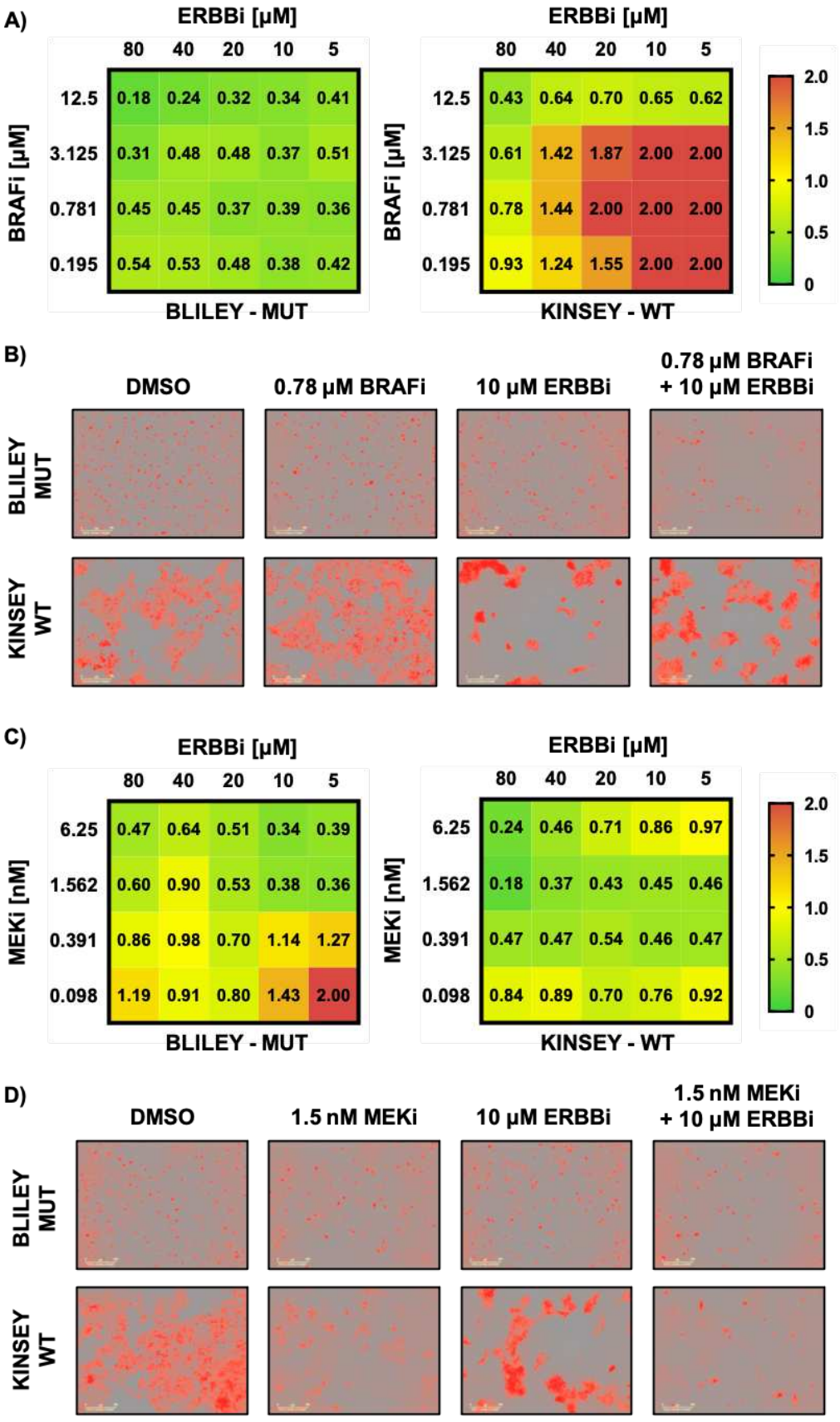
A)
ERBBi [μM]
80 40 20 10 5
BRAFi [μM]
12.5 0.18 0.24 0.32 0.34 0.41
3.125 0.31 0.48 0.48 0.37 0.51
0.781 0.45 0.45 0.37 0.39 0.36
0.195 0.54 0.53 0.48 0.38 0.42
BLILEY - MUT
ERBBi [μM]
80 40 20 10 5
BRAFi [μM]
12.5 0.43 0.64 0.70 0.65 0.62
3.125 0.61 1.42 1.87 2.00 2.00
0.781 0.78 1.44 2.00 2.00 2.00
0.195 0.93 1.24 1.55 2.00 2.00
KINSEY - WT
2.0
1.5
1.0
0.5
0
B)
DMSO
0.78 μM BRAFi
10 μM ERBBi
0.78 μM BRAFi + 10 μM ERBBi
BLILEY MUT
KINSEY WT
C)
ERBBi [μM]
80 40 20 10 5
MEKi [nM]
6.25 0.47 0.64 0.51 0.34 0.39
1.562 0.60 0.90 0.53 0.38 0.36
0.391 0.86 0.98 0.70 1.14 1.27
0.098 1.19 0.91 0.80 1.43 2.00
BLILEY - MUT
ERBBi [μM]
80 40 20 10 5
MEKi [nM]
6.25 0.24 0.46 0.71 0.86 0.97
1.562 0.18 0.37 0.43 0.45 0.46
0.391 0.47 0.47 0.54 0.46 0.47
0.098 0.84 0.89 0.70 0.76 0.92
KINSEY - WT
2.0
1.5
1.0
0.5
0
D)
DMSO
1.5 nM MEKi
10 μM ERBBi
1.5 nM MEKi + 10 μM ERBBi
BLILEY MUT
KINSEY WT

Figure 3.7. Combined MAPK and ErbB inhibition synergizes in canine TCC cell lines. Cells were treated with serial dilutions of the pan-ErbB inhibitor sapitinib (ERBBi) and (A,B) BRAF inhibitor PLX7904 (BRAFi) or (C,D) MEK1/2 inhibitor trametinib (MEKi), and cell proliferation was monitored for 72 hours. Drug synergy was determined using CalcuSyn software. (A,C) Colors on heat maps represent combination index (CI) values, where CI < 1 is synergistic (green), CI = 1 is additive, and CI > 1 is antagonistic (red). CI values were determined from three independent experiments (n=3). (B,D) Representative images of red-labeled TCC cells 72 hours post-treatment. Images were acquired using IncuCyte ZOOM Live-Cell Analysis System at 10X magnification. Scale bars are 300 μm.

DISCUSSION

Recent studies have identified BRAF mutations in approximately 70% of canine TCC tumors (Decker et al., 2015; Mochizuki et al., 2015). Despite this discovery, little is know about the role that BRAF mutations play in canine TCC development and whether targeting mutant BRAF is a feasible therapy for TCC. In this study, we targeted BRAF and its downstream kinase, MEK, in five TCC cell lines: three BRAF mutant, one KRAS mutant, and one BRAF/KRAS wild-type. MAPK inhibitors suppressed proliferation in TCC cell lines with varying degrees of efficacy, but failed to sustain attenuation of MAPK pathway activity. The ErbB family of receptors was identified as a potential therapeutic target for TCC treatment, and inhibition of ErbB receptors synergized with MAPK inhibition in TCC cell lines. These data demonstrate the potential of ErbB receptor inhibition combined with either BRAF or MEK inhibition as an effective therapy for canine TCC. Additionally, our findings illustrate canine TCC's potential utility as a naturally occurring model for investigating intrinsic resistance mechanisms to MAPK inhibition in human cancers and tailoring treatments to combat the emergence of resistance.

BRAF and KRAS mutant cell lines exhibited constitutive MAPK pathway activity based on expression levels of MAPK target genes (MPAS scores) and sustained ERK1/2 phosphorylation in the absence of FBS. Additionally, the Kinsey cell line, with no known MAPK mutation, also exhibited constitutive pathway activity. This phenomenon occurs in human cancers where ERK1/2 phosphorylation and expression of MAPK target genes do not always correlate with RAS/BRAF mutation status (Houben et al., 2008; Levidou et al., 2012; Wagle et al., 2018). Another group previously analyzed five different canine TCC cell lines and also showed sustained ERK1/2 phosphorylation in the absence of FBS for all cell lines (Rathore and Cekanova, 2014). Thus, constitutive MAPK activity seems to be a common occurrence in canine TCC, suggesting a possible causative role for the MAPK pathway in canine TCC pathogenesis. In human bladder cancer, BRAF mutations are rare; however, mutations in NRAS/HRAS occur in 6% of tumors and alterations in the RTK/Ras/PI3K pathway are present in 72% of tumors (Atlas, 2014; Robertson et al., 2017).

All five TCC cell lines were insensitive to BRAF inhibition with vemurafenib relative to human BRAF mutant melanoma (A375) and colorectal (Colo205 and HT29) cell lines. In fact, TCC cell lines exhibited IC_{50} values similar to that of the RKO colorectal cancer cell line, which was previously reported to be insensitive to vemurafenib (Yang et al., 2012). Vemurafenib treatment yielded an initial decrease in MAPK pathway activity in BRAF mutant TCC cell lines, but pathway activity rebounded by 24 hours post-treatment. Human colorectal cancer cell lines also achieve MAPK pathway reactivation following 24 hours of vemurafenib treatment (Corcoran et al., 2012; Yang et al., 2012). Unlike canine TCC and human colorectal cancer cell lines,

vemurafenib treatment in human melanoma cell lines maintains suppression of MAPK activation after 24 hours (Corcoran et al., 2012). Vemurafenib induced the same paradoxical MAPK activation in BRAF wild-type TCC cell lines that has been described in human BRAF wild-type cell lines. The mechanism behind paradoxical activation involves increased transactivation of RAF homo- or heterodimers as a result of vemurafenib binding, causing increased pathway activity (Hatzivassiliou et al., 2010; Heidorn et al., 2010; Poulikakos et al., 2010).

In melanoma patients, decreased BRAF allelic frequency is associated with a poorer clinical outcome to BRAF inhibition and combined BRAF/MEK inhibition (Lebbe et al., 2014; Stagni et al., 2018). The proposed mechanism behind this response is paradoxical MAPK pathway activation due to a higher wild-type allele frequency. BRAF mutations in the canine TCC cell lines used in this study are heterozygous; thus, we hypothesized that their reduced sensitivity to vemurafenib may be the result of paradoxical activation of the MAPK pathway due to the wild-type copy of BRAF. In support of this hypothesis, when treated with the "paradox-breaking" inhibitor PLX7904 BRAF mutant TCC cell lines were equally as sensitive as BRAF mutant human lines. Further studies in canine and human BRAF mutant cell lines are required to establish the role of BRAF zygosity in sensitivity to BRAF inhibitors.

In this study, canine TCC cell lines were equally sensitive to MEK1/2 inhibition with selumetinib or trametinib compared to BRAF mutant human cell lines. Our group assessed trametinib sensitivity for the entire FACC panel of canine cancer cell lines and found that TCC cell lines were more sensitive than other cancer cell types (Das et al., unpublished data). Analysis of ERK1/2 activation following MEK1/2 inhibition for 6

hours showed complete or reduced pathway inhibition with trametinib and selumetinib, respectively. However, similar to the response with BRAF inhibition, TCC cell lines displayed a rebound in pathway activity by 24 hours post-treatment. Collectively, these data suggest canine TCC's initial dependence on the RAS-BRAF-MEK signaling axis; however, intrinsic resistance mechanisms are able to bypass pathway inhibition by 24 hours.

In metastatic melanoma patients, tumor regression in response to BRAF inhibition correlates with sustained inhibition of ERK1/2 phosphorylation. Additionally, patients experiencing tumor regression typically had at least 80% inhibition of ERK1/2 phosphorylation following treatment (Bollag et al., 2010).

This finding likely explains the lack of success of MAPK inhibition as a monotherapy for colorectal cancer treatment (Kopetz et al., 2015). Similar to the response of colorectal cancer cell lines (Corcoran et al., 2012), the TCC cell lines analyzed in this study showed re-activation of the MAPK pathway by 24 hours following MAPK inhibition, suggesting that long-term treatment with a MAPK inhibitor alone may not be an effective therapy for canine TCC.

Human melanoma and colorectal cancer exhibit acquired and innate resistance to BRAF inhibition, respectively. Mechanisms of acquired resistance in melanoma include BRAF splice isoforms, BRAF amplification, secondary NRAS mutations, CRAF overexpression, MEK1/2 mutations, and increased signaling through RTKs such as IGF-1R (Montagut et al., 2008; Nazarian et al., 2010; Poulikakos et al., 2011; Shi et al., 2012; Villanueva et al., 2010; Wagle et al., 2011). Mechanisms of intrinsic resistance in colorectal cancer include activation of RTKs (EGFR) and increased signaling through

the PI3K/AKT pathway (Corcoran et al., 2012; Mao et al., 2013; Prahallad et al., 2012). The majority of these resistance mechanisms involve re-activation of the MAPK pathway, explaining the increased efficacy in melanoma and colorectal cancer patients with dual inhibition of BRAF and MEK compared to monotherapy (Corcoran et al., 2015; Robert et al., 2015). A similar response was observed in this study where combined inhibition of BRAF and MEK was synergistic in the BRAF mutant Bliley TCC cell line.

To identify potential mediators of resistance to MAPK inhibition in TCC, in addition to determining other drivers that may contribute to TCC pathogenesis, we determined cancer genes that are differentially expressed in TCC cell lines versus other canine cancer cell lines. Genes up-regulated in TCC cell lines include *CDH1, PPARG, EGFR, ERBB2, EREG* and *MYC*. EGFR and ERBB2 protein expression is up-regulated in 50% and 8-30% of muscle-invasive human bladder cancers, respectively (Knowles and Hurst, 2015). Additionally, copy number alterations in EGFR (11%), ERBB2 (7%), PPARG (17%), and MYC (13%) are common in human bladder cancer (Atlas, 2014).

Of particular interest to us was the up-regulation of genes encoding ErbB receptors, EGFR and ERBB2, and the ErbB ligand EREG. Previous studies in colorectal cancer cell lines have shown that increased signaling through EGFR and/or ERBB2 allows cells to bypass BRAF inhibition (Corcoran et al., 2012; Prahallad et al., 2012). The mechanism behind the efficacy of combined ErbB and BRAF inhibition in colorectal cancer cell lines involves negative feedback regulation of the MAPK pathway. Increased MAPK signaling results in increased expression of negative regulators such as DUSP and SPRY. DUSP proteins inactivate ERK1/2 and SPRY proteins inhibit RTK-mediated activation of RAS (Lake et al., 2016). BRAF inhibition results in

decreased expression of these negative regulators, thus, relieving negative feedback of the MAPK pathway. In colorectal cancer it was suggested that this decrease in negative feedback results in increased activation of the RTKs EGFR and ERBB2 and subsequent increased MAPK signaling through CRAF (Corcoran et al., 2012; Prahallad et al., 2012). Similar to the response in colorectal cancer cell lines, MAPK inhibition with either a BRAF or MEK inhibitor synergized with a pan-ErbB inhibitor targeting EGFR, ERBB2, and ERBB3. These results suggest that the ErbB family of receptors and ligands may facilitate resistance to MAPK inhibition in canine TCC. Overall, the findings in this study suggest that dogs with BRAF mutant TCC may benefit from combined treatment with a pan-ErbB inhibitor and a “paradox-breaking” BRAF inhibitor, while dogs with BRAF wild-type TCC may benefit from combined pan-ErbB and MEK inhibition. Clinical trials evaluating the efficacy of these combinations in dogs with TCC may inform treatment modalities in human MAPK-driven cancers.

REFERENCES

Ascierto PA, McArthur GA, Dreno B, Atkinson V, Liszkay G, Di Giacomo AM, Mandala M, Demidov L, Stroyakovskiy D, Thomas L, de la Cruz-Merino L, Dutriaux C, Garbe C, Yan Y, Wongchenko M, Chang I, Hsu JJ, Koralek DO, Rooney I, Ribas A and Larkin J (2016) Cobimetinib combined with vemurafenib in advanced BRAF(V600)-mutant melanoma (coBRIM): updated efficacy results from a randomised, double-blind, phase 3 trial. *Lancet Oncol* **17**(9): 1248-1260.

Atlas TCG (2014) Comprehensive molecular characterization of urothelial bladder carcinoma. *Nature* **507**(7492): 315-322.

Bollag G, Hirth P, Tsai J, Zhang J, Ibrahim PN, Cho H, Spevak W, Zhang C, Zhang Y, Habets G, Burton EA, Wong B, Tsang G, West BL, Powell B, Shellooe R, Marimuthu A, Nguyen H, Zhang KY, Artis DR, Schlessinger J, Su F, Higgins B, Iyer R, D'Andrea K, Koehler A, Stumm M, Lin PS, Lee RJ, Grippo J, Puzanov I, Kim KB, Ribas A, McArthur GA, Sosman JA, Chapman PB, Flaherty KT, Xu X, Nathanson KL and Nolop K (2010) Clinical efficacy of a RAF inhibitor needs broad target blockade in BRAF-mutant melanoma. *Nature* **467**(7315): 596-599.

Chapman PB, Hauschild A, Robert C, Haanen JB, Ascierto P, Larkin J, Dummer R, Garbe C, Testori A, Maio M, Hogg D, Lorigan P, Lebbe C, Jouary T, Schadendorf D, Ribas A, O'Day SJ, Sosman JA, Kirkwood JM, Eggermont AM, Dreno B, Nolop K, Li J, Nelson B, Hou J, Lee RJ, Flaherty KT, McArthur GA and Group B-S (2011) Improved survival with vemurafenib in melanoma with BRAF V600E mutation. *N Engl J Med* **364**(26): 2507-2516.

Corcoran RB, Atreya CE, Falchook GS, Kwak EL, Ryan DP, Bendell JC, Hamid O, Messersmith WA, Daud A, Kurzrock R, Pierobon M, Sun P, Cunningham E, Little S, Orford K, Motwani M, Bai Y, Patel K, Venook AP and Kopetz S (2015) Combined BRAF and MEK Inhibition With Dabrafenib and Trametinib in BRAF V600-Mutant Colorectal Cancer. *J Clin Oncol* **33**(34): 4023-4031.

Corcoran RB, Ebi H, Turke AB, Coffee EM, Nishino M, Cogdill AP, Brown RD, Della Pelle P, Dias-Santagata D, Hung KE, Flaherty KT, Piris A, Wargo JA, Settleman J, Mino-Kenudson M and Engelman JA (2012) EGFR-mediated re-activation of MAPK signaling contributes to insensitivity of BRAF mutant colorectal cancers to RAF inhibition with vemurafenib. *Cancer Discov* **2**(3): 227-235.

Dankner M, Rose AAN, Rajkumar S, Siegel PM and Watson IR (2018) Classifying BRAF alterations in cancer: new rational therapeutic strategies for actionable mutations. *Oncogene* **37**(24): 3183-3199.

Das S, Idate R, Cronise KE, Gustafson DL and Duval DL (2019) Identifying Candidate Druggable Targets in Canine Cancer Cell Lines Using Whole-Exome Sequencing. *Mol Cancer Ther* **18**(8): 1460-1471.

Decker B, Parker HG, Dhawan D, Kwon EM, Karlins E, Davis BW, Ramos-Vara JA, Bonney PL, McNiel EA, Knapp DW and Ostrander EA (2015) Homologous Mutation to Human BRAF V600E Is Common in Naturally Occurring Canine Bladder Cancer--Evidence for a Relevant Model System and Urine-Based Diagnostic Test. *Mol Cancer Res* **13**(6): 993-1002.

Dhillon AS, Hagan S, Rath O and Kolch W (2007) MAP kinase signalling pathways in cancer. *Oncogene* **26**(22): 3279-3290.

Duval DL, Hernandez B, Brown J, Lana SE, Page R and Jones KL (2014) 13 Whole exome sequence analysis of canine transitional cell carcinoma of the bladder. *European Journal of Cancer* **50, Supplement 6**: 11.

Forbes SA, Beare D, Boutselakis H, Bamford S, Bindal N, Tate J, Cole CG, Ward S, Dawson E, Ponting L, Stefancsik R, Harsha B, Kok CY, Jia M, Jubb H, Sondka Z, Thompson S, De T and Campbell PJ (2017) COSMIC: somatic cancer genetics at high-resolution. *Nucleic Acids Res* **45**(D1): D777-D783.

Fowles JS, Dailey DD, Gustafson DL, Thamm DH and Duval DL (2017) The Flint Animal Cancer Center (FACC) Canine Tumour Cell Line Panel: a resource for veterinary drug discovery, comparative oncology and translational medicine. *Vet Comp Oncol* **15**(2): 481-492.

Fulkerson CM, Dhawan D, Ratliff TL, Hahn NM and Knapp DW (2017) Naturally Occurring Canine Invasive Urinary Bladder Cancer: A Complementary Animal Model to Improve the Success Rate in Human Clinical Trials of New Cancer Drugs. *Int J Genomics* **2017**: 6589529.

Fulkerson CM and Knapp DW (2015) Management of transitional cell carcinoma of the urinary bladder in dogs: a review. *Vet J* **205**(2): 217-225.

Gordon I, Paoloni M, Mazcko C and Khanna C (2009) The Comparative Oncology Trials Consortium: using spontaneously occurring cancers in dogs to inform the cancer drug development pathway. *PLoS Med* **6**(10): e1000161.

Halper-Stromberg E, Frelin L, Ruczinski I, Scharpf R, Jie C, Carvalho B, Hao H, Hetrick K, Jedlicka A, Dziedzic A, Doheny K, Scott AF, Baylin S, Pevsner J, Spencer F and Irizarry RA (2011) Performance assessment of copy number microarray platforms using a spike-in experiment. *Bioinformatics* **27**(8): 1052-1060.

Hatzivassiliou G, Song K, Yen I, Brandhuber BJ, Anderson DJ, Alvarado R, Ludlam MJ, Stokoe D, Gloor SL, Vigers G, Morales T, Aliagas I, Liu B, Sideris S, Hoeflich KP, Jaiswal BS, Seshagiri S, Koeppen H, Belvin M, Friedman LS and Malek S (2010)

RAF inhibitors prime wild-type RAF to activate the MAPK pathway and enhance growth. *Nature* **464**(7287): 431-435.

Heidorn SJ, Milagre C, Whittaker S, Nourry A, Niculescu-Duvas I, Dhomen N, Hussain J, Reis-Filho JS, Springer CJ, Pritchard C and Marais R (2010) Kinase-dead BRAF and oncogenic RAS cooperate to drive tumor progression through CRAF. *Cell* **140**(2): 209-221.

Houben R, Vetter-Kauczok CS, Ortmann S, Rapp UR, Broecker EB and Becker JC (2008) Phospho-ERK staining is a poor indicator of the mutational status of BRAF and NRAS in human melanoma. *J Invest Dermatol* **128**(8): 2003-2012.

Knapp DW and McMillan SK (2013) Tumors of the Urinary System, in *Withrow and MacEwen's Small Animal Clinical Oncology* (Withrow SJ, Page RL and Vail DM eds) pp 572-582, Elsevier Saunders, St. Louis, MO.

Knowles MA and Hurst CD (2015) Molecular biology of bladder cancer: new insights into pathogenesis and clinical diversity. *Nature reviews Cancer* **15**(1): 25-41.

Kopetz S, Desai J, Chan E, Hecht JR, O'Dwyer PJ, Maru D, Morris V, Janku F, Dasari A, Chung W, Issa JP, Gibbs P, James B, Powis G, Nolop KB, Bhattacharya S and Saltz L (2015) Phase II Pilot Study of Vemurafenib in Patients With Metastatic BRAF-Mutated Colorectal Cancer. *J Clin Oncol* **33**(34): 4032-4038.

Lake D, Correa SA and Muller J (2016) Negative feedback regulation of the ERK1/2 MAPK pathway. *Cell Mol Life Sci* **73**(23): 4397-4413.

Lebbe C, How-Kit A, Battistella M, Sadoux A, Podgorniak MP, Sidina I, Pages C, Roux J, Porcher R, Tost J and Mourah S (2014) BRAF(V600) mutation levels predict response to vemurafenib in metastatic melanoma. *Melanoma Res* **24**(4): 415-418.

Levidou G, Saetta AA, Gigelou F, Karlou M, Papanastasiou P, Stamatelli A, Kavantzas N, Michalopoulos NV, Agrogiannis G, Patsouris E and Korkolopoulou P (2012) ERK/pERK expression and B-raf mutations in colon adenocarcinomas: correlation with clinicopathological characteristics. *World J Surg Oncol* **10**: 47.

Long GV, Flaherty KT, Stroyakovskiy D, Gogas H, Levchenko E, de Braud F, Larkin J, Garbe C, Jouary T, Hauschild A, Chiarion-Sileni V, Lebbe C, Mandala M, Millward M, Arance A, Bondarenko I, Haanen J, Hansson J, Utikal J, Ferraresi V, Mohr P, Probachai V, Schadendorf D, Nathan P, Robert C, Ribas A, Davies MA, Lane SR, Legos JJ, Mookerjee B and Grob JJ (2017) Dabrafenib plus trametinib versus dabrafenib monotherapy in patients with metastatic BRAF V600E/K-mutant melanoma: long-term survival and safety analysis of a phase 3 study. *Ann Oncol* **28**(7): 1631-1639.

Mao M, Tian F, Mariadason JM, Tsao CC, Lemos R, Jr., Dayyani F, Gopal YN, Jiang ZQ, Wistuba, II, Tang XM, Bornman WG, Bollag G, Mills GB, Powis G, Desai J,

Gallick GE, Davies MA and Kopetz S (2013) Resistance to BRAF inhibition in BRAF-mutant colon cancer can be overcome with PI3K inhibition or demethylating agents. *Clin Cancer Res* **19**(3): 657-667.

Mochizuki H, Kennedy K, Shapiro SG and Breen M (2015) BRAF Mutations in Canine Cancers. *PLoS One* **10**(6): e0129534.

Montagut C, Sharma SV, Shioda T, McDermott U, Ulman M, Ulkus LE, Dias-Santagata D, Stubbs H, Lee DY, Singh A, Drew L, Haber DA and Settleman J (2008) Elevated CRAF as a potential mechanism of acquired resistance to BRAF inhibition in melanoma. *Cancer Res* **68**(12): 4853-4861.

Nazarian R, Shi H, Wang Q, Kong X, Koya RC, Lee H, Chen Z, Lee MK, Attar N, Sazegar H, Chodon T, Nelson SF, McArthur G, Sosman JA, Ribas A and Lo RS (2010) Melanomas acquire resistance to B-RAF(V600E) inhibition by RTK or N-RAS upregulation. *Nature* **468**(7326): 973-977.

O'Donoghue LE, Rivest JP and Duval DL (2011) Polymerase chain reaction-based species verification and microsatellite analysis for canine cell line validation. *J Vet Diagn Invest* **23**(4): 780-785.

O'Neil NJ, Bailey ML and Hieter P (2017) Synthetic lethality and cancer. *Nat Rev Genet* **18**(10): 613-623.

Poulikakos PI, Persaud Y, Janakiraman M, Kong X, Ng C, Moriceau G, Shi H, Atefi M, Titz B, Gabay MT, Salton M, Dahlman KB, Tadi M, Wargo JA, Flaherty KT, Kelley MC, Misteli T, Chapman PB, Sosman JA, Graeber TG, Ribas A, Lo RS, Rosen N and Solit DB (2011) RAF inhibitor resistance is mediated by dimerization of aberrantly spliced BRAF(V600E). *Nature* **480**(7377): 387-390.

Poulikakos PI, Zhang C, Bollag G, Shokat KM and Rosen N (2010) RAF inhibitors transactivate RAF dimers and ERK signalling in cells with wild-type BRAF. *Nature* **464**(7287): 427-430.

Prahallad A, Sun C, Huang S, Di Nicolantonio F, Salazar R, Zecchin D, Beijersbergen RL, Bardelli A and Bernards R (2012) Unresponsiveness of colon cancer to BRAF(V600E) inhibition through feedback activation of EGFR. *Nature* **483**(7387): 100-103.

Rathore K and Cekanova M (2014) Animal model of naturally occurring bladder cancer: characterization of four new canine transitional cell carcinoma cell lines. *BMC Cancer* **14**: 465.

Robert C, Karaszewska B, Schachter J, Rutkowski P, Mackiewicz A, Stroiakovski D, Lichinitser M, Dummer R, Grange F, Mortier L, Chiarion-Sileni V, Drucis K, Krajsova I, Hauschild A, Lorigan P, Wolter P, Long GV, Flaherty K, Nathan P, Ribas A, Martin AM, Sun P, Crist W, Legos J, Rubin SD, Little SM and

Schadendorf D (2015) Improved overall survival in melanoma with combined dabrafenib and trametinib. *N Engl J Med* **372**(1): 30-39.

Robertson AG, Kim J, Al-Ahmadie H, Bellmunt J, Guo G, Cherniack AD, Hinoue T, Laird PW, Hoadley KA, Akbani R, Castro MAA, Gibb EA, Kanchi RS, Gordenin DA, Shukla SA, Sanchez-Vega F, Hansel DE, Czerniak BA, Reuter VE, Su X, de Sa Carvalho B, Chagas VS, Mungall KL, Sadeghi S, Pedamallu CS, Lu Y, Klimczak LJ, Zhang J, Choo C, Ojesina AI, Bullman S, Leraas KM, Lichtenberg TM, Wu CJ, Schultz N, Getz G, Meyerson M, Mills GB, McConkey DJ, Network TR, Weinstein JN, Kwiatkowski DJ and Lerner SP (2017) Comprehensive Molecular Characterization of Muscle-Invasive Bladder Cancer. *Cell* **171**(3): 540-556 e525.

Shi H, Moriceau G, Kong X, Lee MK, Lee H, Koya RC, Ng C, Chodon T, Scolyer RA, Dahlman KB, Sosman JA, Kefford RF, Long GV, Nelson SF, Ribas A and Lo RS (2012) Melanoma whole-exome sequencing identifies (V600E)B-RAF amplification-mediated acquired B-RAF inhibitor resistance. *Nat Commun* **3**: 724.

Siegel RL, Miller KD and Jemal A (2018) Cancer statistics, 2018. *CA Cancer J Clin* **68**(1): 7-30.

Sosman JA, Kim KB, Schuchter L, Gonzalez R, Pavlick AC, Weber JS, McArthur GA, Hutson TE, Moschos SJ, Flaherty KT, Hersey P, Kefford R, Lawrence D, Puzanov I, Lewis KD, Amaravadi RK, Chmielowski B, Lawrence HJ, Shyr Y, Ye F, Li J, Nolop KB, Lee RJ, Joe AK and Ribas A (2012) Survival in BRAF V600-mutant advanced melanoma treated with vemurafenib. *N Engl J Med* **366**(8): 707-714.

Stagni C, Zamuner C, Elefanti L, Zanin T, Bianco PD, Sommariva A, Fabozzi A, Pigozzo J, Mocellin S, Montesco MC, Chiarion-Sileni V, De Nicolo A and Menin C (2018) BRAF Gene Copy Number and Mutant Allele Frequency Correlate with Time to Progression in Metastatic Melanoma Patients Treated with MAPK Inhibitors. *Mol Cancer Ther* **17**(6): 1332-1340.

Villanueva J, Vultur A, Lee JT, Somasundaram R, Fukunaga-Kalabis M, Cipolla AK, Wubbenhorst B, Xu X, Gimotty PA, Kee D, Santiago-Walker AE, Letrero R, D'Andrea K, Pushparajan A, Hayden JE, Brown KD, Laquerre S, McArthur GA, Sosman JA, Nathanson KL and Herlyn M (2010) Acquired resistance to BRAF inhibitors mediated by a RAF kinase switch in melanoma can be overcome by cotargeting MEK and IGF-1R/PI3K. *Cancer Cell* **18**(6): 683-695.

Wagle MC, Kirouac D, Klijn C, Liu B, Mahajan S, Junttila M, Moffat J, Merchant M, Huw L, Wongchenko M, Okrah K, Srinivasan S, Mounir Z, Sumiyoshi T, Haverty PM, Yauch RL, Yan Y, Kabbarah O, Hampton G, Amler L, Ramanujan S, Lackner MR and Huang SA (2018) A transcriptional MAPK Pathway Activity Score (MPAS) is a clinically relevant biomarker in multiple cancer types. *NPJ Precis Oncol* **2**(1): 7.

Wagle N, Emery C, Berger MF, Davis MJ, Sawyer A, Pochanard P, Kehoe SM, Johannessen CM, Macconaill LE, Hahn WC, Meyerson M and Garraway LA

(2011) Dissecting therapeutic resistance to RAF inhibition in melanoma by tumor genomic profiling. *J Clin Oncol* **29**(22): 3085-3096.

Yang H, Higgins B, Kolinsky K, Packman K, Bradley WD, Lee RJ, Schostack K, Simcox ME, Kopetz S, Heimbrook D, Lestini B, Bollag G and Su F (2012) Antitumor activity of BRAF inhibitor vemurafenib in preclinical models of BRAF-mutant colorectal cancer. *Cancer Res* **72**(3): 779-789.

Yang W, Soares J, Greninger P, Edelman EJ, Lightfoot H, Forbes S, Bindal N, Beare D, Smith JA, Thompson IR, Ramaswamy S, Futreal PA, Haber DA, Stratton MR, Benes C, McDermott U and Garnett MJ (2013) Genomics of Drug Sensitivity in Cancer (GDSC): a resource for therapeutic biomarker discovery in cancer cells. *Nucleic Acids Res* **41**(Database issue): D955-961.

CHAPTER 4

Characterizing a canine model of acquired trametinib resistance[3]

SUMMARY

Activating BRAF mutations are drivers of oncogenesis in several human cancers. Selective BRAF inhibitors are effective alone and in combination with MEK inhibitors in half of BRAF mutant melanoma cases, but the majority of these patients develop resistance. Trametinib is an ATP-noncompetitive inhibitor of MEK1/2 that is FDA-approved for treatment of several BRAF mutant cancers, both as a single-agent and in combination with the BRAF inhibitor dabrafenib. However, intrinsic and acquired resistance remains a major challenge. Our aim was to use a comparative approach to identifying determinants of trametinib sensitivity and resistance. We applied the human-derived MAPK Pathway Activity Score (MPAS), a predictor of sensitivity to MEK inhibition in human cancer cell lines, to a panel of 32 canine cancer cell lines and found that the MPAS correlates with trametinib sensitivity in this canine dataset. We also identified 30 non-MPAS genes whose expression levels are significantly correlated with trametinib sensitivity, suggesting their role in *de novo* sensitivity to trametinib. To investigate mechanisms of acquired resistance, we generated six trametinib-resistant (TramR) clonal derivatives of the BRAF mutant Tyler1 canine transitional cell carcinoma (cTCC) cell line (Tyler1-TramR), with trametinib IC_{50} values greater than 500 nM versus

[3] A big thanks to Dawn Duval, Dan Gustafson, Sunetra Das, David Ackart, and Rupa Idate for their contributions to this chapter.

1 nM in parental Tyler1. Tyler1-TramR cell lines exhibited sustained inhibition of ERK1/2 when treated with trametinib and were resistant to pharmacologic inhibition of ERK1/2. Collectively, these data suggested an ERK-independent mechanism of resistance. Gene expression analysis of two Tyler1-TramR clones identified dramatic downregulation of epithelial markers accompanied by an increase in expression of mesenchymal genes and transcription factors that regulate the epithelial-to-mesenchymal transition (EMT). One Tyler1-TramR clone exhibited metabolic alterations including decreased basal and maximal oxygen consumption rates, diminished spare respiratory capacity, and reduced glycolytic capacity. Overall, the findings in this study suggest that the mechanisms of acquired and intrinsic MEK inhibitor resistance are conserved between man and dog, further elucidating the translational value of cTCC as a model for improving MAPK pathway-targeted therapies

INTRODUCTION

BRAF mutations serve as the driving alteration in a number of human neoplasms, including 50% of melanoma, 60% of thyroid carcinomas, 15% of colon adenocarcinomas, as well as nearly 100% of hairy-cell leukemia cases (Davies et al., 2002; Grossman et al., 2016; Tiacci et al., 2011). The majority of BRAF mutations are valine-to-glutamic acid missense substitutions at amino acid 600 (V600E) (Davies et al., 2002). This substitution promotes increased BRAF kinase activity, irrespective of upstream RAS activation, resulting in constitutive activation of downstream MEK1 and

MEK 2 (MEK1/2), as well as ERK1 and ERK2 (ERK1/2) (Davies et al., 2002; Wan et al., 2004).

Vemurafenib and dabrafenib and ATP-competitive inhibitors of BRAF approved for treatment of BRAF mutant V600E (or V600K) melanoma (Falchook et al., 2012; Flaherty et al., 2010). Vemurafenib produced impressive results in a randomized, phase III clinical trial assessing its therapeutic value for treatment of metastatic melanoma, achieving a 48% response rate relative to 5% with the standard of care dacarbazine (Chapman et al., 2011). Similar efficacy was observed with dabrafenib, reaching a 50% response rate versus 6% with dacarbazine (Hauschild et al., 2012). Sadly, these responses were typically short-lived, with the majority of patients eventually experiencing disease relapse (Hauschild et al., 2012; McArthur et al., 2014). The mechanisms underlying resistance are heterogeneous; however, reactivation of MAPK signaling occurs in the majority of cases (Johnson et al., 2015; Shi et al., 2014). In 2013, trametinib, an allosteric, ATP-noncompetitive inhibitor of MEK1/2, was FDA-approved as a single-agent therapy for metastatic melanoma (Flaherty et al., 2012b; Gilmartin et al., 2011). The response rate associated with single-agent trametinib (22%) was less impressive than that of vemurafenib or dabrafenib, but the progression-free and overall survival benefit was similar to that of single-agent BRAF inhibition (Flaherty et al., 2012b). Treatment strategies combining BRAF and MEK1/2 inhibition were employed to stave off the emergence of resistance associated with reactivation of the MAPK pathway. Indeed, combined trametinib and dabrafenib treatment extends the progression free survival of patients with advanced melanoma relative to single-agent dabrafenib or vemurafenib (Flaherty et al., 2012a; Long et al., 2014; Robert et al.,

2015). Combined vemurafenib and the MEK1/2 inhibitor cobimetinib was also found to extend the duration of response relative to vemurafenib as a monotherapy (Ascierto et al., 2016). Despite these improvements, acquired resistance still poses a major challenge to treatment (Ascierto et al., 2016; Robert et al., 2015).

Comparative oncology is the study of cancers in companion animals with the goal of understanding cancer biology and assessing novel therapies in order to advance cancer treatment in both humans and dogs. Spontaneous tumors in dogs undergo the same natural processes as human cancers, including the emergence of drug resistance (Paoloni and Khanna, 2007). Canine transitional cell carcinoma (cTCC), the most common bladder cancer in dogs, exhibits a high frequency of activating BRAF mutations (Decker et al., 2015; Mochizuki et al., 2015). We previously evaluated the efficacy of MAPK inhibition in 5 cTCC cell lines (3 BRAF600E, 1 KRASG12D, and 1 BRAF/KRAS wild type) identifying sensitivity to trametinib as a common feature, independent of mutation status (Cronise et al., 2019). Furthermore, cTCC cell lines were the most sensitive histotype out of a panel of 33 canine cancer cell lines (Das et al., 2019). Interestingly, despite trametinib initially attenuating ERK1/2 activation, several cTCC cell lines exhibited reactivation of ERK1/2 by 24 hours post-treatment (Cronise et al., 2019). Thus, cTCC provides the unique opportunity to interrogate mechanisms of acquired and intrinsic resistance to MAPK inhibition that may inform treatment of human MAPK-driven cancers. Herein, we generate and characterize what is, to our knowledge, the first canine model of acquired resistance to MEK1/2 inhibition.

MATERIALS AND METHODS

Cell culture and small molecule inhibitors

The Tyler1 cell line was obtained from Dr. Elizabeth McNeil (Tufts University) (Sledge et al., 2012). Tyler1 cells were maintained in Dulbecco's Modified Eagle's Medium (#10-017-CV, Corning Inc., Corning, NY) supplemented with 10% fetal bovine serum (FBS; #PS-FB3, Peak Serum, Inc., Wellington, CO), 1X penicillin/streptomycin (#30-002-CI, Corning), 10 mM 2-[4-(2-hydroxyethyl)piperazin-1-yl]ethanesulfonic acid (HEPES, pH 7.4), and 1 mM sodium pyruvate (#25-000-CI, Corning). All cells were grown at 37 °C in a humidified incubator with 5% CO_2. Trametinib and ravoxertinib were purchased from Selleck Chemicals (Houston, TX), and stock solutions of drug were prepared in DMSO and stored at -80 °C.

Generation of trametinib-resistant Tyler1

Trametinib-resistant Tyler1 cells (Tyler1-TramR) were generating by repeated exposure to trametinib over the course of nine months. Briefly, Tyler1 cells were cultured in complete media plus trametinib, starting at the IC_{50} dose for three days followed by a three-day recovery in complete media. This "three days on, three days off" cycle was repeated while gradually increasing the concentration of trametinib. Following generation of a stable pool of trametinib-resistant Tyler1, short tandem repeat (STR) analysis was performed as previously described to validate Tyler1 as the cell line of origin (O'Donoghue et al., 2011). Furthermore, Tyler1 shares the same STR profile, but has a different mutation profile, than the cTCC Tyler2 cell line (Das et al., 2019). To determine that Tyler1 was the cell line of origin we performed Sanger sequencing to

identify a previously described mutation in *BECN2* that is present in Tyler1, but not Tyler2 (Das et al., 2019). Polymerase chain reaction was perofrmed to amplify *BECN2* using the following primers: forward 5'-CAAATATTGGAGGGGGAGAATA-3' and reverse 5'-CTTAAAGAAACCCAAGTGAGAC-3'. An 850-bp product was gel-extracted (QIAquick Gel Extaction Kit, Qiagen, Hilden, Germany) and sequenced via Sanger sequencing (GENEWIZ, South Plainfield, NJ) to confirm the presence of the *BECN2* G>C mutation in Tyler1 (Das et al., 2019). To isolate individual clones, 200 Tyler1-TramR cells were seeded into 15-cm petri dishes in complete media plus 25 nM trametinib and grown at 37 °C for approximately 10 days. Plates were washed with PBS, after which, individual colonies were detached by carefully pipetting up and down 50 µL of Trypsin/EDTA (#25-053-CI, Corning) and then were transferred into a 24-well plate containing drug-free media to expand. Once clones were expanded into 10-cm dishes, the "3 days on, 3 days off" cycle was repeated three times using a trametinib maintenance concentration of 10 nM prior to freezing back cell lines stocks. All future downstream maintenance of Tyler1-TramR cell lines was performed in drug-free, complete media.

Seahorse assays

Cells were plated 24 hours prior to analysis at a density of 2.0×10^4 cells per well in a tissue culture-treated Seahorse XF24 Cell Culture Microplate (Agilent Technologies, Santa Clara, CA) in complete DMEM. Following a 24-hour incubation under normal growth conditions, complete DMEM was replaced with FBS-free, un-buffered Seahorse XF DMEM (Agilent) and cells were equilibrated at 37 °C in a CO_2-free incubator prior to analysis. Oxygen consumption rate (OCR) and extracellular

acidification rate (ECAR) were measured on a Seahorse XFe24 Analyzer (Agilent) using a Seahorse XF Cell Mito Stress Kit (Agilent) with sequential injection of oligomycin (1 μM final), carbonyl cyanide-4 (trifluoromethoxy) phenylhydrazone (FCCP; 1 μM final), rotenone/antimycin A (0.5 μM final each) and 2-deoxyglucose (2-DG; 50 mM final). Following metabolic flux analysis, plates were stained with Calcein-AM (BioLegend, San Diego, CA) and read on a plate reader according to the manufacturer's protocol as a surrogate for relative cell number. OCR and ECAR readings were normalized to relative cell number. Metabolic parameters were determined based on the results of three independent biological replicates, each of which was conducted in technical triplicates.

Proliferation and cell cycle analysis

Proliferation was measured using a Click-iT Plus EdU Pacific Blue Flow Cytometry Assay Kit (#C10636; Thermo Fisher Scientific, Waltham, MA). 1.0 x 10^6 cells were plated into a 10-cm petri dish and incubated overnight in complete media under normal growth conditions. The next day, media was replaced with fresh complete media plus 25 nM trametinib or DMSO control, and plates were incubated for 24 hours at 37 °C. 5-ethynyl-2´-deoxyuridine (EdU) was then added to each plate at a concentration of 10 μM and plates were incubated for 1 hour at 37 °C. A negative control without the addition of EdU was conducted for each condition. Cells were fixed, permeabilized, and stained according to the Click-iT Plus EdU Pacific Blue Flow Cytometry Assay Kit guidelines. Cells were then stained for DNA content by incubating with FxCycle Propidium Iodide (PI)/RNase Staining Solution for 15 minutes protected from light (#F10797; Thermo Fisher Scientific). Cells were then analyzed on a

Beckman Coulter Gallios flow cytometer (Brea, CA) and data were analyzed using FlowJo software (v10.6; Becton, Dickson, and Company, Franklin Lakes, NJ).

Drug sensitivity assays

Parental and trametinib-resistant Tyler1 cell lines were seeded into 96-well plates (1,500 cells per well) in 100 µl of complete media and incubated at 37 °C for 24 hours. Cells were then treated with serial dilutions of drug or DMSO control prepared in 100 µl of complete media. A resazurin-based assay was used to determine the relative cell number in each well. Briefly, media was aspirated and replaced with 200 µl of fresh media followed by 20 µl of resazurin for a final concentration of 20 µg/mL. Plates were incubated for three hours at 37 °C and then read on a 96-well plate reader with an emission wavelength of 530 and an excitation wavelength of 590. IC_{50} values were calculated from three independent biological replicates as previously described (Holbeck, 2004). Dose-response graphs were generated using GraphPad Prism software (v8).

Western blotting

Western blotting for phosphorylated ERK1/2 (pERK1/2), total ERK1/2, and tubulin were performed as described in Chapter 3.

RNA sequencing and analysis

Total RNA was isolated using an RNeasy Mini Kit (Qiagen) according to the manufacturer's protocol. Cells were homogenized using QIAshredder columns (Qiagen). A poly(A) selected library was generated using the Universal mRNA-Seq Library Preparation Kit (NuGEN Technologies, Inc., Redwood City,CA). 150 bp, paired-end reads were sequenced on the NovaSeq 6000 (Illumina, San Diego, CA). Library

preparation and sequencing was performed at the Genomics and Microarray Shared Resource at the University of Colorado Cancer Center. Three independent biological replicates were sequenced for each sample.

Raw FASTQ reads were trimmed using Trimmomatic (v0.36) and quality check was performed using FASTQC (v0.11.5) (Bolger et al., 2014). Trimmed reads were mapped to the CanFam3.1 reference genome using STAR (v2.6.1a), and Ensembl v99 was used for annotation of genes (Dobin et al., 2013). Gene counts were determined using htseq-count (v0.6.0) and relative FPKM expression values were determined using cufflinks (v2.2.1) (Anders et al., 2015; Trapnell et al., 2010).

Differentially expressed genes (DEGs) were identified using R statistical software with the 'edgeR' package (McCarthy et al., 2012; Robinson et al., 2010). Filtering of unexpressed genes and TMM normalization were performed using the built-in functions 'filterByExpr' and 'calcNormFactors' with default parameters, respectively. Normalized count data were fitted to a quasi-likelihood negative binomial generalized log-linear model using the 'glmQLFit' function with 'robust = T'. An empirical Bayes quasi-likelihood F-test was performed for each contrast using the 'glmQLFTest' function with default parameters. A minimum $\log_2$ fold change of 1 and a Benjamini-Hochberg adjusted p-value < 0.01 were required for statistical significance. All heatmaps were generated using the 'ComplexHeatmap' R package with $\log_2$ FPKM expression values as input (Gu et al., 2016). Functional annotation of DEGs was performed using the GSEAPreranked tool (GSEA v4.0.3) with $\log_2$ fold change values as the ranking metrics (Subramanian et al., 2005). GSEAPreranked was performed using default parameters with a minimum gene set size of 10. DEGs were analyzed for enrichment of gene sets

within the following Molecular Signatures Database (MSigDB) collections: Hallmark, Canonical Pathways, Gene Ontology (GO) Biological Process (BP), GO Cellular Component (CC), and GO Molecular Function, and Oncogenic Signatures (Liberzon et al., 2011; Subramanian et al., 2005).

Identifying transcriptomic correlates with trametinib sensitivity in canine cancer cell lines

RNA-Seq gene expression data, in total counts and relative log_2-FPKM, for 32 canine cancer cell lines were provided by Drs. Sunetra Das and Dawn Duval. Counts-per-million (CPM) expression values were determined using edgeR. MPAS were calculated using CPM expression for the 32 cell lines as previously described (Wagle et al., 2018). MPAS were correlated with previously determined $logIC_{50}$ values to trametinib (Das et al., 2019) using a Pearson correlation. Individual genes whose expression is associated with trametinib sensitivity were identified by determining Pearson correlations between z-score normalized CPM expression and trametinib $logIC_{50}$ values, requiring a Benjamini and Hochberg false discovery rate less than 0.05. Functional annotation of gene hits was performed with Enrichr (Chen et al., 2013; Kuleshov et al., 2016).

RESULTS

Transcriptomic determinants of de novo sensitivity to trametinib in canine cancer cell lines

The MPAS is a gene signature quantifying relative MAPK activity that consists of 10 gene targets of the MAPK pathway that show dose-dependent reductions in expression in response to pharmacologic inhibition of MEK1/2 (Wagle et al., 2018). The MPAS is predictive of sensitivity to MEK inhibition in cancer cell lines and is associated with a better response to vemurafenib in BRAF mutant melanoma (Wagle et al., 2018). We determined the MPAS for 32 canine cancer cell lines using RNA-Seq expression data. The leukemia cell line 1771 had the highest MPAS (5.7); while the soft tissue sarcoma cell line STSA-1 and the TCC cell line Kinsey had the second and third highest MPAS at 2.9 and 2.0, respectively (**Figure 4.1**). TCC cell lines exhibited high MPAS as measured via RNA-Seq relative to other canine cancer cell lines, similar to our analysis with microarray data in Chapter 3 (**Figure 3.2**).

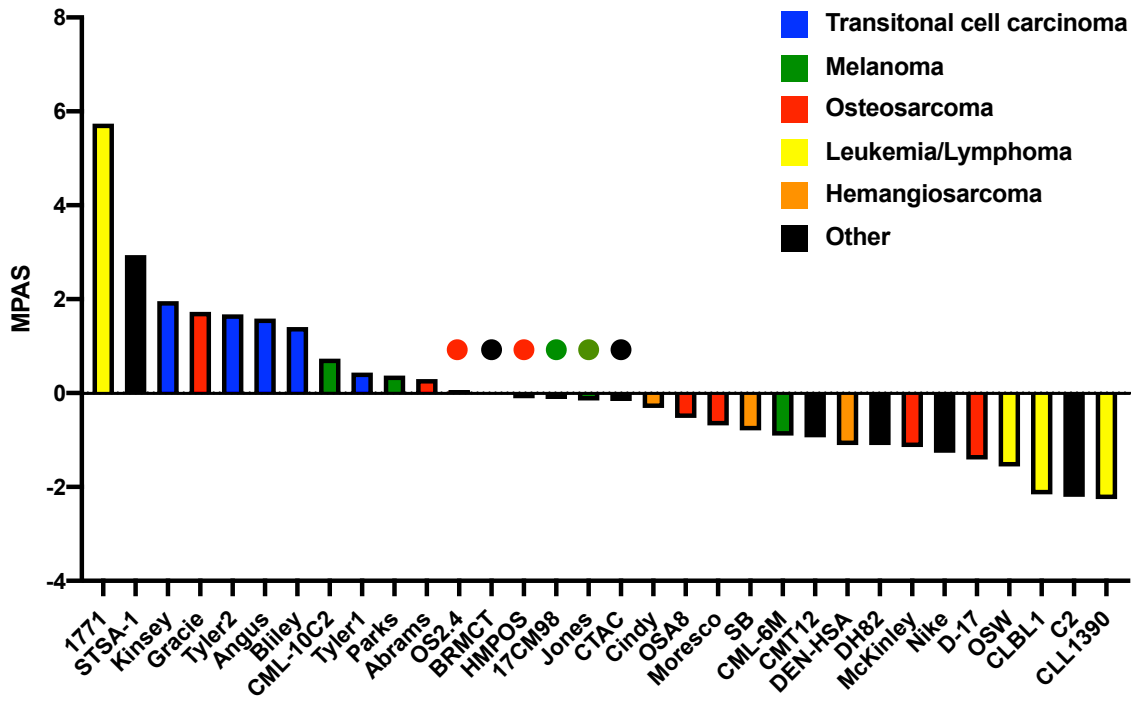

Figure 4.1 MPAS of canine cancer cell lines.
MPAS values for canine cancer cell lines representing relative basal MAPK pathway activation. Cell lines are colored by histotype.

Next, we wanted to determine whether the MPAS correlates with sensitivity to MEK inhibition in canine cancer cell lines. Using previously published trametinib IC_{50} values (Das et al., 2019), we observed a weak negative correlation between MPAS and trametinib logIC_{50} (**Figure 4.2**; Pearson r = -0.355, p = 0.046). The 1771 cell line, which has an extremely high MPAS, was insensitive (IC_{50} = 1.8 uM). This cell line harbors a mutation in the gene encoding protein capicua homolog (CIC) (Das et al., 2019). CIC is a transcriptional repressor of downstream gene targets of the MAPK pathway, including many MPAS genes, and loss of CIC function promotes resistance to trametinib (Wang et al., 2017; Weissmann et al., 2018). Since the MPAS is a relative score we elected to perform the analysis both with and without the 1771 cell line. Removing the 1771 cell

line from our analysis revealed a much stronger correlation between MPAS and trametinib sensitivity (Pearson r = -0.670 and p < 0.0001).

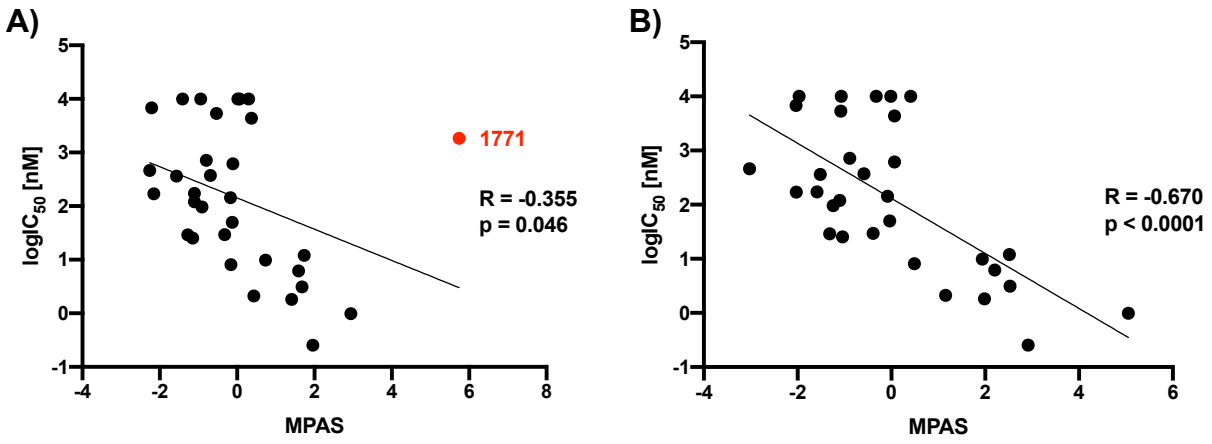

Figure 4.2 Correlation of MPAS with trametinib sensitivity in canine cancer cell lines.
MPAS values for canine cancer cell lines versus trametinib $logIC_{50}$ values (A) with all 32 cell lines included in the analysis. The 1771 cell line with the deleterious CIC mutation is indicated in red. (B) Correlation of MPAS with trametinib sensitivity with the 1771 cell line excluded from the analysis. The relationship between MPAS and $logIC_{50}$ values was determined using a Pearson correlation.

We next sought to determine the association between each MPAS gene individually with trametinib sensitivity. When including 1771 in the analysis, *CCND1* and *DUSP6* were the only genes whose expression correlated significantly with trametinib $logIC_{50}$ values (**Table 4.1**). When 1771 is excluded from the analysis, *CCND1*, *DUSP6*, *ETV4*, *ETV5*, and *SPRY4* expression levels each correlated with trametinib $logIC_{50}$ values. Expression of *EPHA2* and *EPHA4*, which encode ephrin type-A receptors 2 and 4, respectively, exhibited the weakest correlations with trametinib sensitivity.

Table 4.1 Correlation of MPAS gene expression with trametinib logIC_{50} values. Pearson correlations between MPAS and trametinib logIC_{50} values were determined both with (n = 32) and without the 1771 cell line (n = 31).

		With 1771		Without 1771	
Gene	**Gene Name**	***r***	**p-value**	***r***	**p-value**
CCND1	cyclin D1	-0.533	0.002	-0.609	<0.001
DUSP4	dual specificity phosphatase 4	-0.064	0.729	-0.146	0.433
DUSP6	dual specificity phosphatase 6	-0.58	0.001	-0.602	<0.001
EPHA2	EPH receptor A2	-0.07	0.704	-0.048	0.798
EPHA4	EPH receptor A4	-0.071	0.7	-0.052	0.78
ETV4	ETS variant transcription factor 4	0.096	0.601	-0.647	<0.001
ETV5	ETS variant transcription factor 5	0.109	0.551	-0.459	0.009
PHLDA1	pleckstrin homology like domain family A member 1	-0.248	0.171	-0.251	0.173
SPRY2	sprouty RTK signaling antagonist 2	-0.322	0.073	-0.307	0.093
SPRY4	sprouty RTK signaling antagonist 4	-0.211	0.246	-0.704	<0.001

Next, we identified other genes that correlate with trametinib sensitivity in this canine dataset. Our goal was to determine transcriptional determinants of trametinib sensitivity; thus, we elected to include the 1771 cell line in our analysis. We identified 30 genes whose expression significantly correlated with trametinib logIC_{50} values (**Table 4.2**). Only two genes exhibited a positive correlation with logIC_{50} values, *ITPKA* and *TCF15*, possibly suggesting their role in *de novo* trametinib resistance. In contrast, 28 genes exhibited negative correlations with trametinib logIC_{50} values (**Table 4.2**). The top three scoring positive gene correlates were *HMGA1*, *ARF6*, and *MPZL1*. Enrichr was used to identify pathways or processes among the list of 28 negatively correlated genes. Endocytosis was the most strongly enriched BioPlanet (adjusted p-value =

0.0015) and KEGG pathway (adjusted p-value = 0.026). Five out of the 28 genes analyzed were associated with endocytosis: *ARF6, F2R, PLD1, CHMP2A,* and *EHD4*.

Table 4.2 Genes significantly correlated with trametinib sensitivity.
30 genes whose expression levels are significantly correlated with trametinib logIC_{50} values (n=32, fdr < 0.05). Statistical significance was determined using a Pearson correlation with a Benjamini and Hochberg correction for multiple comparisons.

Gene	Gene Name	r	fdr
HMGA1	high mobility group AT-hook 1	-0.722	0.018
ARF6	ADP ribosylation factor 6	-0.724	0.018
MPZL1	myelin protein zero like 1	-0.723	0.018
ITPKA	inositol-trisphosphate 3-kinase A	0.711	0.022
F2R	coagulation factor II thrombin receptor	-0.698	0.023
PLD1	phospholipase D1	-0.705	0.023
MRPL14	mitochondrial ribosomal protein L14	-0.697	0.023
CHMP2A	charged multivesicular body protein 2A	-0.684	0.027
CD9	CD9 molecule	-0.686	0.027
UACA	uveal autoantigen with coiled-coil domains and ankyrin repeats	-0.683	0.027
LRRC8A	leucine rich repeat containing 8 VRAC subunit A	-0.68	0.027
SLC39A10	solute carrier family 39 member 10	-0.674	0.028
NSD1	nuclear receptor binding SET domain protein 1	-0.668	0.034
ATG7	autophagy related 7	-0.666	0.034
ZFPM2	zinc finger protein, FOG family member 2	-0.657	0.041
OCIAD1	OCIA domain containing 1	-0.655	0.041
EHD4	EH domain containing 4	-0.654	0.041
MGST3	microsomal glutathione S-transferase 3	-0.653	0.041
CALM1	calmodulin 1	-0.653	0.041
ANXA1	annexin A1	-0.646	0.044
DCUN1D4	defective in cullin neddylation 1 domain containing 4	-0.645	0.044
SBF2	SET binding factor 2	-0.646	0.044
PPP2R2A	protein phosphatase 2 regulatory subunit Balpha	-0.646	0.044
GMFB	glia maturation factor beta	-0.641	0.049
ANKH	ANKH inorganic pyrophosphate transport regulator	-0.639	0.049
ELK3	ETS transcription factor ELK3	-0.634	0.049
TCF15	transcription factor 15	0.634	0.049
ZDHHC3	zinc finger DHHC-type palmitoyltransferase 3	-0.636	0.049
FRMD6	FERM domain containing 6	-0.634	0.049
LURAP1L	leucine rich adaptor protein 1 like	-0.636	0.049

Generating trametinib-resistant Tyler1

Next, we aimed to identify determinants of acquired resistance to trametinib using BRAF mutant cTCC as a model. Trametinib-resistant Tyler1 (Tyler-TramR) were generated over the course of 9 months by gradually exposing Tyler1 parental cells to increasing concentrations of trametinib (**Figure 4.3**). Following generation of a stable pool of Tyler1-TramR, we isolated six individual clones and evaluated their sensitivity to trametinib (**Figure 4.3**). The IC_{50} of the parental Tyler1 cell line was approximately 1 nM; whereas, with all of the Tyler-TramR resistant clones, an IC_{50} was not reached even at concentrations as high as 500 nM. All resistant clones retained constitutive activation of ERK1/2, as evidenced by sustained ERK1/2 phosphorylation in the absence of growth serum (**Figure 4.4**).

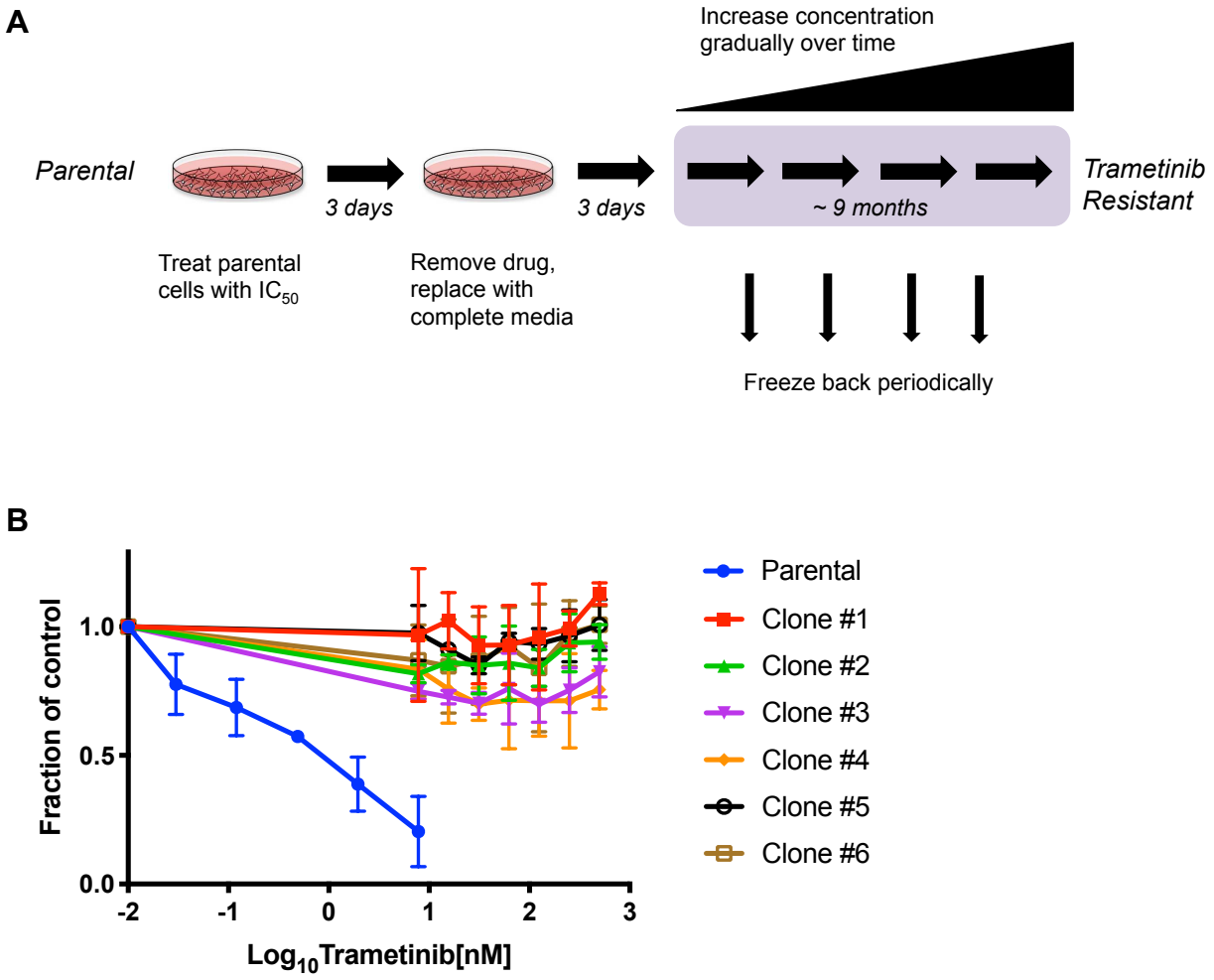

Figure 4.3 Generation of Tyler1-TramR clones.
(A) Schematic for generation of Tyler1-TramR cells. (B) Sensitivity of Tyler1 Parental and TramR clones to trametinib. Cell lines were treated with serial dilutions of trametinib and relative cell number was determined as a fraction of DMSO control. Error bars represent standard deviations of the fraction of control determined from three independent biological replicates, each of which was conducted in technical triplicate.

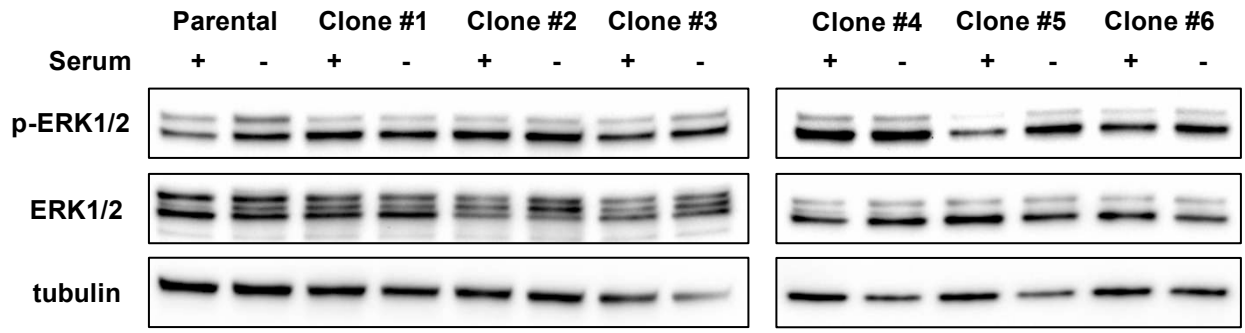

Figure 4.4 Tyler1-TramR clones exhibit constitutive activation of ERK1/2. Serum starvation of Tyler1 parental and TramR cell lines, followed by western blot analysis of phosphorylated ERK1/2 abundance.

We next analyzed the effects of trametinib treatment on proliferation and cell cycle distribution in Tyler1 parental and TramR-Clone2. In Tyler1 Parental cells, trametinib treatment results in a significant reduction in the percentage of cells in S phase (**Figure 4.5**; 44% to 11%) and a slight reduction in the percentage in G2/M (21% to 15%). This change was accompanied by an increase in the percentage of cells in G1/G0 (33% to 66%) and Sub-G1 (0.3% to 6%), suggestive of arrest in G1 and cell death, respectively. In TramR-Clone2, trametinib treatment decreased the percentage of cells in S phase, from 54% to 32%, and increased the percentage of cells in G1/G0, from 36% to 61% (**Figure 4.5**).

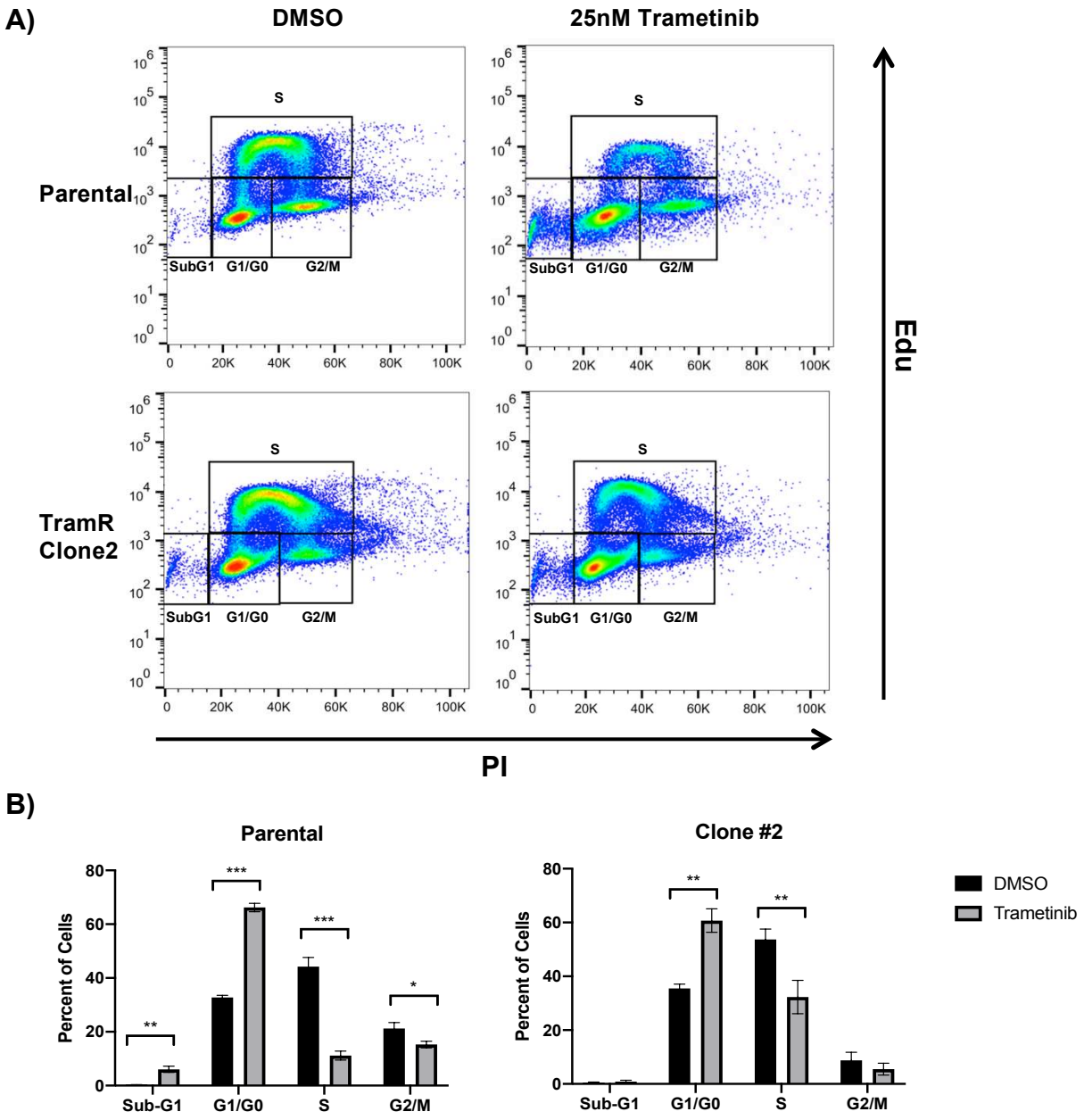

Figure 4.5 Cell cycle analysis of Tyler1 parental and TramR-Clone2 following trametinib treatment. Tyler1 parental and TramR-Clone2 cells were treated with 25 nM trametinib or DMSO control for 24 hours, followed by exposure to EdU for 1 hour. EdU incorporation was detected using Click-iT chemistry with a Pacific Blue conjugated azide. Cells were also stained for DNA content with PI. (A) Representative flow cytometry dot plots with gates indicating the fraction of cells in Sub-G1, G1/G0, S, and G2/M phases. (B) Graphs illustrating the percent of cells in each cell cycle phase in control and treated cells. Error bars represent standard deviations from three biological replicates. Asterisks represent statistical significance as determined using multiple unpaired t tests with the Benjamini, Krieger, and Yekutieli correction for multiple comparisons.

Trametinib resistance in this model is ERK1/2-indepdendent

Analysis of ERK1/2 phosphorylation following trametinib yielded similar results for parental and trametinib-resistant Tyler1, whereby ERK phosphorylation remained inhibited after 24 hours of treatment (**Figure 4.6**). This response differs from many other *in vitr*o models of MAPK pathway inhibitor resistance where treatment with a MAPK pathway inhibitor causes an initial attenuation in ERK activation followed by a rapid rebound (Corcoran et al., 2012). In addition to sustained inhibition of ERK1/2 phosphorylation, parental Tyler1 and two Tyler1-TramR clones showed a marked reduction in MPAS gene expression following 24 hours of trametinib treatment (**Figure 4.6**). Tyler1-TramR-Clone2 also exhibited decreased basal MPAS gene expression relative to parental Tyler1 or TramR-Clone4. Collectively, these results suggested that resistant Tyler1 do not exhibit ERK1/2 reactivation when treated with trametinib, hinting at a possible ERK-independent resistance mechanism. This theory was supported when we evaluated parental and TramR Tyler1 for sensitivity to the ERK1/2 inhibitor ravoxertinib (**Figure 4.7**). While the parental cell line exhibited an IC_{50} value of 312 nM, all six of the trametinib-resistant cell lines were insensitive and did not reach an IC_{50} at concentrations greater than 10 μM.

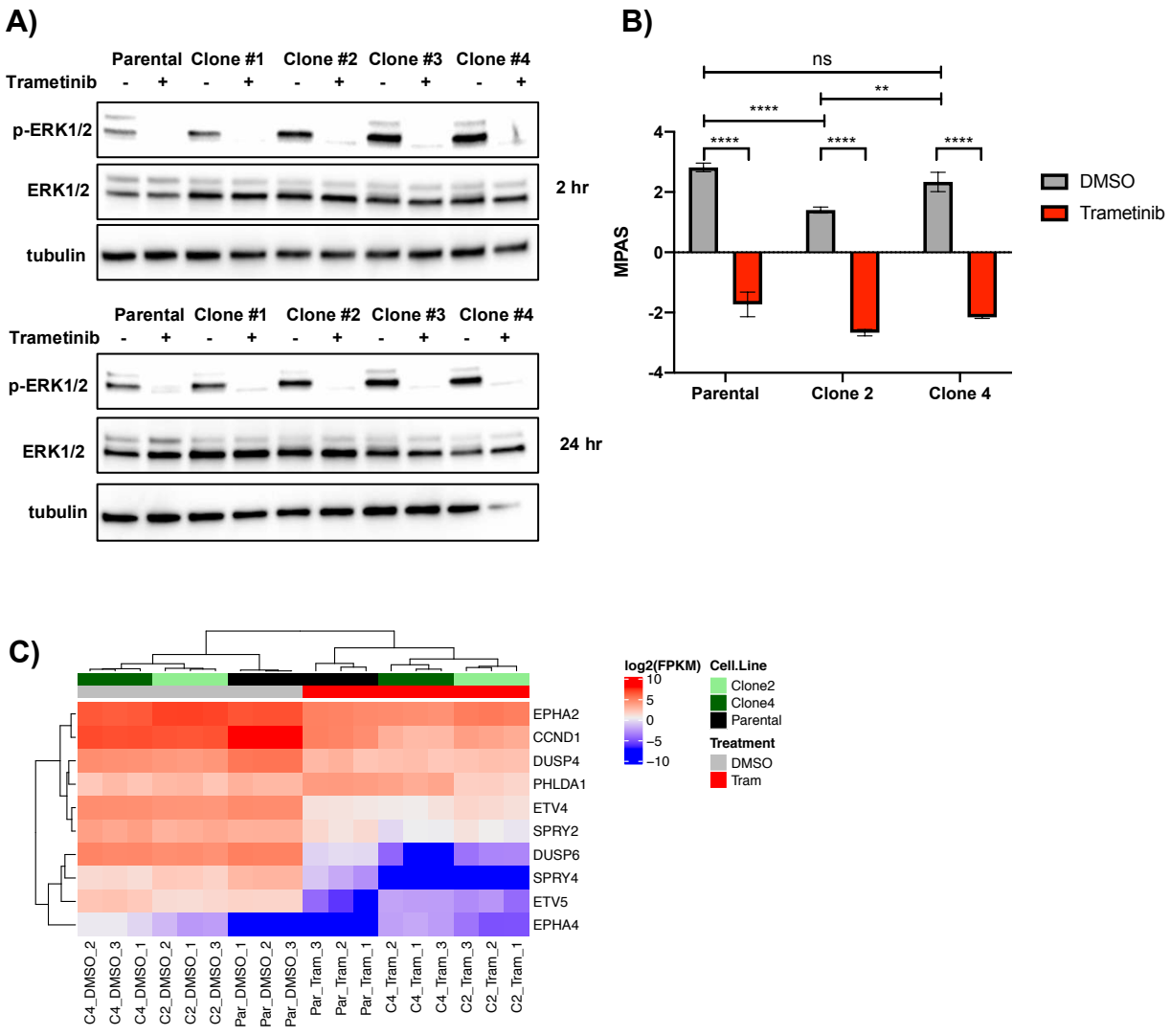

Figure 4.6 Sustained inhibition of ERK1/2 activation trametinib-treated Tyler1-TramR cell lines. (A) Parental and TramR Tyler1 cell lines were treated with 25 nM trametinib or DMSO control for 2 and 24 hours, followed by western blot analysis for phosphorylated ERK1/2 abundance. (B) MPAS for Tyler1 Parental, TramR-Clone2 and TramR-clone 4 following a 24-hour treatment with 25 nM trametinib or DMSO control. Error bars represent the standard deviation from three biological replicates. Statistical significance was determined using a two-way ANOVA with Tukey's adjustment for multiple comparisons. (C) Heatmap illustrating $\log_2$ FPKM expression of MPAS genes in control and trametinib-treated Tyler1 parental, TramR-Clone2, and TramR-Clone4.

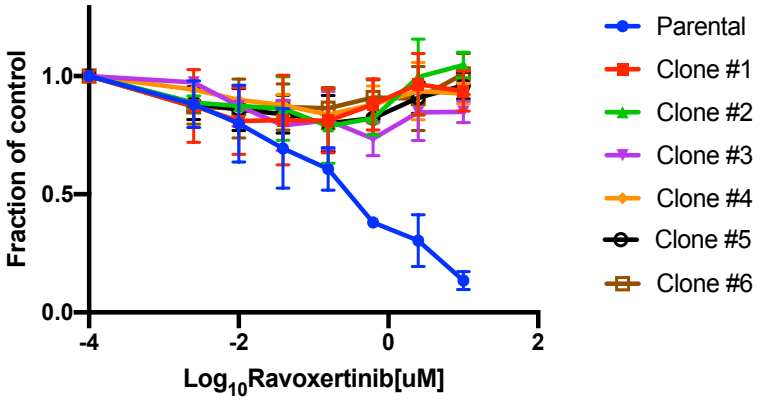

Figure 4.7. Tyler1-TramR clones are insensitive to ERK1/2 inhibition.
Cell lines were treated with serial dilutions of ravoxertinib and relative cell number was determined as a fraction of DMSO control. Error bars represent standard deviations of the fraction of control determined from three independent biological replicates, each of which was conducted in technical triplicate.

Trametinib-induced gene expression alterations in parental and trametinib-resistant Tyler1

Next, we analyzed gene expression changes in response to trametinib in parental Tyler1 and Tyler1-TramR-Clone2 and –Clone4. Cell lines were treated with 25 nM trametinib or DMSO control for 24 hours, after which, cells were harvested for RNA-Seq analysis. In parental Tyler1, 1,525 and 358 genes were up- and downregulated following trametinib treatment, respectively. Downregulated genes were primarily involved in cell cycle control (E2F Targets, DNA Replication, G2/M Checkpoint) as well as negative regulation of MAPK signaling (**Table 4.4**). Upregulated genes were involved in a variety of processes including chemokine signaling, extracellular matrix components (GO Core Matrisome), and neuronal genes (CAHOY Astroglial; **Table 4.4**).

Table 4.4 Enriched processes among trametinib-induced DEGs in parental Tyler1. Top 10 enriched processes among up- and downregulated DEGs in Tyler1 in response to 24-hour treatment with 25 nM trametinib. Enrichment was determined using GSEA Preranked with log_2 fold-change values as the ranking metric. Statistical enrichment was determined with a nominal p-value cutoff of 0.01.

NAME	# genes	ES	NES	p-val
Upregulated				
GO CHEMOKINE RECEPTOR BINDING	12	0.707	2.081	<0.001
GO GLYCOSAMINOGLYCAN BINDING	46	0.497	2.013	<0.001
GO SULFUR COMPOUND BINDING	42	0.499	2.01	0.002
CAHOY ASTROGLIAL	10	0.563	2.007	<0.001
REACTOME CHEMOKINE RECEPTORS BIND CHEMOKINES	34	0.717	1.996	0.001
GO HEPARIN BINDING	12	0.505	1.965	0.001
GO RETINA HOMEOSTASIS	27	0.661	1.952	0.002
GO SENSORY PERCEPTION OF LIGHT STIMULUS	53	0.526	1.944	0.002
NABA CORE MATRISOME	14	0.46	1.91	<0.001
GO RESPONSE TO CHEMOKINE	23	0.609	1.901	<0.001
Downregulated				
HALLMARK E2F TARGETS	19	-0.833	-4.2	<0.001
GO DNA DEPENDENT DNA REPLICATION	17	-0.825	-3.828	<0.001
GO DNA REPLICATION	26	-0.674	-3.826	<0.001
GO DNA RECOMBINATION	17	-0.753	-3.453	<0.001
HALLMARK G2M CHECKPOINT	18	-0.713	-3.373	<0.001
REACTOME CELL CYCLE	39	-0.502	-3.359	<0.001
GO CHROMOSOMAL REGION	28	-0.626	-3.279	<0.001
REACTOME CELL CYCLE MITOTIC	14	-0.528	-3.245	<0.001
GO CATALYTIC ACTIVITY ACTING ON DNA	17	-0.752	-3.19	<0.001
GO NEGATIVE REGULATION OF MAP KINASE ACTIVITY	11	-0.702	-3.184	<0.001

Trametinib treatment upregulated 520 genes and downregulated 299 genes in Tyler1-TramR-Clone2. Of these DEGs, 339 (65%) and 111 (37%) were also up- and downregulated in parental Tyler1 treated with trametinib, respectively. GSEA Preranked analysis of trametinib-induced DEGs in TramR-Clone2 identified only one upregulated process (Tube Formation); whereas, several downregulated processes

were identified, including KRAS signaling and interleukin signaling (**Table 4.5**). Unlike parental Tyler1, TramR-Clone2 does not exhibit downregulation of cell cycle-related genes in response to trametinib. Loss of genes that are normally induced in response to oncogenic KRAS suggests a decrease in MAPK pathway (and possibly AKT pathway) signaling in response to trametinib, which is consistent with sustained suppression of ERK1/2 phosphorylation and an ERK-independent mechanism of resistance.

Table 4.5 Enriched processes among trametinib-induced DEGs in Tyler1-TramR-Clone2. Top enriched processes among up- and downregulated DEGs in Tyler1 in response to 24-hour treatment with 25 nM trametinib. Enrichment was determined using GSEA Preranked with $\log_2$ fold-change values as the ranking metric. Statistical enrichment was determined with a nominal p value cutoff of 0.01.

NAME	SIZE	ES	NES	p-val
Upregulated				
GO TUBE FORMATION	10	0.575	1.767	0.006
Downregulated				
KRAS.300 UP.V1 UP	17	-0.75	-2.726	<0.001
KRAS.600 UP.V1 UP	27	-0.637	-2.624	<0.001
HALLMARK KRAS SIGNALING UP	27	-0.609	-2.547	<0.001
GO BEHAVIOR	37	-0.524	-2.436	<0.001
IL15 UP.V1 UP	23	-0.594	-2.4	<0.001
IL2 UP.V1 UP	22	-0.624	-2.39	<0.001
KEGG JAK STAT SIGNALING PATHWAY	14	-0.678	-2.345	<0.001
GO NEGATIVE REGULATION OF KINASE ACTIVITY	25	-0.558	-2.338	<0.001
REACTOME SIGNALING BY INTERLEUKINS	33	-0.542	-2.337	0.002
KRAS.BREAST UP.V1 UP	17	-0.63	-2.322	<0.001

In TramR-Clone4, 1,140 and 450 genes were up- and downregulated following trametinib treatment, respectively, of which 617 (54%) and 161 (36%) were similarly up

and downregulated in parental Tyler1, respectively. Functional analysis of DEGs identified upregulation of a variety of processes including heparin binding, GPCR ligand binding, and extracellular matrix components (Matrisome; **Table 4.6**). Many downregulated processes were related to RNA processing and ribosome/ribonucleoprotein biogenesis. Additionaly, TramR-Clone4 exhibited downregulation of downstream targets of KRAS signaling and E2F targets, possibly suggesting decreased MAPK pathway activity and decreased expression of cell cycle genes.

Table 4.6 Enriched processes among trametinib-induced DEGs in Tyler1-TramR-Clone4. Top enriched processes among up- and downregulated DEGs in Tyler1 in response to 24-hour treatment with 25 nM trametinib. Enrichment was determined using GSEA Preranked with log_2 fold-change values as the ranking metric. Statistical enrichment was determined with a nominal p value cutoff of 0.01.

NAME	SIZE	ES	NES	p-val
Upregulated				
GO HEPARIN BINDING	23	0.631	2.323	<0.001
GO SULFUR COMPOUND BINDING	28	0.548	2.133	<0.001
GO GLYCOSAMINOGLYCAN BINDING	33	0.536	2.13	0.001
GO ENDOPEPTIDASE ACTIVITY	37	0.504	2.1	<0.001
REACTOME GPCR LIGAND BINDING	23	0.547	2.031	<0.001
GO SOMATODENDRITIC COMPARTMENT	66	0.398	1.948	<0.001
GO REGULATION OF CALCIUM ION TRANSPORT INTO CYTOSOL	12	0.635	1.941	0.001
NABA MATRISOME	137	0.356	1.932	<0.001
GO INNER EAR MORPHOGENESIS	18	0.556	1.927	0.003
GO DIVALENT INORGANIC CATION HOMEOSTASIS	39	0.459	1.918	0.001
Downregulated				
GO NCRNA PROCESSING	39	-0.688	-3.663	<0.001
GO NCRNA METABOLIC PROCESS	42	-0.634	-3.533	<0.001
GO RIBONUCLEOPROTEIN COMPLEX BIOGENESIS	40	-0.663	-3.425	<0.001
GO RIBOSOME BIOGENESIS	35	-0.684	-3.421	<0.001
GO RRNA METABOLIC PROCESS	31	-0.678	-3.317	<0.001

HALLMARK E2F TARGETS	22	-0.717	-3.127	<0.001
KRAS.300 UP.V1 UP	22	-0.678	-3.024	<0.001
KRAS.600 UP.V1 UP	40	-0.577	-2.973	<0.001
REACTOME METABOLISM OF RNA	32	-0.608	-2.939	<0.001
GO RNA PROCESSING	64	-0.483	-2.903	<0.001

Trametinib-resistant Tyler1 exhibit upregulation of EMT genes and altered expression of immune-related genes

The basal gene expression profiles of trametinib resistant clones (Tyler1-TramR-Clone2 and Tyler1-TramR-Clone4) were compared against that of the parental Tyler1 cell line. DEG analysis identified upregulation of 1,720 and 1,472 genes in Tyler1-TramR-Clone2 and Tyler1-TramR-Clone4, respectively. The two lists of DEGs were compared, revealing 1,133 co-upregulated genes. Additionally, 1,630 and 1,739 genes were downregulated in TramR-Clone2 and -Clone4, respectively, of which, 1,298 were co-downregulated. Functional analysis of the DEGs common to both clones was performed. A total of 34 terms representing various pathways and processes were enriched in Tyler1-TramR clones relative to the parental cell line (**Table 4.7**). 35% of these terms (12/34) are involved in EMT. **Figure 4.8** shows a heatmap of DEGs within the leading edge subset of the Hallmarks EMT gene set. The most strongly upregulated leading edge genes are decorin (*DCN*) and tenascin C (*TNC*), which encode extracellular matrix components. The EMT leading edge genes also include those encoding type I collagens (*COL1A1* and *COL1A2*) and matrix metalloproteases (*MMP1* and *MMP3*). Concurrently, terms related to epithelium growth and cell-cell junctions were downregulated in TramR relative to parental Tyler1 (43%, 19 out of 44 terms) (**Table 4.8**).

Table 4.7 Top 20 enriched terms that are upregulated in TramR versus parental Tyler1. Enrichment was determined using GSEA Preranked with log_2 fold-change values as the ranking metric. Statistical enrichment was determined with a nominal p value cutoff of 0.01.

Gene Set	# genes	ES	NES	p-val
GO COMPLEMENT ACTIVATION	11	0.76	2.3	<0.001
GO COLLAGEN TRIMER	17	0.64	2.3	<0.001
KEGG PROGESTERONE MEDIATED OOCYTE MATURATION	12	0.69	2.3	<0.001
REACTOME COMPLEMENT CASCADE	10	0.75	2.3	<0.001
GO COLLAGEN FIBRIL ORGANIZATION	16	0.63	2.2	<0.001
KEGG COMPLEMENT AND COAGULATION CASCADES	14	0.66	2.2	<0.001
WP COMPLEMENT AND COAGULATION CASCADES	14	0.66	2.2	<0.001
WP HUMAN COMPLEMENT SYSTEM	16	0.62	2.1	<0.001
GO SKELETAL MUSCLE ORGAN DEVELOPMENT	30	0.50	2.1	<0.001
GO SMAD BINDING	12	0.64	2.1	<0.001
HALLMARK EPITHELIAL MESENCHYMAL TRANSITION	63	0.40	2.0	<0.001
GO CILIARY PLASM	17	0.56	1.9	0.004
GO EXTRACELLULAR MATRIX STRUCTURAL CONSTITUENT CONFERRING TENSILE STRENGTH	11	0.60	1.9	0.004
NABA CORE MATRISOME	60	0.37	1.9	<0.001
GO NEUROMUSCULAR JUNCTION	11	0.59	1.9	0.007
REACTOME COLLAGEN DEGRADATION	19	0.49	1.8	0.004
GO FC EPSILON RECEPTOR SIGNALING PATHWAY	10	0.59	1.8	0.009
GO ACTIVATION OF IMMUNE RESPONSE	50	0.37	1.8	<0.001
REACTOME REGULATION OF INSULIN LIKE GROWTH FACTOR IGF TRANSPORT AND UPTAKE BY INSULIN LIKE GROWTH FACTOR BINDING PROTEINS IGFBPS	27	0.44	1.8	<0.001
REACTOME TRANSMISSION ACROSS CHEMICAL SYNAPSES	40	0.39	1.8	<0.001

Table 4.8 Top 20 enriched terms that are downregulated in TramR versus parental Tyler1. Enrichment was determined using GSEA Preranked with log_2 fold-change values as the ranking metric. Statistical enrichment was determined with a nominal p value cutoff of 0.01.

Gene Set	# genes	ES	NES	p-val
AKT UP.V1 UP	45	-0.56	-2.0	<0.001
GO CYTOKINE ACTIVITY	40	-0.56	-2.0	<0.001
REACTOME FORMATION OF THE CORNIFIED ENVELOPE	18	-0.67	-1.9	<0.001
REACTOME KERATINIZATION	18	-0.67	-1.9	<0.001
HALLMARK INTERFERON GAMMA RESPONSE	56	-0.52	-1.9	<0.001
REACTOME INTERFERON ALPHA BETA SIGNALING	20	-0.62	-1.9	<0.001
GO RESPONSE TO TYPE I INTERFERON	24	-0.60	-1.9	<0.001
GO REGULATION OF SYMBIOTIC PROCESS	31	-0.55	-1.9	0.001
GO CORNIFICATION	18	-0.64	-1.8	0.001
GO TIGHT JUNCTION	39	-0.53	-1.8	<0.001
GO BASOLATERAL PLASMA MEMBRANE	53	-0.50	-1.8	0.002
GO KERATINIZATION	22	-0.60	-1.8	0.001
GO ENSHEATHMENT OF NEURONS	28	-0.56	-1.8	<0.001
GO DEFENSE RESPONSE TO VIRUS	41	-0.51	-1.8	0.001
GO WATER HOMEOSTASIS	19	-0.59	-1.8	0.004
GO UDP GLYCOSYLTRANSFERASE ACTIVITY	18	-0.60	-1.8	0.007
GO RESPONSE TO VIRUS	53	-0.48	-1.8	0.001
MEK UP.V1 UP	46	-0.48	-1.8	0.001
REACTOME O LINKED GLYCOSYLATION	20	-0.58	-1.7	0.007
REACTOME CELL JUNCTION ORGANIZATION	23	-0.57	-1.7	0.008

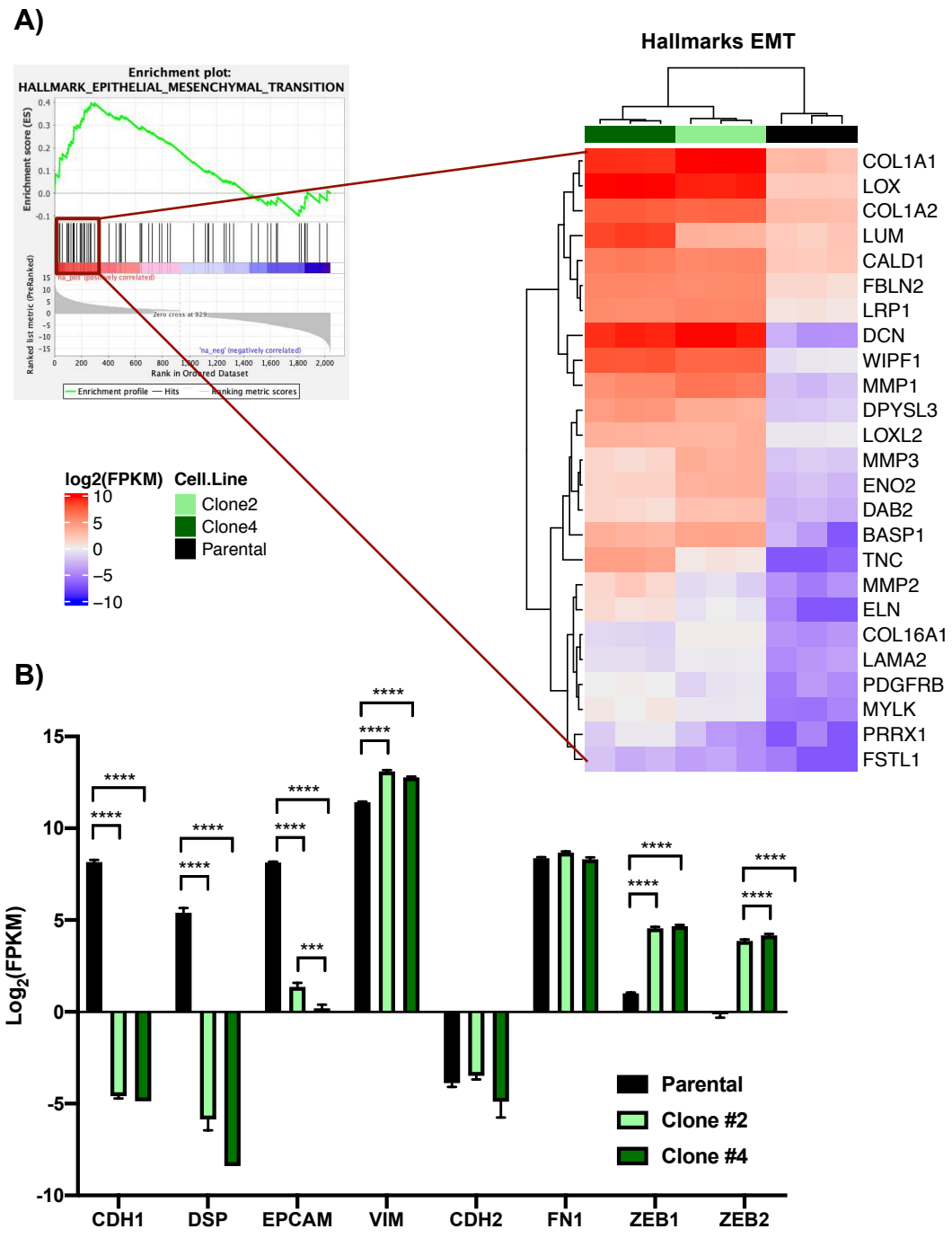

Figure 4.8 Trametinib-resistant Tyler1 exhibit increased expression of EMT markers relative to the parental cell line. (A) Results from GSEA Preranked analysis of shared DEGs between TramR-Clone2 and TramR-Clone4 versus the parental cell line. Heatmap illustrates log_2-FPKM expression of core enrichment genes for the Hallmark EMT gene set. (B) Mean and standard deviation of log_2-FPKM expression of various epithelial and mesenchymal markers (n = 3). Statistical significance was determined in our differential gene expression analysis using 'edgeR' with Benjamini and Hochberg correction for multiple comparisons.

Loss of epithelial markers was observed in TramR clones, including dramatically decreased expression of E-cadherin (*CDH1*) and desmoplakin (*DSP*) relative to the parental cell line (**Figure 4.8**). Vimentin (*VIM*) expression was increased roughly 3-fold in resistant clones, consistent with a shift to a more mesenchymal phenotype; whereas, no change was observed in the expression levels of N-cadherin (*CDH2*) and fibronectin (*FN1*). EMT in cancer is controlled by a variety of signaling pathways that activate EMT-promoting transcription factors including zinc finger E-box binding homeobox 1 and 2 (ZEB1/2). Indeed, ZEB1 and ZEB2 were also upregulated in resistant clones (**Figure 4.8**). Interestingly, a common feature of all 6 Tyler1-TramR clones was a morphology shift from an epithelial-like polygonal shape, characteristic of the parental Tyler1 cell line (Sledge et al., 2012), to a more spindle-shaped, fibroblast-like appearance (**Figure 4.9**).

Other terms enriched in TramR Tyler1 were related to immune (8/34) and neuronal (6/34) processes (**Table 4.7**). However, most of the immune terms involved the complement and coagulation cascade. In contrast, parental Tyler1 exhibited enrichment of many immune-related gene sets (10 out of 44 terms, 23%) involving interferon and cytokine signaling (**Table 4.8**). Several of these terms were specific to antiviral immunity. These data suggest that TramR Tyler1 exhibit a shift in immune signaling pathways, characterized by loss of interferon signaling and an increase in complement/coagulation gene expression.

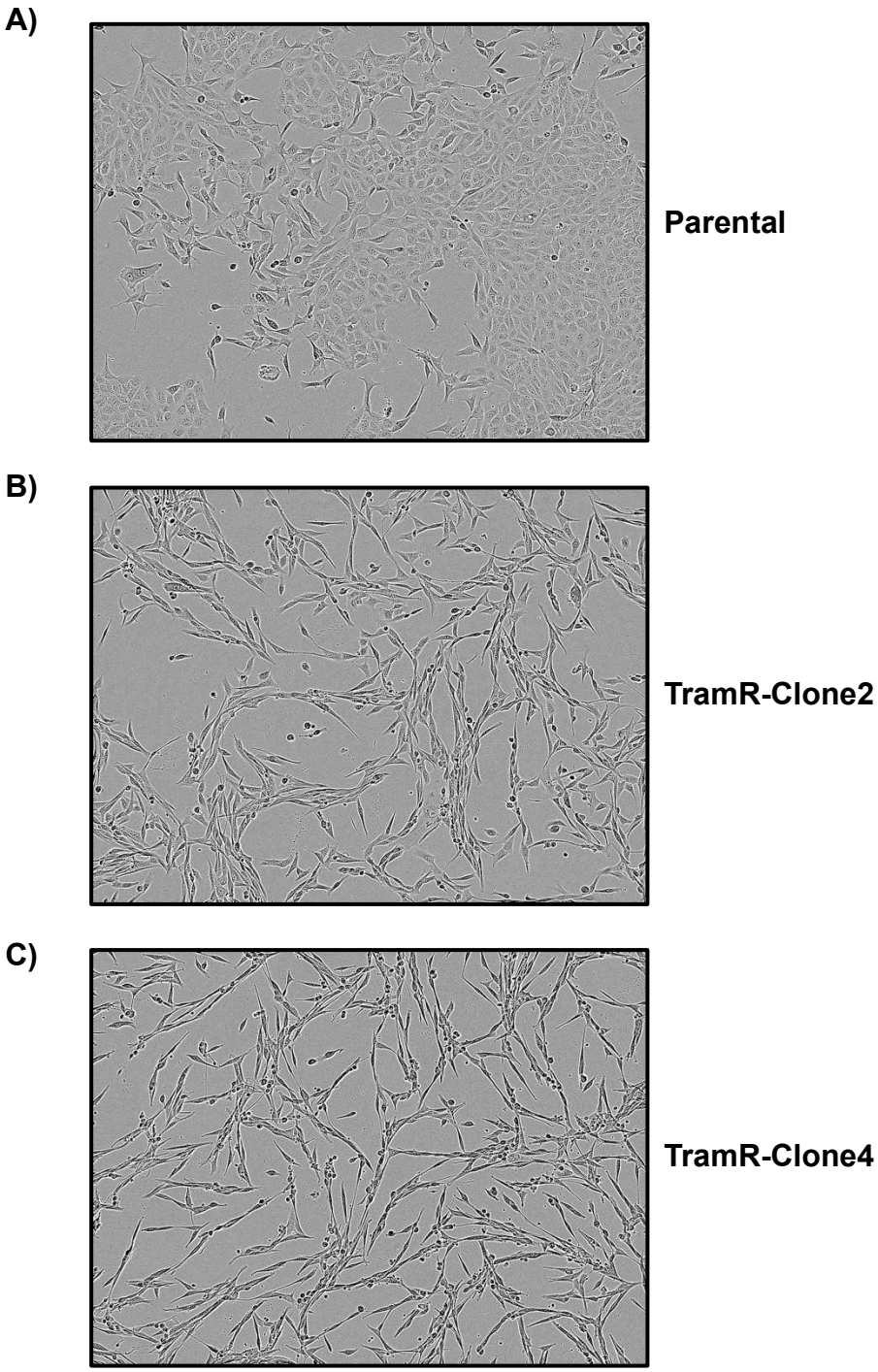

Figure 4.9. Tyler1 TramR cell lines exhibit altered morphology relative to the Tyler1 parental cell line. Cells were seeded in a 96-well plate (1,500 per well) and imaged using IncuCyte ZOOM live-cell imaging system. Representative images were taken 48 hours after plating at a 10x maginification.

Tyler1-TramR-Clone2 and –Clone4 also exhibited decreased expression of genes downstream of AKT and MEK signaling (**Table 4.8**). The gene sets "AKT UP.V1 UP" and "MEK UP.V1 UP", which are within the MSigDB C6: Oncogenic Signatures gene set collection, were enriched in parental Tyler1 relative to the trametinib-resistant cell lines. These gene sets contain genes upregulated in response to transgenic expression of AKT1 and constitutively active MEK1, respectively (Creighton et al., 2006; Majumder et al., 2004).

We also wanted to determine whether expression of any of the 30 genes identified earlier that correlate with *de novo* trametinib sensitivity (**Table 4.2**) was altered in either TramR-Clone2 or –Clone4. Nine out of 30 genes were differentially expressed in both clones relative to the parental cell line: *MPZL1, ITPKA, CHMP2A, UACA, ZFPM2, EHD4, ANKH, TCF15,* and *LURAP1L* (**Figure 4.10**). TramR-Clone2 alone exhibited altered expression of *NSD1*; whereas, TramR-Clone4 exhibited altered expression of *CD9* and *ELK3* (**Figure 4.10**). Low expression of *MPZL1, CHMP2A, UACA, ZFPM1, EHD4, ANKH,* and *LURAP1L* was associated with intrinsic resistance to trametinib in canine cancer cell lines (**Table 4.2**). These seven genes were downregulated in both TramR-Clone2 and –Clone4, suggesting that loss of their expression may be associated with both intrinsic and acquired resistance to trametinib. *LURAP1L*, was the most strongly downregulated gene, with expression levels decreased approximately 400 and 300-fold in TramR-Clone2 and Clone4, respectively. LURAP1L is an activator of canonical NFKB signaling (Jing et al., 2010). High expression of *ITPKA* and *TCF15* was associated with intrinsic trametinib resistance in canine cancer cell lines (**Table 4.2**). *TCF15* expression was increased in both

trametinib-resistant clones compared to the parental cell line, suggesting a possible role for TCF15 in both acquired and intrinsic resistance to trametinib.

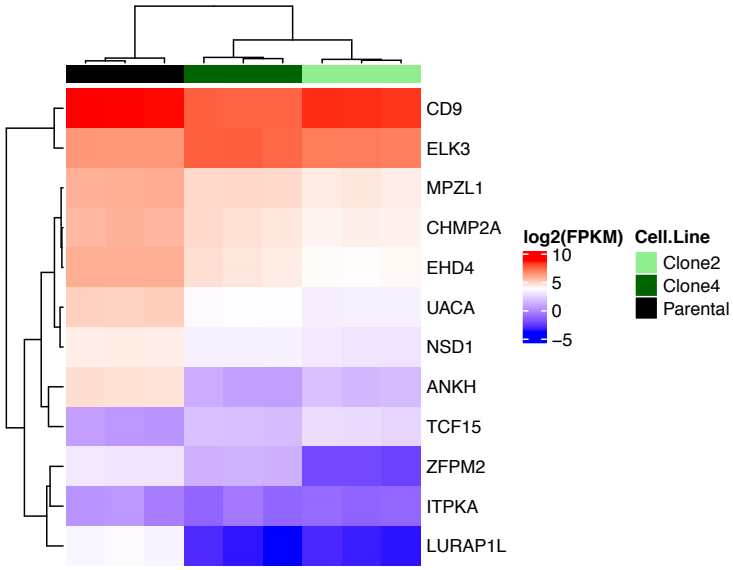

Figure 4.10. Genes correlated with trametinib sensitivity that are differentially expressed in Tyler1-TramR relative to parental Tyler1. Heatmap illustrating log_2-FPKM expression levels of 12 out of the 30 genes associated with trametinib sensitivity (listed in Table 4.2) that are differentially expressed in Tyler1-TramR-Clone2 and/or –Clone4 relative to parental Tyler1.

Tyler1-TramR-Clone2 exhibits altered metabolism relative to parental Tyler1 and Tyler1-TramR-Clone4

We next analyzed Tyler1-TramR for metabolic alterations relative to the parental Tyler1 cell line. Oxygen consumption rates (OCR) and extracellular acidification rates (ECAR) were monitored using the Seahorse XFe24 analyzer. This analysis revealed a decrease in mitochondrial metabolism in TramR-Clone2, but not TramR-Clone4, characterized by decreased basal and maximal OCR (**Figure 4.11**). The mean basal and maximal OCR of TramR-Clone were both approximately 80 nmol O_2/min, versus

325 and 517 nmol O_2/min in the parental cell line, respectively. The lack of difference between basal and maximal OCR in TramR-Clone2 suggests a lack of spare respiratory capacity in this cell line. Additionally, this cell line exhibited lower glycolytic capacity and glycolytic reserve (**Figure 4.12**). To identify potential transcriptomic contributors to this phenotype we specifically analyzed genes that are differentially expressed between TramR-Clone2 and parental Tyler1, but not between TramR-Clone4 and parental Tyler1. Functional analysis of these genes identified enrichment of mitochondrial gene sets among DEGs uniquely upregulated in TramR-Clone2 versus parental Tyler1. These genes include components of the mitochondrial ribosome 39S subunit (*MRPL21*, *MRPL23*, and *MRPL24*), electron transport chain complex I (*NDUFV2* and *NDUFB10*), and mitochondrial transcription (*TFB2M* and *MTERF1*) (**Figure 4.13**).

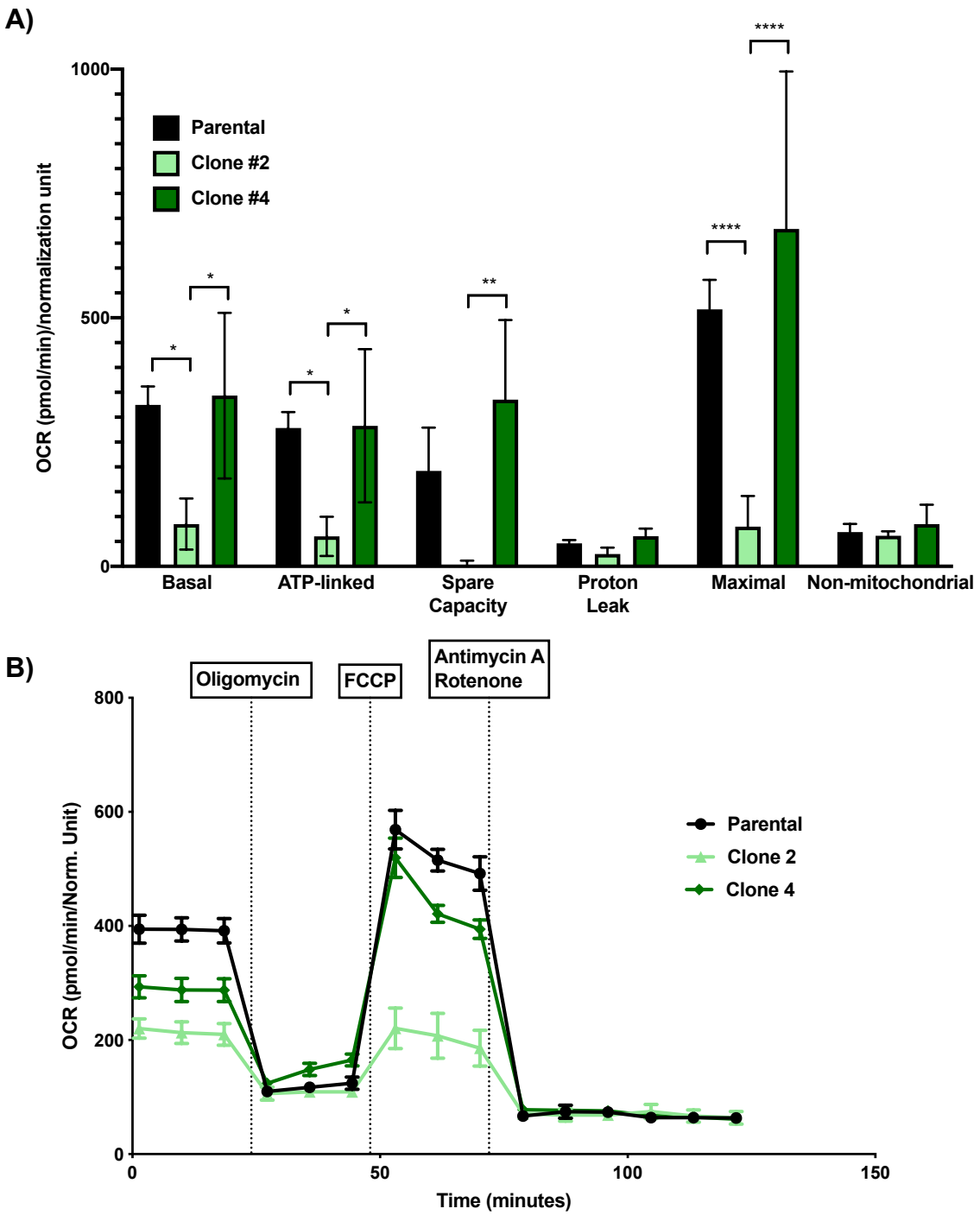

Figure 4.11. Analysis of mitochondrial metabolism in Tyler1 Parental and TramR cell lines. (A) Metabolic parameters of Tyler1 Parental and TramR determined using Seahorse XFe24 measurements. OCR values are the means of three independent biological replicates ± standard deviation. Statistical significance was determined using a two-way ANOVA with Tukey's multiple comparison correction. (B) OCR measurements from a representative biological replicate. Error bars represent standard deviation from three technical replicates.

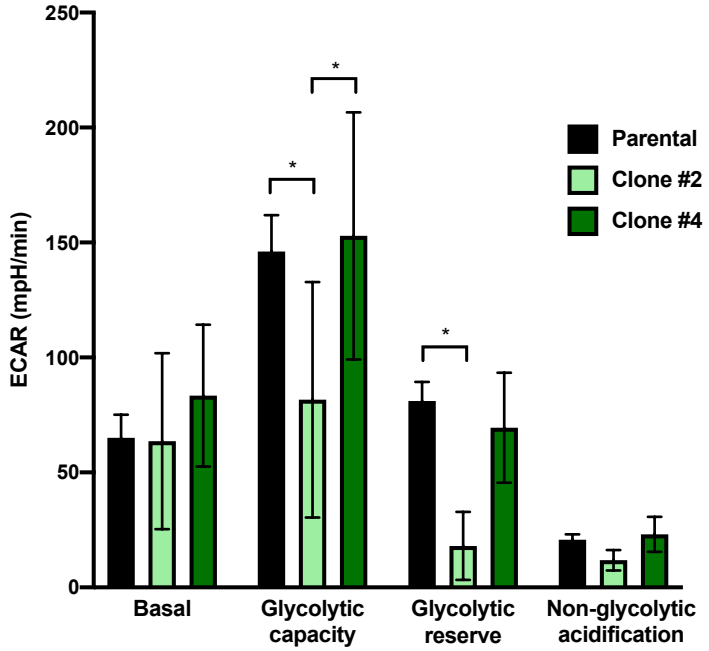

Figure 4.12. Analysis of extracellular acidification in Tyler1 Parental and TramR cell lines. Metabolic parameters of Tyler1 Parental and TramR determined using Seahorse XFe24 measurements. ECAR values are the means of three independent biological replicates ± standard deviation. Statistical significance was determined using a two-way ANOVA with Tukey's multiple comparison correction.

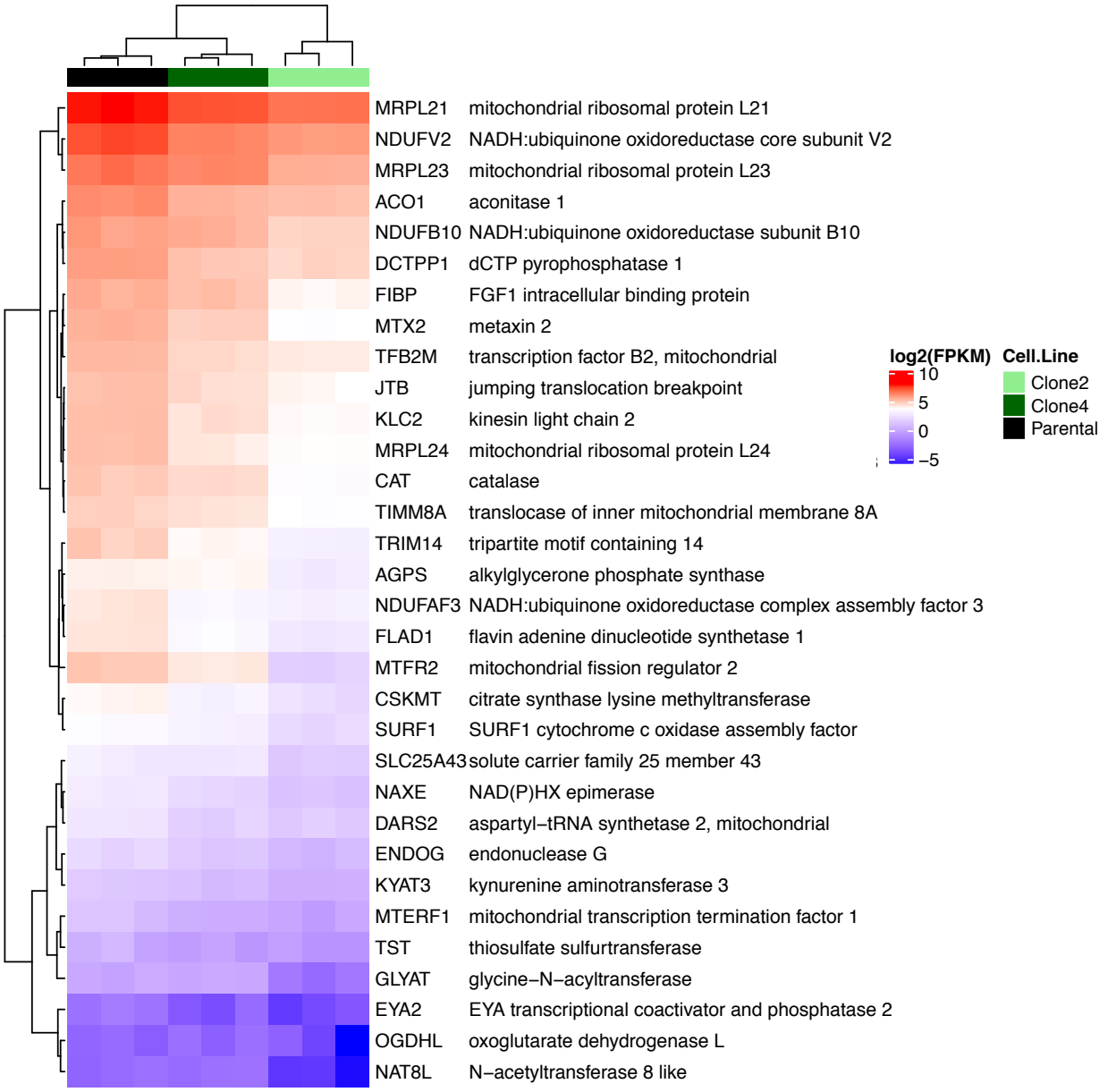

Figure 4.13. Heatmap of mitochondrial genes differentially expressed in TramR-Clone2 but not TramR-Clone4. Heatmap of $\log_2$-FPKM expression of DEGs unique to TramR-Clone2 that are in the Mitochondrion (GO:0005739) MSigDB gene set.

DISCUSSION

Mutations in the proto-oncogene BRAF promote constitutive activation of the MAPK pathway and drive tumorigenesis in several human cancers. Single-agent treatment of BRAF mutant melanoma with BRAF or MEK inhibitors exhibits initial efficacy in half of patients, but most individuals eventually experience disease progression. The majority of resistance mechanisms to BRAF and MEK inhibitors involve reactivation of the MAPK pathway (Shi et al., 2014; Van Allen et al., 2014). These ERK1/2-dependent mechanisms include secondary mutations in NRAS (Nazarian et al., 2010; Trunzer et al., 2013), aberrant spicing of BRAF (Poulikakos et al., 2011), and overexpression of CRAF (Montagut et al., 2008). Combined BRAF and MEK inhibition extends the duration of response, but acquired resistance remains an obstacle to treatment. Other BRAF mutant cancers, such as colorectal cancer, are inherently resistant to BRAF and MEK inhibitors (Kopetz et al., 2015). In this study, we adopt a comparative approach to combating resistance to MEK inhibition, generating and characterizing trametinib-resistant derivatives of the BRAF mutant Tyler1 canine TCC cell line (Tyler1-TramR).

The majority of described resistance mechanisms to MAPK pathway inhibitors involve some means of reactivation of ERK1/2. Interestingly, the mechanism underlying trametinib resistance in the canine model generated in this study appears to be independent of ERK1/2 activation as evidenced by sustained inhibition of ERK phosphorylation, decreased basal expression of MAPK target genes, and insensitivity to

ERK inhibition. Rather, the Tyler1-TramR clones analyzed in this study exhibit alterations in expression of EMT and immune-related genes.

Tyler1-TramR cell lines exhibited characteristics of a shift to a more mesenchymal phenotype, including dramatic loss of genes encoding E-cadherin and desmoplakin, increased expression of vimentin, and increased expression of the EMT transcription factors ZEB1 and ZEB2. TramR cells also exhibited a morphology change consistent with a more mesenchymal appearance relative to parental Tyler1. EMT reprogramming is a recognized contributor to anticancer drug resistance (Singh and Settleman, 2010). Witta et al. described resistance to the EGFR inhibitor gefitinib in non-small cell lung cancer cell lines that have decreased expression of E-cadherin and increased expression of ZEB1 (Witta et al., 2006). Overexpression of E-cadherin in a gefinitib-resistant cell line was found to confer sensitivity. Furthermore, pre-treatment of gefitinib-resistant cells with the HDAC inhibitor entinostat promoted increased expression of E-cadherin and augmented the antiproliferative and pro-apoptotic effects of gefintib (Witta et al., 2006).

Elevated ZEB1 expression is associated with intrinsic resistance to vemurafenib in BRAFV600E mutant melanoma cell lines and patients (Richard et al., 2016). Furthermore, *in vitro* models of acquired vemurafenib resistance exhibited increased ZEB1 expression relative to the parental cell lines, and knockdown of ZEB1 promoted re-sensitization to vemurafenib (Richard et al., 2016). ZEB1 has also been implicated in KRAS mutant lung cancer cell line resistance to selumetinib and trametinib (Peng et al., 2019). Lung cancer cell lines that were more mesencymal-like exhibited decreased sensitivity to MEK inhibition versus epithelial cell lines (Peng et al., 2019). Another

study found that oncogene addiction to mutant KRAS is associated with an epithelial-like gene expression signature (Singh et al., 2009). In our study, Tyler1-TramR cell lines, which have decreased expression of epithelial gene markers, also show loss of expression of genes downstream of AKT and MEK.

Trametinib resistant cTCC also exhibited upregulation of several genes within the complement system. Complement signaling has both pro- and anti-tumorigenic effects depending on the context (Roumenina et al., 2019). Complement components play a role in the EMT. For example, EMT transcription factor TWIST1 promotes expression of C3, causing decreased expression of E-cadherin and EMT induction in ovarian cancer cells (Cho et al., 2016). Thus, it is possible that the increased expression of complement and coagulation genes observed in Tyler1-TramR is related to the shift to a more mesenchymal-like state.

Several metabolic effects of oncogenic BRAF have been described, including suppression of mitochondrial biogenesis via decreased expression of peroxisome proliferator-activated receptor gamma coactivator 1-alpha (PGC-1α) (Haq et al., 2013), increased glycolysis as a result of upregulation of glucose transporters 1 and 3 (GLUT1/3) and hexokinase 2 (HK2) (Parmenter et al., 2014), and increased oxidative metabolism as a result of increased pyruvate dehydrogenase activity (Kaplon et al., 2013). Resistance to MAPK pathway inhibitors in BRAF mutant cancers is often accompanied by a metabolic shift. Several groups have described increased mitochondrial metabolism in cell lines exhibiting acquired or intrinsic resistance to BRAF or MEK inhibition (Corazao-Rozas et al., 2013; Gopal et al., 2014; Zhang et al., 2016).

In these instances, the metabolic alterations often render the resistant cells more sensitive to oxidative stress (Corazao-Rozas et al., 2013; Zhang et al., 2016).

Interestingly, one of the trametinib-resistant Tyler1 clones, Tyler1-TramR-Clone2, exhibited decreased mitochondrial respiration relative to the parental cell line, as evidenced by decreased basal and maximal OCR. In fact, the basal OCR of TramR-Clone2 was roughly equivalent to the maximal OCR, indicating a lack in spare respiratory capacity. The oxidative metabolic profile of TramR-Clone4 was not different from that of the parental cell line. Although increased oxidative phosphorylation has been implicated in resistance to vemurafenib, other instances of cancer drug resistance involve decreased mitochondrial metabolism and spare respiratory capacity. For instance, acquired resistance to the EGFR inhibitor erlotinib in non-small cell lung cancer is associated with decreased spare respiratory capacity, in part due to increased mTORC2 activation, and increased sensitivity to glucose deprivation (Chiang et al., 2018). Multidrug resistance as a result of P-glycoprotein overexpression in cancer cells is characterized by altered metabolism including diminished spare respiratory capacity and increased glycolysis and glutathione metabolism (Lopes-Rodrigues et al., 2017).

We determined that the MPAS, a gene signature predictive of sensitivity to MEK inhibitors in human cancer cell lines, is also associated with sensitivity to trametinib in canine cancer cell lines. This finding suggests that transcriptional determinants of sensitivity and resistance to MEK inhibition may be conserved between human and canine cancers. We identified 30 non-MPAS genes exhibiting significant correlations with trametinib sensitivity. 28 genes were negatively correlated with trametinib IC_{50} values suggesting their association with increased sensitivity to MEK1/2 inhibition with

trametinib. Five of these genes were involved in endocytosis (*ARF6, F2R, PLD1, CHMP2A,* and *EHD4*). Most canine cancer cell lines that are sensitive to trametinib harbor oncogenic MAPK pathway alterations and exhibit constitutive MAPK activity. It is possible that the increased expression of these genes observed in trametinib sensitive cell lines is actually due to increased MAPK signaling. Indeed, pharmacologic inhibition of MEK1/2 or ERK1/2 decreases clathrin-mediated endocytosis in cancer cells, but not in normal cells (Xiao et al., 2018). Activation of ERK1/2 leads to phosphorylation of the endocytic adaptor protein FCHSD2, resulting in FCHSD2 recruitment to clathrin-coated pits (Xiao et al., 2018). On the other hand, endocytosis has been identified as a process necessary for receptor-mediated activation of MEK and ERK in several models (Daaka et al., 1998; Kranenburg et al., 1999; Rizzo et al., 2001). To our knowledge a relationship between endocytosis and sensitivity to MAPK pathway-targeted agents has not been established. Decreased endocytosis has, however, been implicated in resistance to cisplatin (Chauhan et al., 2003; Liang et al., 2006).

Overall, our findings demonstrate that determinants of sensitivity and resistance to MEK-targeted agents are similar between canines and humans. The trametinib-resistant cell lines generated in this study exhibited an ERK-independent mechanism of resistance, which was associated with an EMT transcriptional signature and, in one clone, decreased mitochondrial metabolism – features that have been associated with insensitivity to MAPK pathway-targeted agents in human cancer. We also found that a gene signature that predicts sensitivity to MEK inhibition in human cancer cell lines and patients also predicts sensitivity to MEK inhibition in canine cancer cell lines. Preclinical studies and clinical trials in BRAF mutant canine TCC can, therefore, serve to improve

BRAF- and MEK-targeted therapies for both dogs and humans with MAPK pathway-driven cancers.

REFERENCES

Anders S, Pyl PT and Huber W (2015) HTSeq--a Python framework to work with high-throughput sequencing data. *Bioinformatics* **31**(2): 166-169.

Ascierto PA, McArthur GA, Dreno B, Atkinson V, Liszkay G, Di Giacomo AM, Mandala M, Demidov L, Stroyakovskiy D, Thomas L, de la Cruz-Merino L, Dutriaux C, Garbe C, Yan Y, Wongchenko M, Chang I, Hsu JJ, Koralek DO, Rooney I, Ribas A and Larkin J (2016) Cobimetinib combined with vemurafenib in advanced BRAF(V600)-mutant melanoma (coBRIM): updated efficacy results from a randomised, double-blind, phase 3 trial. *Lancet Oncol* **17**(9): 1248-1260.

Bolger AM, Lohse M and Usadel B (2014) Trimmomatic: a flexible trimmer for Illumina sequence data. *Bioinformatics* **30**(15): 2114-2120.

Chapman PB, Hauschild A, Robert C, Haanen JB, Ascierto P, Larkin J, Dummer R, Garbe C, Testori A, Maio M, Hogg D, Lorigan P, Lebbe C, Jouary T, Schadendorf D, Ribas A, O'Day SJ, Sosman JA, Kirkwood JM, Eggermont AM, Dreno B, Nolop K, Li J, Nelson B, Hou J, Lee RJ, Flaherty KT, McArthur GA and Group B-S (2011) Improved survival with vemurafenib in melanoma with BRAF V600E mutation. *N Engl J Med* **364**(26): 2507-2516.

Chauhan SS, Liang XJ, Su AW, Pai-Panandiker A, Shen DW, Hanover JA and Gottesman MM (2003) Reduced endocytosis and altered lysosome function in cisplatin-resistant cell lines. *Br J Cancer* **88**(8): 1327-1334.

Chen EY, Tan CM, Kou Y, Duan Q, Wang Z, Meirelles GV, Clark NR and Ma'ayan A (2013) Enrichr: interactive and collaborative HTML5 gene list enrichment analysis tool. *BMC Bioinformatics* **14**: 128.

Chiang CT, Demetriou AN, Ung N, Choudhury N, Ghaffarian K, Ruderman DL and Mumenthaler SM (2018) mTORC2 contributes to the metabolic reprogramming in EGFR tyrosine-kinase inhibitor resistant cells in non-small cell lung cancer. *Cancer Lett* **434**: 152-159.

Cho MS, Rupaimoole R, Choi HJ, Noh K, Chen J, Hu Q, Sood AK and Afshar-Kharghan V (2016) Complement Component 3 Is Regulated by TWIST1 and Mediates Epithelial-Mesenchymal Transition. *J Immunol* **196**(3): 1412-1418.

Corazao-Rozas P, Guerreschi P, Jendoubi M, Andre F, Jonneaux A, Scalbert C, Garcon G, Malet-Martino M, Balayssac S, Rocchi S, Savina A, Formstecher P, Mortier L, Kluza J and Marchetti P (2013) Mitochondrial oxidative stress is the Achille's heel of melanoma cells resistant to Braf-mutant inhibitor. *Oncotarget* **4**(11): 1986-1998.

Corcoran RB, Ebi H, Turke AB, Coffee EM, Nishino M, Cogdill AP, Brown RD, Della Pelle P, Dias-Santagata D, Hung KE, Flaherty KT, Piris A, Wargo JA, Settleman J, Mino-Kenudson M and Engelman JA (2012) EGFR-mediated re-activation of MAPK signaling contributes to insensitivity of BRAF mutant colorectal cancers to RAF inhibition with vemurafenib. *Cancer Discov* **2**(3): 227-235.

Creighton CJ, Hilger AM, Murthy S, Rae JM, Chinnaiyan AM and El-Ashry D (2006) Activation of mitogen-activated protein kinase in estrogen receptor alpha-positive breast cancer cells in vitro induces an in vivo molecular phenotype of estrogen receptor alpha-negative human breast tumors. *Cancer Res* **66**(7): 3903-3911.

Cronise KE, Hernandez BG, Gustafson DL and Duval DL (2019) Identifying the ErbB/MAPK Signaling Cascade as a Therapeutic Target in Canine Bladder Cancer. *Mol Pharmacol* **96**(1): 36-46.

Daaka Y, Luttrell LM, Ahn S, Della Rocca GJ, Ferguson SS, Caron MG and Lefkowitz RJ (1998) Essential role for G protein-coupled receptor endocytosis in the activation of mitogen-activated protein kinase. *J Biol Chem* **273**(2): 685-688.

Das S, Idate R, Cronise KE, Gustafson DL and Duval DL (2019) Identifying Candidate Druggable Targets in Canine Cancer Cell Lines Using Whole-Exome Sequencing. *Mol Cancer Ther* **18**(8): 1460-1471.

Davies H, Bignell GR, Cox C, Stephens P, Edkins S, Clegg S, Teague J, Woffendin H, Garnett MJ, Bottomley W, Davis N, Dicks E, Ewing R, Floyd Y, Gray K, Hall S, Hawes R, Hughes J, Kosmidou V, Menzies A, Mould C, Parker A, Stevens C, Watt S, Hooper S, Wilson R, Jayatilake H, Gusterson BA, Cooper C, Shipley J, Hargrave D, Pritchard-Jones K, Maitland N, Chenevix-Trench G, Riggins GJ, Bigner DD, Palmieri G, Cossu A, Flanagan A, Nicholson A, Ho JW, Leung SY, Yuen ST, Weber BL, Seigler HF, Darrow TL, Paterson H, Marais R, Marshall CJ, Wooster R, Stratton MR and Futreal PA (2002) Mutations of the BRAF gene in human cancer. *Nature* **417**(6892): 949-954.

Decker B, Parker HG, Dhawan D, Kwon EM, Karlins E, Davis BW, Ramos-Vara JA, Bonney PL, McNiel EA, Knapp DW and Ostrander EA (2015) Homologous Mutation to Human BRAF V600E Is Common in Naturally Occurring Canine Bladder Cancer--Evidence for a Relevant Model System and Urine-Based Diagnostic Test. *Mol Cancer Res* **13**(6): 993-1002.

Dobin A, Davis CA, Schlesinger F, Drenkow J, Zaleski C, Jha S, Batut P, Chaisson M and Gingeras TR (2013) STAR: ultrafast universal RNA-seq aligner. *Bioinformatics* **29**(1): 15-21.

Falchook GS, Long GV, Kurzrock R, Kim KB, Arkenau TH, Brown MP, Hamid O, Infante JR, Millward M, Pavlick AC, O'Day SJ, Blackman SC, Curtis CM, Lebowitz P, Ma B, Ouellet D and Kefford RF (2012) Dabrafenib in patients with melanoma, untreated brain metastases, and other solid tumours: a phase 1 dose-escalation trial. *Lancet* **379**(9829): 1893-1901.

Flaherty KT, Infante JR, Daud A, Gonzalez R, Kefford RF, Sosman J, Hamid O, Schuchter L, Cebon J, Ibrahim N, Kudchadkar R, Burris HA, 3rd, Falchook G, Algazi A, Lewis K, Long GV, Puzanov I, Lebowitz P, Singh A, Little S, Sun P, Allred A, Ouellet D, Kim KB, Patel K and Weber J (2012a) Combined BRAF and MEK inhibition in melanoma with BRAF V600 mutations. *N Engl J Med* **367**(18): 1694-1703.

Flaherty KT, Puzanov I, Kim KB, Ribas A, McArthur GA, Sosman JA, O'Dwyer PJ, Lee RJ, Grippo JF, Nolop K and Chapman PB (2010) Inhibition of mutated, activated BRAF in metastatic melanoma. *N Engl J Med* **363**(9): 809-819.

Flaherty KT, Robert C, Hersey P, Nathan P, Garbe C, Milhem M, Demidov LV, Hassel JC, Rutkowski P, Mohr P, Dummer R, Trefzer U, Larkin JM, Utikal J, Dreno B, Nyakas M, Middleton MR, Becker JC, Casey M, Sherman LJ, Wu FS, Ouellet D, Martin AM, Patel K, Schadendorf D and Group MS (2012b) Improved survival with MEK inhibition in BRAF-mutated melanoma. *N Engl J Med* **367**(2): 107-114.

Gilmartin AG, Bleam MR, Groy A, Moss KG, Minthorn EA, Kulkarni SG, Rominger CM, Erskine S, Fisher KE, Yang J, Zappacosta F, Annan R, Sutton D and Laquerre SG (2011) GSK1120212 (JTP-74057) is an inhibitor of MEK activity and activation with favorable pharmacokinetic properties for sustained in vivo pathway inhibition. *Clin Cancer Res* **17**(5): 989-1000.

Gopal YN, Rizos H, Chen G, Deng W, Frederick DT, Cooper ZA, Scolyer RA, Pupo G, Komurov K, Sehgal V, Zhang J, Patel L, Pereira CG, Broom BM, Mills GB, Ram P, Smith PD, Wargo JA, Long GV and Davies MA (2014) Inhibition of mTORC1/2 overcomes resistance to MAPK pathway inhibitors mediated by PGC1alpha and oxidative phosphorylation in melanoma. *Cancer Res* **74**(23): 7037-7047.

Grossman RL, Heath AP, Ferretti V, Varmus HE, Lowy DR, Kibbe WA and Staudt LM (2016) Toward a Shared Vision for Cancer Genomic Data. *N Engl J Med* **375**(12): 1109-1112.

Gu Z, Eils R and Schlesner M (2016) Complex heatmaps reveal patterns and correlations in multidimensional genomic data. *Bioinformatics* **32**(18): 2847-2849.

Haq R, Shoag J, Andreu-Perez P, Yokoyama S, Edelman H, Rowe GC, Frederick DT, Hurley AD, Nellore A, Kung AL, Wargo JA, Song JS, Fisher DE, Arany Z and Widlund HR (2013) Oncogenic BRAF regulates oxidative metabolism via PGC1alpha and MITF. *Cancer Cell* **23**(3): 302-315.

Hauschild A, Grob JJ, Demidov LV, Jouary T, Gutzmer R, Millward M, Rutkowski P, Blank CU, Miller WH, Jr., Kaempgen E, Martin-Algarra S, Karaszewska B, Mauch C, Chiarion-Sileni V, Martin AM, Swann S, Haney P, Mirakhur B, Guckert ME, Goodman V and Chapman PB (2012) Dabrafenib in BRAF-mutated metastatic melanoma: a multicentre, open-label, phase 3 randomised controlled trial. *Lancet* **380**(9839): 358-365.

Holbeck SL (2004) Update on NCI in vitro drug screen utilities. *Eur J Cancer* **40**(6): 785-793.

Jing Z, Yuan X, Zhang J, Huang X, Zhang Z, Liu J, Zhang M, Oyang J, Zhang Y, Zhang Z and Yang R (2010) Chromosome 1 open reading frame 190 promotes activation of NF-kappaB canonical pathway and resistance of dendritic cells to tumor-associated inhibition in vitro. *J Immunol* **185**(11): 6719-6727.

Johnson DB, Menzies AM, Zimmer L, Eroglu Z, Ye F, Zhao S, Rizos H, Sucker A, Scolyer RA, Gutzmer R, Gogas H, Kefford RF, Thompson JF, Becker JC, Berking C, Egberts F, Loquai C, Goldinger SM, Pupo GM, Hugo W, Kong X, Garraway LA, Sosman JA, Ribas A, Lo RS, Long GV and Schadendorf D (2015) Acquired BRAF inhibitor resistance: A multicenter meta-analysis of the spectrum and frequencies, clinical behaviour, and phenotypic associations of resistance mechanisms. *Eur J Cancer* **51**(18): 2792-2799.

Kaplon J, Zheng L, Meissl K, Chaneton B, Selivanov VA, Mackay G, van der Burg SH, Verdegaal EM, Cascante M, Shlomi T, Gottlieb E and Peeper DS (2013) A key role for mitochondrial gatekeeper pyruvate dehydrogenase in oncogene-induced senescence. *Nature* **498**(7452): 109-112.

Kopetz S, Desai J, Chan E, Hecht JR, O'Dwyer PJ, Maru D, Morris V, Janku F, Dasari A, Chung W, Issa JP, Gibbs P, James B, Powis G, Nolop KB, Bhattacharya S and Saltz L (2015) Phase II Pilot Study of Vemurafenib in Patients With Metastatic BRAF-Mutated Colorectal Cancer. *J Clin Oncol* **33**(34): 4032-4038.

Kranenburg O, Verlaan I and Moolenaar WH (1999) Dynamin is required for the activation of mitogen-activated protein (MAP) kinase by MAP kinase kinase. *J Biol Chem* **274**(50): 35301-35304.

Kuleshov MV, Jones MR, Rouillard AD, Fernandez NF, Duan Q, Wang Z, Koplev S, Jenkins SL, Jagodnik KM, Lachmann A, McDermott MG, Monteiro CD, Gundersen GW and Ma'ayan A (2016) Enrichr: a comprehensive gene set enrichment analysis web server 2016 update. *Nucleic Acids Res* **44**(W1): W90-97.

Liang XJ, Mukherjee S, Shen DW, Maxfield FR and Gottesman MM (2006) Endocytic recycling compartments altered in cisplatin-resistant cancer cells. *Cancer Res* **66**(4): 2346-2353.

Liberzon A, Subramanian A, Pinchback R, Thorvaldsdottir H, Tamayo P and Mesirov JP (2011) Molecular signatures database (MSigDB) 3.0. *Bioinformatics* **27**(12): 1739-1740.

Long GV, Stroyakovskiy D, Gogas H, Levchenko E, de Braud F, Larkin J, Garbe C, Jouary T, Hauschild A, Grob JJ, Chiarion Sileni V, Lebbe C, Mandala M, Millward M, Arance A, Bondarenko I, Haanen JB, Hansson J, Utikal J, Ferraresi V, Kovalenko N, Mohr P, Probachai V, Schadendorf D, Nathan P, Robert C, Ribas

A, DeMarini DJ, Irani JG, Casey M, Ouellet D, Martin AM, Le N, Patel K and Flaherty K (2014) Combined BRAF and MEK inhibition versus BRAF inhibition alone in melanoma. *N Engl J Med* **371**(20): 1877-1888.

Lopes-Rodrigues V, Di Luca A, Mleczko J, Meleady P, Henry M, Pesic M, Cabrera D, van Liempd S, Lima RT, O'Connor R, Falcon-Perez JM and Vasconcelos MH (2017) Identification of the metabolic alterations associated with the multidrug resistant phenotype in cancer and their intercellular transfer mediated by extracellular vesicles. *Sci Rep* **7**: 44541.

Majumder PK, Febbo PG, Bikoff R, Berger R, Xue Q, McMahon LM, Manola J, Brugarolas J, McDonnell TJ, Golub TR, Loda M, Lane HA and Sellers WR (2004) mTOR inhibition reverses Akt-dependent prostate intraepithelial neoplasia through regulation of apoptotic and HIF-1-dependent pathways. *Nat Med* **10**(6): 594-601.

McArthur GA, Chapman PB, Robert C, Larkin J, Haanen JB, Dummer R, Ribas A, Hogg D, Hamid O, Ascierto PA, Garbe C, Testori A, Maio M, Lorigan P, Lebbe C, Jouary T, Schadendorf D, O'Day SJ, Kirkwood JM, Eggermont AM, Dreno B, Sosman JA, Flaherty KT, Yin M, Caro I, Cheng S, Trunzer K and Hauschild A (2014) Safety and efficacy of vemurafenib in BRAF(V600E) and BRAF(V600K) mutation-positive melanoma (BRIM-3): extended follow-up of a phase 3, randomised, open-label study. *Lancet Oncol* **15**(3): 323-332.

McCarthy DJ, Chen Y and Smyth GK (2012) Differential expression analysis of multifactor RNA-Seq experiments with respect to biological variation. *Nucleic Acids Res* **40**(10): 4288-4297.

Mochizuki H, Kennedy K, Shapiro SG and Breen M (2015) BRAF Mutations in Canine Cancers. *PLoS One* **10**(6): e0129534.

Montagut C, Sharma SV, Shioda T, McDermott U, Ulman M, Ulkus LE, Dias-Santagata D, Stubbs H, Lee DY, Singh A, Drew L, Haber DA and Settleman J (2008) Elevated CRAF as a potential mechanism of acquired resistance to BRAF inhibition in melanoma. *Cancer Res* **68**(12): 4853-4861.

Nazarian R, Shi H, Wang Q, Kong X, Koya RC, Lee H, Chen Z, Lee MK, Attar N, Sazegar H, Chodon T, Nelson SF, McArthur G, Sosman JA, Ribas A and Lo RS (2010) Melanomas acquire resistance to B-RAF(V600E) inhibition by RTK or N-RAS upregulation. *Nature* **468**(7326): 973-977.

O'Donoghue LE, Rivest JP and Duval DL (2011) Polymerase chain reaction-based species verification and microsatellite analysis for canine cell line validation. *J Vet Diagn Invest* **23**(4): 780-785.

Paoloni MC and Khanna C (2007) Comparative oncology today. *Vet Clin North Am Small Anim Pract* **37**(6): 1023-1032; v.

Parmenter TJ, Kleinschmidt M, Kinross KM, Bond ST, Li J, Kaadige MR, Rao A, Sheppard KE, Hugo W, Pupo GM, Pearson RB, McGee SL, Long GV, Scolyer RA, Rizos H, Lo RS, Cullinane C, Ayer DE, Ribas A, Johnstone RW, Hicks RJ and McArthur GA (2014) Response of BRAF-mutant melanoma to BRAF inhibition is mediated by a network of transcriptional regulators of glycolysis. *Cancer Discov* **4**(4): 423-433.

Peng DH, Kundu ST, Fradette JJ, Diao L, Tong P, Byers LA, Wang J, Canales JR, Villalobos PA, Mino B, Yang Y, Minelli R, Peoples MD, Bristow CA, Heffernan TP, Carugo A, Wistuba, II and Gibbons DL (2019) ZEB1 suppression sensitizes KRAS mutant cancers to MEK inhibition by an IL17RD-dependent mechanism. *Sci Transl Med* **11**(483).

Poulikakos PI, Persaud Y, Janakiraman M, Kong X, Ng C, Moriceau G, Shi H, Atefi M, Titz B, Gabay MT, Salton M, Dahlman KB, Tadi M, Wargo JA, Flaherty KT, Kelley MC, Misteli T, Chapman PB, Sosman JA, Graeber TG, Ribas A, Lo RS, Rosen N and Solit DB (2011) RAF inhibitor resistance is mediated by dimerization of aberrantly spliced BRAF(V600E). *Nature* **480**(7377): 387-390.

Richard G, Dalle S, Monet MA, Ligier M, Boespflug A, Pommier RM, de la Fouchardiere A, Perier-Muzet M, Depaepe L, Barnault R, Tondeur G, Ansieau S, Thomas E, Bertolotto C, Ballotti R, Mourah S, Battistella M, Lebbe C, Thomas L, Puisieux A and Caramel J (2016) ZEB1-mediated melanoma cell plasticity enhances resistance to MAPK inhibitors. *EMBO Mol Med* **8**(10): 1143-1161.

Rizzo MA, Kraft CA, Watkins SC, Levitan ES and Romero G (2001) Agonist-dependent traffic of raft-associated Ras and Raf-1 is required for activation of the mitogen-activated protein kinase cascade. *J Biol Chem* **276**(37): 34928-34933.

Robert C, Karaszewska B, Schachter J, Rutkowski P, Mackiewicz A, Stroiakovski D, Lichinitser M, Dummer R, Grange F, Mortier L, Chiarion-Sileni V, Drucis K, Krajsova I, Hauschild A, Lorigan P, Wolter P, Long GV, Flaherty K, Nathan P, Ribas A, Martin AM, Sun P, Crist W, Legos J, Rubin SD, Little SM and Schadendorf D (2015) Improved overall survival in melanoma with combined dabrafenib and trametinib. *N Engl J Med* **372**(1): 30-39.

Robinson MD, McCarthy DJ and Smyth GK (2010) edgeR: a Bioconductor package for differential expression analysis of digital gene expression data. *Bioinformatics* **26**(1): 139-140.

Roumenina LT, Daugan MV, Petitprez F, Sautes-Fridman C and Fridman WH (2019) Context-dependent roles of complement in cancer. *Nature reviews Cancer* **19**(12): 698-715.

Shi H, Hugo W, Kong X, Hong A, Koya RC, Moriceau G, Chodon T, Guo R, Johnson DB, Dahlman KB, Kelley MC, Kefford RF, Chmielowski B, Glaspy JA, Sosman JA, van Baren N, Long GV, Ribas A and Lo RS (2014) Acquired resistance and

clonal evolution in melanoma during BRAF inhibitor therapy. *Cancer Discov* **4**(1): 80-93.

Singh A, Greninger P, Rhodes D, Koopman L, Violette S, Bardeesy N and Settleman J (2009) A gene expression signature associated with "K-Ras addiction" reveals regulators of EMT and tumor cell survival. *Cancer Cell* **15**(6): 489-500.

Singh A and Settleman J (2010) EMT, cancer stem cells and drug resistance: an emerging axis of evil in the war on cancer. *Oncogene* **29**(34): 4741-4751.

Sledge DG, Kiupel M, Madrill N and Elizabeth M (2012) Abstract 5258: Characterization of canine lower urinary tract carcinoma cell lines with variable DNA mismatch repair proficiency derived from a single tumor. *Cancer Research* **72**(8 Supplement): 5258-5258.

Subramanian A, Tamayo P, Mootha VK, Mukherjee S, Ebert BL, Gillette MA, Paulovich A, Pomeroy SL, Golub TR, Lander ES and Mesirov JP (2005) Gene set enrichment analysis: a knowledge-based approach for interpreting genome-wide expression profiles. *Proc Natl Acad Sci U S A* **102**(43): 15545-15550.

Tiacci E, Trifonov V, Schiavoni G, Holmes A, Kern W, Martelli MP, Pucciarini A, Bigerna B, Pacini R, Wells VA, Sportoletti P, Pettirossi V, Mannucci R, Elliott O, Liso A, Ambrosetti A, Pulsoni A, Forconi F, Trentin L, Semenzato G, Inghirami G, Capponi M, Di Raimondo F, Patti C, Arcaini L, Musto P, Pileri S, Haferlach C, Schnittger S, Pizzolo G, Foa R, Farinelli L, Haferlach T, Pasqualucci L, Rabadan R and Falini B (2011) BRAF mutations in hairy-cell leukemia. *N Engl J Med* **364**(24): 2305-2315.

Trapnell C, Williams BA, Pertea G, Mortazavi A, Kwan G, van Baren MJ, Salzberg SL, Wold BJ and Pachter L (2010) Transcript assembly and quantification by RNA-Seq reveals unannotated transcripts and isoform switching during cell differentiation. *Nat Biotechnol* **28**(5): 511-515.

Trunzer K, Pavlick AC, Schuchter L, Gonzalez R, McArthur GA, Hutson TE, Moschos SJ, Flaherty KT, Kim KB, Weber JS, Hersey P, Long GV, Lawrence D, Ott PA, Amaravadi RK, Lewis KD, Puzanov I, Lo RS, Koehler A, Kockx M, Spleiss O, Schell-Steven A, Gilbert HN, Cockey L, Bollag G, Lee RJ, Joe AK, Sosman JA and Ribas A (2013) Pharmacodynamic effects and mechanisms of resistance to vemurafenib in patients with metastatic melanoma. *J Clin Oncol* **31**(14): 1767-1774.

Van Allen EM, Wagle N, Sucker A, Treacy DJ, Johannessen CM, Goetz EM, Place CS, Taylor-Weiner A, Whittaker S, Kryukov GV, Hodis E, Rosenberg M, McKenna A, Cibulskis K, Farlow D, Zimmer L, Hillen U, Gutzmer R, Goldinger SM, Ugurel S, Gogas HJ, Egberts F, Berking C, Trefzer U, Loquai C, Weide B, Hassel JC, Gabriel SB, Carter SL, Getz G, Garraway LA, Schadendorf D and Dermatologic Cooperative Oncology Group of G (2014) The genetic landscape of clinical

resistance to RAF inhibition in metastatic melanoma. *Cancer Discov* **4**(1): 94-109.

Wagle MC, Kirouac D, Klijn C, Liu B, Mahajan S, Junttila M, Moffat J, Merchant M, Huw L, Wongchenko M, Okrah K, Srinivasan S, Mounir Z, Sumiyoshi T, Haverty PM, Yauch RL, Yan Y, Kabbarah O, Hampton G, Amler L, Ramanujan S, Lackner MR and Huang SA (2018) A transcriptional MAPK Pathway Activity Score (MPAS) is a clinically relevant biomarker in multiple cancer types. *NPJ Precis Oncol* **2**(1): 7.

Wan PT, Garnett MJ, Roe SM, Lee S, Niculescu-Duvaz D, Good VM, Jones CM, Marshall CJ, Springer CJ, Barford D, Marais R and Cancer Genome P (2004) Mechanism of activation of the RAF-ERK signaling pathway by oncogenic mutations of B-RAF. *Cell* **116**(6): 855-867.

Wang B, Krall EB, Aguirre AJ, Kim M, Widlund HR, Doshi MB, Sicinska E, Sulahian R, Goodale A, Cowley GS, Piccioni F, Doench JG, Root DE and Hahn WC (2017) ATXN1L, CIC, and ETS Transcription Factors Modulate Sensitivity to MAPK Pathway Inhibition. *Cell Rep* **18**(6): 1543-1557.

Weissmann S, Cloos PA, Sidoli S, Jensen ON, Pollard S and Helin K (2018) The Tumor Suppressor CIC Directly Regulates MAPK Pathway Genes via Histone Deacetylation. *Cancer Res* **78**(15): 4114-4125.

Witta SE, Gemmill RM, Hirsch FR, Coldren CD, Hedman K, Ravdel L, Helfrich B, Dziadziuszko R, Chan DC, Sugita M, Chan Z, Baron A, Franklin W, Drabkin HA, Girard L, Gazdar AF, Minna JD and Bunn PA, Jr. (2006) Restoring E-cadherin expression increases sensitivity to epidermal growth factor receptor inhibitors in lung cancer cell lines. *Cancer Res* **66**(2): 944-950.

Xiao GY, Mohanakrishnan A and Schmid SL (2018) Role for ERK1/2-dependent activation of FCHSD2 in cancer cell-selective regulation of clathrin-mediated endocytosis. *Proc Natl Acad Sci U S A* **115**(41): E9570-E9579.

Zhang G, Frederick DT, Wu L, Wei Z, Krepler C, Srinivasan S, Chae YC, Xu X, Choi H, Dimwamwa E, Ope O, Shannan B, Basu D, Zhang D, Guha M, Xiao M, Randell S, Sproesser K, Xu W, Liu J, Karakousis GC, Schuchter LM, Gangadhar TC, Amaravadi RK, Gu M, Xu C, Ghosh A, Xu W, Tian T, Zhang J, Zha S, Liu Q, Brafford P, Weeraratna A, Davies MA, Wargo JA, Avadhani NG, Lu Y, Mills GB, Altieri DC, Flaherty KT and Herlyn M (2016) Targeting mitochondrial biogenesis to overcome drug resistance to MAPK inhibitors. *J Clin Invest* **126**(5): 1834-1856.

CHAPTER 5

Overall Conclusions and Future Directions

CONCLUSIONS

The goals of this dissertation were three-fold, which are all centered around improving therapies for dogs with transitional cell carcinoma (TCC), while simultaneously investigating the translational potential of the disease for the development of anticancer drugs, specifically MAPK pathway-targeted agents, to improve cancer treatment in humans. First, we aimed to provide a molecular characterization of canine bladder cancer by identifying putative drivers of oncogenesis and druggable targets in eleven canine TCC (cTCC) tumors. Based on the identification of BRAF mutations in 70% of samples, we then investigated the therapeutic value of BRAF and MEK inhibitors in cTCC cell lines. Finally, we generated derivatives of the Tyler1 TCC cell line exhbiting acquired resistance to the MEK inhibitor trametinib and aimed to identify determinants of resistance. The results of this dissertation help to solidify the comparative relevancy cTCC as a model for understanding cancer biology and improving drug development for MAPK pathway-driven cancers.

The broader goal of Chapter 2 was to provide a genomic and immune characterization of canine bladder cancer in order to better understand the biology underlying oncogenesis and improve treatment. We analyzed the mutation landscape of 11 TCC tumors using whole exome sequencing, identifying 583 protein-coding

variants. Mutations in BRAF were the most common variant, initially identified in 4 out of 11 samples using whole exome sequencing and later in an additional 3 tumors, as well as 22 out of 32 FFPE samples, using Sanger sequencing. RNA-Seq analysis comparing the transcriptome of TCC to normal bladder tissue identified upregulation of cell cycle and DNA repair genes, as well as antiviral genes. Overall the prevalence of BRAF mutations identified in canine TCC supports its potential as a therapeutic target. Furthermore, since most patients treated with BRAF or MEK inhibitors eventually experience disease relapse, canine TCC may serve as a translational model for identifying potential combination therapies to prevent or delay the onset of resistance.

While the molecular biology of canine TCC is becoming more clear, a basic understanding of the immune landscape of the disease is still lacking. This served as our motivation for the second half of Chapter 2. Using RNA-Seq and immunohistochemical analysis we identified a subset of tumors (4/11) with characteristics of an immunologically hot tumor microenvironment (TME-Hot). TME-Hot tumors exhibited high MHC Class I expression, increased expression of markers for CD8+ T cells and plasmacytoid dendritic cells, as well as elevated co-stimulatory and co-inhibitory receptor expression. Immunotherapy has shown promise as a therapy for bladder cancer; however, only about one-quarter of patients respond, making effective biomarker identification imperative. We show that TME-Hot TCC tumors exhibit elevated expression of genomic indicators of response to PD-1 and PD-L1 inhibitors. These data indicate that a subset of canine bladder cancer exhibits characteristics of an inflamed tumor microenvironment and suggests that this group could respond more favorably to checkpoint inhibition.

Chapters 3 and 4 expand on our major finding in the first half of Chapter 2 – BRAF mutations. Using five canine TCC cell lines (3 BRAF mutant, 1 KRAS mutant, and 1 wild type), we assessed the antiproliferative efficacy of BRAF and MEK inhibitors. We found that BRAF mutant cTCC cell lines were insensitive to vemurafenib. These cell lines exhibited an initial decrease in MAPK pathway activation that eventually rebounded by 24 hours. Both the KRAS mutant and wild type cell lines exhibited paradoxical increased MAPK activation following vemurafenib treatment, a phenomenon that also occurs in human RAS mutant or BRAF/RAS wild type tumors treated with vemurafenib. However, since BRAF mutations in cTCC are heterozygous, we hypothesized that paradoxical activation as a result of the wild type BRAF copy could be contributing to vemurafenib insensitivity. Indeed, BRAF mutant TCC were sensitive to a newer "paradox-breaking" inhibitor PLX7904; however, analysis of downstream ERK1/2 phosphorylation indicated pathway rebound by 24 hours. All TCC cell lines were sensitive to MEK inhibition; however, the majority of cell lines showed ERK reactivation by 24 hours, similar to results with BRAF inhibition.

Another finding of Chapter 3 was the upregualtion of EGFR and ERBB2 receptors in TCC cell lines relative to other canine cancer cell lines, as well as upregulation of the EGFR ligand EREG. Inhibition of ErbB receptors with the pan-ErbB inhibitor sapitnib was synergistic with the BRAF inhibitor PLX7904 in the BRAF mutant Bliley cell line and was synergistic with MEK inhibition in both BRAF mutant Bliley and wild type Kinsey cell lines. The response of BRAF mutant canine TCC was reminiscent of the response of BRAF mutant colorectal cancer cell lines that are typically unresponsive to BRAF inhibition due to feedback activation of EGFR (Corcoran et al.,

2012; Prahallad et al., 2012). Results from clinical trials combining BRAF and MEK inhibition in BRAF mutant colorectal cancer have been largely unimpressive with a 12% response rate relative to a 5% response rate with BRAF inhibition alone (Corcoran et al., 2015; Kopetz et al., 2015). Triple combinations of BRAF, MEK, and EGFR inhibitors improve the overall response rate to roughly 20-25%; however, the majority of patients experienced intrinsic or acquired resistance characterized by other means of reactivating the MAPK pathway (Corcoran et al., 2018; Kopetz et al., 2019). Thus, canine TCC may serve as a translational model for improving BRAF combination therapies, including those targeting the ErbB receptor family.

In Chapter 4, we further explored the utility of this model for interrogating mechanisms of resistance to MAPK-targeted therapies. We knew from Chapter 3 that cTCC cell lines are exquisitely sensitive to the MEK inhibitor trametinib, but that several cell lines exhibit ERK1/2 reactivation, suggesting a built-in level of plasticity that allows cTCC cell lines to bypass MEK inhibition. Thus, we aimed to create a canine model of acquired trametinib resistance by culturing the BRAF mutant Tyler1 cell line in increasing concentrations of trametinib over the course of nine months. In doing so, we generated six trametinib-resistant cell lines of Tyler1 origin, exhibiting IC_{50} values greater than 500 nM relative to 1 nM with the parental Tyler1 cell line. Interestingly, ERK1/2 activation was suppressed at concentrations that do not affect cell proliferation in the resistant cell lines. This finding suggested that TramR cells are able to grow and survive despite trametinib achieving and maintaining target inhibition. TramR cell line insensitivity to the ERK1/2 inhibitor ravoxertinib further supported a mechanism of resistance that is independent of ERK1/2 reactivation.

Tyler1-TramR cell lines exhibited loss of epithelial gene markers and increased expression of mesenchymal markers and EMT transcription factors, which were accompanied by morphology shifts consistent with a transition to a more mesenchymal appearance. One of the TramR clones also exhibited decreased basal and maximal mitochondrial oxygen consumption rates, as well as decreased glycolytic reserve. Future work involving these trametinib-resistant cTCC cell lines is required to pinpoint specific mediators of resistance.

FUTURE DIRECTIONS

In Chapter 4 we describe the generation and characterization of a canine model of acquired trametinib resistance. While we were not able to identify the exact mechanism(s) underlying resistance, we were able to determine that it is independent of ERK1/2 activation. One question that should be addressed is whether or not these cell lines are specifically resistant to MAPK pathway inhibitors or if they are resistant to other non-targeted agents. It is possible that the TramR cells exhibit a general resistance to cell death. For instance, it would be informative to treat Tyler1-TramR cell lines with different cytotoxic chemotherapeutic agents and compare the degree of sensitivity to that of the parental cell line. Mitoxantrone and vinblastine may be of interest, as these drugs are often used in management of canine bladder cancer (Fulkerson and Knapp, 2019).

Another avenue worth investigating is the possibility that Tyler1-TramR cell lines exhibit increased dependence on the PI3K/AKT/mTOR signaling pathway. The

importance of addressing this question is further highlighted by metabolic alterations in one of the trametinib resistant clones. PI3K/AKT signaling regulates metabolism via many mechanisms including increased glucose uptake, activation of glycolytic enzymes, and increased lipid and nucleotide biosynthesis (Hoxhaj and Manning, 2020). The metabolic phenotype of TramR-Clone2 involved diminished spare respiratory capacity with decreased basal and maximal oxygen consumption rates relative to the parental cell line, as well as decreased glycolytic reserve. This phenotype possibly may suggest that increased PI3K/AKT activation is not actually the case in this cell line; however, given the variety of previously identified MAPK inhibitor resistance mechanisms involving increased AKT signaling, determining whether Tyler1 TramR cell lines exhibit increased activation of this pathway is of high importance.

Additional drug sensitivity assays could be performed to determine if TramR-Clone2, which exhibits decreased spare respiratory and capacity, is more sensitive to other forms of oxidative stress. Metformin is an antidiabetic drug with anticancer properties that have been attributed to disruption of complex I of the electron transport chain (El-Mir et al., 2000; Wheaton et al., 2014). Teh et al. have recently shown that cell lines with decreased spare respiratory capacity are more sensitive to metformin; thus, the antiproliferative capacity of metformin should be assessed in parental and trametinib-resistant Tyler1, specifically TramR-Clone2 (Teh et al., 2019).

All six Tyler1-TramR clones described in this dissertation exhibited a morphology shift consistent with EMT. Gene expression analysis of epithelial and mesenchymal markers in two TramR clones supported this notion. However, additional experimentation should be performed to confirm that TramR cells exhibit increased

expression of mesenchymal markers (and loss of epithelial markers) at the protein level. If EMT is confirmed in the TramR cells it would be of interest to determine the metastatic and invasive potential of these TramR cell lines relative to the parental cell line. Knockdown or knockout of ZEB1 or ZEB2, two EMT transcription factors whose expression are increased in Tyler1-TramR cell lines, followed by trametinib treatment would be a valuable means of determining whether reversal of the EMT can confer sensitivity to trametinib. COX-2 inhibition in human bladder cancer cell lines reverses EMT and reduces the metastatic and tumorigenic potential of the cell lines (Adhim et al., 2011). Since the COX-2 inhibitor piroxicam is commonly used in management of canine TCC, it would be worthwhile to determine whether pre-treatment or combined treatment with piroxicam is capable of conferring sensitivity to trametinib.

The acquired resistance of Tyler1-TramR cells developed over the course of nine months. An interesting endeavor would be to go back and analyze gene expression from frozen stocks of these cells at earlier time points during the development of resistance. This analysis could be used to track the transcriptional changes that occurred over time. Furthermore, since transcriptional alterations are not the only known contributors to drug resistance, analyzing the mutation profile of Tyler1-TramR at different time points during the development of resistance could be informative. This mutational analysis may identify and track the emergence of new variants that may contribute to resistance.

Finally, the concept of synthetic lethality in cancer has become increasingly relevant. An oncogenic alteration can confer a specific vulnerability to cancer cells, such that targeting a certain pathway or gene is toxic to cells harboring that alteration

but is innocuous in other instances (O'Neil et al., 2017). An increased emphasis on high-throughput approaches to cancer research and drug development has made the identification of synthetic lethal interactions easier. Performing a CRISPR screen or small molecule library screen on Tyler1-TramR cell lines is likely to be the most informative means of identifying specific gene targets, pathways, or processes that mediate resistance.

REFERENCES

Adhim Z, Matsuoka T, Bito T, Shigemura K, Lee KM, Kawabata M, Fujisawa M, Nibu K and Shirakawa T (2011) In vitro and in vivo inhibitory effect of three Cox-2 inhibitors and epithelial-to-mesenchymal transition in human bladder cancer cell lines. *Br J Cancer* **105**(3): 393-402.

Corcoran RB, Andre T, Atreya CE, Schellens JHM, Yoshino T, Bendell JC, Hollebecque A, McRee AJ, Siena S, Middleton G, Muro K, Gordon MS, Tabernero J, Yaeger R, O'Dwyer PJ, Humblet Y, De Vos F, Jung AS, Brase JC, Jaeger S, Bettinger S, Mookerjee B, Rangwala F and Van Cutsem E (2018) Combined BRAF, EGFR, and MEK Inhibition in Patients with BRAF(V600E)-Mutant Colorectal Cancer. *Cancer Discov* **8**(4): 428-443.

Corcoran RB, Atreya CE, Falchook GS, Kwak EL, Ryan DP, Bendell JC, Hamid O, Messersmith WA, Daud A, Kurzrock R, Pierobon M, Sun P, Cunningham E, Little S, Orford K, Motwani M, Bai Y, Patel K, Venook AP and Kopetz S (2015) Combined BRAF and MEK Inhibition With Dabrafenib and Trametinib in BRAF V600-Mutant Colorectal Cancer. *J Clin Oncol* **33**(34): 4023-4031.

Corcoran RB, Ebi H, Turke AB, Coffee EM, Nishino M, Cogdill AP, Brown RD, Della Pelle P, Dias-Santagata D, Hung KE, Flaherty KT, Piris A, Wargo JA, Settleman J, Mino-Kenudson M and Engelman JA (2012) EGFR-mediated re-activation of MAPK signaling contributes to insensitivity of BRAF mutant colorectal cancers to RAF inhibition with vemurafenib. *Cancer Discov* **2**(3): 227-235.

El-Mir MY, Nogueira V, Fontaine E, Averet N, Rigoulet M and Leverve X (2000) Dimethylbiguanide inhibits cell respiration via an indirect effect targeted on the respiratory chain complex I. *J Biol Chem* **275**(1): 223-228.

Fulkerson CM and Knapp DW (2019) Tumors of the Urinary System, in *Withrow and MacEwen's Small Animal Clinical Oncology (Sxith Edition)* (Vail DM, Thamm DH and Liptak JM eds) pp 645-656, W.B. Saunders, St. Louis (MO).

Hoxhaj G and Manning BD (2020) The PI3K-AKT network at the interface of oncogenic signalling and cancer metabolism. *Nature reviews Cancer* **20**(2): 74-88.

Kopetz S, Desai J, Chan E, Hecht JR, O'Dwyer PJ, Maru D, Morris V, Janku F, Dasari A, Chung W, Issa JP, Gibbs P, James B, Powis G, Nolop KB, Bhattacharya S and Saltz L (2015) Phase II Pilot Study of Vemurafenib in Patients With Metastatic BRAF-Mutated Colorectal Cancer. *J Clin Oncol* **33**(34): 4032-4038.

Kopetz S, Grothey A, Yaeger R, Van Cutsem E, Desai J, Yoshino T, Wasan H, Ciardiello F, Loupakis F, Hong YS, Steeghs N, Guren TK, Arkenau HT, Garcia-Alfonso P, Pfeiffer P, Orlov S, Lonardi S, Elez E, Kim TW, Schellens JHM, Guo

C, Krishnan A, Dekervel J, Morris V, Calvo Ferrandiz A, Tarpgaard LS, Braun M, Gollerkeri A, Keir C, Maharry K, Pickard M, Christy-Bittel J, Anderson L, Sandor V and Tabernero J (2019) Encorafenib, Binimetinib, and Cetuximab in BRAF V600E-Mutated Colorectal Cancer. *N Engl J Med* **381**(17): 1632-1643.

O'Neil NJ, Bailey ML and Hieter P (2017) Synthetic lethality and cancer. *Nat Rev Genet* **18**(10): 613-623.

Prahallad A, Sun C, Huang S, Di Nicolantonio F, Salazar R, Zecchin D, Beijersbergen RL, Bardelli A and Bernards R (2012) Unresponsiveness of colon cancer to BRAF(V600E) inhibition through feedback activation of EGFR. *Nature* **483**(7387): 100-103.

Teh JT, Zhu WL, Newgard CB, Casey PJ and Wang M (2019) Respiratory Capacity and Reserve Predict Cell Sensitivity to Mitochondria Inhibitors: Mechanism-Based Markers to Identify Metformin-Responsive Cancers. *Mol Cancer Ther* **18**(3): 693-705.

Wheaton WW, Weinberg SE, Hamanaka RB, Soberanes S, Sullivan LB, Anso E, Glasauer A, Dufour E, Mutlu GM, Budigner GS and Chandel NS (2014) Metformin inhibits mitochondrial complex I of cancer cells to reduce tumorigenesis. *Elife* **3**: e02242.